STREAM CORRIDOR CONNECTIVITY CONTROLS

ON NITROGEN CYCLING

by

JOEL GREENE SINGLEY

B.S., Cornell University, 2010

M.S., University of Colorado, 2017

A thesis submitted to the

Faculty of the Graduate School of the

University of Colorado in partial fulfillment

of the requirement for the degree of

Doctor of Philosophy

Environmental Studies Program

2021

Committee Members:

Eve-Lyn S. Hinckley

Michael N. Gooseff

Kamini Singha

Diane M. McKnight

Nichole N. Barger

Singley, Joel Greene (Ph.D., Environmental Studies)

Stream Corridor Connectivity Controls on Nitrogen Cycling

Thesis directed by Asst. Prof. Eve-Lyn S. Hinckley and Prof. Michael N. Gooseff

As water flows downstream, it is transported to and from environments that surround the visible stream. Along with surface water, these laterally and vertically connected environments comprise the stream corridor. Stream corridor connectivity influences many ecosystem services, including retention of excess nutrients. The subsurface area where stream water and groundwater mixes—the hyporheic zone—represents one of the most biogeochemically active parts of stream corridors.

The goal of my research is to advance understanding of how connectivity between different parts of a stream corridor controls the availability and retention of nitrogen (N), a nutrient that can limit primary productivity (low-N) and negatively impact water quality (excess N). First, I developed and applied a new machine learning method to objectively characterize the extent and variability of hyporheic exchange in terms of statistically unique functional zones using geophysical data. In applying this method to a benchmark dataset, I found that hyporheic extent does not scale uniformly with streamflow and that changes in the heterogeneity of connectivity differ over small (<10 m) distances. Next, I leveraged the relative simplicity of ephemeral streams of the McMurdo Dry Valleys (MDVs), Antarctica, to isolate stream corridor processes that influence the fate of N. Through intensive field sampling campaigns, I found that the hyporheic zone can be a persistent source of N even in this low nutrient environment. Next, I combined historic sample data and remote sensing analysis to estimate how much N is stored in an MDV stream corridor. My results indicate that up to 10^3 times more N is stored in this system than is exported each year, with most of this storage in the shallow (< 10 cm) hyporheic zone. Lastly, I examined 25 years of data for 10 streams to assess how stream corridor processes control concentration-discharge relationships. I found that in the absence of hillslope connectivity, stream corridor processes alone can maintain chemostasis – relatively small

concentration changes with large fluctuations in streamflow – of both geogenic solutes and primary nutrients. My analysis also revealed that solutes subject to greater control by biological processes exhibit more variability within chemostatic relationships than weathering solutes that are only minimally influenced by biota.

Altogether, this research advances understanding of processes that are difficult to measure or are often overlooked in typical studies of temperate stream corridors. My findings provide insight into the surprising ways in which N is mobilized, transformed, and retained due to stream corridor connectivity in intermittent stream systems with few N inputs.

DEDICATION

For my Little Adventure Bird

ACKNOWLEDGMENTS

CONTENTS

TABLES

Table

FIGURES

Chapter I

Introduction

As water flows, it is transported to and from environments that surround the visible stream. Along with surface water, these laterally and vertically connected environments comprise the stream corridor (Harvey & Gooseff, 2015). Stream corridor connectivity influences many ecosystem services, including retention of excess nutrients, that are of importance to humans and downstream ecosystems (Peterson et al., 2001; Gomez-Velez et al., 2015). The subsurface area where stream water and groundwater mixes—the hyporheic zone—represents one of the most biogeochemically active parts of stream corridors due to strong redox zonation, extended residence time, and increased contact with sediment and microbial communities (Boano et al., 2014). With this dissertation, I advance the current state of knowledge regarding (1) how hyporheic connectivity is spatially structured and (2) how this connectivity controls the availability and retention of nitrogen (N), a primary nutrient that can negatively impact water quality and influence the function of downstream ecosystems.

Hydrologic connectivity has served as useful framework for investigating and characterizing integrated hydro-biogeochemical functioning of stream corridors from the scale of pore spaces and bedforms up to stream reaches, networks, and entire basins (Harvey & Gooseff, 2015; Magliozzi et al., 2018; Gomez-Velez et al., 2015). Within stream corridors, hydrologic connectivity influences the development of distinct biogeochemical processing along exchange gradients (Boano et al., 2014; Krause et al., 2017) as well as their significance over larger scales (Harvey et al., 2018; Bernhardt et al., 2017).

Amongst the compartments connected by hydrologic exchange flows, hyporheic and parafluvial zones are of particular importance for many biogeochemical processes, especially N retention and transformation (Harvey et al., 2018; Jones et al., 1995a, 1995b; Mulholland et al., 2008). Despite decades of research, it remains challenging to quantitatively characterize, numerically represent, and accurately predict the spatiotemporal heterogeneity of hyporheic

connectivity and biogeochemical function (Boano et al., 2014, Lewandowski et al., 2019; Ward et al., 2016). The challenges in this area largely reflect more general issues with understanding how multi-scale heterogeneity impacts emergent hydro-biogeochemical processes in natural systems (Blöschl et al., 2019, Li et al., 2021).

Connectivity between landscapes and stream corridors is often leveraged in the analysis of concentration-discharge (C-Q) relationships to infer distributed hydro-biogeochemical processes over large scales. Utilizing simple C-Q analysis frameworks has provided significant insight into how catchments store, mobilize, and transform solutes (Evans & Davies, 1998; Godsey et al., 2009; Knapp et al., 2020). Yet, despite recognition of streams as biogeochemically active conduits, few studies employing the C-Q framework have attempted to isolate stream corridor effects on C-Q relationship form and variability from those of the surrounding catchment (e.g., Moatar et al., 2017).

Since nutrient and organic matter fluxes in most systems are dominated by allochthonous inputs from the surrounding landscape (e.g., Mulholland et al., 2008; Tank et al., 2010), hydrologic connectivity often determines the availability of nutrients in streams and strongly modulates the balance between autotrophic and heterotrophic metabolic processes (Mulholland et al., 2001), as well as N cycling (Alexander et al., 2009). This has resulted in extensive research on how stream corridors remove excess allochthonous organic matter and N (e.g., Alexander et al., 2007; Boyer et al., 2002; Gomez-Velez et al., 2015). However, in environments with limited canopy cover (e.g., alpine, arid, or polar systems), autochthonous contributions to organic matter and N from benthic algal biofilms can be significant (Fellman et al., 2011; Fenoglio et al., 2015; Marcarelli et al., 2008). Attention to the ways in which autochthonous organic matter and N are transformed and stored in such systems has been overshadowed by the general focus on systems in which excess N is exported from the surrounding landscape.

Additionally, very few streams are characterized by stable hydrologic conditions either in space or time. Hydrologic variability has profound implications for where and how N and other nutrients are cycled and whether short-term studies can adequately characterize variability in

their biogeochemical function. This is especially true of intermittent streams, which comprise more than half the length of global river networks, are becoming more prevalent due to anthropogenic activities, are often ignored in environmental policy, and exert an outsize influence on water availability and quality (Acuña et al., 2014; Datry et al., 2014). Intermittent streams exhibit unique hydro-biogeochemical behaviors that require more nuanced characterization and representation of spatial and temporal variability in connectivity, especially in terms of biogeochemical cycling (Allen et al., 2020; Larned et al., 2010). To address broadly relevant issues, advances in stream corridor science will increasingly need to incorporate the biogeochemical consequences associated with intermittent hydrologic connectivity.

In this dissertation, I seek to characterize processes that are difficult to measure or are often overlooked in typical studies of temperate and perennial stream corridors. To do so, I combined data science techniques and geophysical data to enhance objective characterization of heterogenous hyporheic connectivity. I also leveraged the relative simplicity of ephemeral streams of the McMurdo Dry Valleys (MDVs), Antarctica, to isolate stream corridor processes that influence the fate of N. These studies provide insight into the surprising ways in which N is mobilized, transformed, and retained in intermittent stream systems with few N inputs. Chapters II – V of this dissertation include conceptual and methodological advice, analytical assistance, and guidance on writing by many coauthors, including committee members, who I have recognized in the Acknowledgements section. These chapters are formatted for submission to scientific journals, with the style of the text, graphics, and citations reflecting the target journal for each chapter. In the final chapter (VI), I summarize findings from Chapters II – V and provide recommendations for future lines of research, both in the MDVs and other stream systems.

Chapter II: Estimation of hyporheic extent and functional zonation during seasonal streamflow recession by unsupervised clustering of time-lapse electrical resistivity models. Analysis of time-lapse ER data from tracer studies has shown great potential to address problems associated with characterizing the spatiotemporal complexity of hyporheic exchange processes

from limited point-scale sampling (i.e., wells and piezometers; Ward et al., 2010). However, its utility in objectively delimiting the extent and quantifying changes in connectivity has been impeded by reliance on qualitative analysis or the use of *a priori* assumptions about data quality and signal strength. In particular, it has been difficult to objectively and quantitatively interpret small scale (<25 cm) heterogeneity modeled in ER inversions relative to larger-scale functional differences within the hyporheic zone. Here, I develop and apply a machine learning method coupled with a statistical test to identify the spatial structure and transport behavior of distinct functional zones during seasonal flow recession in a headwater stream.

Chapter III: The Role of Hyporheic Connectivity in Determining Nitrogen Availability: Insights from an Intermittent Antarctic Stream. In some systems, N fixation along stream corridors has been shown to be a relatively large compared to allochthonous inputs, but relatively little is known about how spiraling of this autochthonous N occurs and its impact on N availability. I conducted intensive field sampling campaigns involving concurrent sampling of surface and hyporheic water from an MDV stream along with a laboratory assay on the nitrification potential of hyporheic microbial communities. I used data from these efforts to assess the role of the hyporheic zone in cycling autochthonous N across flow conditions. This chapter has been published (Singley et al., 2021) in the *Journal of Geophysical Research: Biogeosciences*.

Chapter IV: Differentiating Physical and Biological Storage of Nitrogen Along an Intermittent Antarctic Stream Corridor. Given the global increases in reactive N availability due to anthropogenic activities, most studies on N cycling in streams have focused on N export flux reductions, especially through biological uptake processes. Very few studies have determined how this N removal relates to N storage in the stream corridor, especially for intermittent systems where allochthonous N inputs are low and transport of N may only occur during brief periods. In this chapter, I combined historic datasets and remote sensing analysis to estimate how much N is stored in an MDV stream corridor in periphyton biomass and the hyporheic zone. I conducted a simple laboratory assay to assess whether fluid conductivity fluctuations

characteristic of MDV streams can release ammonium stored by sorption to sediment – which is generally understudied in small, intermittent streams. Lastly, I utilize a simple reactive transport model to assess the longitudinal distances over which allochthonous N inputs are attenuated by uptake to evaluate the prior inference that fluxes from internal N pools are needed to explain downstream concentration observations.

Chapter V: Stream Corridor Processes Sustain Chemostasis of Weathering Solutes and Primary Nutrients in Antarctic Streams. Long-term C-Q relationships provide information about integrated hydro-biogeochemical processes occurring throughout catchments. Due to the challenges of parsing the influence of catchment and stream corridor biogeochemical processes on C-Q relationships, the latter are often ignored or assumed to be negligible. In this chapter, I analyze 25 years of data for 10 MDV streams to assess how stream corridor processes alone control C-Q relationship form and variability among a suite of solutes spanning geogenic solutes to primary nutrients.

References

Acuña, V., Casellas, M., Corcoll, N., Timoner, X., & Sabater, S. (2015). Increasing extent of periods of no flow in intermittent waterways promotes heterotrophy. *Freshwater Biology*, *60*(9), 1810–1823. https://doi.org/10.1111/fwb.12612

Alexander, R. B., Boyer, E. W., Smith, R. A., Schwarz, G. E., and Moore, R. B. (2007). The role of headwater streams in downstream water quality1. *JAWRA Journal of the American Water Resources Association*, *43*(1), 41–59.

Alexander, R. B., Bohlke, J. K., Boyer, E. W., David, M. B., Harvey, J. W., Mulholland, P. J., et al. (2009). Dynamic modeling of nitrogen losses in river networks unravels the coupled effects of hydrological and biogeochemical processes. *Biogeochemistry*, *93*(1–2), 91–116. https://doi.org/10.1007/s10533-008-9274-8

Allen, D. C., Datry, T., Boersma, K. S., Bogan, M. T., Boulton, A. J., Bruno, D., et al. (2020). River ecosystem conceptual models and non-perennial rivers: A critical review. *Wiley Interdisciplinary Reviews: Water*. John Wiley and Sons Inc. https://doi.org/10.1002/wat2.1473

Bernhardt, E. S., Blaszczak, J. R., Ficken, C. D., Fork, M. L., Kaiser, K. E., & Seybold, E. C. (2017). Control Points in Ecosystems: Moving Beyond the Hot Spot Hot Moment Concept. *Ecosystems*, *20*(4), 665–682. https://doi.org/10.1007/s10021-016-0103-y

Blöschl, G., M. F. P. Bierkens, A. Chambel, C. Cudennec, et al. (2019) Twenty-three unsolved problems in hydrology (UPH) – a community perspective, *Hydrological Sciences Journal*, 64:10, 1141-1158, https://doi.org/10.1080/02626667.2019.1620507

Boano, F., J. W. Harvey, Boano, F., Harvey, J. W., et al. (2014), Hyporheic flow and transport processes: Mechanisms, models, and biogeochemical implications, *Rev. Geophys.*, 52, 603–679, https://doi.org/10.1002/2012RG000417.

Boyer, E. W., C. L. Goodale, N. A. Jaworski, and R. W. Howarth (2002). Anthropogenic nitrogen sources and relationships to riverine nitrogen export in the northeastern USA. *Biogeochemistry* 57:137–169.

Datry, T., Larned, S. T., & Tockner, K. (2014). Intermittent Rivers: A Challenge for Freshwater Ecology. *BioScience*, *64*(3), 229–235. https://doi.org/10.1093/biosci/bit027

Evans, C., & Davies, T. D. (1998). Causes of concentration/discharge hysteresis and its potential as a tool for analysis of episode hydrochemistry. *Water Resources Res. 34*(1), 129–137.

Fellman, J. B., Dogramaci, S., Skrzypek, G., Dodson, W., & Grierson, P. F. (2011). Hydrologic control of dissolved organic matter biogeochemistry in pools of a subtropical dryland river. *Water Resources Research*, *47*(6). https://doi.org/10.1029/2010WR010275

Fenoglio, S., Bo, T., Cammarata, M., López-Rodríguez, M. J., & Tierno De Figueroa, J. M. (2015). Seasonal variation of allochthonous and autochthonous energy inputs in an Alpine stream. *Journal of Limnology*, *74*(2), 272–277. https://doi.org/10.4081/jlimnol.2014.1082

Godsey, S. E., Kirchner, J. W., & Clow, D. W. (2009). Concentration–discharge relationships reflect chemostatic characteristics of US catchments. *Hydrological Processes*, *23*(13), 1844–1864.

Gomez-Velez, J. D., J. W. Harvey, M. Bayani Cardenas, and B. Kiel (2015). Denitrification in the Mississippi River network controlled by flow through river bedforms. *Nature Geoscience*, 8:941.

Harvey, J. W., & Gooseff, M. N. (2015). River corridor science: Hydrologic exchange and ecological consequences from bedforms to basins. *Water Resources Research*. https://doi.org/10.1002/2015WR017617

Knapp, J. L. A., Von Freyberg, J., Studer, B., Kiewiet, L., & Kirchner, J. W. (2020). Concentration-discharge relationships vary among hydrological events, reflecting differences in event characteristics. *Hydrology and Earth System Sciences*, *24*(5), 2561–2576. https://doi.org/10.5194/hess-24-2561-2020

Krause, S., et al. (2017), Ecohydrological interfaces as hot spots of ecosystem processes, *Water Resources Research*, 53, 6359–6376, https://doi.org/10.1002/2016WR019516.

Larned, S. T., Datry, T., Arscott, D. B., & Tockner, K. (2010). Emerging concepts in temporary-river ecology. *Freshwater Biology*, *55*(4), 717–738.

Lewandowski, J., Arnon, S., Banks, E., et al. (2019). Is the hyporheic zone relevant beyond the scientific community? *Water*, *11*(11), 2230. https://doi.org/10.3390/w11112230

Li, L., Sullivan, P. L., Benettin, P., Cirpka, O. A., Bishop, K., Brantley, S. L., et al. (2021). Toward catchment hydro-biogeochemical theories. *Wiley Interdisciplinary Reviews: Water*, *8*(1), e1495. https://doi.org/10.1002/wat2.1495

Magliozzi, C., Grabowski, R. C., Packman, A. I., & Krause, S. (2018). Toward a conceptual framework of hyporheic exchange across spatial scales. *Hydrology and Earth System Sciences*, *22*(12), 6163–6185. https://doi.org/10.5194/hess-22-6163-2018

Marcarelli, A. M., Baker, M. A., & Wurtsbaugh, W. A. (2008). Is in-stream N2 fixation an important N source for benthic communities and stream ecosystems? *Journal of the North American Benthological Society*. https://doi.org/10.1899/07-027.1

Moatar, F., Abbott, B. W., Minaudo, C., Curie, F., & Pinay, G. (2017). Elemental properties, hydrology, and biology interact to shape concentration-discharge curves for carbon, nutrients, sediment, and major ions. *Water Resources Research*, *53*(2), 1270–1287. https://doi.org/https://doi.org/10.1002/2016WR019635

Mulholland, P. J., C. S. Fellows, J. L. Tank, N. B. Grimm, et al. (2001), Inter-biome comparison of factors controlling stream metabolism. *Freshwater Biology*, 46: 1503-1517. https://doi.org/10.1046/j.1365-2427.2001.00773.x

Mulholland, P. J. (2004). The importance of in-stream uptake for regulating stream concentrations and outputs of N and P from a forested watershed: Evidence from long-term chemistry records for Walker Branch Watershed. *Biogeochemistry*, *70*(3), 403–426. https://doi.org/10.1007/s10533-004-0364-y

Mulholland, P. J., Helton, A. M., Poole, G. C., Hall, R. O., Hamilton, S. K., Peterson, B. J., et al. (2008). Stream denitrification across biomes and its response to anthropogenic nitrate loading. *Nature*, *452*(7184), 202–205. https://doi.org/10.1038/nature06686

Singley, J. G., Gooseff, M. N., McKnight, D. M., & Hinckley, E.-L. S. (2021). The Role of Hyporheic Connectivity in Determining Nitrogen Availability: Insights from an Intermittent Antarctic Stream. *Journal of Geophysical Research: Biogeosciences*, *126*, e2021JG006309. https://doi.org/10.1029/2021JG006309

Tank, J. L., Rosi-Marshall, E. J., Griffiths, N. A., Entrekin, S. A., & Stephen, M. L. (2010). A review of allochthonous organic matter dynamics and metabolism in streams. *Journal of the North American Benthological Society*, *29*(1), 118–146. https://doi.org/10.1899/08-170.1

Ward, A. S., Gooseff, M. N., & Singha, K. (2010). Imaging hyporheic zone solute transport using electrical resistivity. *Hydrological Processes*, *24*(7). https://doi.org/10.1002/hyp.7672

Ward, A. S. (2016). The evolution and state of interdisciplinary hyporheic research. *Wiley Interdisciplinary Reviews: Water*, *3*(1), 83–103. https://doi.org/10.1002/wat2.1120

Chapter II

Estimation of hyporheic extent and functional zonation during seasonal streamflow recession by unsupervised clustering of time-lapse electrical resistivity models

2.1. Introduction

The exchange and mixing of surface and groundwater in stream corridors exerts a strong control on hydrologic transport, biogeochemical reactions, and the existence of ecological refugia (Harvey & Bencala, 1993; Ward, 2016; Harvey et al., 2018; Lewandowski et al., 2019). Despite decades of research, estimating the extent and spatiotemporal variability of the hyporheic zone remains challenging due to the structural heterogeneity of the subsurface and the difficulty of making direct observations beyond a few discrete points (i.e., wells and piezometers). Numerous studies have sought to determine how the extent of hyporheic exchange responds to variable hydrologic conditions, often with an interest in the implications for which biogeochemical reactions can occur and their reach-scale significance, but results are often in conflict between sites and few generalizable behaviors have been identified (Ward, 2016). The capability for predictive modeling is similarly limited either by overly simplistic representation of the hyporheic zone as a single well-mixed storage zone (Marion et al., 2003; Wondzell, 2006) or the rarity of sufficient data needed to inform accurate representation of transport heterogeneity at scales beyond individual channel features (Schmadel et al., 2017; Ward et al., 2017). Consequently, advances in observing and modeling both the dynamic behavior of hyporheic exchange will depend on developing data-driven techniques that can constrain the spatiotemporal complexity of hyporheic exchange at functionally meaningful and tractable scales.

Numerous definitions of the hyporheic zone have been proposed, with specific criteria reflecting the primary discipline of a given study (White, 1993; Tonina & Buffington, 2007; Gooseff, 2010; Ward, 2016). A primary challenge in defining the hyporheic zone originates from the heterogeneity of nested flow paths that govern both reach-scale hydrologic transport and the significance of biogeochemical reactions. In an effort to incorporate prior studies and promote

interdisciplinary synthesis, Ward (2016) suggested that the region encompassing the HZ must (1) be in the saturated subsurface, (2) include flow paths that originate from and return to surface water, and (3) interact with the stream water within a specified temporal scale related to hydrologic or biogeochemical processes of interest. While this definition is flexible, it remains practically difficult to simultaneously delineate both the spatial and temporal boundaries implied by this definition in an actual field study.

Interactions between surface water and the hyporheic zone are most often assessed through conservative-solute tracer injections (Harvey & Bencala, 1993; Harvey et al., 1996; Kasahara & Wondzell, 2003; Ward et al., 2019). The resulting solute breakthrough curves (BTCs) reflect the effects of advection, dispersion, and transient-storage processes (both surface and subsurface) that are integrated over space and time (Stream Solute Workshop, 1990). Point-scale subsurface sampling combined with surface-water data is often used for model tuning to estimate lumped transport and storage parameters, but the results are often not clearly meaningful (Marion et al., 2003; Wondzell, 2006). Additionally, main-channel BTC observations reflect the convolution of surface and subsurface transient-storage processes, yet these compartments are known to exhibit distinct biogeochemical functions, especially aerobic versus anaerobic processes, making the need to parse their effects important in many studies (Knapp et al., 2018). Despite the computational feasibility of numerically modeling spatially explicit heterogeneity of coupled transport and biogeochemical reactions (e.g., Marzadri et al., 2011), it is rarely possible to overcome issues of equifinality in parameterizing multiple storage-zone models from surface and well BTC observations alone (e.g., Bottacin-Busolin, 2019), especially for reactive solutes (e.g., Kelleher et al., 2019).

The use of time-lapse electrical resistivity (ER) imaging of hyporheic exchange during tracer injections was introduced over a decade ago (Ward et al., 2010b) as a promising method for characterizing time-varying hyporheic extent. Fundamentally, ER methods utilize surface measurements of electrical potentials from induced current flow to inversely model subsurface properties that are sensitive to the introduction and transport of electrically conductive solute

tracers (Singha et al., 2008). Since its adaptation to stream tracer studies, ER imaging has been employed to investigate how hyporheic exchange, especially its extent, responds to in-channel woody debris (Doughty et al., 2020), seasonal flow recession (Ward et al., 2012, 2014), flow regulation by dam operation (Cardenas & Markowski, 2011), and structural variations in bedrock boundaries (Rucker et al., 2021).

Successful application of ER for delimiting and quantifying changes in hyporheic exchange has been impeded by reliance on qualitative analysis or *a priori* assumptions about the consequences of data quality and inversion decisions on the final model images to attempt more quantitative analysis. Prior studies have relied on evaluation of time-lapse 2D ER model images to compare hyporheic extent between times of data collection (e.g., Ward et al. 2010b), largely ignoring sensitivity issues (e.g., Day-Lewis et al., 2005). This approach is flexible but, like nearly all geophysical analyses, does not allow for robust quantitative comparison or prediction between stream reaches or injections. Alternatively, some studies (e.g., Doughty et al., 2020) have analyzed spatially lumped changes in bulk apparent resistivity data, which provide a basis for quantitatively describing temporal variations in exchange but sets aside spatially resolved information inherent in the time-lapse ER models. Finally, a few studies (e.g., Ward et al., 2010b, 2012) have applied *a priori* signal thresholds to delimit and estimate hyporheic extent from model images. Unfortunately, the resulting estimates of hyporheic extent are particularly sensitive to the subjectively selected change in resistivity ($\Delta\rho$) threshold (Ward et al., 2010b), so only relative changes, not the actual extents, are meaningful. Application of a standard threshold (i.e., $\Delta\rho > 2.5\%$) across multiple datasets does not account for actual differences in either the quality of the data or the relative strength of tracer injection signals compared to noise.

In this study, we introduce a novel method for analyzing inverted ER images based on unsupervised time-series clustering that addresses the challenge of resolving both the extent and spatial heterogeneity of hyporheic exchange. Unsupervised clustering is a data-mining technique in which time series are objectively grouped based on structures within the data rather than *a priori* assumptions (e.g., Aghabozorgi et al., 2015). We apply unsupervised clustering to time-

lapse ER models from a benchmark dataset (Ward et al., 2012, 2020) to assess how the extent and heterogeneity of hyporheic connectivity changes during baseflow recession in a headwater stream. We demonstrate that unsupervised clustering of inverted ER model time series from tracer injections can be used to (1) delimit hyporheic extent by distinguishing solute transport signals from noisy background inversions (adjacent hillslopes or at depth), and (2) characterize transport heterogeneity within the hyporheic zone in terms of spatially defined functional zones. Clustering of inverted ER models, therefore, represents a shift towards a data-driven functional zonation representation of hyporheic connectivity, which is akin to other facies frameworks in which complex heterogeneity is simplified by characterizing compartments for which in-group heterogeneity is smaller than between-group differences (e.g., Sassen et al., 2012; Wainwright et al., 2014; Hou et al., 2019; Hermes et al., 2020).

2.2. Methods

The principles of ER data collection and its application in stream tracer studies have been described extensively by prior studies (Singha et al., 2008; Ward et al., 2010a-b, 2012, 2014; McLachlan et al., 2017). Briefly, ER measurements are sensitive to lithology, porosity, connectivity of pore spaces, pore fluid conductivity, temperature and moisture content. The introduction of an electrically conductive tracer alters only pore-fluid conductivity, thereby allowing detection of solute transport through the subsurface (Singha et al., 2008). Data are collected by applying an electric current (I, A) to the ground surface and measuring the resulting potential difference (V) between two locations to calculate the geometry-dependent resistance (R, Ω) by Ohm's Law ($R = V/I$). Then, depending on the arrangement of electrodes, a geometric factor (K) can be calculated for each measurement (see Binley et al., 2015) which is used to convert R to apparent resistivity (ρ, Ωm) as $\rho = KR$. Apparent resistivity can, in turn, be converted to apparent electrical conductivity (σ, S/m) as $\sigma = 1/\rho$. We present results for this study in terms of σ, which is more intuitively related to fluid conductivity (σ_{fl}) typically measured in surface water or wells during tracer studies.

2.2.1 Injections and ER Collection from a Benchmark Dataset

We use ER survey data and main channel σ_{fl} from tracer studies conducted in a forested second-order stream within the H. J. Andrews Experimental Forest, Oregon (48º10'N, 122º15'W) during the summer of 2010 (Ward et al., 2020). This dataset has been previously used to examine hyporheic connectivity throughout baseflow recession (Ward et al., 2012, 2014) and, therefore, serves as a useful benchmark for comparison of new methods. We focus our analysis on four 48-hr tracer tests that were conducted in a 50-m reach of a headwater stream in Watershed 3 (101 ha) for discharges decreasing from 35 to 4 L s^{-1}. All injection solutions contained only sodium chloride (NaCl) as a conservative tracer. A two-week recovery period was observed between injections. Electrical resistivity data were collected using dipole-dipole configurations with an IRIS Syscal Pro (Orleans, France) on lateral transects, each consisting of 12 surface electrodes with approximately 1 m spacing (Figure 2.1). While data were collected from six transects, we consider ER data from Transects 2 and 3 as only they have complete data from all four injections; they also cross different channel morphologies.
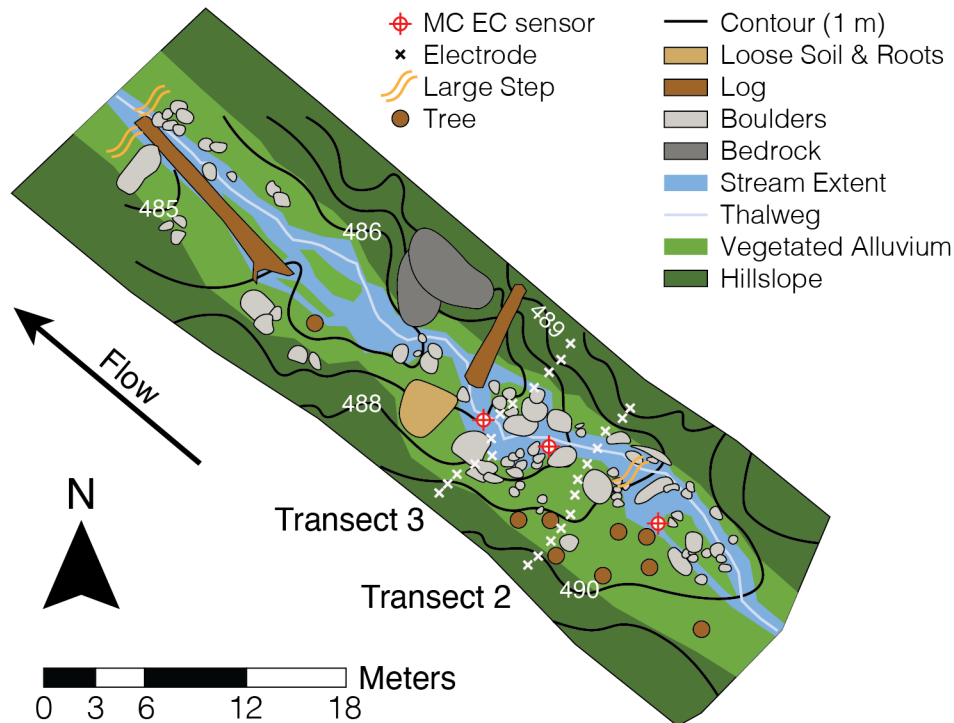
Figure 2.1. Site location and instrumentation map for WS3 in the H. J. Andrews Experimental Forest, located in the Cascade Range of central Oregon. Main channel electrical conductivity sensors are identified as A–C from upstream to downstream locations in the text. Modified from Ward et al. (2012).

2.2.2 ER Inversions

We inverted resistance data from surface measurements with R2 (v2.7b compiled for Unix), which uses a regularized objective function and weighted least-squares regression approach to model and solve current flow in a quadrilateral finite-element mesh for each transect and injection (Binley & Kemna, 2005; Binley, 2015). The number of nodes in the inversion meshes for this study ranged from 2,394–2,698 due to differences in transect widths. The inversion mesh was generated with 25-cm spacing horizontally and 20-cm spacing vertically down to a relative depth of 6 m, with spacing doubling to each node thereafter. In all cases, we extended the inversion mesh at least 100 m horizontally beyond the outermost electrode locations and to a depth of about 150 m to reduce boundary effects. Surface topography for the inversion mesh was linearly interpolated between surveyed electrode locations. For comparability between injections, we limited analysis to data collected between, at most, 8 hours prior to and 96 hours after the beginning of each injection.

For the time-lapse inversions we utilized a difference method wherein the first timestep data and ER model are used as a starting model and target dataset to which subsequent inversions are regularized (Binley, 2015). Changes in resistivity ($\Delta\rho$) and its inverse, changes in conductivity ($\Delta\sigma$), from the starting model are provided for each time period of collection (timestep, hereafter) during the inversion process. For each injection and transect we calculated the resolution matrix as described by Binley & Kemna (2005) to quantify nodal sensitivity within the inversion mesh. We then used the diagonal of the resolution matrix to select nodes for subsequent analyses with a resolution of at least 1%, meaning that at least 1% of the node's modeled resistivity was independent of adjacent nodes (Binley & Kemna, 2005; Ward et al.,

2012). Areas with resolution values < 1% were parts of the inverted model for which temporal changes in conductivity could not be meaningfully interpreted.

2.2.3 Unsupervised Clustering of Time-lapse ER Models

As an alternative to qualitative assessments, spatially lumped analysis, or *a priori* selection of signal thresholds, we used unsupervised hierarchical clustering of nodal $\Delta\sigma$ time series to identify clusters of nodes for which within-zone differences in tracer response are smaller than between-group differences. In so doing, we (1) estimated the spatial arrangement of functional zones, (2) identified characteristic $\Delta\sigma$ BTCs for each cluster, and (3) estimated total hyporheic extent. Applying this method to time-lapse ER models identifies emergent patterns within the model outputs and retains both spatial and temporal information but does not require selection of arbitrary cutoffs in $\Delta\sigma$ to determine where meaningful changes have occurred.

2.2.3.1 Clustering of Nodal ER Time Series

From the time-lapse ER models, we calculated a metric describing the dissimilarity between pairs of nodal $\Delta\sigma$ time series (Figure 2.2a-c). To do so, we calculated the absolute value of Euclidean distances at each timestep for all pairwise combinations of the $\Delta\sigma$ time series using the *TSclust* package in *R* (Montero & Vilar, 2014; R Core Team, 2019). The absolute Euclidean distance (d) between the time series for any two nodes (j and k) with $\Delta\sigma_{j,t}$ and $\Delta\sigma_{k,t}$ as their respective percent change in electrical conductivity at timestep *t* is:

$$d_{j,k}^{t} = \left|\Delta\sigma_{j,t} - \Delta\sigma_{k,t}\right| \qquad (2.1)$$

We summed these distances for *t* between 8 hours prior to (t_i) and 96 hours after (t_f) the injection began to give the individual elements of the dissimilarity matrix (***D***):

$$\boldsymbol{D}_{j,k} = \sum_{t_i}^{t_f} d_{j,k}^{t} \qquad (2.2)$$

We opted to use Euclidean distances to construct a dissimilarity matrix as they represent the simplest distance metric that retains the physical meaning of the time-series values (no unit conversion) and are sensitive to both scaling and synchronicity in structure among time series, unlike other metrics used for time-series comparisons (e.g., Aghabozorgi et al., 2015).

Consequently, the resulting distance measure $D_{j,k}$ is indicative of how similar two time series are in both shape and timing of the response to tracer transport. Additional discussion of alternative distance-metric selection as well as time-series normalization is provided in the supplemental information.
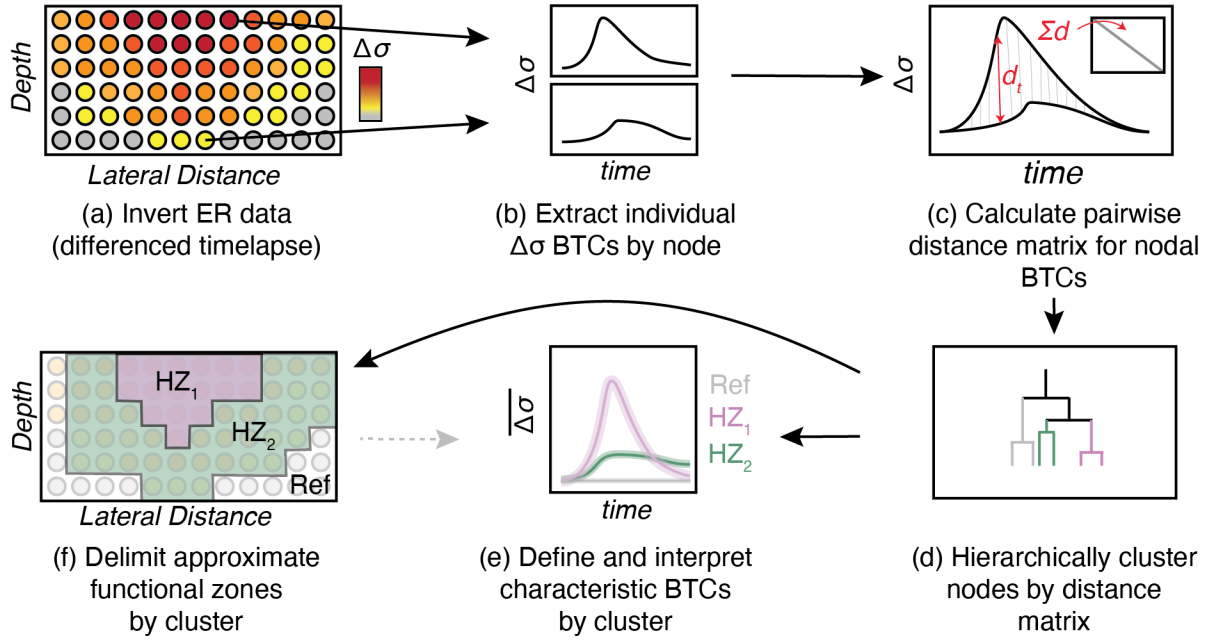
Figure 2.2. Conceptual depiction of unsupervised clustering analysis of time-lapse ER models from tracer injections. At each timestep (a) percent change in modeled conductivity ($\Delta\sigma$) relative to the pre-injection condition is output, then (b) time series of $\Delta\sigma$ are extracted for each node in the inversion mesh, (c) Euclidean distances are calculated and summed for each pairwise comparison of nodes to construct a dissimilarity matrix, which is then used to (d) hierarchically cluster nodes. The resulting clusters can then be analyzed for (e) characteristic BTCs and (f) approximate spatial extent.

To identify similarities in hyporheic exchange processes within the subsurface, we then applied the built-in agglomerative hierarchical clustering algorithm in *R* (*hclust*; R Core Team, 2019) to *D* (Figure 2.2d). Individual nodes are first assigned to their own clusters, then at each subsequent iteration the most similar clusters are merged until a single cluster is formed. Here we use the default complete-linkage method to identify the nearest clusters to be merged at each step. The resulting dendrogram consists of *n-1* branching events, where *n* is the number of nodes retained from the ER inversion mesh with resolution > 1%.

2.2.3.2 Identifying the Number of Clusters and Characteristic BTCs

There is no absolute best approach to selecting the "correct" number of clusters or how to cut a dendrogram (Liao, 2005) and many different cluster-validity indices have been proposed (Aghabozorgi et al., 2015). We pass the dendrogram data through a non-parametric permutation-based test of within- versus between-branch variances (Park et al., 2009) to determine whether each branching event results in the formation of clusters with statistically different responses to the tracer addition. Significant branching events are identified if they satisfy a Bonferroni corrected p-value threshold ($p < 0.05/[n\text{-}1]$, where n is the number of nodes). In selecting this approach, we base cluster retention on patterns and structures that exist within the data in a way that allows for asymmetric combination of non-significant branching events (Park et al., 2009). With this method any number of clusters that is statistically supported can be retained depending on the end goal or application of the resulting information. We present results for four statistically unique clusters for each transect and injection. Objectively parsing the hyporheic zone into a few functional zones signifies an advance beyond treating it as a single well-mixed compartment while not exceeding the complexity represented in widely available, computationally inexpensive multiple transient storage zone models.

After identifying four statistically unique clusters and the membership of individual nodes, we determined the characteristic $\Delta\sigma$ BTC for each cluster by calculating the mean and standard error (SE) of individual nodal $\Delta\sigma$ values within a cluster by timestep (Figure 2.2e). We calculated the SE on the mean instead of the standard deviation as the number of nodes within each cluster can vary largely, with some clusters potentially including fewer than 10 nodes while others may include hundreds.

2.2.3.3 Identifying and Delimiting Extent of Hyporheic Exchange

Next, we identified which of the retained clusters represent the effective hyporheic zone – that is, which groups of nodes have time series that are reflective of tracer transport at the timescale of interest for a particular injection as informed by the BTC observed in the stream.

We used the dendrogram and cluster-wise characteristic BTCs to subjectively distinguish clusters comprising the effective hyporheic zone and those that behave as non-responsive "reference" nodes. Specifically, reference nodes lack BTC structure related to the tracer injection and exhibit a signal akin to white noise. However, reference nodes may exhibit some temporal patterns deviating from white noise due to variations in temperature and soil moisture, or the spatial smearing of signals through the mesh by the inversion algorithm (Day-Lewis et al., 2005). In contrast, we interpret clusters representing the effective hyporheic zone as exhibiting BTCs with systematic increases in σ (decreases in ρ) from the pre-injection state, which is indicative of conductive solute transport (Singha et al., 2008; Ward et al., 2010b). In the event that such qualitative distinctions between BTC shapes for reference and hyporheic clusters were not obvious, we utilized the branching structure of the dendrogram to inform decision making.

We then qualitatively categorized the clusters comprising the effective hyporheic zone based on the speed and magnitude of their $\Delta\sigma$ BTC as "fast", "moderate", or "slow". These descriptors reflect the relative $\Delta\sigma$ BTC behaviors that indicate differences in advective solute transport between the clusters (Ward et al., 2010a).

We then calculated the approximate extent of the clusters comprising the effective hyporheic zone based on the location of nodes within the inversion mesh. Due to the ill-determined nature of the inverse problem and resolution limitations, neither the ER models nor our calculated hyporheic extents represent a precise quantification of the system. Rather, they are simply estimates based on a smoothed approximation of subsurface properties, from which we more objectively, but imprecisely, map patterns via hierarchical clustering.

2.2.3.4 Quantifying Heterogeneity of Hyporheic Exchange Over Time

While clusters represent coarse spatial characterization of hyporheic complexity into just a few functional zones based on modeled responses over the entire injection, we also seek to estimate the heterogeneity of tracer transport into and from the subsurface at different times during the injection. Therefore, we quantified the magnitude and trajectory of heterogeneity in

modeled tracer signal (as $\Delta\sigma$) at particular times throughout a tracer study and how that changes under different flow conditions. Specifically, we characterized the temporal patterning of modeled $\Delta\sigma$ by calculating the mean and standard deviation of d (Eqn 2.1) across all nodal pairings within the interpreted effective hyporheic zone for individual timesteps. This metric is a rough proxy for heterogeneity of tracer exchange into and from the subsurface. We included only nodes interpreted as belonging to effective hyporheic clusters, such that differences between those and reference clusters did not influence the results.

2.2.4 Threshold-based Estimates of Hyporheic Extent

Prior studies (e.g., Ward et al., 2010b, 2012) have estimated hyporheic extent based on *a priori* selection of $\Delta\rho$ (or $\Delta\sigma$) thresholds. Because the resulting estimates of hyporheic extent are particularly sensitive to the selected threshold (Ward et al., 2010b), only relative changes, not the actual extents, are likely meaningful—ignoring issues with out-of-plane effects (e.g., Bentley and Gharibi, 2004). Therefore, we identified the nodes for each injection and transect for which $\Delta\sigma \geq 2$, 3, 4, 5, and 10% for at least one timestep during the injection to compare to Ward et al. (2012). We then estimated the hyporheic extent by calculating the total area within the inversion mesh represented by the nodes retained by each of these 5 thresholds. We compared the directionality and magnitude of changes in threshold-based and clustering-based extent estimates in response to seasonally declining streamflow.

2.3 Results and Discussion

2.3.1 Spatial Arrangement and Transport Characteristics of Hyporheic Clusters

The total number of nodes with resolution $\geq 1\%$ varied for each set of inverted ER data, with fewer nodes retained (n) for Transect 2 than 3. Over the four injections, n ranged from 300–324 for Transect 2 and 318–408 for Transect 3. In all instances, a permutational test (Park et al., 2009) of inter- versus intra-cluster variances identified > 50 significant branching events such that there are more statistically unique clusters than can be individually interpreted. Therefore, we analyzed the four clusters resulting from the four highest branching events for each transect

and injection (Figure 2.3) – these four clusters were all statistically significantly different ($p \ll 0.001$) from each other. While this approach joins clusters formed by subsequent branching events that exhibit significantly different $\Delta\sigma$ responses to the tracer, all of the within-cluster differences are significantly smaller than those between clusters and no clusters from non-significant branching events are retained. Given the ill-determined nature of inverse modeling from surface ER data and resolution limitations, we chose to avoid retaining large numbers of clusters, wherein the size of some clusters would potentially become too small to generate valid statistical comparisons or meaningful hydrological interpretations.
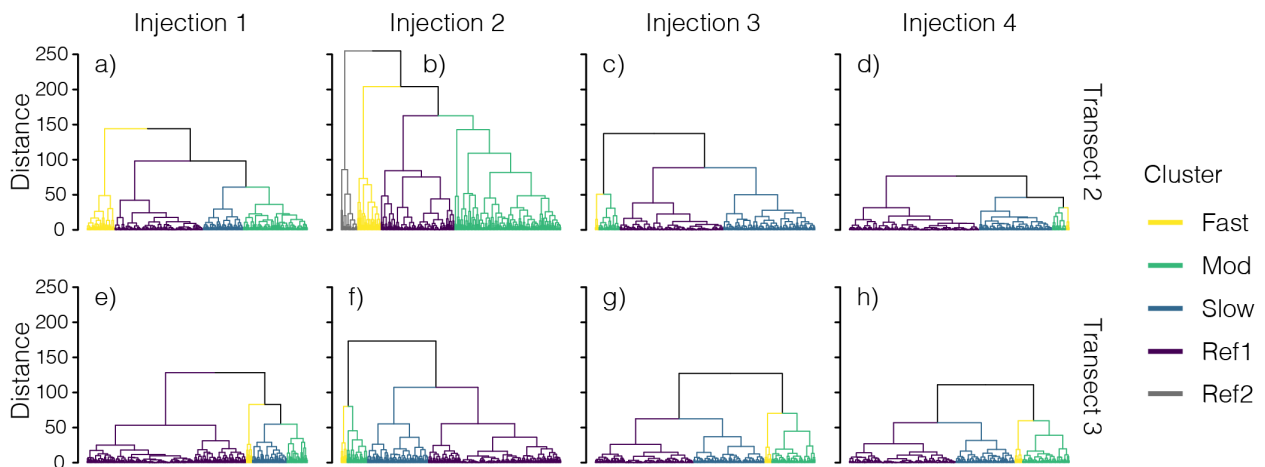
Figure 2.3. Individual injection dendrograms based of hierarchical clustering of nodal $\Delta\sigma$ time series for Transect 2 (a-d) and Transect 3 (e-h). Clusters are labeled by qualitative descriptors of characteristic BTCs (Figure 2.5).

In general, the hillslopes to either side of the stream clustered together with additional clusters forming in a radial pattern within the valley bottom (Figure 2.4). Based on relative differences in the characteristic $\Delta\sigma$ BTCs (Figure 2.5), we found that the clusters with the most advective signatures ("fast") occurred nearest to surface. These regions were ringed by the cluster exhibit moderately ("mod") advective behavior while the least advective ("slow") clusters were located at even greater depths and lateral distances within the subsurface. This spatial organization matches both conceptual expectations of hyporheic exchange and prior visualizations of ER data from tracer studies in streams (e.g. Ward et al., 2010a, 2010b, 2012;

Doughty et al., 2020). It is notable, however, that this pattern is neither explicitly defined by nor provided as an input in the cluster-identification algorithm.

While the nodal membership and spatial arrangement of clusters shifted over the four injections, we observed some persistent patterns in the organization of functional zones. For Transect 2, the primary pattern is the assignment of two spatially separated regions on either side of the valley bottom to the same cluster (i.e., "Fast" cluster for injections 1 and 2, shifting to "Slow" for injections 3 and 4). In contrast, a singular radial clustering pattern was exhibited in Transect 3 throughout all four injections. This difference highlights the ability of hierarchical clustering to parse the effective hyporheic area into functional zones with spatial arrangements that reflect connectivity to surface water at a particular transect, but that are not necessarily contiguous. Additionally, the location and extent of certain functional zones (i.e., "fast" for Transect 3) change very little even as flow changes suggesting that this functional zonation approach based on clustering is sensitive to spatial differences in hyporheic exchange that reflect stable physical properties.
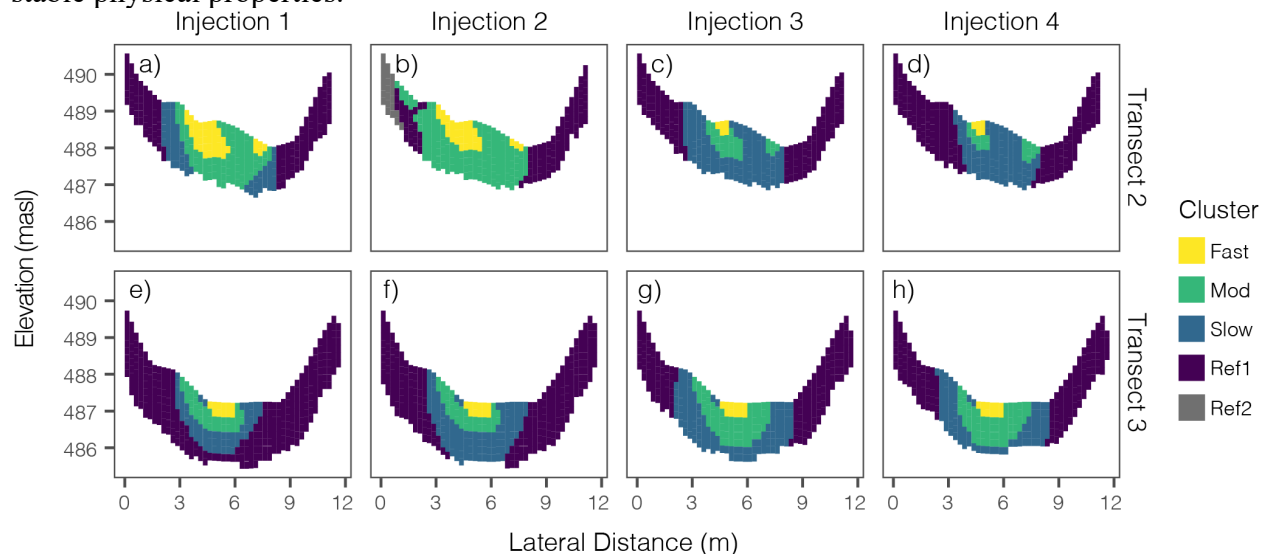
Figure 2.4. Inversion mesh cross-sections with individual node regions colored by cluster membership for Transect 2 (a-d) and Transect 3 (e-h) across each of the four injections. Vertical relief is exaggerated two fold. Clusters are labeled by qualitative descriptors of characteristic BTCs (Figure 2.5).
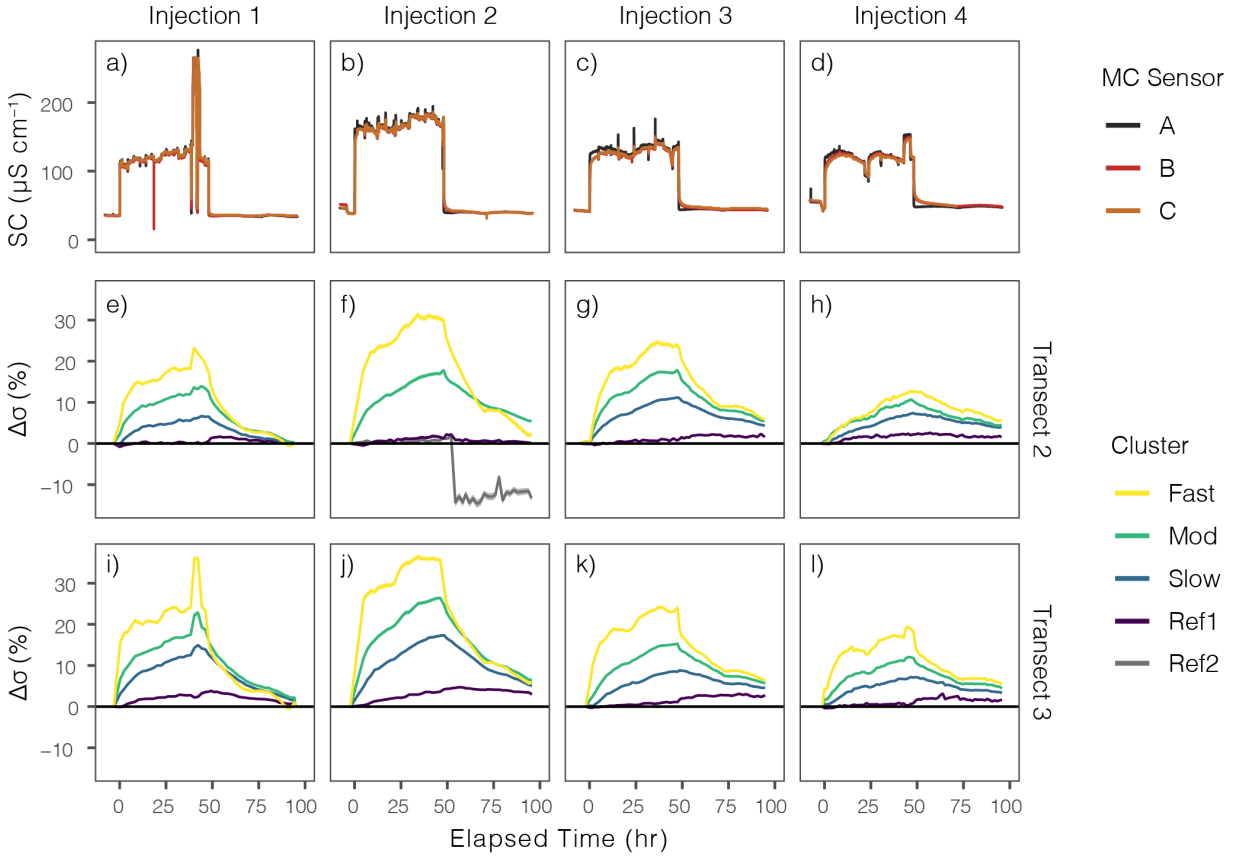
Figure 2.5. Observed specific conductivity BTCs for main channel sensors (a-d) and cluster-wise $\Delta\sigma$ BTCs for Transect 2 (e-h) and Transect 3 (i-l). The $\Delta\sigma$ traces (e-l) are presented as ribbon plots (mean $\pm$ SE) representing $\Delta\sigma$ values for nodes within each cluster at teach timestep. Errors are relatively small compared to line width in most cases. Clusters are labeled by qualitative descriptors of characteristic BTCs (Figure 2.4).

As noted by prior studies (e.g., Ward et al., 2012), main-channel fluid-conductivity BTCs from each injection reached a plateau quickly (< 1 hour) and returned to background levels over slightly longer, but still fairly rapid time spans (< 2 hours), after the injection ended (Figure 2.5a-d). In contrast, characteristic $\Delta\sigma$ BTCs for each cluster show a much more gradual shift from background conditions and most do not reach a fully plateaued state (Figure 5e-l), especially for injection 4 at the lowest flows. While many clusters show an initially rapid response to the end of the injection, the rate at which characteristic $\Delta\sigma$ BTCs return to their pre-injection state generally slows after a few hours, and most do not return to the initial state even 48 hours later. These behaviors reflect the sensitivity of ER to low concentrations of solute that are retained in and slowly released from relatively immobile pore spaces and diluted below detection in stream

water (Singha et al., 2008; Ward et al., 2010a). Notably, the "fast" clusters appear to load and unload with tracer the most rapidly and exhibit the greatest change in σ, reflecting more advective transport and greater dominance by mobile domains. In contrast, the "slow" clusters show the smallest and most gradual σ responses, indicative of less advective transport and more immobile pore spaces. Clustering of inverted ER data, therefore, categorizes portions of the subsurface in terms of BTC behavior that emerges from distinctive combinations of transport phenomena (i.e., advection vs dispersion) and relative density of mobile versus immobile domains within the subsurface.

By providing a means to quantify how these behaviors differ at each timestep for spatially defined sets of nodes, clustering improves upon approaches that either lump all surface ER data together (i.e., bulk apparent-resistivity time series; Doughty et al., 2020) or characterize spatial trends within modeled cross-sections for only a small subset of times (i.e., $\Delta\rho$ cross-sectional images at a few selected timesteps; Ward et al., 2012). Thus, this application illustrates how functional zones defined by their transport characteristics can be identified and approximately mapped in space by hierarchical clustering of inverted ER data.

We interpreted reference clusters ("ref1") across injections and transects when they did not exhibit an obvious BTC response to the tracer addition (Figure 2.5) and were mostly located within adjacent hillslopes above the streambed where exchange is unlikely (Figure 2.4). Generally, this reference cluster was the largest across all injections and exhibited $\Delta\sigma$ traces that were flat and near zero ($< \pm 5\%$) as would be expected. Notably, however, for Transect 2 injection 2, cluster "ref2" showed a flat $\Delta\sigma$ response during the injection but had a large negative $\Delta\sigma$ step change in the post-injection period. Such a negative $\Delta\sigma$ response is likely an artifact of the second-derivative smoothing incorporated into the inversion process. Altogether, these examples demonstrate that hierarchical clustering is useful for identifying spatial organization of distinct tracer transport signals in the subsurface, distinguishing unresponsive nodes from those in the effective hyporheic zone and detecting inversion-process artifacts.

While main-channel fluid conductivity BTCs vary between injections (Figure 2.5a-d), some notable patterns reflective of seasonally evolving subsurface solute transport emerge across the injections. Specifically, cluster-wise $\Delta\sigma$ BTC shapes (particularly the "fast" clusters) shift temporally toward slower loading and weaker plateauing. That change in the "fast" cluster behavior is most apparent for Transect 2 and to lesser extent for Transect 3. This difference between transects is suggestive of subsurface advective transport declining more substantially for Transect 2 as surface flow (35 L/s at injection 1 to 4 L/s during injection 4). Temporal moment analysis on nodal BTCs for this dataset by Ward et al. (2014) similarly reported larger changes in first-arrival time, mean-arrival time, and skewness for Transect 2 than Transect 3. That analysis required lumping data for all nodes identified as part of the effective hyporheic zone, while our analysis parses this into spatially defined functional zones.

2.3.2 Comparison of Methods for Estimating Effective Hyporheic Extent

We compared the total effective hyporheic extent among injections with different streamflow rates estimated by hierarchical clustering with $\Delta\sigma$ thresholds (Figure 2.6). We limit analysis of relative differences in extent to a single significant digit due to the imprecise nature of models resulting from inversion of field data. Based on the clustering method, we found that total effective hyporheic extent for Transect 2 decreased by ~40% (10 to 6 m^2) between the highest and lowest flows. In contrast, for Transect 3 cluster-based analysis resulted in a ~30% increase (6 to 8 m^2). For Transect 2, threshold-based estimates of hyporheic extent were relatively stable for flows of 35 and 14 L s^{-1}, with decreasing extents observed as flow fell from 14 to 7 and then 4 L s^{-1}, except for $\Delta\sigma \geq 2\%$. For Transect 3, estimated hyporheic extent increased as flow fell from 35 to 14 L s^{-1} then declined thereafter.
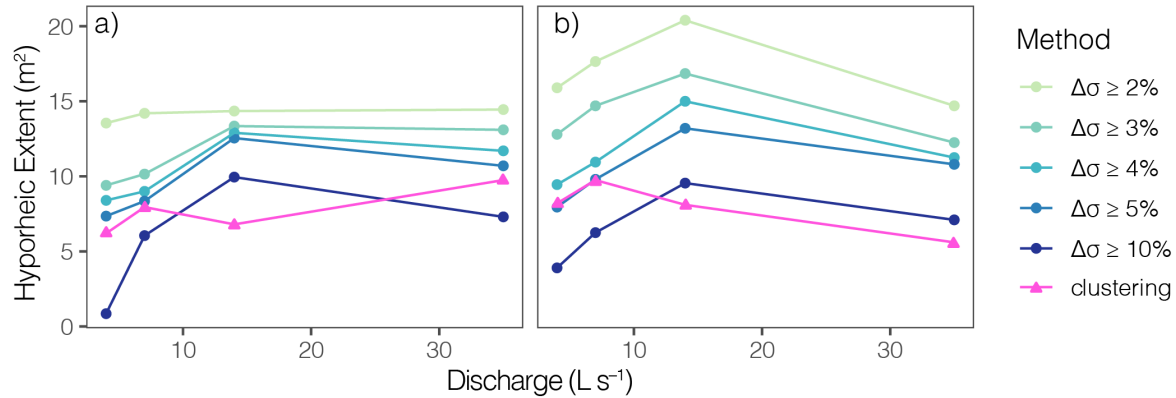
Figure 2.6. Total effective hyporheic extent by method versus surface discharge for (a) Transect 2 and (b) Transect 3.

Interestingly, the cluster-based estimates of total effective hyporheic extent are relatively more stable at the three lowest streamflow conditions and most similar to those generated by different threshold values depending on the injection and transect. For the lowest flow conditions, cluster-based extent estimates for both Transect 2 and Transect 3 are very similar to those generated by a $\Delta\sigma$ threshold of 5%, while this shifts to 10% for the 14 L s^{-1} injection. At the highest-flow condition, the cluster-based extent estimate for Transect 2 was again more similar to a 5% threshold while Transect 3 was more similar to that based on a 10% threshold. Thus, applying a single $\Delta\sigma$ threshold across multiple datasets does not replicate the way in which clustering distinguishes reference from responsive signals to delimit hyporheic extent, likely because clustering is a more robust method than threshold-based analysis of hyporheic extent when comparing inverse model results amongst injections.

The inconsistent relationships between hyporheic extent and streamflow (directionality and magnitude) we found for adjacent transects are reflective of the complex and contradictory patterns reported by many other studies (e.g., Ward, 2016; Magliozzi et al., 2018). Our results demonstrate that analyzing time-lapse inverse ER models generated from data collected along multiple transects can, at least, capture some of the sub-reach variability in how hyporheic extent responds to complex interactions between in-channel hydraulics and riparian head gradients. Therefore, collection and processing of such data in this way can provide estimates of the range of extents and relative spatial structure of hyporheic exchange to variations in discharge, beyond

just a single areal estimate as is often obtained from inverse modeling of surface-water tracer BTCs.

Notably, the total hyporheic extents that we estimate (as well as the depth to which nodes are retained) are much smaller than those reported for prior analysis of these data (Ward et al., 2012, 2014). This result highlights an additional sensitivity not just to the method used to delimit hyporheic extent, but also to small differences in the inversion mesh, models used for regularization, and inversion settings as the underlying data are the same.

2.3.3 Temporal Patterns in the Heterogeneity of Hyporheic Connectivity

We calculated the mean and standard deviation of all pairwise Euclidean distances (d) for modeled $\Delta\sigma$ time series at each timestep (Figure 2.7). Generally, d traces (Figure 2.7) reflect the shape and timing of $\Delta\sigma$ BTCs (Figure 2.5e-l). Increases in mean d at the beginning of an injection suggest heterogeneous loading of flow paths while plateauing would indicate stable, but non-zero, differences amongst nodal responses. For most injections, d nears a plateau but continues to increase slightly throughout the injection. Since characteristic BTCs for hyporheic clusters all begin to respond almost immediately after injections began (Figure 5e-l), these continued increases in d are likely due to slow and heterogeneous loading of relatively immobile pore spaces within the area of the hyporheic zone represented by each cluster over the injection duration, rather than loading of entirely new zones within the streambed. We also note that d begins to decline immediately after the end of the 48-hour injections. Similarly, an initial rapid decline in $\Delta\sigma$ BTCs was noted for clusters that had larger overall responses (Figure 5e-l). Thus, subsurface locations that had exhibited a larger response are flushed more quickly, allowing both individual nodal responses and their heterogeneity to decline simultaneously.
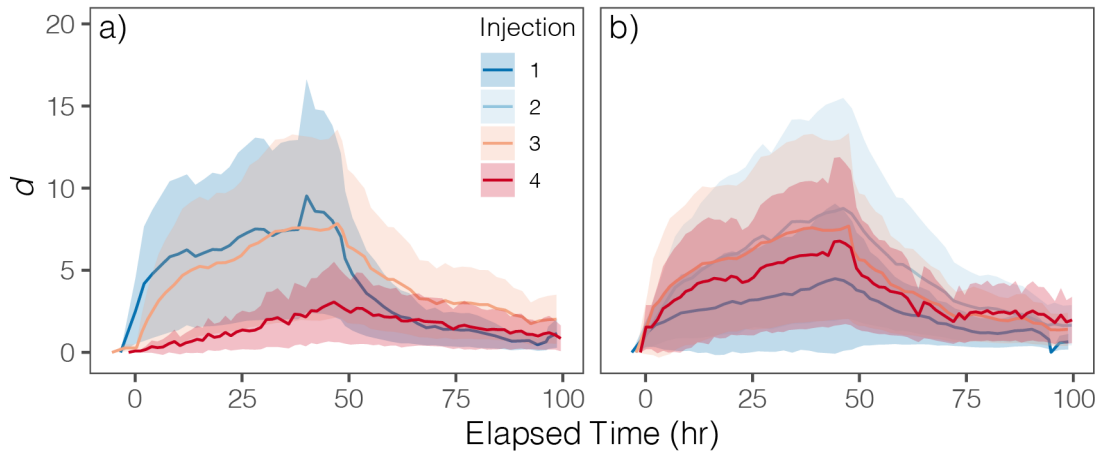
Figure 2.7. Time series of pairwise Euclidean distances (mean ± SD) among effective hyporheic nodes by injection for (a) Transect 2 and (b) Transect 3. Data from Transect 2 during injection 2 is excluded. Elapsed time is relative to the start of each tracer injection. High values of d represent larger differences in the response amongst nodes, while small values are indicative of a similar response amongst hyporheic nodes, not necessarily a lack of response.

Most injections exhibited similar d traces between injections and across the two transects. The most notable deviations, however, is for Transect 2 injection 4, which had both smaller mean and SD values for d than injections at higher flows. Additionally, the data from Transect 2 injection 4 exhibits a much steadier increase throughout the injection period and a steadier decline than for injections 1 and 3. Combined, these patterns indicate that at the lowest flows, hyporheic exchange became less spatially and temporally heterogeneous at Transect 2 while similar declines were not found for Transect 3. This means that transport behavior (i.e., advective timescales) becomes more similar amongst functional zones as flows decline for Transect 2, but not for Transect 3. Ward et al. (2014) reported increased heterogeneity of transport amongst hyporheic flow paths during seasonal flow recession based on the coefficient of variance from normalized temporal moments from time-lapse ER models for the same data. It is not entirely clear why these different metrics give conflicting results, although one explanation may be that our analysis is of a smaller hyporheic region that excludes many nodes with weaker $\Delta\sigma$ signals.

2.3.4 Potential Extensions

While the analyses we introduce are useful for characterizing transport heterogeneity within the effective hyporheic zone, they also have the potential to improve model representation of hyporheic processes. For instance, utilizing our proposed method to identify the extent and characteristic BTCs for regions within the hyporheic zone could be used to parameterize both cross-sectional areas and exchange coefficients in reactive transport models. This is especially important as physical parameters such as the extent of hyporheic exchange cannot be uniquely determined solely by observing surface-water BTCs (Bottacin-Busolin, 2019). Similar progress has been achieved using the hydrologic facies frameworks to parameterize reduced-complexity models based on sediment property observations (Hou et al., 2019).

The utility of clustering could also be further extended through changes to the inversion process. Most obviously, in streams that have a large enough cross-sectional area, the stream itself could be included in the inversion mesh and subsequent clustering. This would provide a more direct point of comparison rather than using observed surface water conductivities and modeled subsurface conductivity as in this study. It may also be possible to develop inversion techniques that solve specifically for functional zones. This may be accomplished by extending alternative inversion techniques that can solve for specific, albeit simple, shapes reflective of hydrologic processes and limited artifacts (e.g., Pidlisecky et al., 2011).

Our method may also be extended to identify the region over which point-scale sampling (i.e., from wells, piezometers, or mini-point samplers) may provide representative information. This information is potentially most useful in the context of reactive-tracer studies, wherein metrics of reactivity or the balance of transport and reaction timescales from particular points could be extrapolated in space based on ER-informed functional-zone mapping. Conversely, such functional-zone mapping could be used to develop testable hypotheses about the spatial structure of biogeochemical activity (i.e., occurrence of oxic or anoxic reactions, relative reaction completion, etc.). For instance, the decreasing heterogeneity we observed amongst functional zones with declining streamflow for Transect 2 but not 3 (Figure 2.7), could be used to predict

whether spatial gradients in biogeochemical reactions remain stable or decline seasonally at each transect. Such extensions would represent a major development in linking heterogeneity of coupled transport and biogeochemical processes occurring at the scale of a few meters to their aggregate significance over entire reaches.

Beyond identifying functional zones representing distinct transport and connectivity signals within the hyporheic zone, there are also potential extensions for this method that could advance synthesis across time (injections) and space (transects or sites). In particular, there is the potential to develop methods that either form clusters across merged datasets or match clusters across datasets through post-hoc comparisons so that the persistence and spatial evolution of particular functional zones can be investigated. The greatest challenge in this area will be determining how to normalize data given differences in forcings from separate solute injections. It is difficult, if not impossible, to perform multiple tracer additions that generate BTCs with the same relative change in stream water fluid conductivities, as is apparent even in this dataset (Figure 2.5a-d). Determining how to quantitatively handle such differences among injections will be necessary to definitively differentiate changes due to the tracer input itself or subsurface transport processes when examining clustering between datasets.

Another intriguing potential extension exists around supervised clustering or similar machine-learning techniques in which cluster characteristics are defined based on an initial training dataset containing time-lapse ER and ancillary measurements to allow for prediction elsewhere. Such methods have been applied to classify and then predict spatiotemporal evolution of other hydrologic behaviors such as seasonal soil moisture (Hermes et al., 2020) and hydrologically homogeneous regions within catchments (Nadoushani et al., 2018) based on topographic indices, but not, to our knowledge, for hyporheic exchange. Doing so could support reduced-complexity modeling that still represents spatial variations in functionally distinct zones at finer resolution along stream reaches than is currently possible. The primary challenge to this extension will be in determining which combination of metrics are obtainable over entire reaches

(at least compared to discrete ER transects) and can provide predictive power of subsurface functional zonation.

2.4. Conclusions

With the goal of developing a more objective approach to evaluating hyporheic extent, we present a method to analyze inverted ER models using unsupervised hierarchical clustering to delimit the extent of hyporheic exchange and to characterize functional zones with distinct transport behaviors within the subsurface. We used this method to show that total hyporheic extent and the spatial heterogeneity of exchange respond differently to seasonal baseflow recession between adjacent (< 10 m) transects in a mountain stream. We also found that the application of a single signal threshold to delimit hyporheic extent across ER datasets cannot replicate statistically supported parsing of active hyporheic and inactive reference regions in the subsurface. While this method does not overcome the inevitable issues of blurring in inverse models of the subsurface, it provides a more objective approach to distinguishing where and to what degree stream tracers may be exchanged with the subsurface from geophysical datasets. It also helps distinguish the spatial structure of zones with distinctive combinations of transport phenomena (i.e., advection vs dispersion) and relative density of mobile versus immobile domains within the subsurface, as well as how these structures persist temporally. To our knowledge, this represents the first application of machine learning to classify statistically unique spatial patterning of hyporheic exchange during tracer studies. Additionally, this approach has the potential to inform data-driven reduced-complexity modeling that could address known shortfalls of representing the hyporheic zone as a single well-mixed compartment.

References

Aghabozorgi, S., Seyed Shirkhorshidi, A., Ying Wah, T., Shirkhorshidi, A. S., & Wah, Y. (2015). Time-series clustering – A decade review. *Information Systems*, *53*, 16–38. https://doi.org/10.1016/j.is.2015.04.007

Bentley, L. R., & Gharibi, M. (2004). Two-and three-dimensional electrical resistivity imaging at a heterogeneous remediation site. *Geophysics*, 69(3), 674-680.

Binley, A. M. (2015). Tools and Techniques: Electrical Methods. In *Treatise on Geophysics: Second Edition* (Vol. 11, pp. 233–259). Elsevier Inc. https://doi.org/10.1016/B978-0-444-53802-4.00192-5

Binley, A. M. (2019). R2: Summary. Retrieved from http://www.es.lancs.ac.uk/people/amb/Freeware/R2/R2_readme.pdf

Binley, A. M., & Kemna, A. (2005). Electrical Methods. In Y. Rubin & S. S. Hubbard (Eds.), *Hydrogeophysics* (pp. 129–156). Springer.

Bottacin-Busolin, A. (2019). Modeling the effect of hyporheic mixing on stream solute transport. *Water Resources Research*, 55, 9995– 10011. https://doi.org/10.1029/2019WR025697

Cardenas, M. B., & Markowski, M. S. (2011). Geoelectrical imaging of hyporheic exchange and mixing of river water and groundwater in a large regulated river. *Environmental Science and Technology*, *45*(4), 1407–1411. https://doi.org/10.1021/es103438a

Day-Lewis, F. D., Singha, K., & Binley, A. (2005). The application of petrophysical models to radar and electrical resistivity tomograms: resolution-dependent limitations. *Journal of Geophysical Research*, 110, B08206, https:doi.org/10.1029/2004JB003569

Doughty, M., Sawyer, A. H., Wohl, E., & Singha, K. (2020). Mapping increases in hyporheic exchange from channel-spanning logjams. *Journal of Hydrology*, *587*, 124931. https://doi.org/https://doi.org/10.1016/j.jhydrol.2020.124931

Fu, T. C. (2011, February 1). A review on time series data mining. *Engineering Applications of Artificial Intelligence*. Elsevier Ltd. https://doi.org/10.1016/j.engappai.2010.09.007

Gooseff, M. N. (2010, August 4). Defining hyporheic zones - advancing our conceptual and operational definitions of where stream water and groundwater meet. *Geography Compass*. John Wiley & Sons, Ltd (10.1111). https://doi.org/10.1111/j.1749-8198.2010.00364.x

Harvey, J. W., & Bencala, K. E. (1993). The Effect of streambed topography on surface-subsurface water exchange in mountain catchments. *Water Resources Research*, *29*(1), 89–98. https://doi.org/10.1029/92WR01960

Harvey, J. W., Wagner, B. J., & Bencala, K. E. (1996). Evaluating the reliability of the stream tracer approach to characterize stream-subsurface water exchange. *Water Resources Research*, *32*(8), 2441–2451. https://doi.org/10.1029/96WR01268

Harvey, J. W., Gomez-Velez, J. D., Schmadel, N. M., Scott, D. T., Boyer, E. W., Alexander, R. B., et al. (2018, April 9). How Hydrologic Connectivity Regulates Water Quality in River Corridors. *Journal of the American Water Resources Association*, pp. 369–381. https://doi.org/10.1111/1752-1688.12691

Hermes, A. L., Wainwright, H. M., Wigmore, O., Falco, N., Molotch, N. P., & Hinckley, E.-L. S. (2020). From Patch to Catchment: A Statistical Framework to Identify and Map Soil Moisture Patterns Across Complex Alpine Terrain. *Frontiers in Water*, *2*. https://doi.org/10.3389/frwa.2020.578602

Hou, Z., Scheibe, T. D., Murray, C. J., Perkins, W. A., Arntzen, E. V., Ren, H., et al. (2019). Identification and mapping of riverbed sediment facies in the Columbia River through integration of field observations and numerical simulations. *Hydrological Processes*, *33*(8), 1245–1259. https://doi.org/10.1002/hyp.13396

Kasahara, T., & Wondzell, S. M. (2003). Geomorphic controls on hyporheic exchange flow in mountain streams. *Water Resources Research*, *39*(1), SBH 3-1-SBH 3-14. https://doi.org/10.1029/2002wr001386

Kelleher, C., Ward, A., Knapp, J. L. A., Blaen, P. J., Kurz, M. J., Drummond, J. D., et al. (2019). Exploring tracer information and model framework trade-offs to improve estimation of stream transient storage processes. *Water Resources Research*, 55, 3481– 3501. https://doi.org/10.1029/2018WR023585

Knapp, J. L. A., González-Pinzón, R., & Haggerty, R. (2018). The Resazurin-Resorufin System: Insights From a Decade of "Smart" Tracer Development for Hydrologic Applications. *Water Resources Research*, *54*(9), 6877–6889. https://doi.org/10.1029/2018WR023103

Lewandowski, J., Arnon, S., Banks, E., Batelaan, O., Betterle, A., Broecker, T., et al. (2019). Is the hyporheic zone relevant beyond the scientific community? *Water (Switzerland)*, *11*(11), 2230. https://doi.org/10.3390/w11112230

Magliozzi, C., Grabowski, R. C., Packman, A. I., & Krause, S. (2018). Toward a conceptual framework of hyporheic exchange across spatial scales. *Hydrology and Earth System Sciences*, *22*(12), 6163–6185. https://doi.org/10.5194/hess-22-6163-2018

Marion, A., Zaramella, M., & Packman, A. I. (2003). Parameter Estimation of the Transient Storage Model for Stream–Subsurface Exchange. *Journal of Environmental Engineering*, *129*(5), 456–463. https://doi.org/10.1061/(asce)0733-9372(2003)129:5(456)

Marzadri, A., Tonina, D., & Bellin, A. (2011). A semianalytical three-dimensional process-based model for hyporheic nitrogen dynamics in gravel bed rivers. *Water Resour. Res.*, 47, W11518, https://doi.org/10.1029/2011WR010583

McLachlan, P. J., Chambers, J. E., Uhlemann, S. S., & Binley, A. M. (2017). Geophysical characterisation of the groundwater–surface water interface. *Advances in Water Resources*, *109*, 302–319. https://doi.org/10.1016/J.ADVWATRES.2017.09.016

Montero, P., & Vilar, J. A. (2014). TSclust: An R package for Time Series Clustering. *Journal of Statistical Software2*, *62*(1), 1–43.

Mueen, A., & Keogh, E. (2016). Extracting optimal performance from dynamic time warping. In *Proceedings of the ACM SIGKDD International Conference on Knowledge Discovery and Data Mining* (Vol. 13-17-August-2016, pp. 2129–2130). New York, NY, USA: Association for Computing Machinery. https://doi.org/10.1145/2939672.2945383

Nadoushani, S. S. M., Dehghanian, N., & Saghafian, B. (2018). A fuzzy hybrid clustering method for identifying hydrologic homogeneous regions. *Journal of Hydroinformatics*, *20*(6), 1367–1386. https://doi.org/10.2166/hydro.2018.004

Park, P. J., Manjourides, J., Bonetti, M., & Pagano, M. (2009). A permutation test for determining significance of clusters with applications to spatial and gene expression data. *Computational Statistics and Data Analysis*, *53*(12), 4290–4300. https://doi.org/10.1016/j.csda.2009.05.031

Pateiro-Lopez, B., Rodriguez-Casal, A., & . (2019). alphahull: Generalization of the Convex Hull of a Sample of Points in the Plane.

Pidlisecky, A., Singha, K., & Day-Lewis, F. D. (2011). A distribution-based parameterization for

improved tomographic imaging of solute plumes. *Geophysical Journal International*, 187(1), doi: 10.1111/j.1365-246X.2011.05131.x

R Core Team. (2019). R: A Language and Environment for Statistical Computing. Vienna, Austria: R Foundation for Statistical Computing.

Rucker, D. F., Tsai, C. H., Carroll, K. C., Brooks, S., Pierce, E. M., Ulery, A., & Derolph, C. (2021). Bedrock architecture, soil texture, and hyporheic zone characterization combining electrical resistivity and induced polarization imaging. *Journal of Applied Geophysics*, *188*, 104306. https://doi.org/10.1016/j.jappgeo.2021.104306

Sassen, D. S., Hubbard, S. S., Bea, S. A., Chen, J., Spycher, N., & Denham, M. E. (2012). Reactive facies: An approach for parameterizing field-scale reactive transport models using geophysical methods. *Water Resources Research*, *48*(10), 10526. https://doi.org/10.1029/2011WR011047

Savoy, P., Appling, A. P., Heffernan, J. B., Stets, E. G., Read, J. S., Harvey, J. W., & Bernhardt, E. S. (2019). Metabolic rhythms in flowing waters: An approach for classifying river productivity regimes. *Limnology and Oceanography*, *64*(5), 1835–1851. https://doi.org/10.1002/lno.11154

Schmadel, N. M., Ward, A. S., & Wondzell, S. M. (2017). Hydrologic controls on hyporheic exchange in a headwater mountain stream. *Water Resources Research*, *53*(7), 6260–6278. https://doi.org/10.1002/2017WR020576

Singha, K., Pidlisecky, A., Day-Lewis, F. D., & Gooseff, M. N. (2008). Electrical characterization of non-Fickian transport in groundwater and hyporheic systems. *Water Resources Research*, *46*(4), 0–07. https://doi.org/10.1029/2008WR007048

Stream Solute Workshop. (1990). Concepts and methods for assessing solute dynamics in stream ecosystems. *Journal of the North American Benthological Society*, *9*(2), 95–119. https://doi.org/10.2307/1467445

Tonina, D., & Buffington, J. M. (2007). Hyporheic exchange in gravel bed rivers with pool-riffle morphology: Laboratory experiments and three-dimensional modeling. *Water Resources Research*, *43*(1). https://doi.org/10.1029/2005WR004328

Wainwright, H. M., Chen, J., Sassen, D. S., & Hubbard, S. S. (2014). Bayesian hierarchical approach and geophysical data sets for estimation of reactive facies over plume scales. *Water Resources Research*, *50*(6), 4564–4584. https://doi.org/10.1002/2013WR013842

Ward, A. S. (2016). The evolution and state of interdisciplinary hyporheic research. *Wiley Interdisciplinary Reviews: Water*, *3*(1), 83–103. https://doi.org/10.1002/wat2.1120

Ward, A. S., Gooseff, M. N., & Singha, K. (2010a). Characterizing hyporheic transport processes - Interpretation of electrical geophysical data in coupled stream-hyporheic zone systems during solute tracer studies. *Advances in Water Resources*, *33*(11), 1320–1330. https://doi.org/10.1016/j.advwatres.2010.05.008

Ward, A. S., Gooseff, M. N., & Singha, K. (2010b). Imaging hyporheic zone solute transport using electrical resistivity. *Hydrological Processes*, *24*(7), 948–953. https://doi.org/10.1002/hyp.7672

Ward, A. S., Fitzgerald, M., Gooseff, M. N., Voltz, T. J., Binley, A. M., & Singha, K. (2012).

Hydrologic and geomorphic controls on hyporheic exchange during base flow recession in a headwater mountain stream. *Water Resources Research*, *48*(4), 4513. https://doi.org/10.1029/2011WR011461

Ward, A. S., Gooseff, M. N., Fitzgerald, M., Voltz, T. J., & Singha, K. (2014). Spatially distributed characterization of hyporheic solute transport during baseflow recession in a headwater mountain stream using electrical geophysical imaging. *Journal of Hydrology*, *517*, 362–377. https://doi.org/10.1016/j.jhydrol.2014.05.036

Ward, A. S., Schmadel, N. M., Wondzell, S. M., Gooseff, M. N., & Singha, K. (2017). Dynamic hyporheic and riparian flow path geometry through base flow recession in two headwater mountain stream corridors. *Water Resources Research*, *53*(5), 3988–4003. https://doi.org/10.1002/2016WR019875

Ward, A. S., Wondzell, S. M., Schmadel, N. M., Herzog, S., Zarnetske, J. P., Baranov, V., et al. (2019). Spatial and temporal variation in river corridor exchange across a 5th-order mountain stream network. *Hydrology and Earth System Sciences*, *23*(12), 5199–5225. https://doi.org/10.5194/hess-23-5199-2019

Ward, A. S., K. Singha, and M. N. Gooseff (2020). Hyporheic exchange studies in H.J. Andrews Watersheds 01 and 03, summer 2010, HydroShare, https://doi.org/10.4211/hs.8207c26f492e49f0be33e7a2427ccfea

Warren Liao, T. (2005). Clustering of time series data - A survey. *Pattern Recognition*, *38*(11), 1857–1874. https://doi.org/10.1016/j.patcog.2005.01.025

Wondzell, S. M. (2006). Effect of morphology and discharge on hyporheic exchange flows in two small streams in the Cascade Mountains of Oregon, USA. *Hydrological Processes*, *20*(2), 267–287. https://doi.org/10.1002/hyp.5902

Chapter III

The Role of Hyporheic Connectivity in Determining Nitrogen Availability:

Insights from an Intermittent Antarctic Stream[1]

3.1 Introduction

   The biogeochemical processing of nitrogen (N) in streams has drawn wide interest related to various water quality problems (Davidson et al., 2011) and the mobilization of N from local human activities adjacent to freshwater systems to downstream locations (Fowler et al., 2013). To date, most research has focused on how human manipulation of N sources – through fertilizer applications or emissions – increase the amount of reactive N that is transported from terrestrial to aquatic systems (Alexander et al., 2007; Bernot & Dodds, 2005; Boyer et al., 2002; Dodds, 2006; Mulholland et al., 2008). Yet, in many oligotrophic systems with little to no input of anthropogenic N, autochthonously derived N (i.e., N fixed by periphyton within the stream) is a significant driver of ecosystem metabolism (Grimm & Petrone, 1997; Kunza & Hall, 2014; Marcarelli & Wurtsbaugh, 2006; McKnight et al., 2004). Largely, these low-N systems are in alpine, arid, or polar environments. Even in low-N systems, directly quantifying N inputs from both autochthonous and allochthonous sources can be difficult (Hamilton et al., 2004), especially because N fixation is highly heterogenous (Grimm & Petrone, 1997; Horne & Carmiggelt, 1975; Marcarelli et al., 2008). Consequently, attributing biologically available N to either source in these oligotrophic streams and determining how internally sourced N is processed remains challenging.

   Nitrogen cycling in streams results from coupled hydrologic and biogeochemical processes, which result in the spiraling of N (Harvey et al., 2018; Stream Solute Workshop, 1990; Webster et al., 2003). The coupling of physical and biological processes control the balance of reaction and transport timescales (Briggs et al., 2014; Harvey et al., 2013; Lansdown et al., 2015; Zarnetske et al., 2011, 2012), redox zonation (Briggs et al., 2015), and the availability of other nutrients (e.g., carbon or phosphorus) (Koch et al., 2010; Oviedo-Vargas et

---

[1] This chapter has been published, see Singley et al. (2021a) in the bibliography for the full citation.

al., 2013). Low-N systems in alpine, arid, or polar environments are often characterized by ephemeral or intermittent streamflow (Jensen et al., 2017; Larned et al., 2010; Robinson et al., 2016). Streamflow variability and intermittence result in heterogenous spatial and temporal patterns of N cycling as a result of variations in connectivity with terrestrial N sources, exchange between the main channel and streambed, and hyporheic residence times relative to process rates (Bernal et al., 2013; Harvey et al., 2018; Mendoza-Lera et al., 2019; von Schiller et al., 2017). While autochthonous N sources are expected to be more important in such systems, flow re-initiation may be accompanied by a first flush of N from the surrounding landscape (Bernal et al., 2005, 2019; Merbt et al., 2016), further obscuring how N is transformed within the stream. Thus, the hydrology of many low-N systems may make it difficult to quantify the importance of internally-sourced N. By altering surface and subsurface connectivity, these streamflow dynamics likely modulate the function of the hyporheic zone as an ecosystem control point (*sensu* Bernhardt et al., 2017) that influences N fate and availability to biota.

Widely distributed autotrophic cyanobacteria (e.g., *Nostoc*) are responsible for N fixation in many streams (Dodds et al., 1995). As a result, the spiraling of internal N is driven by the transport of this autochthonous organic matter (OM) and subsequent heterotrophic respiration. Unlike streams with abundant allochthonous sources (Tank et al., 2010), in environments with limited canopy cover (e.g., alpine, arid, or polar systems), autochthonous contributions to dissolved OM (DOM) from benthic algal biofilms can be significant (Dahm et al., 2003; Fellman et al., 2011; Fenoglio et al., 2015) and serve as a relatively labile source of C and N (Jones et al., 1995b). Consequently, understanding the temporal and spatial dynamics of how internally sourced N is processed will provide insight into multiple facets of stream ecosystem function controlled by both physical and biological processes.

Despite widespread human manipulation of N, there exist some relatively unaltered systems that can serve as models for understanding the cycling of internal N sources in streams. Ephemeral streams in the McMurdo Dry Valleys (MDVs) of Antarctica represent one such system. Streamflow resulting from glacial meltwater generation occurs for 4–10 weeks per year

in MDV streams in a landscape devoid of plants. The extremely arid climate (<10 cm snow water equivalent yr^{-1}, Fountain et al., 2010) and presence of continuous permafrost (Bockheim et al., 2007; Conovitz et al., 2006) result in stream channels that are disconnected from hillslopes or deeper groundwater. Thus, MDV streams provide relatively isolated model systems with a single upstream source of N from atmospheric deposition on glaciers, N sourced from benthic algae within the stream channel (including *Nostoc*), and very limited OM inputs (Howard-Williams et al., 1989; McKnight et al., 1999).

Given the relative simplicity of MDV streams, their nutrient and OM cycling has been studied for over three decades. Previous nutrient tracer additions and longitudinal sampling demonstrated that N uptake occurs in both the main channel via benthic algal mats and the hyporheic zone (Gooseff et al., 2004; Howard-Williams et al., 1989; McKnight et al., 2004). Due to hydrologic isolation and lack of carbon sources, relatively labile OM in dissolved or particulate form is predominantly sourced from benthic algal mats along the stream channel. As flow increases, particulate OM (POM) is scoured from these mats and transported downstream (Cullis et al., 2014). Fortuitously, the sources of N to MDV streams are isotopically distinct (Kohler et al., 2018). Recently, Kohler et al. (2018) found that the abundant *Nostoc* dominated black mats maintained a stable isotopic signature indicative of N-fixation (δ^{15}N ≈ 0‰). By contrast, the δ^{15}N of non-N fixing orange mats increased longitudinally from a depleted signature reflective of glacial inputs (δ^{15}N ≪ 0‰) to that of black mats in the lower reaches. Together with δ^{15}N values in POM matching that of black mats and evidence of POM entrainment in the hyporheic zone (Heindel et al., 2021), these findings imply that internal N sources dominate in lower reaches due to the mobilization, remineralization and subsequent release of black mat derived POM. Yet, it is important to note that neither OM mineralization nor nitrification have been directly investigated in MDV streams.

In this study, we use a MDV stream as an ideal ecosystem to examine the fate of autochthonous N under conditions of limited hydrologic connectivity with the surrounding landscape. We test the hypothesis that the availability of remineralized autochthonous N is

controlled by connectivity between the hyporheic zone and main channel due to the contrasting biogeochemical function of benthic autotrophs and hyporheic heterotrophs. To do so, we collected samples of hyporheic water and surface water frequently (~4–6 hr) over a diel period in January 2019 and opportunistically throughout the 2020 flow season. We used water chemistry to identify signatures of remineralization, nitrification, and hydrologic exchange as well as any spatiotemporal variations of these processes. In addition, we performed a laboratory nitrification potential assay on sediment from the same stream. With this assay, we tested prior inferences that hyporheic microbes possess the functional potential to carry out nitrification, which is essential for the coupled spiraling of OM and N. By leveraging the relative simplicity of MDV streams, we are able to assess the roles of hyporheic residence time and microbial processing on the cycling of autochthonously-derived N sources, which are difficult to examine in other ecosystems.

3.2 Study Site and Methods

3.2.1 McMurdo Dry Valley Streams

The MDVs are part of a polar desert ecosystem that comprises the largest ice-free area in Antarctica (Levy, 2013). The landscape is characterized by large, open expanses of loosely consolidated glacial till, ephemeral stream channels, closed basin lakes, and cold-based alpine glaciers. Flood pulse events generated by diel fluctuations in the net energy balance of source glaciers determine streamflow in the MDVs. These flood pulses punctuate periods of flow intermittence that can be on the order of a few hours to days during the flow season, which only lasts for 4–10 weeks per Austral summer (Wlostowski et al., 2016). Mean transit times for median streamflows (<10 L s^{-1} for most streams) range from days to a few months (Wlostowski et al., 2018). Given the loosely consolidated sediment, hyporheic exchange rates are relatively high in MDV streams (Gooseff et al., 2004; Runkel et al., 1998), although hydrological flow path residence times vary due to the expansion-contraction dynamics and relatively large wetted margins along the stream corridor (Gooseff et al., 2003). At low flows (i.e., < 5 L s^{-1}), the cross-

sectional area that exchanges water with the surface is relatively small, yet preferential flow paths and temperature-dependent variations in viscosity can maintain rapid exchange to limited portions of the hyporheic zone (Cozzetto et al., 2013). Consequently, hyporheic connectivity exhibits marked spatial and temporal variability.

For this study, we focused on Von Guerard Stream, a relatively long (5.2 km) ephemeral stream located in Taylor Valley with an average gradient of 0.078 m m-1 (Wlostowski et al., 2016) (Figure 3.1). Streamflow is derived entirely from glacial melt. The upper reaches of Von Guerard Stream are relatively steep and the streambed consists of cobbles and boulders embedded in sandy gravel. The gradient eases into a broader, sandy area where streamflow is diverted between the main channel to the east (~75% of flow) and a relict channel, which contributes streamflow to Harnish Creek to the west (Alger, 1997; McKnight et al., 2007). Below this diversion, there is a large playa composed of loosely consolidated alluvium. Below the playa, the gradients increase and the streambed re-channelizes, although it remains broader than the upper reaches. The streambed in the lower reaches varies from stone pavements to a braided, sandy delta as it approaches the outlet, where a stream gage is operated by the McMurdo Dry Valleys Long-Term Ecological Research project (mcmlter.org).
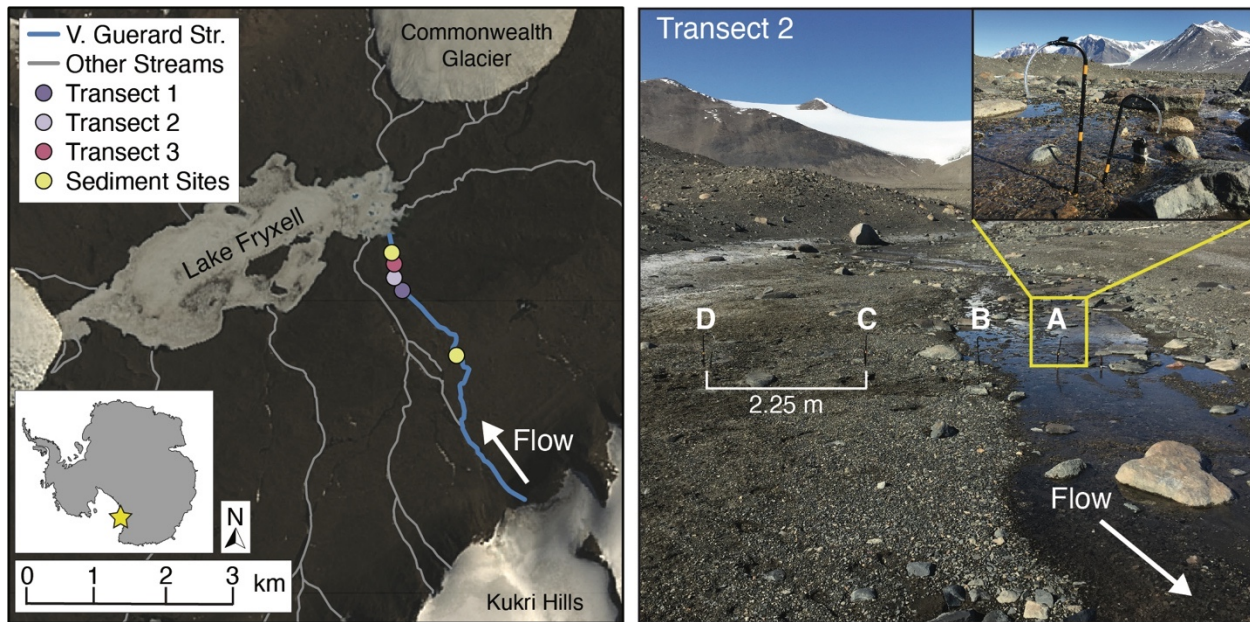
Figure 3.1. Map of sample collection locations along the lower reaches of Von Guerard Stream (left) and photo of Transect 2 (right) with porewater sites A-D and close up of samplers at site A (inset).

Benthic algal mats dominated by cyanobacteria cover substantial portions of the streambed along the length of Von Guerard Stream (Alger, 1997). The perennial mats lie in a freeze-dried state for much of the year and reactivate quickly upon the return of streamflow (McKnight et al., 2007). The dominant species composition of these mat communities varies with mat location and color. Black mats, dominated by *Nostoc spp*., are well developed along the stream margins and in slightly raised areas within the channel that are less frequently inundated. Orange mats, dominated by non-N-fixing cyanobacteria (*Oscillatoria spp*. and *Phormidium spp.*), cover much of the streambed in smooth, tightly-adhered formations (Alger, 1997; Kohler et al., 2015). Kohler et al. (2018) demonstrated that autochthonous N derived from scoured black mat OM dominates the N budget in the lower reaches of Von Guerard Stream and the neighboring stream of similar length, Harnish Creek.

High-frequency (15 min) discharge (Q) data were obtained from the gage at the outlet of Von Guerard Stream into Lake Fryxell (Gooseff & McKnight, 2019). The duration and magnitude of Q varied widely within and between the two seasons (Figure 3.2), as is typical for

MDV streams. Gage data for the final weeks of the 2020 flow season were not recovered by the time of writing due to impacts of the COVID-19 pandemic on fieldwork. However, discrete measurements of Q for the final four sampling events are provided based on portable flume measurements or observations of zero flow (Figure 3.2b). Field teams observed zero or low Q for streams throughout the Lake Fryxell Basin during this period.
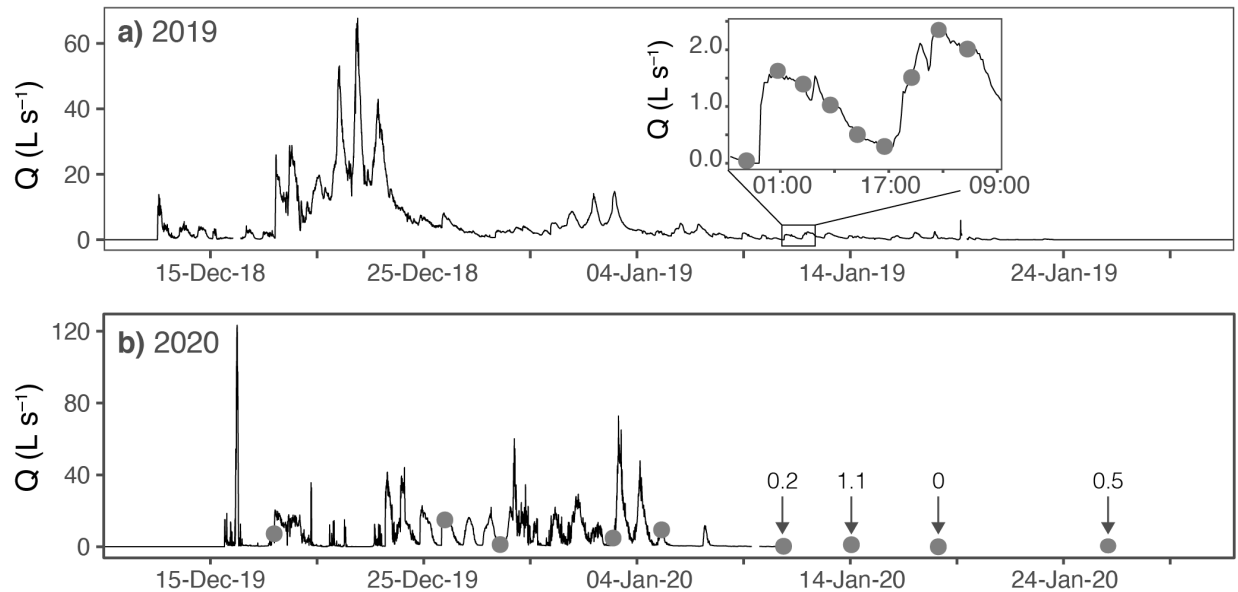
Figure 3.2. Gage for Von Guerard Stream over the 2019 and 2020 flow seasons. Each sampling period is indicated with a single point representing samples across transects and sites. Concurrent manual Q measurements are indicated for samples during the latter part of 2020 where gage data is unavailable.

3.2.2. Hyporheic Water and Surface Water Samples

We established three lateral transects (T1–3) in the lower reaches of Von Guerard Stream (Figure 3.1). Transects extended from the center of the channel (site A) to the wetted margin (site D), with the actual spacing and overall length of each transect varying with channel morphology. Hyporheic water samplers were constructed of flexible polyethylene tubing (3/16" inner diameter) encased in a rigid plastic tube and screened at the bottom with fine metal mesh. We installed samplers to depths of 15 and 30 cm at locations A-D on each transect and allowed them to remain *in situ* 6 hours prior to sample collection so any disturbed sediment could settle.

We collected samples every 4-6 hrs over a 32 hr period during January 2019 (n=192), and periodically throughout the 2020 flow season (n=54, Figure 3.2). For 2019, samples were collected from all three transects at depths of 15 and 30 cm and lateral sites A-D. For 2020, samples were again collected for T1–3, but only at a depth of 15 cm at the thalweg (site A).

To collect samples, we slowly drew 15–20 mL of water into a syringe attached to the sampler tubing, closed a T-valve to prevent backflow, discarded the rinse water, and then slowly drew another 100 mL. The collected water was immediately partitioned into 20 mL glass scintillation vials with no head space for stable isotope analysis (^{18}O and deuterium), a 60 mL HDPE bottle for nutrient and silica (Si) analyses, and 25 mL glass analysis tubes for dissolved organic carbon (DOC). Each vessel was rinsed with ~5 mL of sample water prior to filling. Surface water samples were taken concurrently at site A by triple-rinsing bottles with stream water and filling directly. All samples were kept out of direct sunlight and transported back to the laboratory at F6 Camp. In the lab, we immediately filtered nutrient and DOC samples through pre-combusted (4 hr at 450ºC) Whatman GF/C glass fiber filters. Combined nutrient and Si samples were stored frozen in 60 mL HDPE bottles, while samples for DOC and stable isotope analyses were kept chilled (+4ºC) in the dark prior to analysis. We analyzed DOC in the Crary Lab at McMurdo Station, while samples for nutrient and stable isotope analyses were shipped to the University of Colorado Boulder, USA. Dissolved organic carbon, water isotopes, and Si were not measured for the 2020 season samples due to logistical constraints on fieldwork.

Silica and dissolved inorganic nitrogen (DIN) species concentrations were measured colorimetrically for samples from both seasons immediately after thawing at room temperature by the Arikaree Environmental Laboratory, University of Colorado Boulder, using a Lachat (USA) QuikChem 8500 Flow Injection Autoanalyzer. Nitrate (NO_3^-) – measured as NO_3^-+ nitrite (NO_2^-) – was analyzed by standard method 4500-NO_3 I (cadmium reduction flow injection) with a limit of detection (LOD) of 0.004 mg NO_3^-–N L^{-1}. Samples were analyzed for ammonium (NH_4^+) by standard method 4500-NH_3 H (phenolate flow injection, LOD 0.005 mg NH_4^+–N/L). For Si, the LOD was 0.004 mg Si L^{-1} by standard method 4500-SiO_2 F. We

measured water isotopes ($\delta^{18}O$ and δD) using a cavity ring-down spectrometer (Picarro, USA) and calculated deuterium excess as $\delta D - 8*\delta^{18}O$.

3.2.4. Stream Sediment Nitrification Potential Assay

To verify the functional potential of hyporheic microbes to perform nitrification, we conducted a laboratory assay on sediment from Von Guerard Stream. We collected sediment from mid-channel and lateral locations (equivalent to A and C) from two different transects in the lower half of Von Guerard Stream during January 2018 (Figure 3.1). We first removed the top 5 cm of the streambed to avoid contamination from benthic algal mats, then scooped sediment from approximately 5–10 cm depth into sterile Whirlpaks. These sediment samples were stored frozen and shipped to the University of Colorado Boulder for analysis.

After thawing the samples at room temperature (20ºC), we subsampled 20 g of wet sediment from each site in triplicate into sterile 250 mL HDPE bottles and an additional 20 g in triplicate into pre-weighed aluminum weigh boats. We dried the subsamples in the aluminum weigh boats at 105ºC for 24 hours and reweighed to calculate mean volumetric water content for each sampling location. For the wet subsamples in 250 mL HDPE bottles, we performed a nitrification potential assay using 100 mL of a 0.5 mM phosphate (KH_2PO_4 and K_2HPO_4) buffered solution containing 10 mM perchlorate and 0.5 mM NH_4^+, which was mixed constantly with the sediment on a shaker table. A detailed description of the assay protocol is provided by Schmidt & Belser (1994). We took samples of the solution in triplicate from each replicate flask at 0, 1 and 8 hours then 1, 2, 3, and 5 days from the start of the assay. This extended duration follows prior nitrification assays with MDV microbial communities that found relatively slow NO_2^- accumulation (Hopkins et al., 2006). All subsamples were immediately filtered through Whatman GF/C glass fiber filters and stored frozen (-20ºC) until thawed for analysis. As perchlorate in the incubation solution inhibits the final oxidation of NO_2^- to NO_3^-, we analyzed the filtered aliquots for NO_2^- colorimetrically using a Lachat QuikChem 8500 Flow Injection

Autoanalyzer. Accumulated NO_2^- concentrations were converted to mass NO_2^-–N normalized by the calculated dry weight of sediment in each replicate flask.

Due to a number of factors, the data from this assay is not intended to reflect *in situ* nitrification rates. While sediment in MDV stream corridors frequently experiences freeze-thaw cycles during the Austral summer (and are frozen most of the year) (Wlostowski et al., 2018), it is possible that extended freezing during transportation and thawing immediately prior to analysis may have altered the viable microbial community and observed rates. However, stream sediment temperatures cycle between 4ºC and 12ºC on a daily basis and water advected into the hyporheic zone can be up to 15ºC (Cozzetto et al., 2013; Wlostowski et al., 2018). So, while the assay was conducted at room temperature (20ºC), it is likely that highly temperature sensitive microbes are not dominant in this system. We utilized a perchlorate inhibition protocol (Schmidt & Belser, 1994) originally intended for soils rather than methods designed for streams (Dodds & Jones, 1987; Kemp & Dodds, 2001, 2002) as stream corridor sediments are dry for most of the year and similar perchlorate-based approaches have been used on sediment from MDV stream margins (Hopkins et al., 2006). Consequently, we use the data from this assay as an indication of whether the microbial community of MDV stream sediments possess the functional potential to perform nitrification, not to quantify *in situ* rates.

3.2.5 Data Analysis

In order to assess N cycling, we examined spatial and temporal patterns in solute concentrations (NH_4^+, NO_3^-, DOC, and Si) and water isotopes (^{18}O and deuterium) between surface water and hyporheic water samples. We assessed variability of solute concentrations at each sampling site over the entire 2019 diel-sampling campaign by calculating coefficients of variation (CV = σ/μ, where σ is the standard deviation and μ is the mean for each particular site). To assess net rates of change in the concentration of each solute, we performed simple linear regressions for those sites and solutes for which a significant monotonic trend was detected (Mann-Kendall, $p < 0.05$).

We also analyzed concentration discharge (C-Q) relationships for each solute. To do so, we aggregated data within each type (hyporheic and surface water) across sites, transects, and seasons. We utilized a non-linear least squares regression approach to fit power law relationships ($C=aQ^b$).

Apart from time series and C-Q results, unless otherwise noted, we present time-averaged mean concentrations and masses $\pm$ 1 standard error by sampling site within transects. Due to small and unequal sample sizes across groupings, we performed nonparametric Mann-Whitney U-tests with p-value adjustments on multiple comparisons (Benjamini & Hochberg, 1995) to identify significant differences at the level of hyporheic versus surface water and among lateral and vertical hyporheic locations within each transect. We also analyzed the correlation of each analyte to DIN concentrations to identify factors controlling variability in net N cycling. Based on prior work in MDV streams (Gooseff et al., 2003; Wlostowski et al., 2018), we utilized Si as an indicator of relative residence time and deuterium excess to assess whether evaporation rather than biological processes explained variations in DIN concentrations. We analyzed the correlation between DOC and DIN concentrations to assess whether DOC is an important substrate for remineralization and nitrification (POM was not quantified by this study). In instances where either temporal or spatial variations existed, we also calculated ratios of coefficients of variation to assess the degree of connectivity between hyporheic sites and surface water.

We used the results of our intensive hyporheic and surface water sampling during the 2019 flow season to compare the relative size of DIN pools at a single moment in time (i.e., not accounting for fluxes or spiraling) for Von Guerard Stream under low streamflow conditions. We estimated the total mass of DIN per longitudinal meter in three compartments: (1) surface water as well as hyporheic water from (2) 0-15 cm and (3) 15-30 cm depths. To simplify these calculations, we assumed rectangular cross-sectional areas for each zone where surface water had a width of 1.5 m and a depth of 0.03 m, while each hyporheic compartment had a width of 6 m. These dimensions reflect commonly estimated values (Gooseff et al., 2004; Runkel et al.,

1998) and are within ranges found from surveys of water sampling transects. We used a porosity of 0.34 ± 0.01 (n=18) based on bulk densities observed by a concurrent study and a mineral density of 2.65 g cm^{-3}. We multiplied the mean concentrations of DIN in surface water and hyporheic water from each depth to the resultant fluid volume per meter of stream length – resulting in a mass of N as DIN per unit length along the stream. We propagated errors from bulk density and DIN concentrations by adding in quadrature (Taylor, 1997). Errors were not included for the surface water depth or width and the hyporheic compartment widths; these assumptions were held constant across estimates.

3.3 Results

3.3.1 Hyporheic Water and Surface Water Chemistry

During both the 2019 and 2020 streamflow season, the largest diel pulse events and peak streamflow occurred in late December and gradually tapered off until flow ceased completely in late January (Figure 3.2). Discharge ranged from 0 to 2.4 L s^{-1} during the 2019 diel sampling campaign (Figure 3.2a inset), with two distinct, albeit small (1.5 and 2.4 L s^{-1}), peaking events. While the fluctuation in streamflow was relatively small throughout the diel sampling period, the magnitude of change was large enough that wetted channel expansion and contraction variably inundated and exposed sampling locations at all three transects. For the 2020 season, we conducted opportunistic sampling at streamflow values from 0–15.5 L s^{-1}. While the highest streamflow values for either season were not represented by our sampling, historic streamflow data (1990-2020) for Von Guerard Stream exceed the range over which we obtained samples less than 20% of the time (Figure S3.1). Therefore, although higher flows may alter N cycling dynamics, our data represent the temporally dominant state of the system.

Despite cyclic Q pulsing during the diel sampling campaign in 2019, hyporheic concentrations of all solutes and water isotopes at 26 locations remained relatively stable over time (Figure 3.3), although some significant monotonic patterns (Mann Kendall, $p < 0.05$) were detected. Nitrate concentrations were stable for 17 of the 26 locations, while the remaining 9

sampling locations exhibited significant temporal trends (median rate -15.4 µg NO_3^--N L^{-1} day^{-1}, adj. $R^2 > 0.60$). For all sites, NH_4^+ fluctuated or remained near the LOD throughout the diel period, trends were not significant. Similarly, DOC mostly declined over time, although the trend was only significant for 7 locations (median of -0.18 mg DOC L^{-1} day^{-1}, adj. $R^2 > 0.42$). Dissolved Si concentrations increased significantly at 11 locations (median of 0.38 mg Si L^{-1} day^{-1}, adj. $R^2 > 0.78$), while cyclic behavior reflecting changing Q was observed for T3. Only 4 sites exhibited trends in deuterium excess (T1 C, T2 B, T3 A and D all at 30 cm depths), although cyclic behavior with Q is apparent in a few instances (e.g., T3 surface water).
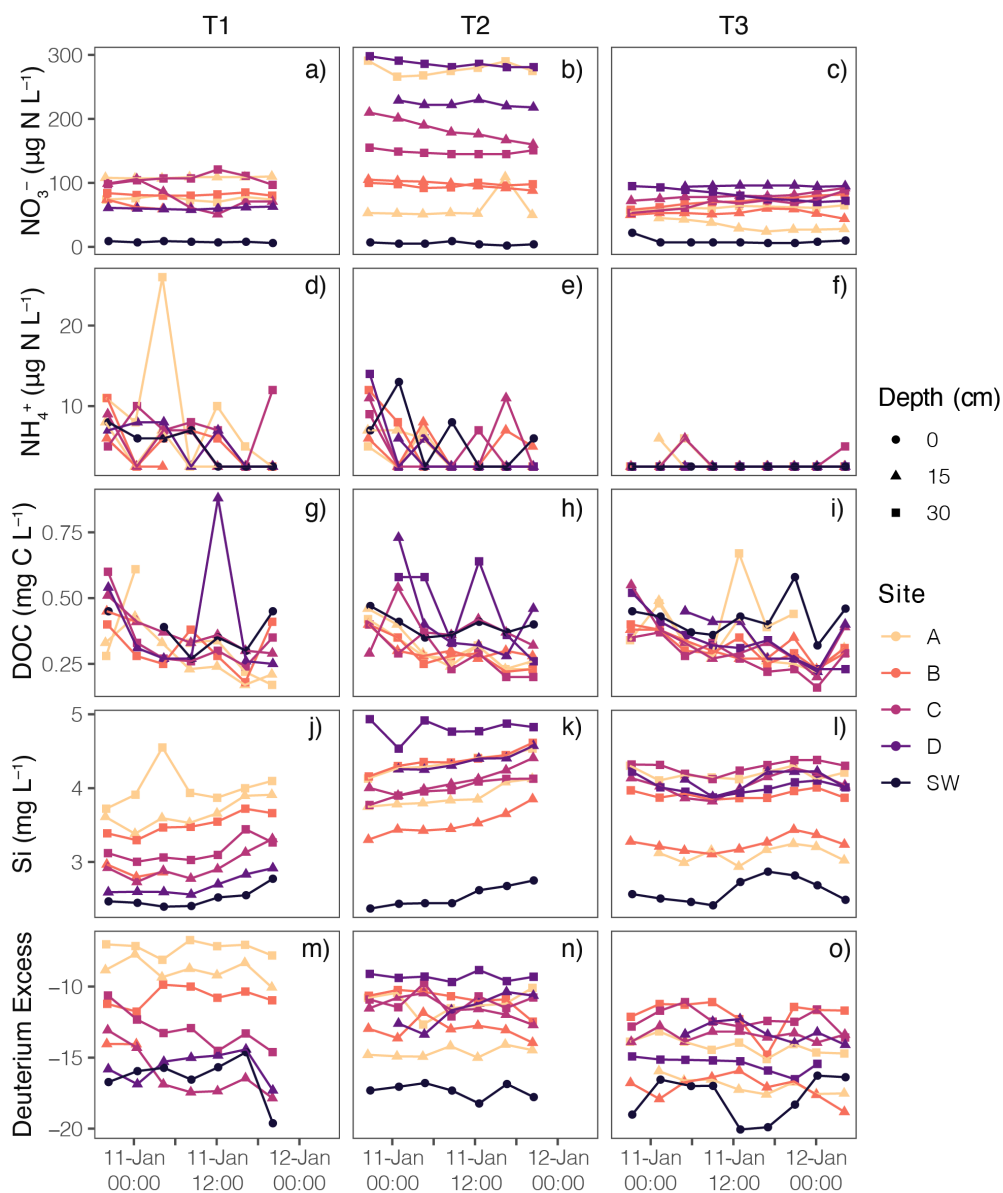
Figure 3.3. Concentration time series for (a-c) NO_3^-, (d-f) NH_4^+, (g-i) DOC, (j-l) Si, and (m-o) deuterium excess by transect during the 2019 diel sampling period. SW indicates surface water samples, all other samples are for hyporheic water.

Median CVs across all sites in 2019 were 0.12, 0.22, 0.04, < 0.01, < 0.01, and 0.07 for NO_3^-, DOC, Si, $\delta^{18}O$, δD, and deuterium excess, respectively. Where mean differences existed, they were most pronounced between surface and hyporheic water samples rather than laterally within or between transects for both seasons (detailed comparisons in the supplemental information, Figures S3.2–7 and Tables S3.1–6). Additionally, relatively sparse sampling

(~weekly) in a system characterized by hydrologic changes on hourly timescales limited the utility of temporal analysis for the 2020 season. Consequently, we present further analysis for both seasons that is organized around aggregate hyporheic versus surface water comparisons.

For both seasons, NO_3^- was above detection (4.0 µg NO_3^-–N L^{-1}) in all surface and hyporheic water samples. While variations exist between sites within a transect and between transect (Figure S3.2), NO_3^- concentrations were about 7 to 30 times higher in hyporheic water than surface water (Figure 3.3). For both seasons, the mean concentration of NO_3^- across all hyporheic water samples was significantly higher ($p < 0.05$, Mann-Whitney U) than in the concurrent surface water samples. Within each transect, spatial differences (lateral and vertical) in mean NO_3^- concentrations existed among sites, but patterns were not consistent across transects in 2019 (Figure S3.2) and sampling only at site A prevented analysis of lateral patterns for 2020. A complete pairwise comparison of NO_3^- concentrations by site and depth within each transect are reported in the supplemental information (Table S3.1).

Ammonium remained below detection (5.0 µg NH_4^+-N L^{-1}) in 71.6 % of the hyporheic water ($n_{total}=169$) and 65.2% of the surface water samples ($n_{total}=23$) in 2019. In contrast, NH_4^+ was above the LOD for all samples ($n_{total}=54$) during the 2020 season. Together, these results are consistent with the long-term surface water sampling record from the MCM LTER: NH_4^+ was below detection in 37.8% ($n_{total}=90$) of samples from the lower reaches of Von Guerard Stream and 42.9% ($n=28$) from the upper reaches over the period from 1994–2018. Furthermore, NH_4^+ was below detection in 31.2% ($n_{total}=3131$) of all samples from all monitored MDV streams from 1993–2018 (*Lyons*, 2015). Mean NH_4^+ concentrations were not significantly different between hyporheic water and surface water for either season (p > 0.05, Mann-Whitney U), but concentrations were higher in 2020 than 2019 (p < 0.001, Mann-Whitney U; Figure 3.4b).
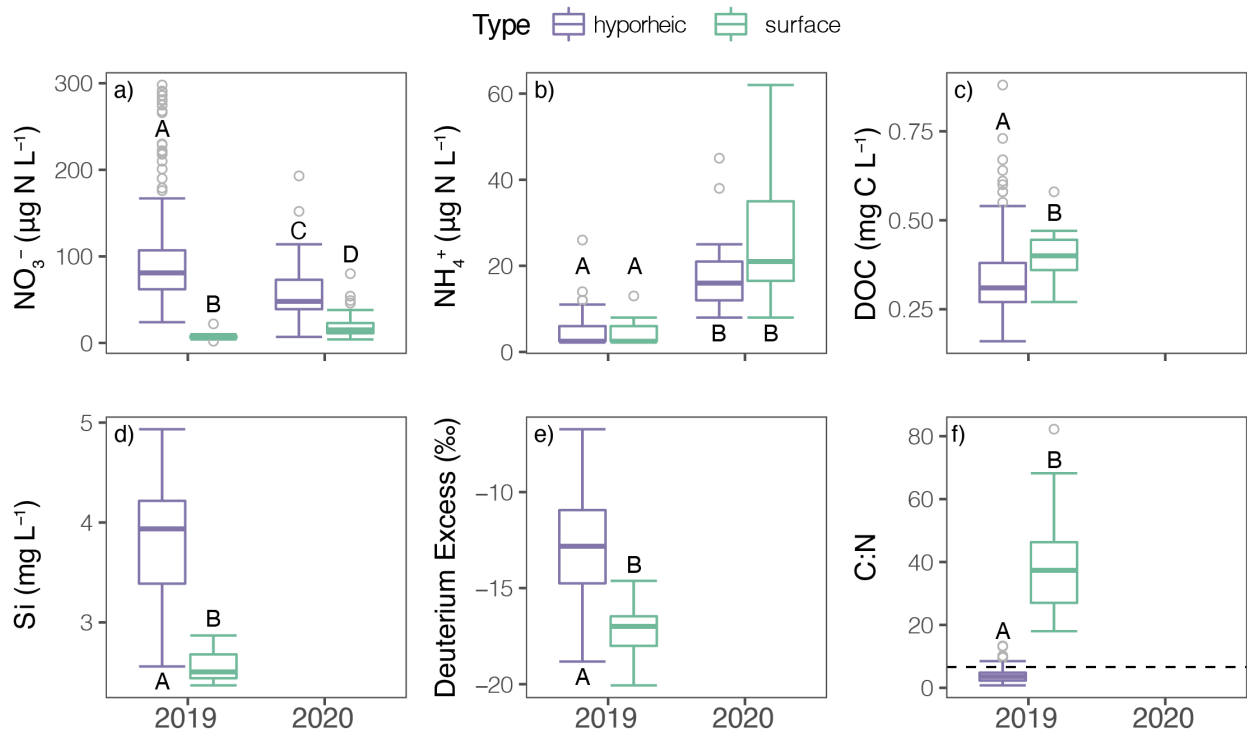
Figure 3.4. Hyporheic and surface water concentrations of (a) NO_3^-, (b) NH_4^+ (c) DOC, (d) dissolved Si, (e) deuterium excess, and (f) C:N (mg DOC mg^{-1} DIN) aggregated by flow season across transects and sites. Non-detections of NH_4^+ were replaced with half of the LOD. The dashed line in (f) represents C:N of the Redfield ratio. DOC was not measured in 2020. Uppercase letters denote significant statistical difference among groups (Mann-Whitney U, $p<0.05$).

DOC concentrations remained very low (< 0.9 mg C L^{-1}) throughout the diel sampling period in 2019 across all sites. Mean surface DOC concentrations aggregated over time across transects were higher than for hyporheic water ($p < 0.001$, Mann-Whitney U), although DOC was more variable in hyporheic samples (Figures 3.4c; S3.3). Despite the expectation that DOC would exhibit the opposite patterns compared to NO_3^-, as it is a substrate for nitrification, our sampling did not provide evidence for consistent lateral or vertical patterning of DOC concentrations in hyporheic water. This finding is likely due to the low concentrations for both solutes. Full pairwise comparisons of DOC by site within each transect are reported in Table S3.3.

Silica was significantly greater ($p < 0.001$, Wilcoxon) in hyporheic water relative to surface water for 2019 (Figure 3.4c; Table S3.4). This pattern held across all transects (Figure S3.5) and was relatively stable over time despite small variations in streamflow or increases in Si with time at low flows (Figure 3.3). Yet the magnitude of difference between hyporheic water and surface water Si concentrations was much less than for NO_3^-. Similar to NO_3^-, the lateral patterning differed between transects; Si concentrations decreased with lateral distance from the channel center for T1, but generally increased across T2 and T3. Furthermore, mean Si concentrations were greater at 30 cm than 15 cm depths except for T2 site C and T3 site D (Figure S3.5; Table S3.4).

Dissolved C:N (mg DOC mg^{-1} DIN) was significantly higher ($p < 0.001$, Mann-Whitney) for surface water samples as was variability in C:N (Figure 3.4e). In calculating DIN we replaced non-detects of NH_4^+ with half of the LOD. The mean C:N of hyporheic water was 5.5 ± 0.3 mg DOC mg^{-1} DIN, which is near a Redfield ratio of 6.6, while the mean C:N of surface water was 47.0 ± 3.9 mg DOC mg^{-1} DIN. While significant lateral and vertical differences in C:N were found within transects these patterns were much smaller than the difference between surface and hyporheic water (Figure S3.5; Table S3.6). This ratio could not be calculated for 2020 samples due to the lack of DOC data.

We found that NO_3^- concentrations were most strongly related to Si and deuterium excess, while there was not a significant relationship between NO_3^- and DOC (Figure 3.5). We predicted that remineralization of OM would drive the production of NO_3^- in the hyporheic zone (*Jones et al.*, 1995a), and, given the low DOC concentrations in these streams, we expected to find a negative correlation between DOC and NO_3^-. However, no such relationship was observed (Figure 3.5a). Across all three transects and both seasons, NO_3^- was positively correlated with Si (Figure 3.5b), indicating that NO_3^- concentrations generally increase with increasing residence time in the hyporheic zone of MDV streams. In MDV streams, more negative deuterium excess values result from evaporative fractionation (Gooseff et al., 2003). We found that NO_3^- was

positively correlated with deuterium excess (Figure 3.5c), which indicates that increasing

concentrations of NO_3^- cannot be attributed to evaporative losses of streamwater.
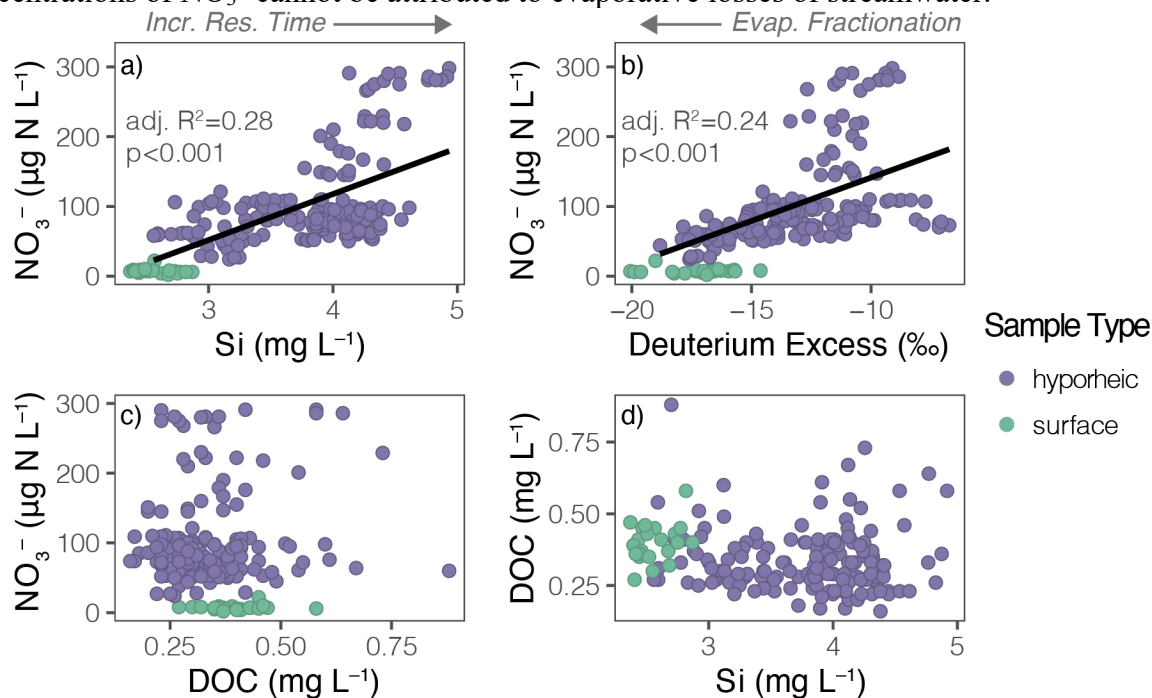
Figure 3.5. Concentrations of NO_3^- by Si, deuterium excess, and DOC (a-c, respectively) as well as DOC by Si (d). Lines denote significant linear relationships ($p<0.05$) for hyporheic water data only – surface water samples are plotted for comparison but were not included in regressions.

For all solutes in this study, C-Q relationships were largely chemostatic over streamflows ranging from 0-15.5 L s^{-1} (Figure 3.6). Power-law C-Q regressions resulted in slope (b) parameters that were not significantly different from 0 ($p>0.05$; $|b| < 0.05$ for all analytes). In all instances, hyporheic water and surface water data from this study were reflective of the range of surface water concentrations in the historic data. Hyporheic water NO_3^- concentrations were generally above the upper limits observed historically in surface water, although surface water samples from this study were similar to historic surface water data. Nitrate also exhibited notably larger variations in this study. Both NH_4^+ and DOC from this study fell well within their historic C-Q patterns. Dissolved Si exhibited similar patterns to NO_3^- insofar as hyporheic water concentrations fell at or above the upper limits observed historically in surface water, although there was notably less variation in concentrations.
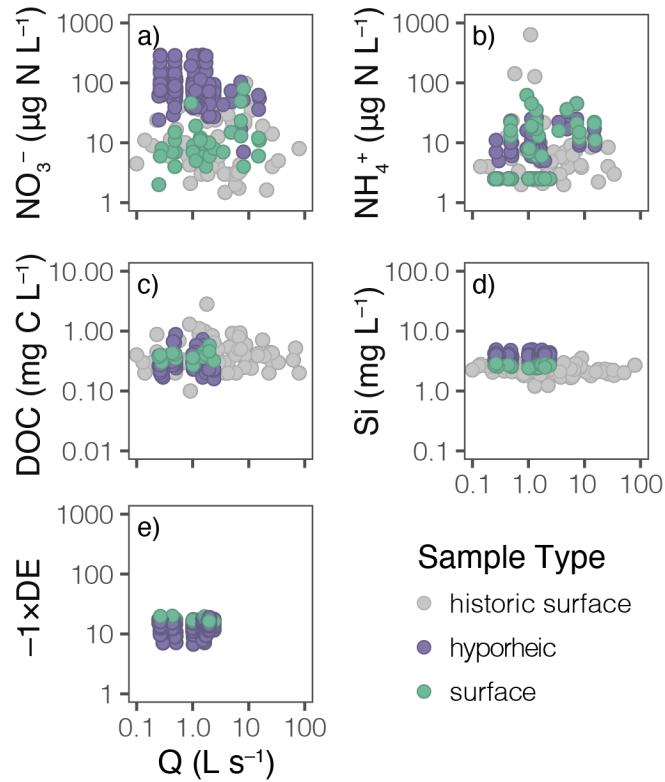
Figure 3.6. Solutes and deuterium excess C-Q relationships for hyporheic water and surface water from the present study as well as historic surface water grab sample data (1994-2018) at the Von Guerard Stream gage. Samples paired to a gage Q of 0 L s^{-1} were assigned a value of 0.01 L s^{-1} due to rating curve errors at low flows. Deuterium excess values, which are all negative, were multiplied by –1 to visualize as positive values in log-log space.

We compared relative DIN concentrations between concurrent surface and hyporheic water samples by Q over both the 2019 and 2020 season (Figure 3.7). Except for a few samples at the A sites (thalweg), DIN remained elevated in hyporheic water (DIN$_{HZ}$:DIN$_{SW}$ >>1) regardless of Q. While the data suggest weakly declining DIN$_{HZ}$:DINS$_W$ for some distal sites (C and D), the pattern is not consistent across transects and only thalweg sites were sampled during the 2019 streamflow season. These data suggest that elevated DIN in hyporheic water is both spatially and temporally ubiquitous for Von Guerard Stream.
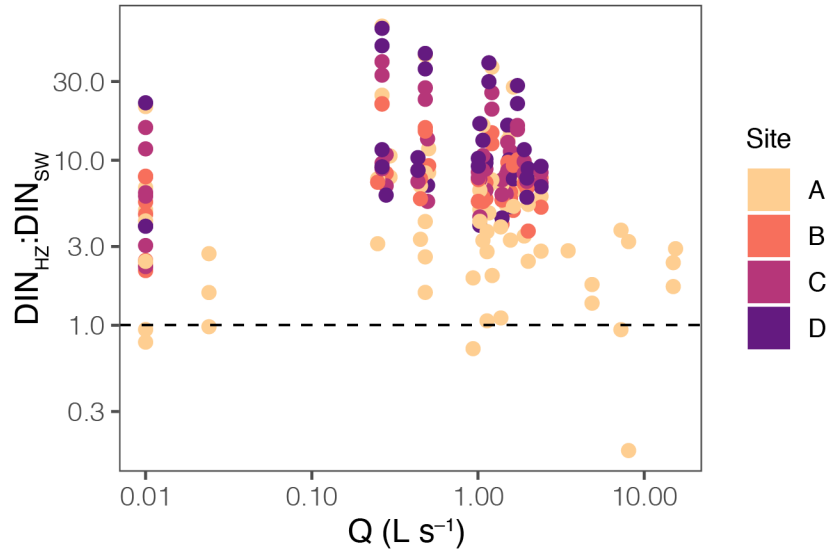
Figure 3.7. Relative DIN concentration in hyporheic water (HW) versus surface water (SW) for concurrent samples during both flow seasons. Samples paired to a gage Q of 0 L s^{-1} were assigned a value of 0.01 L s^{-1} due to rating curve errors at low flows.

We estimated the instantaneous size of DIN pools for surface water and two compartments in the hyporheic zone for depth ranges of 0–15 and 15–30 cm (Table 3.1). We utilized concentrations of NO_3^- only as NH_4^+ was below detection in most samples for 2019 and was relatively low when detected in 2020. For all three transects, the estimated mean mass of N as NO_3^- per meter of stream length was three to four orders of magnitude greater in hyporheic water than surface water.

Table 3.1. Estimated dissolved NO_3^- pools (mg NO_3^-–N m^{-1}) in surface water (SW) and hyporheic (HZ) compartments during 2019 sampling period.

	Transect 1	Transect 2	Transect 3
SW	$6.9 \times 10^{-3} \pm 3.8 \times 10^{-4}$	$4.6 \times 10^{-3} \pm 7.7 \times 10^{-4}$	$8.0 \times 10^{-3} \pm 1.5 \times 10^{-3}$
HZ (0-15 cm)	24.5 ± 17.9	42.2 ± 28.9	19.6 ± 20.5
HZ (15-30 cm)	26.8 ± 11.8	61.8 ± 24.2	21.5 ± 8.7

3.3.2 Nitrification Potential of Hyporheic Microbial Communities

We observed the accumulation of NO_2^- for all replicates from all four sites in a laboratory nitrification potential assay (Figure 3.8). Despite the extended duration of the assay (5 days), it was not clear whether the accumulation of NO_2^- had plateaued, as expected under

Michaelis-Menten kinetics. For this reason and limitations noted above (see 2.4) we did not calculate rates of nitrification. The final normalized accumulation of NO_2^- varied by more than an order of magnitude across the four collection points. For the upstream site (Figure 3.8a, more NO_2^- accumulated in the marginal location (site C) than for the center of the channel (site A), but no such difference was observed at the downstream site (Figure 3.8b).
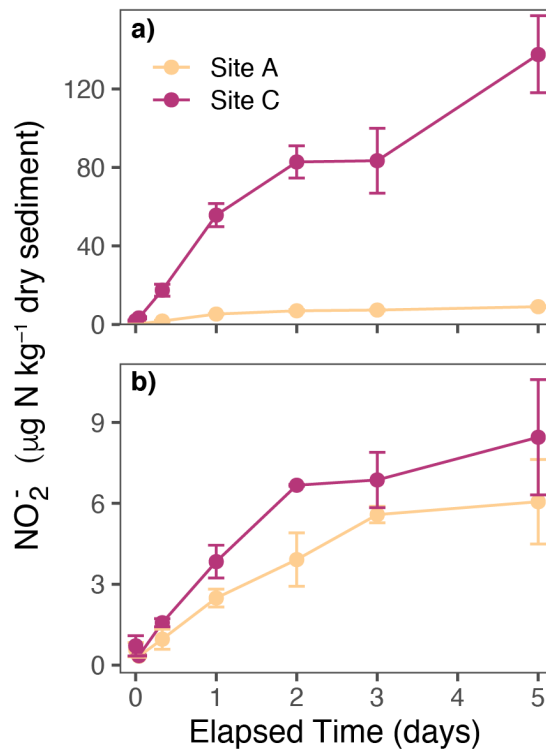
Figure 3.8. Accumulated NO_2^- normalized to sediment dry weight (mean ±1 SE, n=3) by location over time from a laboratory nitrification potential assay for (a) upper and (b) lower sediment collection locations (see Figure 3.1). Site A is located in the channel center while site C is located near the wetted margin.

3.4 Discussion

3.4.1 Hyporheic Contributions to Autochthonous N Availability

We leveraged the relative simplicity of an intermittent stream in the MDVs of Antarctica to test the hypothesis that the biological availability of remineralized autochthonous N is controlled by connectivity between the hyporheic zone and main channel due to the contrasting biogeochemical function of benthic autotrophs and hyporheic heterotrophs. Due to the lack of terrestrial vegetation, limited hillslope connectivity, and stable isotopic evidence that

autochthonous N is the predominant source of N in the lower reaches of Von Guerard Stream (*Kohler et al.*, 2018), our findings can be interpreted as signatures of autochthonous N cycling.

In particular, we found that elevated NO_3^- concentrations in the hyporheic zone (Figure 3.4) were positively related to an indicator of residence time (Si, Figure 3.5a), not due to evapo-concentration (Figure 3.5b), and there are no known subsurface influxes of water and solutes (including allochthonous DIN) via groundwater in MDV streams (Gooseff et al., 2016). Additionally, a laboratory assay demonstrated that hyporheic microbes in Von Guerard Stream possess the functional potential to carry out nitrification (Figure 3.8) – although this assay is not indicative of *in situ* rates. Therefore, we attribute the elevated NO_3^- concentrations in hyporheic water to the net remineralization and nitrification of autochthonous OM. Since much of the autochthonous OM that is mobilized and subsequently entrained in the hyporheic zone of Von Guerard Stream is predominantly sourced from *Nostoc*-dominated N-fixing benthic algal mats (Heindel et al., 2021; Kohler et al., 2018), these elevated NO_3^- concentrations reflect the role of the hyporheic zone in transforming N that is fixed within the stream corridor into readily available and mobile forms.

We found that the NO_3^- pool in the hyporheic zone is approximately three to four orders of magnitude larger than that of surface water per unit of stream length (Table 3.1), indicating a surprisingly large reservoir of mobile N for such a highly-oligotrophic system. Over both seasons, observations of elevated NO_3^- concentrations in hyporheic water were spatially and temporally persistent regardless of changing flow conditions (Figures 3.3, 3.6, and 3.7). Similarly elevated NO_3^- in hyporheic water relative to surface water was also reported in a prior study of MDV streams (McKnight et al., 2004). Surface water samples from the present study match historic surface water C-Q patterns for Von Guerard Stream, yet hyporheic water NO_3^- is at or above the upper limit for historic surface water concentrations (Figure 3.6). While the range of Q represented by our samples does not include the highest flows that occur in this stream, such high flows are relatively short-lived and our samples represent the temporally dominant state of the system (Figure S3.1). Combined with relatively high hyporheic exchange rates in the

loosely consolidated sediment of MDV streams (Cozzetto et al., 2013; Gooseff et al., 2003, 2004; Runkel, 2002; Runkel et al., 1998), these results suggest that the hyporheic zone may be a persistent net source of remineralized autochthonous N to surface water and benthic algal communities even under rapidly varying or intermittent flow.

We would expect autotrophic algal communities that are not capable of N fixation in oligotrophic systems to rapidly remove much of the DIN that returns to surface water from the hyporheic zone (Gooseff et al., 2004; Hall & Tank, 2003; McKnight et al., 2004). This is especially true for MDV streams where N-limited benthic algal mats are capable of removing all NO_3^- added above ambient conditions over short spatial and temporal scales (Gooseff et al., 2004; McKnight et al., 2004). As MDV hyporheic zones are well connected (Cozzetto et al., 2013; Gooseff et al., 2003, 2004; Runkel, 2002; Runkel et al., 1998) and hyporheic processes consequently drive surface water concentration dynamics for many solutes (Singley et al., 2017; Wlostowski et al., 2018), it is unlikely that the hyporheic zone could remain relatively enriched in NO_3^- while also acting as a net sink that prevents return fluxes of N to the main channel. In Mediterranean systems, studies have found that short-term streambed drying can promote nitrification (Gómez et al., 2012) and result in the accumulation of NO_3^-, which can then account for ~50% of NO_3^- mobilized when flow reinitiates (Merbt et al., 2016). Our study uniquely suggests that the processing and temporary storage of autochthonously-derived N could result in contributions of NO_3^- from the hyporheic zone that persist beyond brief fluxes occurring with flow re-initiation, even throughout diel-scale flow pulsing. Thus, the persistently lower NO_3^- concentration in surface water that we found (Figures 3.4 and 3.7) and longitudinal $\delta^{15}N$ patterns (Kohler et al., 2018) are more readily explained by rapid uptake of returned DIN by extensive benthic autotrophs in the main channel than by an absence of fluxes from the hyporheic N pool.

Although N cycling has been investigated in MDV streams for decades, the focus of prior work was on removal of DIN in the main channel and hyporheic zone rather than processes controlling its production from internal N and OM cycling (Gooseff et al., 2004; Koch et al., 2010; McKnight et al., 2004). Our findings complicate interpretation of MDV streams, and

intermittent streams in oligotrophic systems more generally, as functional sinks that retain or remove N (e.g., Bernal & Sabater, 2012; Dubnick et al., 2017; Schade et al., 2005). Instead, we have shown that while surface water and benthic algae may operate as strong DIN sinks, the hyporheic zone may simultaneously serve as a persistent source for DIN. Moreover, our results support prior claims based on stable isotope data (Kohler et al., 2018) that remineralization in the hyporheic zone serves as a pathway through which in-stream N fixation can subsidize downstream N availability to biota. Critically, this is dependent on hyporheic connectivity, including for the import of substrate containing N from N-fixing autotrophs (e.g., *Nostoc*-dominated benthic algal mats) (Cullis et al., 2014; Kohler et al., 2018), retention of POM in the hyporheic zone (Heindel et al., 2021), and the export of DIN to the main channel. Thus, our work necessitates a shift in the conceptualization of N cycling in MDV streams as simple N sinks to recognize the role of hyporheic connectivity in maintaining N availability to biota.

3.4.2 Additional Factors Influencing Autochthonous N Cycling

Both autochthonous N cycling and short-term intermittence (or wetted channel expansion-contraction) have received relatively little attention in previous studies, especially in combination. Based on the results of this study and prior research in both MDV and temperate streams, we discuss further factors and processes likely to be important in controlling autochthonous N cycling, especially under similar short-term hydrologic variability. For much of this section, we refer to autochthonous N simply as N (or DIN), unless otherwise necessary for clarity.

Principally, streamflow variability will influence the cycling of N through its control on benthic primary production and biomass (Datry et al., 2017) as well as hyporheic residence time. The pool of N and OM in benthic algal mats and their N uptake capacity following flood pulse events can be influenced by both the return frequency and magnitude of individual pulsing events as well as seasonal streamflow patterns (Acuña et al., 2015; Cullis et al., 2014; Kohler et al., 2015; Martí et al., 1997). Thus, we would expect streamflow variations to determine the

stability of N source pools as well as the efficiency of sink processes. Surprisingly, our data suggest that variations in streamflow did not result in a shift from transport- to reaction-limitation for remineralization and nitrification in the hyporheic zone as concentrations remained fairly stable. It is notable that, even in well-studied perennial systems, there is conflicting evidence of how hyporheic exchange scales with discharge across geomorphologies (Lee et al., 2020; Ward et al., 2012; Wondzell, 2006; Wondzell & Gooseff, 2013; Zimmer & Lautz, 2014) and how N uptake rates are affected (Webster et al., 2003), although evidence from MDV streams suggests hyporheic turnover increases during periods of higher flow (Singley et al., 2017). While we cannot constrain actual rates on any particular process from the data, it is notable that cycling of autochthonous N in the hyporheic zone of Von Guerard Stream must occur on timescales sufficiently fast to counteract transport losses, or shifts in residence time, that can occur due to successive flow pulses (*Singh et al.*, 2020). Thus, hyporheic function in MDV streams can remain relatively stable even where the timescale of persistent diel flow pulsing and intermittence is much shorter than the seasonal intermittence that dominates well studied Mediterranean streams (e.g., Arce et al., 2014; Bernal et al., 2005; Gómez et al., 2009; von Schiller et al., 2017). This stability may, in part, be due to elevated processing rates stemming from the high lability of autochthonous OM (Bertilsson & Jones, 2003) and its increasing mobilization with increasing flow via scouring (Cullis et al., 2014). Whether this balance exists in other streams characterized by short-term intermittence or pulsing remains an open but important question.

The availability of N to biota is likely further complicated by multiple organic source forms from which DIN can be derived. We found that differences in NO_3^- concentrations were not explained by changing DOC concentrations (Figure 3.5c). This is probably due to the exceedingly low concentrations as well as spatial differences in previous supply of DOC, heterogeneity in processing rates, and contributions of autochthonously-derived N in forms other than DOM. Prior studies of MDV streams have investigated some of the dynamics controlling both DON (Howard-Williams et al., 1989) and POM (Cullis et al., 2014; Heindel et al., 2021),

although the relative importance of these sources for hyporheic DIN production has not yet been investigated. N-fixing autotrophs, such as *Nostoc spp.,* are recognized as relatively leaky with respect to DIN and DON in marine and dryland systems (Glibert & Bronk, 1994; Mayland et al., 1966). Leaching of DIN and DON may increase with elevated N fixation activity (*Barr*, 1999), which can resume rapidly after rewetting (Dodds et al., 1995; McKnight et al., 2007). Nostoc mats often occupy the margins of streams due to their resistance to desiccation (Dodds et al., 1995; McKnight et al., 1999), such that channel expansion and contraction with streamflow variations will likely further control both the timing and the spatial scale over which leached N is transported. Consequently, direct leaching coupled to flow variations are another likely, albeit understudied, pathway by which N from periphyton may subsidize downstream production without POM mobilization, both in MDV streams and elsewhere.

The presence and relative concentrations of C and N species reflect the stoichiometric needs of multiple biotic communities connected by hydrologic exchange. For instance, the production of excess DIN is expected for heterotrophic microbes in the hyporheic zone due to stochiometric demands when OM is predominantly sourced from autotrophic microbes (Jones et al., 1995a). This is consistent with our finding that dissolved C:N (mg DOC mg^{-1} DIN) is significantly lower in the hyporheic zone, largely due to higher DIN concentrations. Studies in other systems have found that NH_4^+ concentrations may increase during periods of declining flow or drying, mainly due to remineralization of less labile allochthonous inputs (Acuña et al., 2005; von Schiller et al., 2011). Yet, we observed that NH_4^+ remained below detection in the majority of both hyporheic water and surface water samples in 2019 and, although concentrations were detectable in 2020, they remained much lower than those of NO_3^-. Consequently, NH_4^+ produced by remineralization of OM (as POM, DOM, or DON) in the hyporheic zone of Von Guerard Stream must be removed from solution relatively quickly. As in semi-arid and arid-land streams, one of the most likely fates for excess NH_4^+ produced by OM mineralization in transient storage is accumulation of NO_3^- via enhanced nitrification (e.g., Gómez et al., 2012; Jones et al., 1995a). The elevated NO_3^- concentrations and potential for

nitrification we observed (Figure 3.8) provide evidence that relatively rapid nitrification is a probable explanation of low NH_4^+ concentrations in this system.

Importantly, denitrification in the hyporheic zone may result in the loss of remineralized N prior to remobilization. However, there is conflicting evidence about whether streamflow intermittence promotes or inhibits denitrification (Gómez et al., 2012; Merbt et al., 2016; von Schiller et al., 2011). Provided that streamflow events are sufficiently large and frequent, we would not expect denitrification to represent a dominant process controlling the fate of accumulated NO_3^- in hyporheic water, although there is evidence that it can still contribute to N losses even in MDV streams (Gooseff et al., 2004; Maurice et al., 2002) and temperate systems characterized by diel-scale hydrologic pulsing (e.g., Knights et al., 2017). It is possible that the small but significant declines in DOC and NO_3^- at lateral and deep locations during the 2019 season (Figure 3.3) were due to denitrification, though it remains unclear how large this loss of N may be for this system. The degree to which denitrification reduces subsidies by in channel N-fixation to downstream communities, or N spiraling more generally, depends on the duration and intensity of hydrologic contraction and expansion cycles.

Ultimately, our work elucidates the role of the hyporheic zone as a source of remineralized autochthonous N. Spiraling of autochthonous N likely occurs in many streams, even though it may be obscured by large allochthonous inputs of N. The controls on hydrochemical variability and biogeochemical cycling in other intermittent and ephemeral streams is often attributed to catchment-scale factors (e.g., geology and land use) while instream factors become dominant only during flow cessation (Vidal-Abarca et al., 2004). Prior work has conceptualized such behavior as the unique 'biogeochemical heartbeat' or 'punctuated biogeochemical reactions' of intermittent and ephemeral systems (Datry et al., 2014; Jacobson & Jacobson, 2013; Larned et al., 2010), but few studies or conceptual models have focused explicitly on autochthonous N. Some traditional conceptual models of river ecosystems must be modified to include the spatiotemporal dynamics of drying as a key process governing connectivity in intermittent rivers (Allen et al., 2020). Similarly, our findings demonstrate that

conceptual models of nutrient dynamics ought to further incorporate autochthonous N (and OM) spiraling and its reliance on hyporheic connectivity, which may be important beyond periods of flow cessation.

In some systems, it may be necessary to better constrain the contributions of instream N sources and cycling to variations of surface water N, especially given the influence of biogeochemical cycling in intermittent and ephemeral systems in modulating downstream N fluxes in many mid-latitude systems (Bernal et al., 2019; Larned et al., 2010; Leigh et al., 2016; von Schiller et al., 2017). Investigating the connections between flow fluctuations and autochthonous N availability will also be increasingly necessary as climate change and intensive management of water resources drive more incidences of short-term intermittency, particularly in previously perennial streams (Krysanova et al., 2008; Larned et al., 2010; Sabater, 2008). Lastly, as N-fixing periphyton, such as the *Nostoc* in Von Guerard Stream, are globally pervasive (Dodds et al., 1995), the role of hydrologic connectivity in modulating autochthonous N cycling may exist in systems other than alpine, arid, or polar streams. For example, network expansion and contraction, which is common in humid temperate climates (Buttle et al., 2012; Jensen et al., 2017), may result in similar autochthonous N cycling processes in the uppermost reaches of headwater systems.

3.5 Conclusions

Despite decades of research on N cycling in streams, large allochthonous N inputs in many systems have obscured or impeded efforts to understand how N fixation by stream periphyton contributes to N cycling. Our study of a relatively simple stream setting (without hillslope or groundwater connectivity) in the McMurdo Dry Valleys, Antarctica, yielded evidence of nitrification following remineralization of autochthonous OM in the hyporheic zone. Our results indicate that the accumulation of remineralized N, which represents a readily-mobile N pool that can subsidize the N budget of downstream autotrophs, is sustained regardless of short-term flow variation and intermittence. Together, the results of this study complicate

simplistic interpretations of oligotrophic intermittent stream systems, and especially their

hyporheic zones—that they function strictly as N sinks. While prior studies demonstrated that

MDV hyporheic zones act as a source for many geogenic solutes (Gooseff et al., 2002), ours is

the first to show that similar hyporheic sourcing occurs for DIN via remineralization processes.

As in other systems, sink processes for N in MDV streams have been quantified (e.g., Gooseff et

al., 2004; Koch et al., 2010; McKnight et al., 2004), but DIN sourcing coupled to in-stream N

fixation remains poorly constrained. Ultimately, this work demonstrates the potential for

hyporheic connectivity both to enhance the contributions of internal N sources to nutrient

budgets in oligotrophic streams and control how tightly and in what form this material it cycles.

References

Acuña, V., Muñoz, I., Giorgi, A., Omella, M., Sabater, F., & Sabater, S. (2005). Drought and postdrought recovery cycles in an intermittent Mediterranean stream: structural and functional aspects. *Journal of the North American Benthological Society*, *24*(4), 919–933.

Acuña, V., Casellas, M., Corcoll, N., Timoner, X., & Sabater, S. (2015). Increasing extent of periods of no flow in intermittent waterways promotes heterotrophy. *Freshwater Biology*, *60*(9), 1810–1823. https://doi.org/10.1111/fwb.12612

Alexander, R. B., Boyer, E. W., Smith, R. A., Schwarz, G. E., & Moore, R. B. (2007). The role of headwater streams in downstream water quality1. *JAWRA Journal of the American Water Resources Association*, *43*(1), 41–59.

Alger, A. S. (1997). Ecological processes in a cold desert ecosystem: the abundance and species distribution of algal mats in glacial meltwater streams in Taylor Valley, Antarctica. *Occasional Paper/University of Colorado*.

Allen, D. C., Datry, T., Boersma, K. S., Bogan, M. T., Boulton, A. J., Bruno, D., et al. (2020, September 28). River ecosystem conceptual models and non-perennial rivers: A critical review. *Wiley Interdisciplinary Reviews: Water*. John Wiley and Sons Inc. https://doi.org/10.1002/wat2.1473

Arce, I. M., Sanchez-Montoya, M. D., Vidal-Abarca, M. R., Suarez, M. L., & Gomez-Velez, J. D. (2014). Implications of flow intermittency on sediment nitrogen availability and processing rates in a Mediterranean headwater stream. *Aquatic Sciences*, *76*(2), 173–186. https://doi.org/10.1007/s00027-013-0327-2

Barr, D. M. (1999). Biotic and abiotic regulation of nitrogen dynamics in biological soil crusts. Northern Arizona University.

Benjamini, Y., & Hochberg, Y. (1995). Controlling the False Discovery Rate: A Practical and

Powerful Approach to Multiple Testing. *Journal of the Royal Statistical Society: Series B (Methodological)*, *57*(1), 289–300. https://doi.org/10.1111/j.2517-6161.1995.tb02031.x

Bernal, S., & Sabater, F. (2012). Changes in discharge and solute dynamics between hillslope and valley-bottom intermittent streams. *Hydrology and Earth System Sciences*, *16*(6), 1595–1605. https://doi.org/10.5194/hess-16-1595-2012

Bernal, S., Butturini, A., & Sabater, F. (2005). Seasonal variations of dissolved nitrogen and DOC:DON ratios in an intermittent Mediterranean stream. *Biogeochemistry*, *75*(2), 351–372. https://doi.org/10.1007/s10533-005-1246-7

Bernal, S., von Schiller, D., Sabater, F., & Martí, E. (2013). Hydrological extremes modulate nutrient dynamics in mediterranean climate streams across different spatial scales. *Hydrobiologia*, *719*(1), 31–42. https://doi.org/10.1007/s10750-012-1246-2

Bernal, S., Lupon, A., Wollheim, W. M., Sabater, F., Poblador, S., & Martí, E. (2019). Supply, Demand, and In-Stream Retention of Dissolved Organic Carbon and Nitrate During Storms in Mediterranean Forested Headwater Streams. *Frontiers in Environmental Science*, *7*(May), 60. https://doi.org/10.3389/fenvs.2019.00060

Bernhardt, E. S., Blaszczak, J. R., Ficken, C. D., Fork, M. L., Kaiser, K. E., & Seybold, E. C. (2017). Control Points in Ecosystems: Moving Beyond the Hot Spot Hot Moment Concept. *Ecosystems*, *20*(4), 665–682. https://doi.org/10.1007/s10021-016-0103-y

Bernot, M. J., & Dodds, W. K. (2005, June 28). Nitrogen retention, removal, and saturation in lotic ecosystems. *Ecosystems*. Springer. https://doi.org/10.1007/s10021-003-0143-y

Bertilsson, S., & Jones, J. B. (2003). Supply of Dissolved Organic Matter to Aquatic Ecosystems: Autochthonous Sources. In S. E. G. Findlay & R. L. Sinsabaugh (Eds.), *Aquatic Ecosystems - Interactivity of Dissolved Organic Matter* (pp. 3–24). Academic Press.

Bockheim, J. G., Campbell, I. B., & McLeod, M. (2007). Permafrost distribution and active-layer depths in the McMurdo Dry valleys, Antarctica. *Permafrost and Periglacial Processes*, *18*(3), 217–227.

Boyer, E. W., Goodale, C. L., Jaworski, N. A., & Howarth, R. W. (2002). Anthropogenic nitrogen sources and relationships to riverine nitrogen export in the northeastern USA. In *The Nitrogen Cycle at Regional to Global Scales* (pp. 137–169). Springer.

Briggs, M. A., Lautz, L. K., & Hare, D. K. (2014). Residence time control on hot moments of net nitrate production and uptake in the hyporheic zone. *Hydrological Processes*, *28*(11), 3741–3751.

Briggs, M. A., Day-Lewis, F. D., Zarnetske, J. P., & Harvey, J. W. (2015). A physical explanation for the development of redox microzones in hyporheic flow. *Geophysical Research Letters*, *42*(11), 4402–4410. https://doi.org/10.1002/2015GL064200

Buttle, J. M., Boon, S., Peters, D. L., Spence, C., (Ilja) van Meerveld, H. J., & Whitfield, P. H. (2012). An Overview of Temporary Stream Hydrology in Canada. *Canadian Water Resources Journal / Revue Canadienne Des Ressources Hydriques*, *37*(4), 279–310. https://doi.org/10.4296/cwrj2011-903

Conovitz, P. A., MacDonald, L. H., & McKnight, D. M. (2006). Spatial and temporal active layer dynamics along three glacial meltwater streams in the McMurdo Dry Valleys, Antarctica. *Arctic, Antarctic, and Alpine Research*, *38*(1), 42–53.

Cozzetto, K. D., Bencala, K. E., Gooseff, M. N., & McKnight, D. M. (2013). The influence of stream thermal regimes and preferential flow paths on hyporheic exchange in a glacial meltwater stream. *Water Resources Research*, *49*(9), 5552–5569.

Cullis, J. D. S., Stanish, L. F., & McKnight, D. M. (2014). Diel flow pulses drive particulate organic matter transport from microbial mats in a glacial meltwater stream in the McMurdo Dry Valleys. *Water Resources Research*, *50*(1), 86–97. https://doi.org/10.1002/2013WR014061

Dahm, C. N., Baker, M. A., Moore, D. I., & Thibault, J. R. (2003). Coupled biogeochemical and hydrological responses of streams and rivers to drought. *Freshwater Biology*, *48*(7), 1219–1231.

Datry, T., Larned, S. T., & Tockner, K. (2014). Intermittent Rivers: A Challenge for Freshwater Ecology. *BioScience*, *64*(3), 229–235. https://doi.org/10.1093/biosci/bit027

Datry, T., Bonada, N., Boulton, A. J., Datry, T., Bonada, N., & Boulton, A. J. (2017). *Intermittent Rivers and Ephemeral Streams - Ecology and Management*. Cambridge, MA, United States: Academic Press.

Davidson, E. A., David, M. B., Galloway, J. N., Goodale, C. L., Haeuber, R., Harrison, J. A., et al. (2011). Excess nitrogen in the US environment: trends, risks, and solutions. *Issues in Ecology*, (15).

Dodds, W. K. (2006). Eutrophication and trophic state in rivers and streams. In *Limnology and Oceanography* (Vol. 51, pp. 671–680). John Wiley & Sons, Ltd. https://doi.org/10.4319/lo.2006.51.1_part_2.0671

Dodds, W. K., & Jones, R. D. (1987). Potential Rates of Nitrification and Denitrification in an Oligotrophic Freshwater Sediment System. *Microbial Ecology*, *14*, 91–100.

Dodds, W. K., Gudder, D. A., & Mollenhauer, D. (1995). The Ecology of Nostoc. *Journal of Phycology*, *31*(1), 2–18. https://doi.org/10.1111/j.0022-3646.1995.00002.x

Dubnick, A., Wadham, J. L., Tranter, M., Sharp, M., Orwin, J., Barker, J., et al. (2017). Trickle or treat: The dynamics of nutrient export from polar glaciers. *Hydrological Processes*, *31*(9), 1776–1789. https://doi.org/10.1002/hyp.11149

Fellman, J. B., Dogramaci, S., Skrzypek, G., Dodson, W., & Grierson, P. F. (2011). Hydrologic

control of dissolved organic matter biogeochemistry in pools of a subtropical dryland river. *Water Resources Research*, *47*(6). https://doi.org/10.1029/2010WR010275

Fenoglio, S., Bo, T., Cammarata, M., López-Rodríguez, M. J., & Tierno De Figueroa, J. M. (2015). Seasonal variation of allochthonous and autochthonous energy inputs in an Alpine stream. *Journal of Limnology*, *74*(2), 272–277. https://doi.org/10.4081/jlimnol.2014.1082

Fountain, A. G., Nylen, T. H., Monaghan, A., Basagic, H. J., & Bromwich, D. (2010). Snow in the McMurdo Dry Valleys, Antarctica. *International Journal of Climatology*, *30*(5), 633–642.

Fowler, D., Coyle, M., Skiba, U., Sutton, M. A., Cape, J. N., Reis, S., et al. (2013). The global nitrogen cycle in the Twentyfirst century. *Philosophical Transactions of the Royal Society B: Biological Sciences*, *368*(1621). https://doi.org/10.1098/rstb.2013.0164

Glibert, P. M., & Bronk, D. A. (1994). Release of dissolved organic nitrogen by marine diazotrophic cyanobacteria, Trichodesmium spp. *Applied and Environmental Microbiology*, *60*(11), 3996–4000. https://doi.org/10.1128/aem.60.11.3996-4000.1994

Gómez, R., García, V., Vidal-Abarca, M. R., & Suárez, L. (2009). Effect of intermittency on N spatial variability in an arid Mediterranean stream. *Journal of the North American Benthological Society*, *28*(3), 572–583.

Gómez, R., Arce, I. M., Sánchez, J. J., & del Mar Sánchez-Montoya, M. (2012). The effects of drying on sediment nitrogen content in a Mediterranean intermittent stream: A microcosms study. *Hydrobiologia*, *679*(1), 43–59. https://doi.org/10.1007/s10750-011-0854-6

Gooseff, M. N., & McKnight, D. M. (2019). McMurdo Dry Valleys LTER: High frequency seasonal stream gauge measurements from Von Guerard Stream at F6 in Taylor Valley, Antarctica from 1990 to present. https://doi.org/https://doi.org/10.6073/pasta/b452c7c780079060e0cd17db08f6089e

Gooseff, M. N., McKnight, D. M., Lyons, W. B., & Blum, A. E. (2002). Weathering reactions and hyporheic exchange controls on stream water chemistry in a glacial meltwater stream in the McMurdo Dry Valleys. *Water Resources Research*, *38*(12), 15-1-15–17. https://doi.org/10.1029/2001WR000834

Gooseff, M. N., McKnight, D. M., Runkel, R. L., & Vaughn, B. H. (2003). Determining long time-scale hyporheic zone flow paths in Antarctic streams. *Hydrological Processes*, *17*(9), 1691–1710. https://doi.org/10.1002/hyp.1210

Gooseff, M. N., McKnight, D. M., Runkel, R. L., & Duff, J. H. (2004). Denitrification and hydrologic transient storage in a glacial meltwater stream, McMurdo Dry Valleys, Antarctica. *Limnology and Oceanography*, *49*(5), 1884–1895.

Gooseff, M. N., Wlostowski, A. N., McKnight, D. M., & Jaros, C. (2016). Hydrologic connectivity and implications for ecosystem processes-Lessons from naked watersheds. *Geomorphology*.

Grimm, N. B., & Petrone, K. C. (1997). Nitrogen fixation in a desert stream ecosystem. *Biogeochemistry*, *37*(1), 33–61. https://doi.org/10.1023/A:1005798410819

Hall, R. O., & Tank, J. L. (2003). Ecosystem metabolism controls nitrogen uptake in streams in Grand Teton National Park, Wyoming. *Limnology and Oceanography*, *48*(3), 1120–1128. https://doi.org/10.4319/lo.2003.48.3.1120

Hamilton, S. K., Tank, J. L., Raikow, D. F., Siler, E. R., Dorn, N. J., & Leonard, N. E. (2004). The role of instream vs allochthonous N in stream food webs: modeling the results of an isotope addition experiment. *Journal of the North American Benthological Society*, *23*(3), 429–448. https://doi.org/10.1899/0887-3593(2004)023<0429:TROIVA>2.0.CO;2

Harvey, J. W., Bohlke, J. K., Voytek, M. A., Scott, D. T., & Tobias, C. R. (2013). Hyporheic zone denitrification: Controls on effective reaction depth and contribution to whole-stream mass balance. *Water Resources Research*, *49*(10), 6298–6316. https://doi.org/10.1002/wrcr.20492

Harvey, J. W., Gomez-Velez, J. D., Schmadel, N. M., Scott, D. T., Boyer, E., Alexander, R. B., et al. (2018, April 9). How Hydrologic Connectivity Regulates Water Quality in River Corridors. *Journal of the American Water Resources Association*, pp. 369–381. https://doi.org/10.1111/1752-1688.12691

Heindel, R. C., Bergstrom, A. J., Singley, J. G., McKnight, D. M., Darling, J., Lukkari, B., et al. (2021). Diatoms trace the retention and processing of organic matter in hyporheic sediments in the McMurdo Dry Valleys, Antarctica. *Journal of Geophysical Research-Biogeosciences*. https://doi.org/10.1029/2020JG006097

Hopkins, D. W., Sparrow, A. D., Elberling, B., Gregorich, E. G., Novis, P. M., Greenfield, L. G., & Tilston, E. L. (2006). Carbon, nitrogen and temperature controls on microbial activity in soils from an Antarctic dry valley. *Soil Biology and Biochemistry*, *38*(10), 3130–3140. https://doi.org/10.1016/j.soilbio.2006.01.012

Horne, A. J., & Carmiggelt, C. J. W. (1975). Algal nitrogen fixation in Californian streams: seasonal cycles. *Freshwater Biology*, *5*(5), 461–470. https://doi.org/10.1111/j.1365-2427.1975.tb00148.x

Howard-Williams, C., Priscu, J. C., & Vincent, W. F. (1989). Nitrogen dynamics in two antarctic streams. *Hydrobiologia*, *172*(1), 51–61. https://doi.org/10.1007/BF00031612

Jacobson, P. J., & Jacobson, K. M. (2013). Hydrologic controls of physical and ecological processes in Namib Desert ephemeral rivers: Implications for conservation and management. *Journal of Arid Environments*, *93*, 80–93. https://doi.org/10.1016/j.jaridenv.2012.01.010

Jensen, C. K., McGuire, K. J., & Prince, P. S. (2017). Headwater stream length dynamics across four physiographic provinces of the Appalachian Highlands. *Hydrological Processes*.

Jones, J. B., Fisher, S. G., & Grimm, N. B. (1995a). Nitrification in the Hyporheic Zone of a

Desert Stream Ecosystem. *Journal of the North American Benthological Society*, *14*(2), 249–258. https://doi.org/10.2307/1467777

Jones, J. B., Fisher, S. G., & Grimm, N. B. (1995b). Vertical hydrologic exchange and ecosystem metabolism in a Sonoran Desert stream. *Ecology*, *76*(3), 942–952.

Kemp, M. J., & Dodds, W. K. (2001). Centimeter-scale patterns in dissolved oxygen and nitrification rates in a prairie stream. *Journal of the North American Benthological Society*, *20*(3), 347–357. https://doi.org/10.2307/1468033

Kemp, M. J., & Dodds, W. K. (2002). Comparisons of nitrification and denitrification in prairie and agriculturally influenced streams. *Ecological Applications*, *12*(4), 998–1009. https://doi.org/10.1890/1051-0761(2002)012[0998:CONADI]2.0.CO;2

Knights, D., Sawyer, A. H., Barnes, R. T., Musial, C. T., & Bray, S. (2017). Tidal controls on riverbed denitrification along a tidal freshwater zone. *Water Resources Research*, *53*(1), 799–816. https://doi.org/10.1002/2016WR019405

Koch, J. C., McKnight, D. M., & Baeseman, J. L. (2010). Effect of unsteady flow on nitrate loss in an oligotrophic, glacial meltwater stream. *Journal of Geophysical Research-Biogeosciences*, *115*(G1), G01001. https://doi.org/10.1029/2009jg001030

Kohler, T. J., Stanish, L. F., Crisp, S. W., Koch, J. C., Liptzin, D., Baeseman, J. L., & McKnight, D. M. (2015). Life in the main channel: long-term hydrologic control of microbial mat abundance in McMurdo Dry Valley streams, Antarctica. *Ecosystems*, *18*(2), 310–327.

Kohler, T. J., Stanish, L. F., Liptzin, D., Barrett, J. E., & McKnight, D. M. (2018). Catch and release: Hyporheic retention and mineralization of N-fixing Nostoc sustains downstream microbial mat biomass in two polar desert streams. *Limnology and Oceanography Letters*. https://doi.org/10.1002/lol2.10087

Krysanova, V., Vetter, T., & Hattermann, F. (2008). Detection of change in drought frequency in the Elbe basin: comparison of three methods. *Hydrological Sciences Journal*, *53*(3), 519–537.

Kunza, L. A., & Hall, R. O. (2014). Nitrogen fixation can exceed inorganic nitrogen uptake fluxes in oligotrophic streams. *Biogeochemistry*, *121*(3), 537–549.

Lansdown, K., Heppell, C. M., Trimmer, M., Binley, A. M., Heathwaite, A. L., Byrne, P., & Zhang, H. (2015). The interplay between transport and reaction rates as controls on nitrate attenuation in permeable, streambed sediments. *Journal of Geophysical Research G: Biogeosciences*, *120*(6), 1093–1109. https://doi.org/10.1002/2014JG002874

Larned, S. T., Datry, T., Arscott, D. B., & Tockner, K. (2010). Emerging concepts in temporary-river ecology. *Freshwater Biology*, *55*(4), 717–738.

Lee, A., Aubeneau, A. F., & Cardenas, M. B. (2020). The Sensitivity of Hyporheic Exchange to Fractal Properties of Riverbeds. *Water Resources Research*, *56*(5).

https://doi.org/10.1029/2019WR026560

Leigh, C., Boulton, A. J., Courtwright, J. L., Fritz, K., May, C. L., Walker, R. H., & Datry, T. (2016). Ecological research and management of intermittent rivers: an historical review and future directions. *Freshwater Biology*, *61*(8), 1181–1199. https://doi.org/10.1111/fwb.12646

Levy, J. S. (2013). How big are the McMurdo Dry Valleys? Estimating ice-free area using Landsat image data. *Antarctic Science*, *25*(01), 119–120.

Lyons, W. B. (2015). McMurdo Dry Valleys Stream Nutrients (nitrate, nitrite, ammonium, reactive phosphorus). *Environmental Data Initiative*. https://doi.org/10.6073/pasta/81cfcad244f7d3f6a6fcdab83ea75849

Marcarelli, A. M., & Wurtsbaugh, W. A. (2006). Temperature and nutrient supply interact to control nitrogen fixation in oligotrophic streams: An experimental examination. *Limnology and Oceanography*, *51*(5), 2278–2289. https://doi.org/10.4319/lo.2006.51.5.2278

Marcarelli, A. M., Baker, M. A., & Wurtsbaugh, W. A. (2008, March 1). Is in-stream N2 fixation an important N source for benthic communities and stream ecosystems? *Journal of the North American Benthological Society*. Society for Freshwater Science. https://doi.org/10.1899/07-027.1

Martí, E., Grimm, N. B., & Fisher, S. G. (1997). Pre-and post-flood retention efficiency of nitrogen in a Sonoran Desert stream. *Journal of the North American Benthological Society*, *16*(4), 805–819.

Maurice, P. A., McKnight, D. M., Leff, L., Fulghum, J. E., & Gooseff, M. N. (2002). Direct observations of aluminosilicate weathering in the hyporheic zone of an Antarctic Dry Valley stream. *Geochimica et Cosmochimica Acta*, *66*(8), 1335–1347.

Mayland, H. F., McIntosh, T. H., & Fuller, W. H. (1966). Fixation of Isotopic Nitrogen on a Semiarid Soil by Algal Crust Organisms. *Soil Science Society of America Journal*, *30*(1), 56–60. https://doi.org/10.2136/sssaj1966.03615995003000010022x

McKnight, D. M., Niyogi, D. K., Alger, A. S., Bomblies, A., Conovitz, P. A., & Tate, C. M. (1999). Dry valley streams in Antarctica: ecosystems waiting for water. *BioScience*, *49*(12), 985–995.

McKnight, D. M., Runkel, R. L., Tate, C. M., Duff, J. H., & Moorhead, D. L. (2004). Inorganic N and P dynamics of Antarctic glacial meltwater streams as controlled by hyporheic exchange and benthic autotrophic communities. *Journal of the North American Benthological Society*, *23*(2), 171–188.

McKnight, D. M., Tate, C. M., Andrews, E. D., Niyogi, D. K., Cozzetto, K. D., Welch, K. A., et al. (2007). Reactivation of a cryptobiotic stream ecosystem in the McMurdo Dry Valleys, Antarctica: a long-term geomorphological experiment. *Geomorphology*, *89*(1), 186–204.

Mendoza-Lera, C., Ribot, M., Foulquier, A., Martí, E., Bonnineau, C., Breil, P., & Datry, T.

(2019). Exploring the role of hydraulic conductivity on the contribution of the hyporheic zone to in-stream nitrogen uptake. *Ecohydrology*, *12*(7). https://doi.org/10.1002/eco.2139

Merbt, S. N., Proia, L., Prosser, J. I., Martí, E., Casamayor, E. O., & von Schiller, D. (2016). Stream drying drives microbial ammonia oxidation and first-flush nitrate export. *Ecology*, *97*(9), 2192–2198. https://doi.org/10.1002/ecy.1486

Mulholland, P. J., Helton, A. M., Poole, G. C., Hall, R. O., Hamilton, S. K., Peterson, B. J., et al. (2008). Stream denitrification across biomes and its response to anthropogenic nitrate loading. *Nature*, *452*(7184), 202–205. https://doi.org/10.1038/nature06686

Oviedo-Vargas, D., Royer, T. V., & Johnson, L. T. (2013). Dissolved organic carbon manipulation reveals coupled cycling of carbon, nitrogen, and phosphorus in a nitrogen-rich stream. *Limnology and Oceanography*, *58*(4), 1196–1206. https://doi.org/10.4319/lo.2013.58.4.1196

Robinson, C. T., Tonolla, D., Imhof, B., Vukelic, R., & Uehlinger, U. (2016). Flow intermittency, physico-chemistry and function of headwater streams in an Alpine glacial catchment. *Aquatic Sciences*, *78*(2), 327–341.

Runkel, R. L. (2002). A new metric for determining the importance of transient storage. *Journal of the North American Benthological Society*, *21*(4), 529–543. https://doi.org/10.2307/1468428

Runkel, R. L., McKnight, D. M., & Andrews, E. D. (1998). Analysis of transient storage subject to unsteady flow: diel flow variation in an Antarctic stream. *Journal of the North American Benthological Society*, 143–154.

Sabater, S. (2008). Alterations of the global water cycle and their effects on river structure, function and services. *Freshwater Reviews*, *1*(1), 75–88.

Schade, J. D., Welter, J. R., Martí, E., & Grimm, N. B. (2005). Hydrologic exchange and N uptake by riparian vegetation in an arid-land stream. *Journal of the North American Benthological Society*, *24*(1), 19–28. https://doi.org/10.1899/0887-3593(2005)024<0019:HEANUB>2.0.CO;2

von Schiller, D., Acuña, V., Graeber, D., Martí, E., Ribot, M., Sabater, S., et al. (2011). Contraction, fragmentation and expansion dynamics determine nutrient availability in a Mediterranean forest stream. *Aquatic Sciences*, *73*(4), 485. https://doi.org/10.1007/s00027-011-0195-6

von Schiller, D., Bernal, S., Dahm, C. N., & Martí, E. (2017). Nutrient and Organic Matter Dynamics in Intermittent Rivers and Ephemeral Streams. *Intermittent Rivers and Ephemeral Streams*, 135–160. https://doi.org/10.1016/B978-0-12-803835-2.00006-1

Schmidt, E. L., & Belser, L. W. (1994). Autotrophic Nitrifying Bacteria. In P. S. Bottomley, J. S. Angle, & R. W. Weaver (Eds.), *Methods of Soil Analysis: Part 2 – Microbiological and Biochemical Properties* (pp. 159–177). Madison, WI: Soil Science Society of America.

https://doi.org/10.2136/sssabookser5.2.c10

Singh, T., Gomez-Velez, J. D., Wu, L., Wörman, A., Hannah, D. M., & Krause, S. (2020). Effects of Successive Peak Flow Events on Hyporheic Exchange and Residence Times. *Water Resources Research*, *56*(8). https://doi.org/10.1029/2020WR027113

Singley, J. G., Wlostowski, A. N., Bergstrom, A. J., Sokol, E. R., Torrens, C. L., Jaros, C., et al. (2017). Characterizing hyporheic exchange processes using high-frequency electrical conductivity-discharge relationships on subhourly to interannual timescales. *Water Resources Research*, *53*(5), 4124–4141. https://doi.org/10.1002/2016WR019739

Singley, J. G., Gooseff, M. N., McKnight, D. M., & Hinckley, E.-L. S. (2021). Surface and hyporheic porewater chemistry and sediment nitrification potentials in Von Guerard Stream, McMurdo Dry Valleys, Antarctica (2018-2020) ver 2. Environmental Data Initiative. https://doi.org/10.6073/pasta/d6e4301bf93fba0fef6fd5c33a092aaf

Stream Solute Workshop. (1990). Concepts and methods for assessing solute dynamics in stream ecosystems. *Journal of the North American Benthological Society*, *9*(2), 95–119. https://doi.org/10.2307/1467445

Tank, J. L., Rosi-Marshall, E. J., Griffiths, N. A., Entrekin, S. A., & Stephen, M. L. (2010). A review of allochthonous organic matter dynamics and metabolism in streams. *Journal of the North American Benthological Society*, *29*(1), 118–146. https://doi.org/10.1899/08-170.1

Taylor, J. R. (1997). *An Introduction to Error Analysis: The Study of Uncertainties in Physical Measurements* (2nd ed.). Sausalito, CA: University Science Books.

Vidal-Abarca, M. R., Gómez, R., & Suarez, M. L. (2004). Los ríos de las regiones semiáridas. *Revista Ecosistemas*, *13*(1), 15–28.

Ward, A. S., Fitzgerald, M., Gooseff, M. N., Voltz, T. J., Binley, A. M., & Singha, K. (2012). Hydrologic and geomorphic controls on hyporheic exchange during base flow recession in a headwater mountain stream. *Water Resources Research*, *48*(4), 4513. https://doi.org/10.1029/2011WR011461

Webster, J. R., Mulholland, P. J., Tank, J. L., Valett, H. M., Dodds, W. K., Peterson, B. J., Bowden, W. B., Dahm, C. N., Findlay, S. E. G., & Gregory, S. V. (2003). Factors affecting ammonium uptake in streams–an inter-biome perspective. *Freshwater Biology*, *48*(8), 1329–1352.

Webster, J. R., Mulholland, P. J., Tank, J. L., Valett, H. M., Dodds, W. K., Peterson, B. J., Bowden, W. B., Dahm, C. N., Findlay, S., Gregory, S. V., et al. (2003). Factors affecting ammonium uptake in streams - an inter-biome perspective. *Freshwater Biology*, *48*(8), 1329–1352. https://doi.org/10.1046/j.1365-2427.2003.01094.x

Wlostowski, A. N., Gooseff, M. N., McKnight, D. M., Jaros, C., & Lyons, W. B. (2016). Patterns of hydrologic connectivity in the McMurdo Dry Valleys, Antarctica: a synthesis of 20 years of hydrologic data. *Hydrological Processes*, *30*, 2958– 2975.

https://doi.org/10.1002/hyp.10818

Wlostowski, A. N., Gooseff, M. N., & Adams, B. J. (2018). Soil Moisture Controls the Thermal Habitat of Active Layer Soils in the McMurdo Dry Valleys, Antarctica. *Journal of Geophysical Research: Biogeosciences*, *123*(1), 46–59. https://doi.org/10.1002/2017JG004018

Wlostowski, A. N., Gooseff, M. N., McKnight, D. M., & Lyons, W. B. (2018). Transit Times and Rapid Chemical Equilibrium Explain Chemostasis in Glacial Meltwater Streams in the McMurdo Dry Valleys, Antarctica. *Geophysical Research Letters*, *45*(24), 13,322-13,331. https://doi.org/10.1029/2018GL080369

Wondzell, S. M. (2006). Effect of morphology and discharge on hyporheic exchange flows in two small streams in the Cascade Mountains of Oregon, USA. *Hydrological Processes*, *20*(2), 267–287. https://doi.org/10.1002/hyp.5902

Wondzell, S. M., & Gooseff, M. N. (2013). 9.13 Geomorphic controls on hyporheic exchange across scales: Watersheds to particles. *Treatise on Geomorphology*, 203–218.

Zarnetske, J. P., Haggerty, R., Wondzell, S. M., & Baker, M. A. (2011). Dynamics of nitrate production and removal as a function of residence time in the hyporheic zone. *Journal of Geophysical Research-Biogeosciences*, *116*. https://doi.org/10.1029/2010jg001356

Zarnetske, J. P., Haggerty, R., Wondzell, S. M., Bokil, V. A., & González-Pinzón, R. (2012). Coupled transport and reaction kinetics control the nitrate source-sink function of hyporheic zones. *Water Resources Research*, *48*(11). https://doi.org/10.1029/2012WR011894

Zimmer, M. A., & Lautz, L. K. (2014). Temporal and spatial response of hyporheic zone geochemistry to a storm event. *Hydrological Processes*, *28*(4), 2324–2337. https://doi.org/10.1002/hyp.9778

Chapter IV

Differentiating Physical and Biological Storage of Nitrogen Along an Intermittent Antarctic Stream Corridor

4.1. Introduction

Biogeochemical processes in small headwater streams modulate nutrient concentrations and exert a strong influence on nutrient fluxes to downstream ecosystems (Peterson et al. 2001, Alexander et al. 2007). Much of the research on biogeochemical cycling within streams has focused on the retention of nutrients, especially nitrogen (N) sources from the surrounding landscape (e.g., Boyer et al. 2002, Duncan et al. 2015, Drummond et al. 2016). Quantification of N retention in streams has centered on relationships between hydrologic connectivity and biogeochemical reactions rates (Gomez-Velez et al. 2015, Harvey et al. 2018) or a simple mass balance approach wherein retention is a residual term between input and output fluxes (Burns 1998, Seitzinger et al. 2006). These flux- or transport-centric approaches have not documented the extent of N storage within stream corridors, especially intermittent streams and oligotrophic environments with low allochthonous N inputs.

Unlike in terrestrial biogeochemistry, where the importance of particular N cycling processes are frequently contextualized by the relative sizes of coupled pools and fluxes (Vitousek and Reiners 1975, Aber et al. 1989, 1998, Lovett and Goodale 2011), only a few studies of streams have actually quantified N pools in stream corridors. In temperate forested systems > 90% of N storage is in the form of allochthonous detritus (Triska et al. 1984, Naiman and Melillo 1984). In contrast, Grimm (1987) found that more than 90% of N storage in a desert stream is in autochthonous detritus, although area normalized N storage was lower than in forested systems (3-9 g/m^2 compared to 12-22 g/m^2). These few studies demonstrate that the form, magnitude, and temporal stability of N storage depends heavily on system characteristics including organic matter (OM) sourcing, hydrologic variability, and net metabolic status.

Storage of N in any particular stream occurs through both physical and biological mechanisms (Naiman and Melillo 1984, Triska et al. 1984, Grimm et al. 1987). Biotic

assimilation into periphyton biomass was more important than denitrification in the stream

benthos in temporarily removing N stream during nutrient uptake experiments (O'Brien et al.

2012). Most studies of N retention by such biological uptake characterize spatial and temporal

variations in small-scale area normalized periphyton biomass (i.e., mg Chlorophyll a/cm^2) in

response to environmental conditions or nutrient availability (e.g., Horner and Welch 1981,

Stelzer and Lamberti 2001, von Schiller et al. 2007, Koch et al. 2018). Focus on area normalized

biomass has ensured comparability of results at small scales among systems and allowed for

cross-system synthesis (e.g., Dodds et al. 2002). But apart from the few whole stream N budget

studies, biomass, or the N contained therein, is never scaled along entire reaches. Such scaling is

hampered by the inherently patchy distribution of periphyton, especially due to physical

disturbance (i.e., scouring with flood pulses) or grazing processes (Hillebrand 2008, Luce et al.

2010). Yet, scaling N and biomass pools across an entire reach would permit benchmarking of

stored mass against total seasonal or annual fluxes.

Apart from algal biomass in the stream, N can be transiently stored by physical processes

in the hyporheic zone such as sorption to sediment (Triska et al. 1994), entrainment of particulate

organic matter (POM) (Triska et al. 1984, Heindel et al. 2021a), and in dissolved form in

interstitial waters (Grimm 1987, Bernhardt et al. 2005). As with total storage, the relative

magnitude and stability of these storage mechanisms at the reach-scale is understudied but likely

varies due to climate and flow regime. For example, it is known that ammonium (NH_4^+) sorption

can compete with biotic uptake (Triska et al. 1994) in temperate systems, but the conditions

under which sorption is reversible and the size of sorbed NH_4^+ pools remain poorly characterized

in most streams. This knowledge gap is particularly relevant to intermittent streams that can be

subject to rapidly changing ionic concentrations and fluid conductivities (Datry et al. 2017),

which could theoretically alter cation exchange dynamics governing NH_4^+ sorption. The

hyporheic zone can also entrain POM (which contains N) but this storage is also transient due to

mineralization and remobilization processes (Bernhardt et al. 2005, Burrows et al. 2017), which

vary widely as a function of the climatic characteristics (especially temperature and annual

precipitation) of intermittent stream systems (Shumilova et al. 2019). Lastly, N storage as dissolved solutes in the stream corridor, mainly in interstitial waters of hyporheic and riparian areas, is potentially even more transient due to relatively rapid turnover resulting from hydrologic exchange flows. In intermittent streams, much longer residence times result from diminished surface flow such that transient storage in the hyporheic zone may actually occur over longer timescales and with greater variations in space (Gómez et al. 2009). Therefore, the importance of particular N retention mechanisms may differ between perennial and intermittent streams.

Proglacial intermittent streams of the McMurdo Dry Valleys (MDVs), Antarctica, are often invoked as an ideal natural setting to investigate coupled physical and biological stream corridor processes (McKnight et al. 2015). Even in a cold and hyper-arid environment that is devoid of high-order plants and allochthonous OM inputs, cyanobacteria algal mats cover extensive portions of streambeds (Alger 1997, McKnight et al. 1999). Along with heterotrophic microbes in the hyporheic and parafluvial zones, these mats contribute to biogeochemical cycling of N (Koch et al. 2010, Kohler et al. 2018; Singley et al. 2021a) including relatively rapid N removal from surface water (Gooseff et al. 2004b, McKnight et al. 2004) and N fixation (Howard-Williams et al. 1989, McKnight et al. 2007). The hyporheic zone of MDV streams contain elevated concentrations of dissolved and sorbed N (Heindel et al. 2021a, Singley et al. 2021a) and autochthonous OM in various states of decomposition (Heindel et al. 2021a). A prior study of the stable isotopic composition of mat biomass indicated that N-fixed within the stream corridor supplants N inputs from glacial meltwater as the primary N source with increasing distance downstream (Kohler et al. 2018).

Despite their relative simplicity, N budgets for MDV streams remain poorly constrained. We seek to better characterize stream corridor N storage and fluxes in this system by addressing four questions:

1. How large are annual N fluxes into and from an MDV stream corridor?

2. How much N is stored within stream corridor biomass and the hyporheic zone?

3. Is NH_4^+ stored by sorption to sediment released in response to short-term changes in cation concentrations?

4. What is longitudinal distance over which allochthonous N inputs are removed?

To address these questions, we take advantage of multiple field, lab, and modeling techniques. We combined data from historic point-scale sampling of water, sediment, and biomass along with remote sensing analysis and uncertainty propagation to uniquely characterize N storage over an entire stream corridor and compare these results to other stream systems. We also conducted a laboratory assays to assess the stability of NH_4^+ sorption as an N storage mechanism in light of observed short-term changes in stream water conductivity. Lastly, we used a reactive transport model with unsteady flow routing to evaluate whether upstream fluxes of N can account for downstream exports given biotic uptake. By synthesizing historic point-scale observations, a laboratory assay, and these model simulations we evaluate differentiate the contributions of physical and biological processes to annual N fluxes and storage.

4.2. Study Site

We focused our analysis on Von Guerard Stream, a fairly long (5 km) stream that runs north from its source glacier in the Kukri Hills to Lake Fryxell in Taylor Valley, Antarctica (Figure 4.1). This stream has been gaged and sampled for both algal biomass and surface water chemistry by the McMurdo Long-Term Ecological Research project (MCM LTER) each Austral summer since 1994. Channel morphology, streambed composition, and algal mat coverage vary along Von Guerard Stream (Alger 1997, Wlostowski et al. 2016), making it a useful model for the diversity of stream characteristics present in the MDVs. Streamflow in Von Guerard Stream occurs for just a few months each year and is characterized by large diel pulsing events and periods of intermittency (Wlostowski et al., 2016). The stream corridor is largely hydrologically disconnected from adjacent hillslopes due to the hyper-arid climate (Gooseff et al. 2016). Continuous permafrost in the prevents groundwater exchange beyond the seasonally-thawed active layer (Conovitz et al. 2006, Bockheim et al. 2007), thereby further constraining hydrologic

connectivity. While there is evidence of deep groundwater system beneath the permafrost layer (Mickuki et al. 2015), there is no evidence that substantial exchange occurs between this system and Von Guerard Stream.

Figure 4.1. Von Guerard Stream in Taylor Valley, Antarctica, with stream corridor buffer (blue) used for remote sensing analysis and total area calculations.

Inputs of N to the stream corridor generally occur via meltwater mobilization of N deposited on glaciers and directly into the stream corridor (Witherow et al. 2006, Deuerling et al., 2014). Further N additions occur via in-channel N-fixation by *Nostoc*-dominated black algal mats (Howard-Williams et al. 1989, McKnight et al. 2007). Extensive *Phormidium*-dominated orange algal mats form broad cohesive films across many reaches but are not thought to be capable of N-fixation (McKnight et al. 2007; Kohler et al. 2018). N can be exported by DIN, DON, and PON fluxes with streamflow at the outlet into Lake Fryxell. While denitrification is

possible in MDV streams during nutrient addition experiments (Gooseff et al. 2004), little is known about its contribution to N losses under ambient conditions.

4.3. Methods

For this study, we estimated N import and export fluxes for the Von Guerard stream corridor as well as N storage by mining historic field and laboratory data from the MCM LTER. We scaled site specific data over areal and volumetric footprints representing the whole Von Guerard Stream corridor. We also propagated uncertainty from observational data using Monte Carlo simulations based on fitting distributions to the field data with *fitdistrplus* in R (Delignette-Muller and Dutang 2015, R Core Team 2019) or drawing from normal distributions described by summary statistics (mean and SD) reported in the literature. For each flux and N pool calculation, we randomly sampled 10,000 values for each variable and repeated the calculation based on these parameterizations. Table 4.1 defines each parameter used in the calculations presented below and the references for publications or datasets from which values were obtained.

4.3.1 Estimation of stream corridor N fluxes

We estimated seasonal dissolved and particulate N import and export fluxes based on 15-minute discharge data (Gooseff and McKnight 2019b) and concentration observations from the gage at the outlet of Von Guerard Stream into Lake Fryxell (Figure 4.1). For each season, we calculated total flow (Q_{total}) as the cumulative trapezoidal integration over the gap-filled discharge time series using the *pracma* package (Borchers 2021). We assumed no majors gains or losses in discharge along the stream corridor such that we used the same Q_{total} values to calculate the fluxes at the head and outlet. For import fluxes, we used concentration data from MDV ice cores and supraglacial streams (Howard-Williams et al. 1989; Bergstrom and Gooseff 2021a, 2021b), while export fluxes were based on observations of surface water in Von Guerard Stream (Lyons 2019; Singley et al. 2021b). The flux (F, kg N) for each dissolved and particulate constituent in a given flow season was calculated as:

$$F = CQ_{total}\left(\frac{1\ kg}{10^9\ \mu g}\right) \tag{4.1}$$

Table 4.1 Literature-derived values used to estimate N fluxes and pools (Eqns. 4.1–4.9). Parameters are listed in the order that they first appear in the manuscript.

Symbol	Description	Value or Distribution Type*	Units	Sample Count	Source[†]
Q_{total}	Total seasonal stream discharge	varies by season	L		Gooseff and McKnight 2019b
DIN_{gl}	DIN concentration in glacial ice and supraglacial meltwater	gamma	µg N/L	875 ice	Bergstrom and Gooseff 2021a
				287 melt	Bergstrom and Gooseff 2021b
DIN_{sw}	DIN concentration in stream water from lower reaches	21.2 ± 22.5	µg N/L	74	Lyons 2019
DON_{gl}	DON concentration in glacial ice melt	92.5	µg N/L	2	Howard-Williams et al. 1989
DON_{sw}	DON concentration in stream water from lower reaches	34.0 ± 19.0	µg N/L	15	Singley et al. 2021b
PON_{gl}	PON concentration in glacial ice melt	0	mg N/L	2	Howard-Williams et al. 1989
POM_{sw}	POM concentration in stream water from lower reaches	min = 1×10^{-4} max = 2.59×10^{-2}	mg/L	35	Cullis et al. 2014
CN_{POM}	C:N of POM in stream water from lower reaches	9.51 ± 1.92		13	Kohler 2018
ω	N-fixation rate of *Nostoc* mats	8.11 ± 5.45	mg N/m^2 day	16	McKnight et al. 2007
D	Flow season duration	49.8 ± 15.3	days	22	Gooseff and McKnight 2019b
A_{blk}	Total areal coverage by *Nostoc* mats	4000	m^2		McKnight et al. 1998
φ	Inorganic N deposition rate for Lake Fryxell	2.68	µg N/m^2 year		Deuerling et al. 2014
A_{VG}	Von Guerard Stream corridor area	134,112.5	m^2		
l_1	Upper reach length	1000	m		McKnight et al. 1998
l_2	Middle reach length	3500	m		McKnight et al. 1998
l_3	Lower reach length	500	m		McKnight et al. 1998
$w_{blk,1}$	*Nostoc* mat width in upper reach	0	m		McKnight et al. 1998
$w_{blk,2}$	*Nostoc* mat width in middle reach	1.0	m		McKnight et al. 1998
$w_{blk,3}$	*Nostoc* mat width in lower reach	1.0	m		McKnight et al. 1998
$w_{or,1}$	*Phormidium* mat width in upper reach	0.5	m		McKnight et al. 1998
$w_{or,2}$	*Phormidium* mat width in middle reach	3.0	m		McKnight et al. 1998
$w_{or,3}$	*Phormidium* mat width in lower reach	0.5	m		McKnight et al. 1998
$Chl_{blk,1}$	Chl a content of *Nostoc* mats in upper reach	0	µg Chl a/cm^2		McKnight et al. 1998
$Chl_{blk,2}$	Chl a content of *Nostoc* mats in middle reach	31.0	µg Chl a/cm^2		McKnight et al. 1998
$Chl_{blk,3}$	Chl a content of *Nostoc* mats in lower reach	9.0	µg Chl a/cm^2		McKnight et al. 1998
$Chl_{or,1}$	Chl a content of *Phormidium* mats in upper reach	4.7	µg Chl a/cm^2		McKnight et al. 1998
$Chl_{or,2}$	Chl a content of *Phormidium* mats in middle reach	12.0	µg Chl a/cm^2		McKnight et al. 1998
$Chl_{or,3}$	Chl a content of *Phormidium* mats in lower reach	31.0	µg Chl a/cm^2		McKnight et al. 1998
γ_{blk}	AFDM:Chl a of *Nostoc* mats	gamma	mg AFDM/µg Chl a	130	McKnight et al. 2019
γ_{or}	AFDM:Chl a of *Phormidium* mats	gamma	mg AFDM/µg Chl a	141	McKnight et al. 2019
CN_{blk}	C:N of *Nostoc* mats	9.10 ± 0.80		32	Kohler 2018
CN_{or}	C:N of *Phormidium* mats	10.50 ± 1.54		32	Kohler 2018
A_p	Pixel area from WorldView-3 imagery	1.95	m^2		
τ_{blk}	Spatial coverage by *Nostoc* mats	varies by pixel	percent		
τ_{or}	Spatial coverage by *Phormidium* mats	varies by pixel	percent		
β_{blk}	Areal AFDM content of *Nostoc* mats	gamma	AFDM/m^2	130	McKnight et al. 2019
β_{or}	Areal AFDM content of *Phormidium* mats	exponential	AFDM/m^2	141	McKnight et al. 2019
l	Total stream length	5000	m		
w_{hz}	Saturated hyporheic zone width	6	m		
d	Hyporheic zone depth of seasonally-thawed active layer	0.5	m		Conovitz et al. 2006
Φ	Hyporheic sediment porosity	0.34 ± 15.3		18	Heindel et al. 2021b
C_{nitr}	NO$_3$–N concentration of interstitial hyporheic water	78.6 ± 0.66	µg N/L	255	Singley et al. 2021b
w_{wet}	Wetted corridor width	9.54 ± 5.45	m	9	Heindel et al. 2021b
ρ	Hyporheic sediment bulk density	1749 ± 269.2	kg/m^3	18	Heindel et al. 2021b
C_{amm}	Sorbed NH$_4^+$–N concentration for hyporheic sediment	0.679 ± 0.655	mg N/kg dry sed	45	Heindel et al. 2021b
$d_{shallow}$	Shallow hyporheic depth based on sediment sample collection	0.1	m		Heindel et al. 2021b
LOI	Hyporheic organic matter content as AFDM	6.24 ± 1.34	g AFDM/kg dry sed	45	Heindel et al. 2021b

*Values are provided where only a single value could be derived from the literature or where a normal distribution with the indicated mean ± SD were used. In all other instances the distribution type that was fitted to the raw data is identified.

[†]Values derived or assumed by this study do not have a source listed

where C is concentration (µg N/L). This calculation was repeated for each flow season (1995-2018) for both DIN and dissolved organic nitrogen (DON) concentrations. For imports from glacial sources, we calculated DIN concentrations as the sum of NH_4^+ and NO_3^- (combined analysis for $NO_3^- + NO_2^-$). Individual concentrations that were below the detection limits were treated as zeros in the DIN sum. For glacier ice, 58.6% and 18.7% of samples were below detection for NO_3^- and NH_4^+, respectively. For supraglacial stream water, 0.3% and 20.6% of samples were below detection for NO_3^- and NH_4^+, respectively.

Similarly, we used DIN concentration data from historic grab samples collected in the lower reaches of Von Guerard Stream (1995-2018; Lyons 2019) to calculated export fluxes. For each grab sample, we calculated the DIN concentration as the sum of NO_3^-, NH_4^+ and NO_2^-. Individual concentrations that were below their respective detection limits (37.6% and 54.8% of all samples for NH_4^+ and NO_2^-, respectively) were again treated as zeros in the DIN sum. For the Monte Carlo simulations, we propagated uncertainty in these fluxes due to the variations in observed concentration data, except for the DON input flux from the glacier, for which only a single value is available.

To our knowledge, only one prior study analyzed PON in MDV glacial ice melt, but none was detected (Howard-Williams et al. 1989). Consequently, we assume that the PON flux into Von Guerard from its source glacier is negligible (~0 kg N/yr). Along Von Guerard Stream, POM, which contains N, is mobilized from algal mats with each meltwater pulse in a hysteretic pattern (Cullis et al., 2014). Both POM concentrations and total fluxes differ amongst individual flood pulses as a function of the time since a resetting flood event and the regrowth of potentially mobile benthic biomass. Currently, there is insufficient information to adequately model these time varying biomass pool dynamics and generate continuous estimates of POM concentrations (C_{POM}), especially for multiple seasons. Thus, for tractability, we simply calculate the absolute boundaries of seasonal PON export fluxes (F_{PON}, kg N) as:

$$F_{PON} = \left(\frac{C_{POM}Q_{total}}{CN_{POM}}\right)\left(\frac{1\ kg}{10^6\ mg}\right) \tag{4.2}$$

For each season, we repeated this calculation with both the minimum and maximum C_{POM} observations reported by Cullis et al. (2014). The resulting estimates do not account for the complex interactions between biomass regrowth and POM mobilization, but rather represent extremely conservative estimates for the range of F_{PON}. We propagated uncertainty for CN_{POM} via the Monte Carlo simulations.

We calculated the annual biological N fixation flux for the stream corridor by scaling areal N fixation rates (ω) over the approximate black mat area (A_{blk}) and stream season flow length (D) as:

$$F_{fix} = \omega A_{blk} D \left(\frac{1\ kg}{10^6\ mg} \right) \tag{4.3}$$

We calculated the flow season duration (D) from 1995-2018 as the elapsed time in days between the first and final gaged flows. We held the *Nostoc* area constant and propagated uncertainty for ω and D using Monte Carlo simulations.

Lastly, we estimated total annual atmospheric deposition of inorganic N (F_{dep}) directly into the stream corridor. To do so, we scaled annual deposition rates estimated from Lake Fryxell (φ; Deuerling et al. 2014) over the entire Von Guerard stream corridor (A_{VG}, see 3.2.1).

$$F_{dep} = \varphi A_{VG} \left(\frac{1\ kg}{10^9\ \mu g} \right) \tag{4.4}$$

4.3.2 Estimation of stream corridor N pools

To quantify the relative importance of different storage mechanisms, we estimated total N in periphyton biomass, shallow (<10 cm) hyporheic OM, NH_4^+ sorbed to hyporheic sediment, and dissolved NO_3^- in hyporheic water along the entire stream corridor. For all N pool estimates, we again propagated uncertainty using Monte Carlo simulations based on fitting distributions to the field data or summary statistics.

4.3.2.1 N storage in periphyton biomass

We estimated the total mass of N stored in benthic algal mat biomass in two different ways. First, we estimated N in algal biomass (N_{bio}) in each mat type (black and orange) over

three reaches (*r*) representing the entire length of Von Guerard Stream using a simple scaling calculation based on McKnight et al. (1998) as:

$$N_{bio} = \sum_{r=1}^{3} \left(\frac{l_r w_{blk,r} chl_{blk,r} \gamma_{blk}}{CN_{blk}} + \frac{l_r w_{or,r} chl_{or,r} \gamma_{or}}{CN_{or}} \right) \left(\frac{10^4 \, cm^2}{1 \, m^2} \right) \left(\frac{1 \, kg}{10^6 \, mg} \right) \qquad (4.5)$$

Here, we calculate areal coverage of each mat type and converted these footprints to N content based on relationships between Chlorophyll a, AFDM, and C:N from analysis of mat cores. type as the product of mat width (*w*) and reach length (*l*). Then we determine total biomass content based on areal Chlorophyll a (Chl-a, *chl*) data and Chl-a to AFDM ratios (γ) for each mat type. Lastly, we convert this biomass pool to N mass using C:N ratio data (*CN*) calculated for each type based on historic samples. We propagated uncertainty for γ and *CN* using Monte Carlo simulations.

We also estimated spatial coverage of algal mats and N content based on analysis of multispectral satellite imagery and an MDV-specific spectral mixing model (Salvatore et al. 2020). We based our analysis on data from a WorldView-3 (DigitalGlobe, Inc., now Maxar Technologies) image taken on January 26, 2019. This image was acquired towards the end of the streamflow season and showed relatively snow-free conditions across most of the landscape. As per Salvatore et al. (2020), we leveraged the unique spectral reflectance signature of black and orange algal mats, moss, bare soil, and water to determine the percent coverage of each pixel by spectral endmember. We used a non-negative spectral unmixing model that linearly combines a suite of endmember spectra to produce the best mathematical fit between the input spectrum and the model output. It has been demonstrated that surface endmembers in Taylor Valley, Antarctica, are optically opaque and, therefore, can be appropriately modeled as a linear combination of their areal abundances at each pixel (Salvatore et al., 2020, 2021). The root mean square error (RMSE) on modeled versus observed spectra across all pixels ranged from 0.00 to 81.35%. Most model fits were very good with a mean ± SD RMSE of 1.63 ± 2.35% (median of 1.19%), with less than 0.5% of all pixels exhibiting RMSE > 10%.

From the individual mat coverage estimates by type and pixel, we then calculated N content of all algal biomass (N_{bio*}) in the stream corridor as:

$$N_{bio*} = \sum_i^{n_p} \left(\frac{\tau_{blk,i} \beta_{blk,i} A_p}{CN_{blk}} \right) + \left(\frac{\tau_{or,i} \beta_{or,i} A_p}{CN_{or}} \right) \qquad (4.6)$$

Here, we sum the N content of each mat type for each pixel (i), across the 68,767 pixels (n_p) within a 134,112.5 m^2 region that encompasses an approximately 10 m wide buffer to either side of the thalweg of Von Guerard Stream (Figure 4.1). This width is approximately double the distance between the visible wetted margins for Von Guerard Stream reported by Heindel et al. (2021b) at low flows (< 0.5 L s^{-1}). We converted percent coverage (τ) for each pixel by mat type to AFDM based on areal biomass (β) from field samples for Von Guerard Stream and average pixel area (A_p). Lastly, we used the same C:N ratios noted above to convert AFDM to N content. In this estimation, we propagated uncertainty for β and CN by mat type.

4.3.2.2 N storage in the hyporheic zone

Following Singley et al. (2021a), we estimated the mean N pool contained in dissolved NO$_3^-$ in interstitial hyporheic waters of Von Guerard Stream as:

$$N_{nitr} = l w_{hz} d \Phi C_{nitr} \left(\frac{10^3 \ L}{1 \ m^3} \right) \left(\frac{1 \ kg}{10^9 \ \mu g} \right) \qquad (4.7)$$

where l is the length of the stream, w_{hz} is the saturated hyporheic width, and d is the hyporheic depth within the seasonally thawed active layer. We used NO$_3^-$ concentrations (C_{nitr}) from an extensive set of samples (n = 255) from the lower reaches of Von Guerard Stream (Singley et al. 2021b). Then we determined total hyporheic fluid volume based on estimates of porosity (Φ) for the Von Guerard Stream bed as 0.34 ± 0.10 from bulk density measurements (n = 18; Heindel et al. 2021b) and an assumed mineral density of 2.65 g/cm^3. We limited this analysis to NO$_3^-$ (as NO$_3^-$ + NO$_2^-$) since NH$_4^+$ concentrations were often much lower than NO$_3^-$ (Singley et al., 2021a) or below detection (64.9%, Singley et al. 2021b). Uncertainty was propagated for Φ and C_{nitr} using normal distributions fitted to each dataset.

Hyporheic sediments of Von Guerard Stream also contain OM (both heterotrophic bacteria and POM from algal mats) as well as a NH_4^+ sorbed to sediment (Heindel et al. 2021a). We calculated the total N mass in each of these pools as:

$$N_{sorbed} = lw_{wet}d\rho C_{amm}\left(\frac{1\,kg}{10^6 mg}\right)$$ (4.8)

$$N_{hyp,OM} = \frac{lw_{wet}d_{shallow}\rho LOI}{CN_{blk}}\left(\frac{1\,kg}{10^3\,g}\right)$$ (4.9)

Here we used wetted corridor width (w_{wet}), bulk density (ρ), total extractable NH_4^+ (C_{amm}), and loss on ignition (*LOI*) from 9 sediment transects in the lower half of Von Guerard Stream (Heindel et al. 2021b). We set *d* to 0.5 m as described above for dissolved NO_3^-. For *$N_{hyp,om}$* we limited the analysis to a shallow depth ($d_{shallow}$) of only 0.1 m, given the sample collection protocol used by Heindel et al. (2021b). Using these physical values, we scaled up mean OM content from *LOI* (as AFDM/g dry soil) and C_{amm} (mg NH_4^+–N/kg dry sediment) across the estimated mass of sediment in their respective volumes. As most POM entrained in the hyporheic zone can be traced to black mats (Heindel et al., 2021a), we used the *CN_{blk}* data described above to convert AFDM to N in the *$N_{hyp,OM}$* calculation. For these estimations, we propagated uncertainty in the Monte Carlo simulations by fitting and drawing values from normal distributions based on the data for *w_{wet}*, *ρ*, *C_{amm}*, *LOI*, and *CN_{blk}*.

4.3.3 Assay on desorption of NH_4^+ from stream sediment

We performed a laboratory assay on sediment samples collected from the lower reaches of Von Guerard Stream (Figure 4.1) to assess the availability of NH_4^+ adsorbed to stream sediment as a potential source for internal DIN fluxes. We conducted an assay to determine whether NH_4^+ desorbed over the range of conductivities observed in Von Guerard Stream from 1995-2015 (Figure 4.2A).

Sediment samples were collected from the top 10 cm of the streambed at 5 locations along a transect spanning between the wetted margins of the stream corridor. Subsamples from this sediment was previously analyzed for OM content through loss on ignition (LOI) in a muffle

furnace and total extractable NH_4^+ by 2M potassium chloride (KCl) extraction. A full description of sediment sample collection, storage and analytic methods is provided by Heindel et al. (2021a, 2021b). For this study, we thawed sediment samples at +4ºC and weighed 15 sub-samples (approximately 20 g of sediment each) for 5 lateral locations into 250 mL HDPE bottles. We prepared treatment solutions containing KCl and deionized water to achieve specific conductivity (SC) values that reflect the range of diel to seasonal fluctuations of SC observed in Von Guerard Stream (Figure 4.2B). Based on measurements with a temperature corrected benchtop conductivity probe, the treatment solution SC values were 0.06 (DIW only), 40.7, 77.1, 155.9, and 317.7 µS/cm.
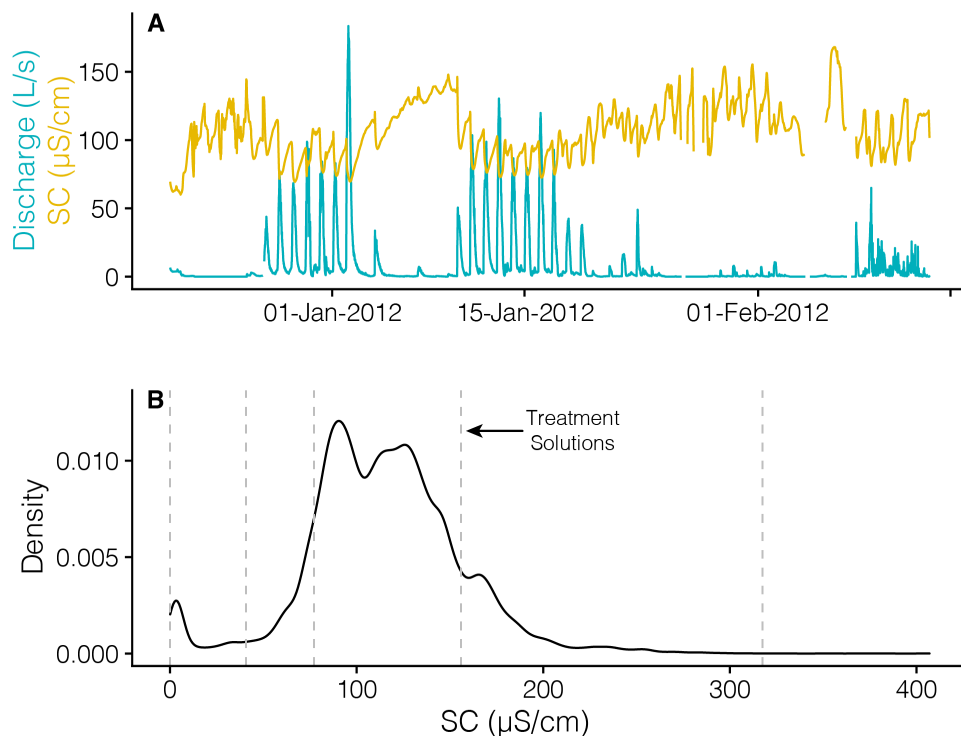
Figure 4.2. (A) Illustrative discharge and specific conductivity variability from the 2012 flow season in Von Guerard Stream. (B) Historic (1995-2015) specific conductivity distribution for high-frequency surface water observations with laboratory assay treatment solution values.

Homogenized sediment subsamples were taken in triplicate from each location then mixed with each treatment solution at a 2:5 ratio of sediment to solution by mass. The resulting sediment slurries and solution blanks for each treatment were immediately placed on a rotary shaker table at 300 rpm for 1 hour, then centrifuged at 3000 rpm for 5 minutes, and filtered via

GF/F filters (Whatman). The filtrate was stored frozen (-20ºC) until analysis. We analyzed NH_4^+ concentrations with a Lachat Quickchem Flow Injection Analysis System (Hach, USA) according to standard protocol 4500-NH3 H (phenolate FIA), with a minimum detection limit of 5 µg NH_4^+-N/L. We analyzed NO_3^- as the sum of NO_3^- and nitrite (NO_2^-) by standard method 4500-NO_3 I (cadmium reduction flow injection) with a detection limit of 4 µg NO_3^-–N/L. The resultant concentrations were normalized to sediment dry weights, which were calculated using transect location-specific gravimetric moisture content determined during the LOI protocol performed by Heindel et al. (2021a). Incubation solution concentrations of K^+ and Cl^- were measured by atomic absorption spectrophotometry with detection limits of 4 and 30 µg L^{-1}, respectively.

We analyzed these data for relationships between solution SC and the net mass of DIN released per mass sediment and the percentage of total extractable NH_4^+ for each site. We also compared changes in concentrations of K^+ and Cl^- to determine whether cation exchange was a likely explanation for any observed release of NH_4^+.

We did not utilize a kill treatment to limit biological activity as preliminary trials found that 1% formalin solutions may have substantially altered cation exchange through changes to solution pH. Similarly, buffered formalin contains ion concentrations that exceeded the low conductivities needed to replicate MDV stream water observations, so a formalin kill was not suitable for this assay. We also did not autoclave sediment as a prior study reported potential releases of N and phosphorus during such treatment of MDV sediments (Bergstrom et al. 2020). Consequently, the results from this assay reflect only the potential for NH_4^+ to desorb from stream sediment in response to changing stream water conductivities, not *in situ* dynamics or kinetics.

4.3.4 Modeling longitudinal attenuation of allochthonous N inputs

The relatively simple hydrologic characteristics of MDV streams ensure that N concentrations are predominately controlled by meltwater inputs and stream corridor processes –

namely advection, dispersion, transient storage through hyporheic exchange, and reactions in the hyporheic zone and main channel. Lateral inflows from adjacent hillslopes are negligible as are groundwater gains and losses. To represent this system, we coupled kinematic wave routing (Koohafkan and Younis 2015) with a one-dimensional transport and storage model (OTIS; Runkel et al., 1998) to assess the spatial scales over which glacially derived N inputs are attenuated in MDV streams. The OTIS model has been widely utilized for both conservative and reactive transport simulation, including in the MDVs (Runkel et al. 1998, Gooseff et al. 2004a, 2004b, McKnight et al. 2004). Given the ability of OTIS to handle unsteady flow, hyporheic exchange, and multiple reaction processes along with estimates of reasonable parameters from prior tracer studies, it is well suited to approximating the longitudinal distance over which allochthonous N inputs are removed in MDV streams.

Due to the lack of gage data at the head of most MDV streams, including Von Guerard Stream, we used a proxy from another stream gage on a shorter stream. This approach has been applied in prior studies of discharge pulse routing in MDV streams (e.g., Koch et al. 2011). To this end, we selected the 2009 seasonal hydrograph for Commonwealth Stream (Gooseff and McKnight 2019a), also located in Taylor Valley. These data were selected as the gage is located within 0.7 km from the toe of its source glacier and flow varied by three orders of magnitude (0.8 to 888.1 L/s) with diel pulsing that is characteristic of this system (Figure 4.3A). Although the selected hydrograph is not likely to be a perfect representation of flow pulse shape for Von Guerard Stream, which flows from a different source glacier, it captures the general unsteady flow that governs transport in MDV streams.

We routed this upstream boundary condition (USBC) for stream flow down an idealized model reach based on the upper portions of Von Guerard Stream using the *Rivr* package in R (Koohafkan and Younis 2015, R Core Team 2019). The model channel was 1100 m long, with a Manning's roughness coefficient of 0.066, a slope of 0.078 m/m, and a constant wetted width of 2 m. These parameters were drawn from prior descriptions and modeling of MDV streams (e.g., Runkel et al. 1998, Wlostowski et al. 2016). We linearly interpolated the USBC hydrograph from

15 to 1 minute resolution and routed the flow with a 5 m spatial step size. We extracted time series for locations spaced 100 m apart and used the discharge and main channel area data in as inputs for the unsteady flow files for the OTIS model.

Here, we utilize the standard version of OTIS to model solute concentrations in the main channel (C) and the hyporheic zone (C_{HZ}), with the following governing equations:

$$\frac{\partial C}{\partial t} = -\frac{Q}{A}\frac{\partial C}{\partial x} + \frac{1}{A}\frac{\partial}{\partial x}\left(AD\frac{\partial C}{\partial x}\right) + \alpha(C_{HZ} - C) - \lambda C \qquad (4.10)$$

$$\frac{dC_{HZ}}{dt} = \alpha\frac{A}{A_{HZ}}(C - C_{HZ}) - \lambda_{HZ}C_{HZ} \qquad (4.11)$$

where Q is surface water discharge (m³/s), α is the hyporheic exchange coefficient (/s), D is the dispersion coefficient (m²/s), A and A_{HZ} are the cross-sectional areas (m²) of the main channel and hyporheic zone. Here λ and λ_{HZ} are first-order uptake coefficients (/s) for the main channel and hyporheic zone. As described above, Q and A vary with time based on kinematic routing. We set α to 4.34×10^{-4} /s, which is the median exchange coefficient from prior studies in which OTIS parameters were fitted to MDV tracer data (Runkel et al. 1998, Gooseff et al. 2004b, McKnight et al. 2004). To deal with the uncertainty in uptake due to changing biotic activity and algal mat coverage, we ran simulations with "slow", "moderate", and "fast" λ values set to 3.74×10^{-4}, 3.74×10^{-3}, and 3.74×10^{-2} (/s), respectively. The moderate uptake rate represents the mean main channel uptake for NO_3^- tracer studies in another MDV stream (Gooseff et al. 2004b), while the slow and fast scenarios represent an order of magnitude change in either direction. We held λ_{HZ} constant at 3.29×10^{-5} /s, which is the average hyporheic removal rate for NO_3^- from the same studies.
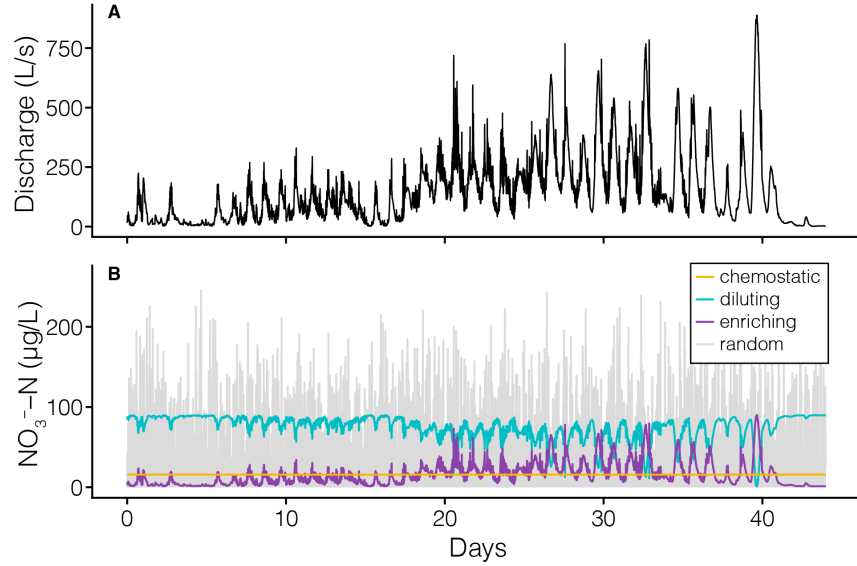
Figure 4.3. Reactive transport model inputs for (A) discharge and (B) concentration-discharge typologies at the upstream boundary over the simulation duration (44 days).

Historically, surface water sampling in MDV streams has occurred primarily at gage locations, resulting in a lack of information on the relationship between concentrations and flow at the head of each stream. To overcome this gap, we simulated four different possible USBC for NO_3^- concentration (C_0) [ppm]:

$$C_0^{chemo} = 0.044 \tag{4.12}$$

$$C_0^{dil} = (2.10 \times 10^{-3})Q_0^{-0.671} \tag{4.13}$$

$$C_0^{enr} = 0.175Q_0^{0.731} \tag{4.14}$$

$$C_0^{rand} = \Gamma(1.42, 0.039) \tag{4.15}$$

where Eqn. 4.12 represents chemostasis set to the mean NO_3^- concentration in glacial ice and supraglacial stream samples (excluding 18 values comprising 2.5% of the data with DIN > 200 µg N/L; Bergstrom et al., 2021a, 2021b); Eqns. 4.13 and 4.14 represent power-law diluting and enriching relationships, respectively. We derived Eqn. 4.13 by pairing the minimum concentration with the maximum discharge, the medians of each, and maximum concentration with the minimum discharge, then fitting the coefficient and exponent parameters to these three points (R^2 = 0.840). Similarly, we derived Eqn 4.14 by pairing the minimum, median, and maximum concentrations with those for discharge and fitting the coefficient and exponent parameters (R^2 = 0.997). Eqn. 4.15 is a random selection of values drawn from a gamma

distribution with the noted shape and inverse rate parameters fit to that data. The resulting USBC time series for each typology are presented in Figure 4.3B. Concentration-discharge plots for each USBC are provided in Figure S4.1.

We ran simulations (n = 9) representing each combination of λ and C_0 over the model reach at 1 minute and 10 m resolution. We summarized longitudinal patterns in C (mean ± SD) at sites located at distances of 5 m, 10-100 (by 10 m increments), and every 50 m thereafter, across the entire time span for each simulation (44 days).

4.4. Results

4.4.1 Seasonal N fluxes to and from the Von Guerard Stream corridor

On an annual basis, the interquartile ranges (IQR, first to third quartiles) of Monte Carlo estimates for input fluxes from the source glacier meltwater totaled 1.2-29.8 kg N/yr. This total flux was composed of 1.1–4.3 kg N/yr as DIN, 0.1–25.5 kg N/yr as DON, and negligible PON imports. We estimated that N fixation by *Nostoc* in the stream corridor adds a further 0.7–2.3 kg N/yr while direct atmospheric deposition of inorganic N is very small (<< 0.1 kg N/yr). Combined, these fluxes amount to total imports of 2.2–32.2 kg N/yr, which normalized over the entire stream corridor is equivalent to a gross input of 16.4–240 mg N/m^2 yr.

We estimated that in total 0.3–5.6 kg N/yr (IQR) is exported from the stream corridor in particulate and dissolved form. Specifically, we estimated that N fluxes as DIN from Von Guerard Stream into Lake Fryxell ranged from 0.1–1.9 kg N/yr. DON exports were slightly larger at 0.2–3.4 kg N/yr. while N export as PON must be no more than 0.3 kg N/yr. Notably, cumulative seasonal streamflow varies widely (719.5 to 2.76×10^8 L) and with no identified directional relationship between DIN or DON concentrations and discharge (i.e., diluting or enriching), N flux estimates into Lake Fryxell are primarily governed by variations in Q_{total} from one season the next. We estimated that only ~17% of N imports are likely exported from the Von Guerard Stream corridor on an annual basis, although we could not account for losses via

denitrification. Scaled to stream corridor area, exports amount to a gross N release of 2.2–41.8 mg N/m^2 yr, resulting in a net increase in storage of 14.2–198.2 mg N/m^2 yr.

4.4.2 Estimates of periphyton biomass coverage by remote sensing

Estimates of algal biomass and N stored therein were remarkably consistent between simple back-of-the-envelope estimates and those based on spectral analysis of satellite imagery (15% and 27% difference on the means and medians, respectively). Generally, modeled abundances show the greatest biomass in the stream channel, especially for orange mats (Figure 4.4). Patchy black mats are known to occur throughout the landscape, especially where snow patches form each winter. However, the modeled presence of orange mats outside the channel is unexpected. This is most likely due to the presence of chlorophyll-bearing photosynthetic species present at small abundances throughout the landscape, either as mosses or disaggregated mat communities, that are contributing to weakly photosynthetic signatures in the surrounding soils (Adams et al. 2006). The spectral absorption of chlorophyll-a is most easily identified in multispectral satellite data in the absence of dark sunscreen pigments, which is likely why the unmixing model is indicating the presence of orange mat over black mat or other spectral signatures. The high abundance of orange mats within the stream corridor, in addition to the dominance of black mats along the stream margins, matches in situ observations (Alger 1997, McKnight et al. 1998, 1999) and previously published remote sensing results (Salvatore et al., 2020, 2021 [*in review*]).
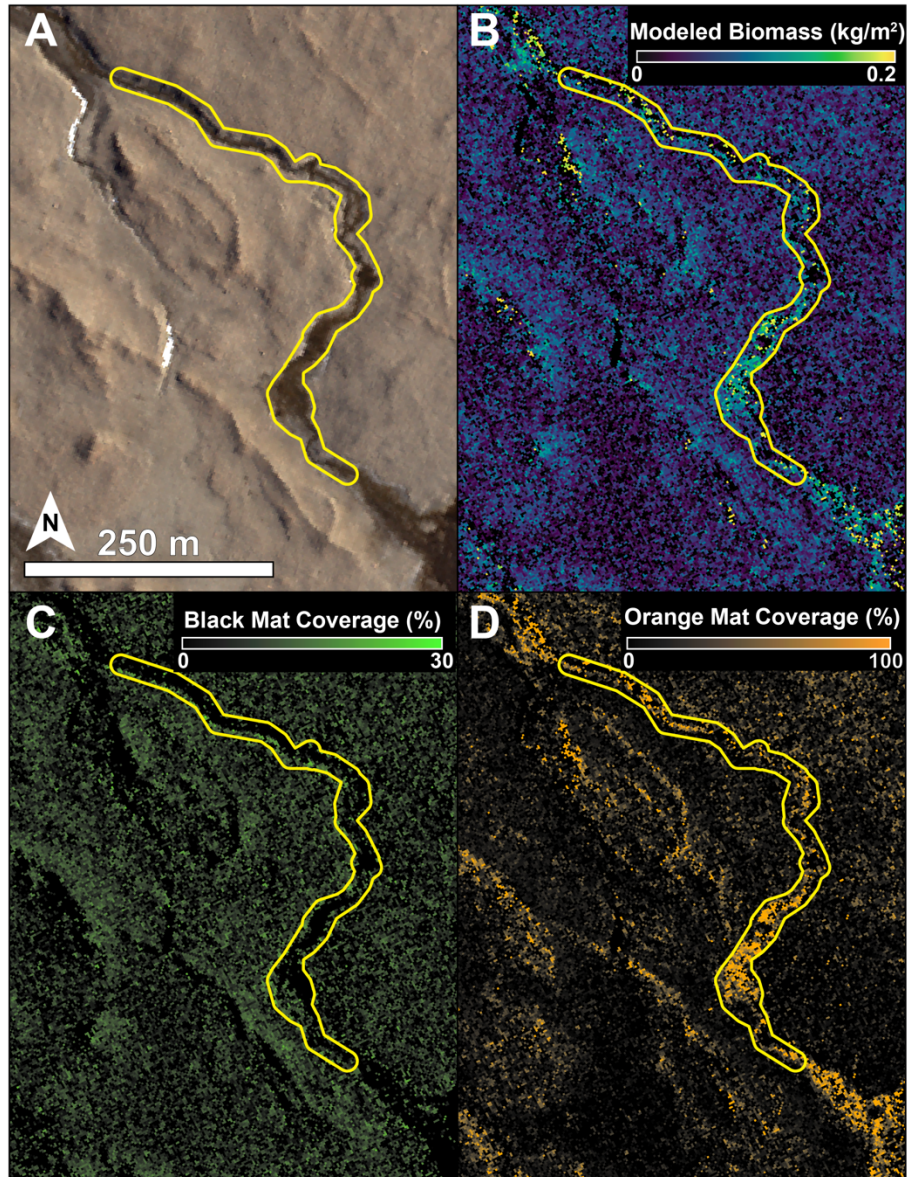
Figure 4.4. Modeled biomass and mat coverage from multispectral remote sensing data along Reach 6 of the Von Guerard Stream corridor. (A) Visible spectrum with corridor buffer ~10 m to either side of the thalweg, flow is from bottom to top. (B) Modeled biomass, (C) percent coverage by *Nostoc*-dominated "black" mats, and (D) percent coverage by *Phormidium*-dominated "orange" mats from linear unmixing model applied to multispectral data. Scale and orientation are the same for all panels.

4.4.3 Stream corridor N storage

We found that relative to the seasonal import and export fluxes, large masses of N are physically and biologically stored along the stream corridor (Figure 4.5, Table S1). Across the

10,000 Monte Carlo simulations for each pool, we estimated that algal biomass contains

approximately 297.2 kg N (mean), while multispectral imagery analysis resulted in a mean

estimate of 349.7 kg N. The vast majority of Monte Carlo simulations (>70%) resulted in

estimates wherein more than 90% of the total N stored in the stream corridor is found in the

hyporheic zone. Organic matter in just the top 10 cm of sediment may account for approximately

5051 kg N. Additionally, we estimate that the hyporheic zone likely stores on the order of 35.7

kg N in sorbed NH_4^+ and 0.4 kg N in dissolved NO_3^-. We do not report standard deviations on

these means as multiple pool estimates have highly skewed non-normal distributions resulting

from the underlying distributions of field measurements. Table S4.1 in the supplemental

information provides the mean, median, and first and third quartile values for each of the pool

estimates that are depicted in Figure 4.5. Combining the mean estimate for each N pool and

normalizing over the largest pool area (134,112.5 m^2), we obtain total N storage estimates of

about 40 g/m^2.

It is important to note that total N storage exceeds the mean annual flux of N at the outlet

of Von Guerard Stream (Figure 4.5). The only exception is for N stored in dissolved NO_3^- in

hyporheic waters, which is expected to be more transiently mobile and was of comparable size

to, or slightly below, seasonal N fluxes. In total, mean annual imports and exports are less than

0.5% and 0.1% of mean N storage in all pools, respectively.
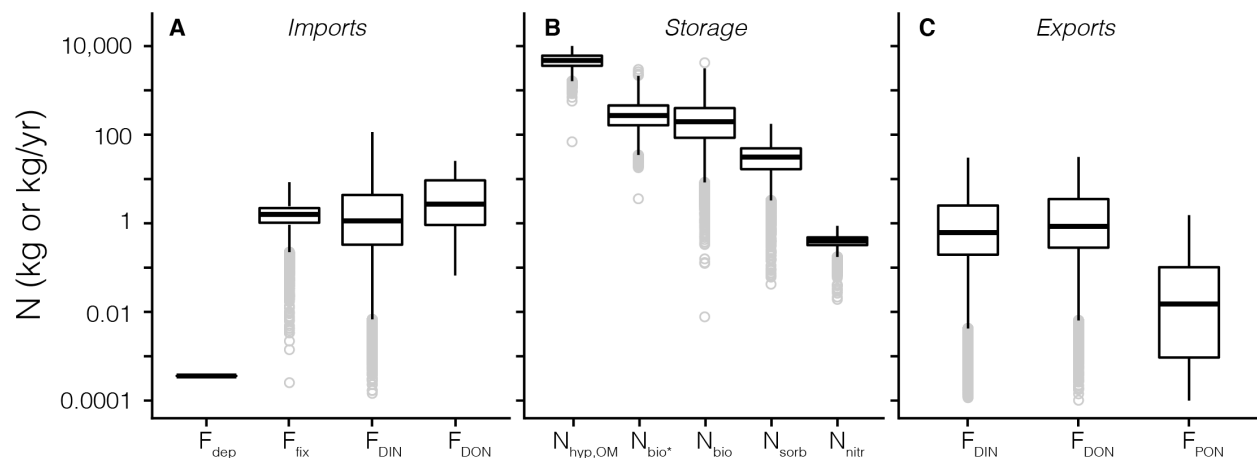
Figure 4.5. Estimates (A) annual N import fluxes, (B) storage pool sizes, and (C) annual export
fluxes with uncertainty propagation through Monte Carlo simulations (n=10,000). The lower and

upper box boundaries correspond to the first and third quartiles while the inner horizontal line is the mean. Whiskers extend to 1.5 times the interquartile range above and below the first and third quartiles. Data beyond these ranges are denoted with light gray circles.

4.4.4 Ammonium desorption in response to changing fluid conductivity

Through a laboratory assay on stream sediment, we found that more K^+ than Cl^- was lost from solution with increasing concentrations (Figure 4.6A). For the two lowest concentration treatments, K^+ and Cl^- concentrations increased slightly, suggesting that some additional ions were mobilized from the sediment as they were wetted. Losses of K^+ in the 77.1, 155.9, and 317.6 µS/cm treatments were not matched by similar losses of Cl^- despite comparable ionic masses. This result suggested that greater net cation but not anion exchange was occurring. The pattern is consistent with field observations of ion exchange during a previous tracer study in an MDV stream (Gooseff et al. 2004a).

We also found that NH_4^+ sorbed to the sediment of Von Guerard Stream can be rapidly liberated into solution as fluid conductivities increase (Figure 4.6B–C). This relationship was fairly strong for each location (linear regressions gave adjusted R^2 values from 0.44–0.89, p < 0.005). We also found that differences in the net mass of NH_4^+ released normalized to sediment dry mass among sample sites was reflective of differences in the amount of total extractable NH_4^+. In other words, while the concentration of NH_4^+ stored by sorption varies laterally across the stream (Heindel et al. 2021a), similar proportions of total stored NH_4^+ are released for particular fluid conductivities (Figure 4.6B). We also observed a trend towards plateauing of K^+ losses at higher concentrations (4.6A), which may indicate an upper limit to cation exchange and, potentially, NH_4^+ desorption (i.e., neither 100% of K^+ was lost or NH_4^+ released) under reasonably representative SC values for Von Guerard Stream.

93
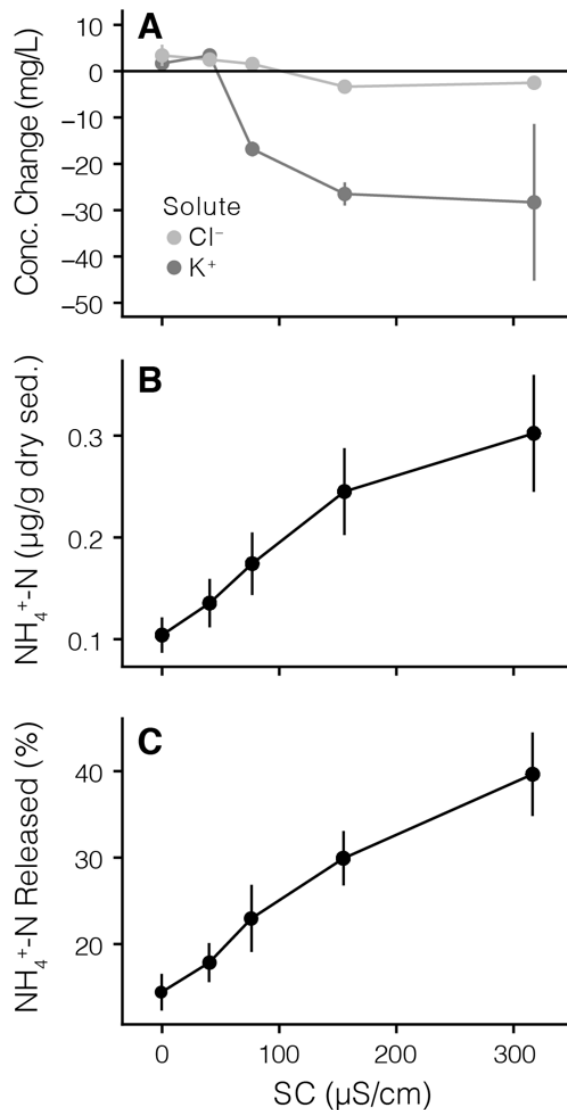
Figure 4.6. Changes in incubation solution ion concentrations and responses of sediment sorbed NH_4^+ to increasing fluid conductivity. (A) Changes in solution concentrations of Cl^- and K^+ (mean ± SE) by treatment conductivity. Assay treatment solution specific conductivity against (B) mean (± SE) net mass of desorbed NH_4^+ normalized to dry sediment mass and (C) mean (± SE) net percent of total extractable NH_4^+ desorbed. Treatment sample size is 5 for panel A and 15 in panels B and C.

4.4.5 Longitudinal attenuation of allochthonous N inputs

Modeling results demonstrate that for the probable range of uptake rates, glacial inputs of NO_3^- at the head of an MDV stream are removed over very short distances (<500 m) regardless of USBC form (Figure 4.7). For all simulations, larger variations in concentration were modeled for slower uptake rates at each longitudinal location. In "moderate" uptake simulations, which

are based on the mean uptake coefficients from prior tracer studies, allochthonous NO_3^-

concentrations reached or were near zero within 500 m. For uptake rates an order of magnitude

larger ("fast" simulations), all allochthonous N was removed within the first 100 meters. Uptake

rates that were one order of magnitude slower than the mean of prior estimates from in situ tracer

studies, resulted in concentrations at 1000 m that were comparable to historic observations made

much further downstream (Figure 4.7A-D).
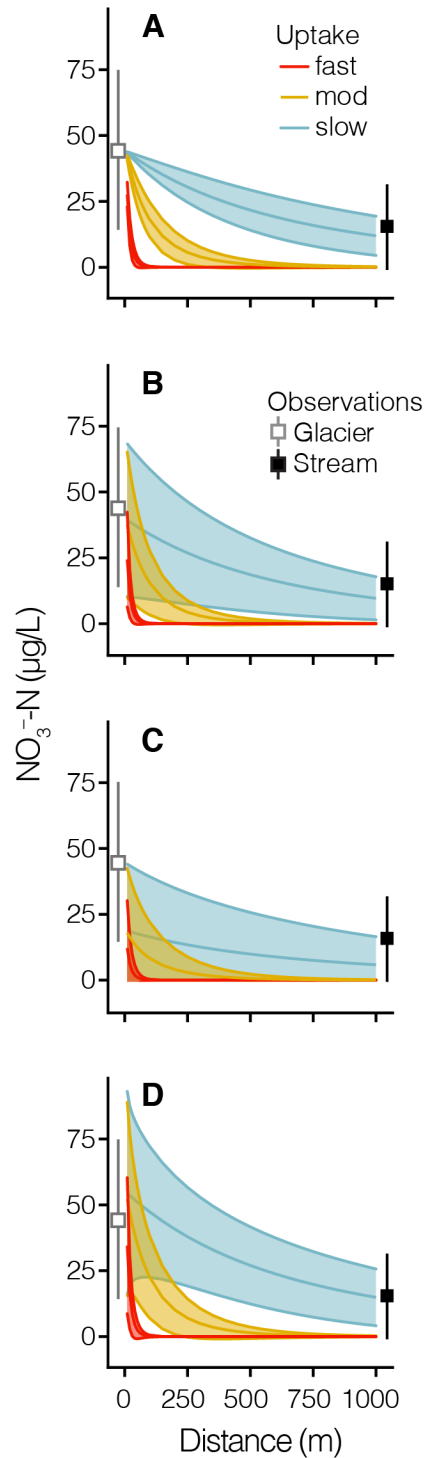
Figure 4.7. Modeled NO_3^- concentration (mean ± SD) by longitudinal location for each reactive transport simulation. Simulations represent various boundary concentration-discharge typologies as (A) chemostatic, (B) enriching, (C) diluting, and (D) random. Observed NO_3^- concentrations are shown for reference by point and whiskers (mean ± SD) in each panel for glacial ice and historical grab samples at Von Guerard Stream gage located at a distance of 5 km.

4.5. Discussion

4.5.1 High stream corridor storage of N relative to fluxes

We found that, despite the uncertainty in field data and scaling values over large areas, there is likely substantially more N stored in biomass and the hyporheic zone than is exported from the stream corridor in any given flow season (Figure 4.5, S4.1). We estimated that mean annual import and export of N represents less than 0.5% of the N that is physically and biologically stored within the stream corridor. Our results reveal that relatively substantial N storage in the stream corridor can occur even without allochthonous POM inputs, which dominate stream corridor N storage in forested temperate catchments (Triska et al. 1984). At about 40 g/m^2, the N storage rates we estimated for Von Guerard Stream are larger than the 12-22 g/m^2 estimated for headwater streams in temperate forests or the 3-9 g/m^2 for a mid-latitude desert stream (Triska et al. 1984, Naiman and Melillo 1984, Grimm 1987). While we expected biomass to store the largest mass of N, given extensive benthic algal mat coverage (Alger 1997), we found that the majority (> 90%) of stored N is likely held in the hyporheic zone.

It is possible that our mean estimates of N storage in Von Guerard Stream are inaccurate due to utilizing values from point-scale samples in the calculations. It is notable that even an order of magnitude reduction in total N mass stored would result in area normalized storage that is comparable to that of Sycamore Creek, AZ (Grimm 1987). Importantly, we constrained our estimates of N in hyporheic OM content – by far the largest N pool – to only the top 10 cm of sediment, although the active layer thaws to depths of up to 60 cm (Conovitz et al. 2006), such that we may have underestimated the size of this pool. Ultimately, our total N storage calculations would need to be reduced by approximately three to four orders of magnitude to equal the highest fluxes at the stream outlet. It is unlikely that the data from historic samples that we used are that unrepresentative of the overall system. In summary, despite uncertainty related to propagating point-scale measures to the entire reach, it is highly likely that substantial N

97

storage occurs relative to import and export fluxes in this hyper-arid, highly intermittent, polar desert stream.

4.5.2 Rapid reversible sorption is an import mechanism for inorganic N storage

Physicochemical storage of NH_4^+ by sorption to stream sediment represents a dynamic N storage process that can vary over both space and time in temperate systems while also competing with microbial N demand (Triska et al. 1994). Our relatively simple laboratory assay demonstrates that NH_4^+ sorption to MDV stream sediments is likely reversible over the range of fluid conductivities observed in Von Guerard Stream. Specifically, the net release of NH_4^+ into solution increases with increasing cation concentrations (K^+ only in the assay; Figure 4.6). Similar sensitivity has been documented in coastal sediment at much higher fluid conductivities (Seitzinger et al. 1991), but remains generally understudied in small headwater streams. The exact kinetics of NH_4^+ desorption may vary *in situ*, but our results indicate that 20-40% of sorbed NH_4^+ can likely be released into solution rapidly (< 1 hr). As sorbed NH_4^+ content varies in space for MDV streams (Heindel et al. 2021a), channel expansion and contraction cycles with diel flow pulsing likely plays an important role in when and where such releases occur.

MDV stream sediments modulate other cation fluxes (K^+, Na^+, and Li^+) through concentration-dependent sorption and release in well-connected hyporheic zones (Gooseff et al. 2004a). This is reflected in how fluid conductivities exhibit small fluctuations during diel flow pulsing and rise during sustained low flow periods (e.g., Figure 4.2A) due to evapoconcentration and hyporheic weathering (Maurice et al. 2002, Barrett et al. 2009, Singley et al. 2017). Extending our laboratory results, we conclude that it is probable that NH_4^+ sorption and desorption similarly varies over time in Von Guerard Stream. Interestingly, it is possible that the net direction of NH_4^+ sorption may shift over time, just as occurs for other cations. While we cannot conclude that this behavior occurs or the exact conditions that may control such shifts, our findings represent an interesting topic for future investigations into how physicochemical processes govern N availability in these oligotrophic and intermittent stream corridors.

4.5.3 Fluxes from internal pools sustain N availability

Our modeling results suggest that regardless of upstream C-Q form and a wide range of uptake rates, N in glacial meltwater could be removed over relatively short longitudinal distances (Figure 4.7). Except for simulations with uptake rates that are an order of magnitude lower than direct observations (Gooseff et al. 2004b, McKnight et al. 2004), concentrations at 1 km are already lower than historic observations collected at 5 km.

From these results, we conclude that there must be an additional source flux of DIN along the stream corridor to explain consistent observations of measurable DIN made much farther downstream (4 km beyond model boundary). Without substantial hydrologic connectivity to adjacent hillslopes or groundwater (Gooseff et al. 2016), the most likely source of this flux is through widely distributed N-fixing *Nostoc* (black) algal mats and remineralization of stored OM, especially in the hyporheic zone (Singley et al. 2021a). This conclusion aligns with stable N isotope analysis showing a shift from a predominance of glacially-sourced N in the upper reaches to autochthonously-sourced N in the lower reaches of MDV streams (Kohler et al. 2018). While our flux estimates agree with prior characterization of MDV streams as net N sinks (e.g., Gooseff et al. 2004b, McKnight et al. 2004, Dubnick et al. 2017), this simple modeling exercise suggests that much more complicated spiraling of OM an N governs N availability rather simply removal from stream water along the entire reach.

Our N pool estimates indicate that there is a sufficiently large pool of N stored in the hyporheic zone to help maintain DIN sourcing from the hyporheic zone even during extended periods (or whole seasons) when streamflow pulses are not large enough to mobilize POM. The same is likely true for sorbed NH_4^+ as low flow periods result in rising fluid conductivities (Figure 4.2A), potentially driving releases of physically stored N (Figure 4.6) when POM import to the hyporheic zone ceases. We would expect that the relative stability of each of these N pools plays an important role in governing N availability. Diel flow pulses in MDV streams mobilize POM, especially from *Nostoc*-dominated mats, resulting in a transfer of autochthonous OM and N into the hyporheic zone (Cullis et al. 2014, Heindel et al. 2021a). Remineralization of this OM

is thought to sustain elevated DIN concentrations in hyporheic water even as flow fluctuates (Singley et al. 2021a). In quantifying the extent of this hyporheic OM pool, we show that it does not need to be continually replenished to allow for DIN production by remineralization. Thus, this dynamic physical retention and release of OM and NH_4^+ in the hyporheic zone likely plays a critical role in sustaining N availability and downstream productivity in this highly oligotrophic system, especially at distances from the source glacier greater than 500–1000 m.

There are, of course, a number of assumptions underlying our simulations which preclude our results from representing the exact behavior of any particular MDV stream. First, mat coverage varies longitudinally and amongst streams (Alger 1997, McKnight et al. 1998), which would impact uptake rates and the distance over which allochthonous DIN signals diminish. However, mat coverage can now be modeled for specific stream corridors in the MDVs based on multi-spectral remote sensing data. Secondly, we include only NO_3^- removal processes, although there is evidence for NO_3^- production and release from the hyporheic zone due to remineralization (Kohler et al. 2018, Singley et al. 2021a). Such production would allow glacially-sourced N signals (both isotopic signatures and concentrations) to propagate further downstream than shown in our results. There has been insufficient quantification of DON concentration dynamics to determine the importance of DON production, uptake, and transformation along the stream, but there is evidence that it is not simply transported conservatively (Howard-Williams et al. 1989). Regardless of the limitations, our approach using uptake rates spanning two orders of magnitude and all USBC forms explores the widest range of plausible system behaviors. Through this approach we show that rapid attenuation of glacially-derived DIN inputs in MDV streams is highly likely even with widely variable diel flow pulses.

4.5.4 Implications for studies of intermittent streams in the MDVs and beyond

A few major knowledge gaps must be addressed to better constrain the longitudinal evolution of dominant N sources and actually close N budgets in MDV streams. Foremost is the need to document upstream boundary conditions for N inputs – including C-Q typology, DIN

and DON concentrations, and meltwater hydrographs at the glacier face. Quantifying spatiotemporal variation of N fixation rates would further limit uncertainty surrounding N inputs. There is also a need to better quantify N export dynamics for DON and POM, not just DIN. At present, none of the specific reaction rates linking these N pools (i.e., hyporheic OM mineralization, nitrification, POM entrainment, NH_4^+ sorption/desorption, etc.) have been determined in situ. Thus, our findings raise questions about how stream corridor N pools change over time such as: When does each pool act as a source or sink? Does this behavior change within and between seasons? Which pools are most sensitive to changes in streamflow, water temperature, and microbial activity that may occur with climate change? What is the importance of N in hyporheic OM pools to the recovery of periphyton following massive disturbance from large flow years (e.g. 2001-2002, Gooseff et al. 2017)? How common is reversible sorption of NH_4^+ in other intermittent streams? Resolving how N pools change over time is critical for explaining how and why streams regulation of N fluxes varies over time, rather than only during narrow discrete periods (i.e., nutrient addition studies).

Beyond these questions, our study also extends the work of Salvatore (2020; 2021 [*in review*]) in demonstrating the potential to map and quantify biomass of benthic algae, and the nutrients stored therein, in intermittent and ephemeral streams using multispectral remote sensing imagery. For alpine, arid, and polar environments without canopy cover obscuring the streambed, this method provides a promising means for characterizing spatial and temporal heterogeneity when flow is reduced or ceases altogether. A few studies have used various remote sensing platforms to map intermittent stream networks (Yang and Smith 2013, Spence and Mengistu 2016, Hamada et al. 2016), but little has been done to leverage such imaging to analyze exposed periphyton along the stream corridor when flow ceases and, to our knowledge, none have attempted to quantify nutrient storage over large areas. The use of spectral libraries based on the particular system of interest offers an intriguing means to provide more nuanced characterization of biotic communities than, say, simply detecting biomass in aggregate. Applying such tools will advance investigations into the processes governing patchy and

temporally variable ecosystem production, carbon and nutrient storage, and ecological responses to disturbance in intermittent streams.

More broadly, the results of our study taken together demonstrate that progress in our understanding of stream biogeochemistry may occur by more closely examining stream corridor N storage in the context of flux modulation at the reach scale, especially beyond perennial streams in forested temperate catchments. We have highlighted the utility of relatively simple scaling calculations with uncertainty propagation that serves as an initial approach for future studies in more complex systems. By applying this approach to MDV streams, we have illuminated the surprising magnitude of N storage over large regions in systems that appear starved for N.

4.6. Conclusions

In this study we leveraged historic point-scale sampling, remote sensing analysis, numerical modeling and a laboratory assay to demonstrate that N storage can be surprisingly high compared to observed fluxes in an intermittent Antarctic stream corridor. We uniquely scale biological and physical N storage over the entire stream corridor scale ($> 100,000$ m^2) to contextualize the importance of N storage at the system rather than centimeter scale. We find that even without significant allochthonous N inputs, N storage, especially in the hyporheic zone, can be comparable (or potentially higher) than has been reported for temperate forested systems. We also demonstrate that, despite generally being ignored outside of tracer addition studies, NH_4^+ sorption to stream sediment may be an important transient physicochemical storage mechanism that responds to short-term fluctuations in streamflow and governs the mobility of inorganic N. Altogether, this work illustrates the importance of quantifying N storage within stream corridors to understand the importance of internal cycling and retention in modulating and sustaining the availability of N in dissolved, mobile forms.

References

Aber, J. D., W. H. McDowell, K. J. Nadelhoffer, A. H. Magill, G. Berntson, M. Kamakea, S. G. McNulty, W. S. Currie, L. Rustad, and I. J. Fernandez. 1998. Nitrogen saturation in

temperate forest ecosystems - Hypotheses revisited. Bioscience 48:921–934.

Aber, J. D., K. J. Nadelhoffer, P. Steudler, and J. M. Melillo. 1989. Nitrogen Saturation in Northern Forest Ecosystems Published by : University of California Press on behalf of the American Institute of Biological Sciences Stable URL : http://www.jstor.org/stable/1311067 . BioScience 39:378–386.

Adams, B. J., R. D. Bardgett, E. Ayres, D. H. Wall, J. Aislabie, S. Bamforth, R. Bargagli, C. Cary, P. Cavacini, L. Connell, P. Convey, J. W. Fell, F. Frati, I. D. Hogg, K. K. Newsham, A. O'Donnell, N. Russell, R. D. Seppelt, and M. I. Stevens. 2006. Diversity and distribution of Victoria Land biota. Soil Biology and Biochemistry 38:3003–3018.

Alexander, R. B., E. W. Boyer, R. A. Smith, G. E. Schwarz, and R. B. Moore. 2007. The role of headwater streams in downstream water quality1. JAWRA Journal of the American Water Resources Association 43:41–59.

Alger, A. S. 1997. Ecological processes in a cold desert ecosystem: the abundance and species distribution of algal mats in glacial meltwater streams in Taylor Valley, Antarctica. Occasional paper/University of Colorado.

Barrett, J. E., M. N. Gooseff, and C. D. Takacs-Vesbach. 2009. Spatial variation in soil active-layer geochemistry across hydrologic margins in polar desert ecosystems. Hydrology and Earth System Sciences 13:2349–2358.

Bergstrom, A. J., M. N. Gooseff, J. G. Singley, M. J. Cohen, and K. A. Welch. 2020. Nutrient Uptake in the Supraglacial Stream Network of an Antarctic Glacier. Journal of Geophysical Research: Biogeosciences 125:e2020JG005679.

Bergstrom, A.J., Gooseff, M.N. 2021a. Chemical and sediment characteristics of ice cores collected from the ablation zones of Canada, Commonwealth, Howard, Hughes, and Seuss Glaciers in the McMurdo Dry Valleys, Antarctica from 2015 to 2019. Environmental Data Initiative. DOI: 10.6073/pasta/9943dc9f5b04e9d24424911c19349b58. Dataset accessed 3 June 2021.

Bergstrom, A.J., Gooseff, M.N. 2021b. Chemical characteristics of supraglacial stream water on Canada Glacier, McMurdo Dry Valleys, Antarctica during the 2015-2016 austral summer. Environmental Data Initiative. DOI: 10.6073/pasta/ea75e039fb7b6314e1c555c9ff8a5009. Dataset accessed 3 June 2021.

Bernhardt, E. S., G. E. Likens, R. O. Hall, D. C. Buso, S. G. Fisher, T. M. Burton, J. L. Meyer, W. H. McDowell, M. S. Mayer, and W. B. Bowden. 2005. Can't see the forest for the stream? In-stream processing and terrestrial nitrogen exports. BioScience 55:219–230.

Bockheim, J. G., I. B. Campbell, and M. McLeod. 2007. Permafrost distribution and active-layer depths in the McMurdo Dry valleys, Antarctica. Permafrost and Periglacial Processes 18:217–227.

Borchers, H. W. 2021. pracma: Practical Numerical Math Functions.

Boyer, E. W., C. L. Goodale, N. A. Jaworski, and R. W. Howarth. 2002. Anthropogenic nitrogen sources and relationships to riverine nitrogen export in the northeastern USA. Biogeochemistry 57:137–169.

Burrows, R. M., H. Rutlidge, N. R. Bond, S. M. Eberhard, A. Auhl, M. S. Andersen, D. G. Valdez, and M. J. Kennard. 2017. High rates of organic carbon processing in the hyporheic zone of intermittent streams. Scientific Reports 7:1–11.

Conovitz, P. A., L. H. MacDonald, and D. M. McKnight. 2006. Spatial and temporal active layer dynamics along three glacial meltwater streams in the McMurdo Dry Valleys, Antarctica. Arctic, Antarctic, and Alpine Research 38:42–53.

Cullis, J. D. S., L. F. Stanish, and D. M. McKnight. 2014. Diel flow pulses drive particulate organic matter transport from microbial mats in a glacial meltwater stream in the McMurdo Dry Valleys. Water Resources Research 50:86–97.

Datry, T., N. Bonada, A. J. Boulton, T. Datry, N. Bonada, and A. J. Boulton. 2017. Intermittent Rivers and Ephemeral Streams - Ecology and Management. Academic Press, Cambridge, MA, United States.

Delignette-Muller, M. L., and C. Dutang. 2015. fitdistrplus: An R Package for Fitting Distributions. Journal of Statistical Software 64:1–34.

Dodds, W. K., V. H. Smith, and K. Lohman. 2002. Nitrogen and phosphorus relationships to benthic algal biomass in temperate streams. Canadian Journal of Fisheries and Aquatic Sciences 59:865–874.

Drummond, J. D., S. Bernal, D. Von Schiller, and E. Martí. 2016. Linking in-stream nutrient uptake to hydrologic retention in two headwater streams. Freshwater Science 35:1176–1188.

Duncan, J. M., L. E. Band, P. M. Groffman, and E. S. Bernhardt. 2015. Mechanisms driving the seasonality of catchment scale nitrate export: Evidence for riparian ecohydrologic controls. Water Resources Research 51:3982–3997.

Gomez-Velez, J. D., J. W. Harvey, M. Bayani Cardenas, and B. Kiel. 2015. Denitrification in the Mississippi River network controlled by flow through river bedforms. Nature Geoscience 8:941.

Gómez, R., V. García, M. R. Vidal-Abarca, and L. Suárez. 2009. Effect of intermittency on N spatial variability in an arid Mediterranean stream. Journal of the North American Benthological Society 28:572–583.

Gooseff, M. N., D. M. McKnight, P. T. Doran, A. G. Fountain, and W. B. Lyons. 2011. Hydrological connectivity of the landscape of the McMurdo Dry Valleys, Antarctica. Geography Compass 5:666–681.

Gooseff, M. N., D. M. McKnight, and R. L. Runkel. 2004a. Reach-Scale Cation Exchange

Controls on Major Ion Chemistry of an Antarctic Glacial Meltwater Stream. Aquatic Geochemistry 10:221–238.

Gooseff, M. N., D. M. McKnight, R. L. Runkel, and J. H. Duff. 2004b. Denitrification and hydrologic transient storage in a glacial meltwater stream, McMurdo Dry Valleys, Antarctica. Limnology and Oceanography 49:1884–1895.

Gooseff, M. N., A. N. Wlostowski, D. M. McKnight, and C. Jaros. 2016. Hydrologic connectivity and implications for ecosystem processes-Lessons from naked watersheds. Geomorphology.

Grimm, N. B. 1987. Nitrogen Dynamics During Succession in a Desert Stream. Ecology 68:1157–1170.

Hamada, Y., B. L. O'Connor, A. B. Orr, and K. K. Wuthrich. 2016. Mapping ephemeral stream networks in desert environments using very-high-spatial-resolution multispectral remote sensing. Journal of Arid Environments 130:40–48.

Harvey, J. W., J. D. Gomez-Velez, N. M. Schmadel, D. T. Scott, E. W. Boyer, R. B. Alexander, K. Eng, H. Golden, A. Kettner, C. Konrad, R. B. Moore, J. Pizzuto, G. E. Schwarz, C. Soulsby, and J. Choi. 2018, April 9. How Hydrologic Connectivity Regulates Water Quality in River Corridors. Journal of the American Water Resources Association 55:369–381. Wiley/Blackwell (10.1111).

Heindel, R. C., A. J. Bergstrom, J. G. Singley, D. M. McKnight, J. Darling, B. Lukkari, K. A. Welch, and M. N. Gooseff. 2021a. Diatoms trace the retention and processing of organic matter in hyporheic sediments in the McMurdo Dry Valleys, Antarctica. Journal of Geophysical Research-Biogeosciences.

Heindel, R. C., J. G. Singley, A. J. Bergstrom, J. Darling, K. A. Welch, D. M. McKnight, and M. N. Gooseff. 2021b. Hyporheic sediment characteristics from Von Guerard Stream, Taylor Valley, McMurdo Dry Valleys, Antarctica in January 2019 ver 2. Environmental Data Initiative.

Hillebrand, H. 2008. GRAZING REGULATES THE SPATIAL VARIABILITY OF PERIPHYTON BIOMASS. Ecology 89:165–173.

Horner, R. R., and E. B. Welch. 1981. Stream Periphyton Development in Relation to Current Velocity and Nutrients. Canadian Journal of Fisheries and Aquatic Sciences 38:449–457.

Howard-Williams, C., J. C. Priscu, and W. F. Vincent. 1989. Nitrogen dynamics in two antarctic streams. Hydrobiologia 172:51–61.

Koch, J. C., D. M. McKnight, and J. L. Baeseman. 2010. Effect of unsteady flow on nitrate loss in an oligotrophic, glacial meltwater stream. Journal of Geophysical Research-Biogeosciences 115:G01001.

Koch, J. C., D. M. McKnight, and R. M. Neupauer. 2011. Simulating unsteady flow,

anabranching, and hyporheic dynamics in a glacial meltwater stream using a coupled surface water routing and groundwater flow model. Water Resources Research 47.

Koch, R., D. Kerling, and J. M. O'Brien. 2018. Effects of chronic elevated nitrate concentrations on the structure and function of river biofilms. Freshwater Biology 63:1199–1210.

Kohler, T. J. 2018. McMurdo Dry Valleys Microbial mat biomass, isotopes, and nutrient ratios sampled over a longitudinal gradient of two McMurdo Dry Valley streams ver 2. Environmental Data Initiative.

Kohler, T. J., L. F. Stanish, D. Liptzin, J. E. Barrett, and D. M. McKnight. 2018. Catch and release: Hyporheic retention and mineralization of N-fixing Nostoc sustains downstream microbial mat biomass in two polar desert streams. Limnology and Oceanography Letters.

Koohafkan, M. C., and B. A. Younis. 2015. Open-channel computation with R. The R Journal 7:249–262.

Lovett, G. M., and C. L. Goodale. 2011. A New Conceptual Model of Nitrogen Saturation Based on Experimental Nitrogen Addition to an Oak Forest. Ecosystems 14:615–631.

Luce, J. J., A. Cattaneo, and M. F. Lapointe. 2010. Spatial patterns in periphyton biomass after low-magnitude flow spates: geomorphic factors affecting patchiness across gravel–cobble riffles. Journal of the North American Benthological Society 29:614–626.

Maurice, P. A., D. M. McKnight, L. Leff, J. E. Fulghum, and M. N. Gooseff. 2002. Direct observations of aluminosilicate weathering in the hyporheic zone of an Antarctic Dry Valley stream. Geochimica et Cosmochimica Acta 66:1335–1347.

McKnight, D. M. 2019. McMurdo Dry Valleys LTER: Algal microbial mat biomass measurements from the McMurdo Dry Valleys and Cape Royds, Antarctica from 1994 to present. Environmental Data Initiative.

McKnight, D. M., A. Alger, C. Tate, G. Shupe, and S. Spaulding. 1998. Longitudinal Patterns in Algal Abundance and Species Distribution In Meltwater Streams In Taylor Valley, Southern Victoria Land, Antarctica. Pages 109–127 in J. C. Priscu (editor). Ecosystem Dynamics in a Polar Desert: The McMurdo Dry Valleys, Antarctica. American Geophysical Union (AGU).

McKnight, D. M., K. D. Cozzetto, J. D. S. Cullis, M. N. Gooseff, C. Jaros, J. C. Koch, W. B. Lyons, R. Neupauer, and A. N. Wlostowski. 2015. Potential for real-time understanding of coupled hydrologic and biogeochemical processes in stream ecosystems: Future integration of telemetered data with process models for glacial meltwater streams. Water Resources Research 51:6725–6738.

McKnight, D. M., D. K. Niyogi, A. S. Alger, A. Bomblies, P. A. Conovitz, and C. M. Tate. 1999. Dry valley streams in Antarctica: ecosystems waiting for water. BioScience 49:985–995.

McKnight, D. M., R. L. Runkel, C. M. Tate, J. H. Duff, and D. L. Moorhead. 2004. Inorganic N and P dynamics of Antarctic glacial meltwater streams as controlled by hyporheic exchange and benthic autotrophic communities. Journal of the North American Benthological Society 23:171–188.

Mikucki, J., Auken, E., Tulaczyk, S. et al. (2015) Deep groundwater and potential subsurface habitats beneath an Antarctic dry valley. *Nature Communications*, 6, 6831, https://doi.org/10.1038/ncomms7831

Naiman, R. J., and J. M. Melillo. 1984. Nitrogen budget of a subarctic stream altered by beaver (Castor canadensis). Oecologia 62:150–155.

O'Brien, J. M., S. K. Hamilton, L. Podzikowski, and N. Ostrom. 2012. The fate of assimilated nitrogen in streams: An in situ benthic chamber study. Freshwater Biology 57:1113–1125.

Peterson, B. J., W. M. Wollheim, P. J. Mulholland, J. R. Webster, J. L. Meyer, J. L. Tank, E. Martí, W. B. Bowden, H. M. Valett, and A. E. Hershey. 2001. Control of nitrogen export from watersheds by headwater streams. Science 292:86–90.

R Core Team. 2019. R: A Language and Environment for Statistical Computing. R Foundation for Statistical Computing, Vienna, Austria.

Runkel, R. L., D. M. McKnight, and E. D. Andrews. 1998. Analysis of transient storage subject to unsteady flow: diel flow variation in an Antarctic stream. Journal of the North American Benthological Society 143–154.

Salvatore, M. R., S. R. Borges, J. E. Barrett, E. R. Sokol, L. F. Stanish, S. N. Power, and P. Morin. 2020. Remote characterization of photosynthetic communities in the Fryxell basin of Taylor Valley, Antarctica. Antarctic Science 32:255–270.

Von Schiller, D., E. Martí, J. L. Riera, and F. Sabater. 2007. Effects of nutrients and light on periphyton biomass and nitrogen uptake in Mediterranean streams with contrasting land uses. Freshwater Biology 52:891–906.

Seitzinger, S. P., W. S. Gardner, and A. K. Spratt. 1991. The effect of salinity on ammonium sorption in aquatic sediments: Implications for benthic nutrient recycling. Estuaries 14:167–174.

Shumilova, O., D. Zak, T. Datry, D. Schiller, R. Corti, A. Foulquier, B. Obrador, K. Tockner, D. et al. 2019. Simulating rewetting events in intermittent rivers and ephemeral streams: A global analysis of leached nutrients and organic matter. Global Change Biology 25:1591–1611.

Singley, J. G., M. N. Gooseff, D. M. McKnight, and E.-L. S. Hinckley. 2021a. The Role of Hyporheic Connectivity in Determining Nitrogen Availability: Insights from an Intermittent Antarctic Stream. Journal of Geophysical Research: Biogeosciences 126:e2021JG006309.

Singley, J. G., M. N. Gooseff, D. M. McKnight, and E.-L. S. Hinckley. 2021b. Surface and

hyporheic porewater chemistry and sediment nitrification potentials in Von Guerard Stream, McMurdo Dry Valleys, Antarctica (2018-2020) ver 2. Environmental Data Initiative.

Singley, J. G., A. N. Wlostowski, A. J. Bergstrom, E. R. Sokol, C. L. Torrens, C. Jaros, C. E. Wilson, P. J. Hendrickson, and M. N. Gooseff. 2017. Characterizing hyporheic exchange processes using high-frequency electrical conductivity-discharge relationships on subhourly to interannual timescales. Water Resources Research 53:4124–4141.

Spence, C., and S. Mengistu. 2016. Deployment of an unmanned aerial system to assist in mapping an intermittent stream. Hydrological Processes 30:493–500.

Stelzer, R. S., and G. A. Lamberti. 2001. Effects of N: P ratio and total nutrient concentration on stream periphyton community structure, biomass, and elemental composition. Limnology and Oceanography 46:356–367.

Triska, F. J., A. P. Jackman, J. H. Duff, and R. J. Avanzino. 1994. Ammonium sorption to channel and riparian sediments: A transient storage pool for dissolved inorganic nitrogen. Biogeochemistry 26:67–83.

Triska, F. J., J. R. Sedell, K. Cromack, S. V. Gregory, and F. M. McCorison. 1984. Nitrogen Budget for a Small Coniferous Forest Stream. Ecological Monographs 54:119–140.

Vitousek, P. M., and W. A. Reiners. 1975. Ecosystem Succession and Nutrient Retention: A Hypothesis. BioScience 25:376–381.

Witherow, R. A., W. B. Lyons, N. A. N. Bertler, K. A. Welch, P. A. Mayewski, S. B. Sneed, T. Nylen, M. J. Handley, and A. Fountain. 2006. The aeolian flux of calcium, chloride and nitrate to the McMurdo Dry Valleys landscape: Evidence from snow pit analysis. Pages 497–505 Antarctic Science.

Wlostowski, A. N., M. N. Gooseff, D. M. McKnight, C. Jaros, and W. B. Lyons. 2016. Patterns of hydrologic connectivity in the McMurdo Dry Valleys, Antarctica: a synthesis of 20 years of hydrologic data. Hydrological Processes 30:2958– 2975.

Yang, K., and L. C. Smith. 2013. Supraglacial streams on the greenland ice sheet delineated from combined spectral-shape information in high-resolution satellite imagery. IEEE Geoscience and Remote Sensing Letters 10:801–805.

Chapter V

Stream Corridor Processes Sustain Chemostasis of Weathering Solutes

and Primary Nutrients in Antarctic Streams

5.1. Introduction

Analysis of concentration-discharge (C-Q) relationships has been widely applied across many solutes and systems to infer integrated catchment-scale hydrological and biogeochemical processes (e.g., Anderson et al., 1997; Chorover et al., 2017; Godsey et al., 2009, 2019; Rice et al., 2004). Most studies have focused on C-Q pattern classification or event-scale hysteretic form (Evans & Davies, 1998; Fazekas et al., 2020; Godsey et al., 2019). The causes of variability within long-term C-Q relationships for particular sites and solutes have received less attention (Knapp et al., 2020; Thompson et al., 2011) or are often ignored altogether as "noise" within the data. Stream corridor biogeochemical processes are widely acknowledged modulators of observed solute concentrations (Bernhardt et al., 2005; Duncan et al., 2015; Harvey & Gooseff, 2015; Peterson et al., 2001), but are rarely invoked in explanations of either the form or variability within long-term C-Q relationships because isolating their influence remains difficult.

The form and variability in C-Q relationships typically explained by hillslope controls on hysteretic patterns through mixing or hydrochemical non-stationarity of source waters (Chanat et al., 2002; Evans & Davies, 1998; Knapp et al., 2020; McDonnell et al., 1990; Pilgrim et al., 1979). Such catchment-focused studies have shown that for a particular location, land cover, lithology, and climate determine both the mean concentrations and variations in C-Q form across catchments (Fazekas et al., 2020; Godsey et al., 2019).

Similar catchment-centric explanations are invoked to explain chemostasis, in which concentrations remain relatively stable over large fluctuations in discharge (Clow & Mast, 2010; Godsey et al., 2009; Thompson et al., 2011). Chemostasis of geogenic solutes has nearly always, heretofore, been attributed to either large terrestrial source pool reservoirs or mobilization of relatively "old" subsurface water that has reached chemical equilibrium within the landscape (Clow & Mast, 2010; Godsey et al., 2009; Kirchner, 2003; Thompson et al., 2011). Chemostasis

of primary nutrients, such as nitrogen (N), has been narrowly reported in systems with large legacy stores from fertilizer additions (Basu et al., 2010; Marinos et al., 2020). Apart from Thompson et al. (2011), studies of chemostasis rarely discuss the ubiquity of variability within the general C-Q pattern (i.e., residuals from the general trend) at a particular site rather than spatially throughout networks.

While a small number of studies have considered how biogeochemical processing and network connectivity stabilize C-Q patterns for carbon (C) and N (e.g., Creed et al., 2015; Marinos et al., 2020), or may alter the slope or breakpoints in C-Q relationships (Moatar et al., 2017), many investigations have ignored stream corridor biogeochemical processes as a potential control of C-Q relationship form and variability. Yet, streams are recognized as strong modulators of primary nutrient concentrations, especially for N (Alexander et al., 2009; Harvey et al., 2018; Mulholland, 2004; Peterson et al., 2001). The general form of C-Q patterns (both event-hysteresis and long-term) may be primarily governed by catchment hydro-biogeochemistry in most systems, but signals from stream corridor biogeochemical activity will further modulate these underlying patterns for some solutes. This influence may be particularly important to long-term C-Q analysis as biogeochemical processes within stream corridors vary considerably over time (Hoellein et al., 2013; Martí & Sabater, 1996; Savoy et al., 2019). The effects of such temporal variations have been analyzed in terms of alteration of seasonal fluxes (Bernhardt et al., 2005; Mulholland, 2004), but not explicitly in terms of C-Q variability. Temporal changes in stream-corridor biogeochemical kinetics are not solely controlled by seasonal Q patterns (Matheson et al., 2012; Rusjan & Mikoš, 2010; Seybold & McGlynn, 2018) or may even differ among solutes in the same stream (Simon et al., 2005). Therefore, ignoring time variable stream corridor processes may over attribute variations in C-Q patterns to catchment processes alone. To our knowledge, no study has isolated solute specific differences in long-term C-Q form and variability due to stream corridor biogeochemical processes.

Here, we leverage the relative simplicity of ephemeral proglacial streams in the McMurdo Dry Valleys (MDVs), Antarctica, to isolate stream corridor controls on C-Q form and

variability across a range of solutes. Streamflow in the MDVs varies by orders of magnitude on the timescale of hours with diel glacial meltwater pulses and frequent periods of intermittency (Wlostowski et al., 2016). Due to a hyper-arid climate and the presence of continuous permafrost, MDV streams are hydrologically disconnected from adjacent hillslopes and associated solute pools therein (Bockheim et al., 2007; Conovitz et al., 2006; Fountain et al., 2010; Gooseff et al., 2016). Consequently, most solute concentrations are controlled by processes occurring in the main channel and well-connected hyporheic zones (Gooseff et al., 2002, 2016; Green et al., 1988; Lyons et al., 2021; Wlostowski et al., 2018). Wlostowski et al. (2018) demonstrated that due to rapid chemical equilibrium in hyporheic waters, MDV stream corridors can maintain chemostasis of geogenic solutes (i.e., silica, potassium, calcium, and bicarbonate).

Whether similar patterns exist for other solutes, especially primary nutrients (C, N, P) that are controlled by coupled physical and biological processes, remains an open question. Large portions of MDV streambeds are covered by cyanobacterial mats that persist in a freeze-dried state throughout much of the year and reactivate quickly upon rewetting (Kohler et al., 2015; McKnight et al., 1999, 2007). These mats, along with heterotrophic microbial communities in hyporheic sediment, strongly drive autochthonous organic matter (OM) and primary nutrient cycling (Gooseff et al., 2004; Koch et al., 2010; Kohler et al., 2018; McKnight et al., 2004). In this highly oligotrophic system, biotic demand exerts a strong influence on the stoichiometric ratio of primary nutrients (Barret et al., 2007). Compared to annual fluxes, MDV stream corridors can store relatively large N and OM pools (Chapter IV) and P is readily released by apatite weathering (Green et al., 1988; Heindel et al., 2018), but it has not been determined whether the reactions governing release from these pools are sufficiently rapid to sustain chemostasis.

In this study, we investigate the role of stream corridor processes in driving C-Q relationship form and variability for both geogenic solutes and primary nutrients, that are largely independent of hillslope influences. We hypothesize that:

H1: *Unlike geogenic solutes, the production and mobilization of solutes dependent on autochthonous organic matter cycling in stream corridors will be reaction limited due to relatively slower biotic process rates.* Consequently, we predict that despite relatively large source pools within MDV stream corridors, C-Q patterns for primary nutrients will be characterized by dilution.

H2: *Stream corridor biological processes are likely to exhibit greater spatial and temporal variability than weathering reactions of broadly distributed mineral substrate.* Therefore, we predict that stream corridors will impart larger variability into C-Q patterns for primary nutrients than geogenic solutes that are only minimally influenced by biota. Secondly, we predict that variations in C not controlled by Q will be correlated with primary drivers of biological activity including light, temperature, and antecedent flow conditions.

To evaluate these hypotheses and the resulting predictions, we analyze historic (1994-2018) C-Q form and variability for six solutes in ten MDV streams with varying flow characteristics. We also assess C-Q variability against concurrent environmental data (water temperature and light), antecedent flow metrics, and stream characteristics. The selected solutes range from those for which concentrations are most strongly influenced by physical processes alone (i.e., chloride and silica) to those governed by coupled physical and biological processes (i.e., dissolved organic carbon, ammonium, and nitrate). While dissolved P, represents an intermediate case as a primary nutrient sourced from mineral weathering.

5.2. Study System Background

The MDVs are a large, relatively ice-free polar desert landscape characterized by unvegetated expanses of glacial till and very little precipitation (10-50 mm water equivalent per year; Fountain et al., 2010; Levy, 2013). Stream gage maintenance and operation is notably challenging in such a hydrodynamic, cold, and arid landscape (Chinn & Mason, 2016), and weather often prevents regular site visits. Thus, we selected ten streams in Taylor Valley (Figure 5.1) gauged by the McMurdo Dry Valleys Long-Term Ecological Research (MCM LTER)

project based on the number of historic surface water grab samples, duration and quality of their gaging record (≥ 15 years), and representative variability in stream length and flow intermittence (Table 5.1).
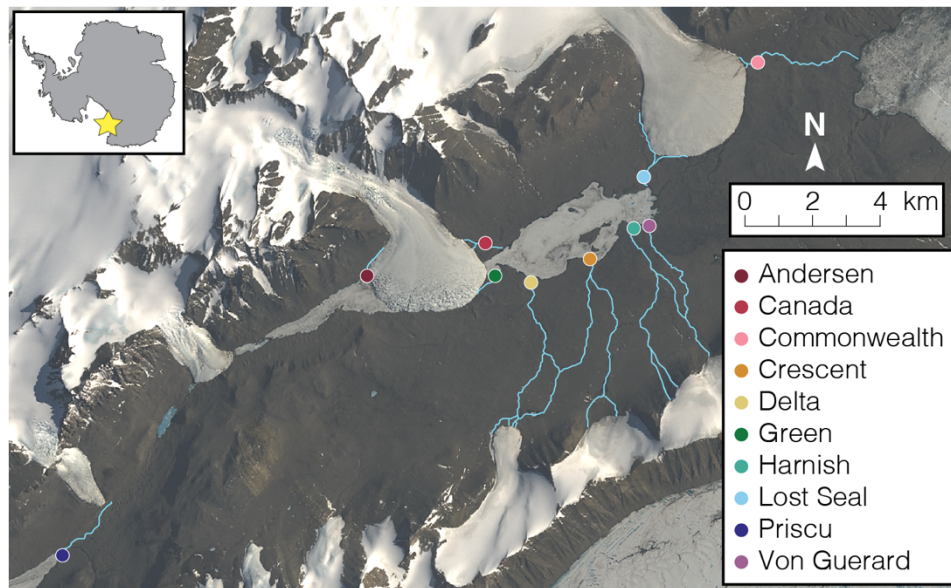
Figure 5.1. Study stream locations within Taylor Valley, Antarctica. Points denote gage locations.

Table 5.1. Study stream characteristics and historic record details.

Stream Name	Length to Gage (km)	Record Duration[1]	Grab Samples (n)	Median[2] Q (L s^{-1})	Seasonal Flashiness[3] (mean±sd)	MFMTT[4] (days)
Andersen	1.4	1994-2018	138	7.5	0.57±0.17	–
Canada	0.7	1994-2018	194	8.6	0.43±0.07	3.95
Commonwealth	0.7	1994-2018	113	15.2	0.44±0.08	2.04
Crescent	5.5	1994-2018	112	5.9	0.58±0.18	48.83
Delta	7.5	1994-2018	121	3.3	0.67±0.27	105.82
Green	0.7	1994-2018	180	12.2	0.46±0.11	3.69
Harnish	5.7	2002-2017	57	2.1	0.69±0.32	–
Lost Seal	2.0	1994-2018	139	11.1	0.58±0.14	10.21
Priscu	2.3	1994-2011	85	9.0	0.50±0.12	–
Von Guerard	4.7	1994-2018	107	3.7	0.62±0.18	54.13

[1]Seasons are indicated by the year in which flow ends (i.e., 2006 denotes the 2005-2006 Austral summer)
[2]Calculated for non-zero flows only over entire record
[3]Mean of seasonal Richards-Baker Index (Baker et al., 2004) based on daily Q volumes
[4]Median flow mean transit time (Wlostowski et al., 2018)

We matched historic surface water grab sample data (Lyons, 2021a-b; Lyons & Welch, 2021) with 15-minute Q data (Gooseff & McKnight, 2021a-j) from the 1994-2018 Austral summer streamflow seasons for the 10 selected streams. For each grab sample, we utilized data for chloride (Cl^-), silica (Si), soluble reactive phosphorus (SRP), dissolved organic carbon (DOC), ammonium (NH_4^+), and nitrate (NO_3^-). Detailed sampling, handling, and analytic procedures are provided in the grab sample metadata (Lyons, 2021a-b; Lyons & Welch, 2021). To minimize the influence of contaminated samples or analytic errors, we removed outliers with concentrations more than 1.5 times the interquartile range above or below the first and third quartiles for a given stream and solute. Outliers represented only 0.0–9.2% (median = 1.0%) of the reported data for each solute and stream.

The stream corridor cycles influencing the selected solutes span a continuum of complexity ranging from only a few physical processes (i.e., mineral weathering or atmospheric deposition) to numerous biological processes (Figure 5.2). Here, we provide an overview of which source and sink processes influence each solute, as well as a qualitative assessment of their relative importance. Of the solutes we consider, Cl^- has the simplest of cycles, at least in terms of the number of coupled processes and lack of biological influence. Deposition of marine aerosols represents the dominant flux of Cl^- into the system, while salt crust precipitation and dissolution along stream margins primarily contribute to observed stream water Cl^- patterns (Keys & Williams, 1981; Welch et al., 2010; Witherow et al., 2006).

	Cl	Si	SRP	DOC	N
1. Glacier	+ Deposition	+ Mineral Wx	+ Mineral Wx +/– Sediment sorption	+ OM Leaching – Heterotroph. metab.	+ Deposition +/– Heterotroph. metab.
2. Channel	+/– SC dissol./precip.	– Diatom uptake	– AM assimilation	+ OM leaching + AM scouring – AM assimilation	+ AM fixation + AM DON/DIN leaching – AM assimilation
3. Hyporheic/ Parafluvial Zones	+/– SC dissol./precip.	+ Sediment Wx + Diatom frustule Wx	+ Mineral wx + OM mineralization	+ OM leaching – OM mineralization – Denitrification	+ OM mineralization + Nitrification +/– Sediment sorption – Assimilation – Denitrification

+ Major source
+ Minor source
– Minor sink
– Major sink

Abbreviations
SC = salt crust
Wx = weathering
AM = algal mat
OM = organic matter

Figure 5.2. Conceptual depiction of MDV stream corridor characteristics and summary of the physical and biogeochemical source and sink processes controlling cycling of selected solutes (N species lumped). Supporting studies are cited in the main text.

Dissolved Si concentrations are similarly controlled predominantly by physical processes in MDV stream corridors. Aluminosilicate mineral weathering occurs in the hyporheic zone (Lyons et al., 2021; Maurice et al., 2002) resulting in longitudinal increases in Si concentrations (Gooseff et al., 2002). Wlostowski et al. (2018) determined that timescales for chemical equilibrium associated with mineral weathering are relatively fast compared to transit times, resulting in Si chemostasis. In addition to primary mineral weathering, some Si cycling occurs through biological uptake by diatoms, precipitation and dissolution associated with freeze-thaw cycles, and chemical equilibrium with secondary mineral Si products that occur relatively homogenously throughout the hyporheic zone (Hirst et al., 2020). Intact and fragmented diatom frustules have been observed in hyporheic sediment (Heindel et al., 2021), suggesting that weathering of biogenic Si could also be a minor influence on observed concentrations.

Dissolved phosphorus is dominantly sourced from mineral weathering of apatite (Green et al., 1988; Heindel et al., 2018), resulting in relatively elevated SRP concentrations in hyporheic water (McKnight et al., 2004). While aeolian transport deposits sediment on glaciers,

SRP is typically undetectable in supraglacial streams and ice cores (Bergstrom et al., publication pending), but can be elevated in cryoconite holes (Bagshaw et al., 2013). Combined with physical and biological removal of SRP in supraglacial sediment deposits (Bergstrom et al., 2020), the glacial inputs of SRP at the head of proglacial streams appears to be relatively minor most of the time. In the stream corridor, added SRP is removed rapidly in the main channel by algal mats (McKnight et al., 2004). The release of SRP by organic matter remineralization has not been specifically quantified, but is likely, given the retention of algal mat particulate organic matter (POM) in the hyporheic zone (Heindel et al., 2021) and indications of subsequent remineralization (Kohler et al., 2018; Singley et al., 2021). Even with these biological influences, SRP concentrations, especially in lower Taylor Valley, are likely predominantly controlled by mineral weathering in the hyporheic zone.

In contrast, DOC and N cycling involve many more complexly coupled biological and physical processes. Active biota exist in cryoconite holes and supraglacial streams (Bagshaw et al., 2011, 2013; Bergstrom et al., 2020), yet organic matter export from glaciers tends to be relatively small, although not zero (Bagshaw et al., 2013; Howard-Williams et al., 1989). Atmospheric deposition of NO_3^- is important on source glaciers (Witherow et al., 2006) and supraglacial streams do have the potential to modulate fluxes prior to meltwater reaching the head of proglacial streams (Bergstrom et al., 2020; Fortner et al., 2005). Dissolved inorganic nitrogen (DIN) concentrations observed at stream gages are often about equal to those in glacial ice, but N stable isotope data indicate that glacially sourced N is supplanted by N fixed by algal mats along the length of MDV streams (Kohler et al., 2018). Autotrophic production by benthic algal mats represents the largest C flux into MDV streams, but net productivity remains near zero for many mats (Hawes & Howard-Williams, 1998). The spiraling of autochthonous C and N is reliant upon mobilization of DON or POM from algal mats in response to flow pulses (Cullis et al., 2014), transport of this material into the hyporheic zone (Heindel et al., 2021) and subsequent remineralization and nitrification, which results in elevated DIN concentrations in hyporheic water (Singley et al., 2021). Uptake of DIN by benthic algal mats act as a strong sink in the main

channel (Gooseff et al., 2004; McKnight et al., 2004) and likely quickly depletes elevated DIN concentrations associated with hyporheic exchange flows (Singley et al., 2021). Additionally, NH_4^+ is subject to reversible sorption to hyporheic sediment, which may represent an important physical source and sink in the hyporheic zone (Chapter IV). Compared to the other solutes we consider, C and N are much more strongly influenced by heterotrophic and autotrophic processes that are coupled to physical drivers of transport and storage.

5.3. Analysis of Concentration-Discharge Relationships

Using the paired C and Q data, we fit power-law relationships ($C = aQ^b$) to quantitively characterize C-Q relationships as diluting ($b < -0.2$), chemostatic ($|b| < 0.2$), or enriching ($b > 0.2$; Godsey et al., 2009). We then calculated coefficients of variations (CV = σ/μ, where σ is the standard deviations and μ is the mean of samples) for both Q and individual solute concentrations. We analyzed long-term, system-wide differences in CV_C/CV_Q by solute using pairwise Mann-Whitney U tests. We assessed the stability of C-Q patterns over time by calculating CV_C/CV_Q values and power-law fits using an overlapping 5-year sliding window approach over the entire period of record for each stream and solute. A 5-year moving window was selected to overcome limitations from low sample numbers in particular seasons due to the difficulty in regularly accessing sites and frequent periods of flow cessation.

To identify potential drivers of variability within chemostatic patterns, we analyzed relationships between observed C and light, water temperature, and Q metrics. We paired grab sample data with 15 minute photosynthetically active radiation (PAR) data from the Lake Fryxell met station (Doran & Fountain, 2019) as well as concurrent water temperature data from each stream gage (Gooseff & McKnight, 2021a-j). We characterized short-term changes in Q as the average dQ/dt (n=4) for the hour preceding each grab sample. To assess the influence of Q over longer-timescales on C variations, we also calculated the cumulative flow (ΣQ) over the prior 12, 24, and 48 hours and the for the entire season to the time of sample collection. As the selected streams differ dramatically in their geomorphic and hydrologic characteristics, we also compared

CV_C/CV_Q values to stream length to gage, flashiness (sensu Baker et al., 2004), and median flow mean transit time (MFMTT; Wlostowski et al., 2018). We visually inspected the relationships between each of these metrics and solute concentrations for each stream and fit linear relationships for each case.

5.4. Results

Despite the highly dynamic nature of MDV streams and limited hillslope interaction, both weathering solutes and primary nutrient data indicate that chemostasis is remarkably ubiquitous and persists over decades (Figures 5.3-5.4). All C-Q relationships had a log-log slope parameter close to zero (Figure 5.5), while CV_C/CV_Q values ranged from 0.07–0.64. Regardless of solute or stream, the C-Q relationships satisfy definitions of chemostasis (i.e., $|b| < 0.20$ and $CV_C/CV_Q < 1$; Godsey et al., 2009; Thompson et al., 2011). The only case in which this definition may not be met is for NO_3^- in Priscu Stream ($b = 0.23\pm0.06$, $CV_C/CV_Q = 0.35$), largely due to higher concentration variability at low flows. We also found that chemostatic means (or "set points", *sensu* Godsey et al., 2019) varied both among solutes for particular streams and across streams for each solute. Generally, Cl^- and Si concentrations were the highest, followed by DOC while concentrations of DIN species and SRP were lower, but set points varied by a few orders of magnitude amongst streams.
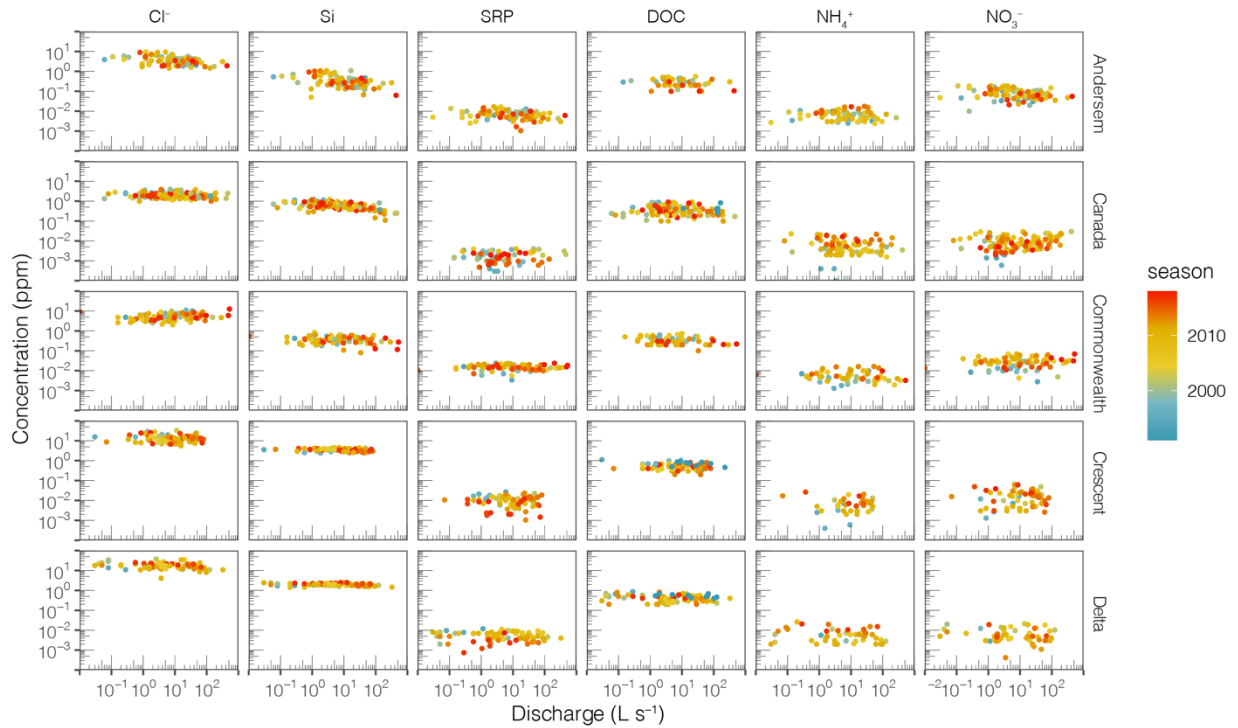
Figure 5.3. Historic C-Q relationships by solute for Andersen Creek, Canada Stream, Commonwealth Stream, Crescent Stream, and Delta Stream.
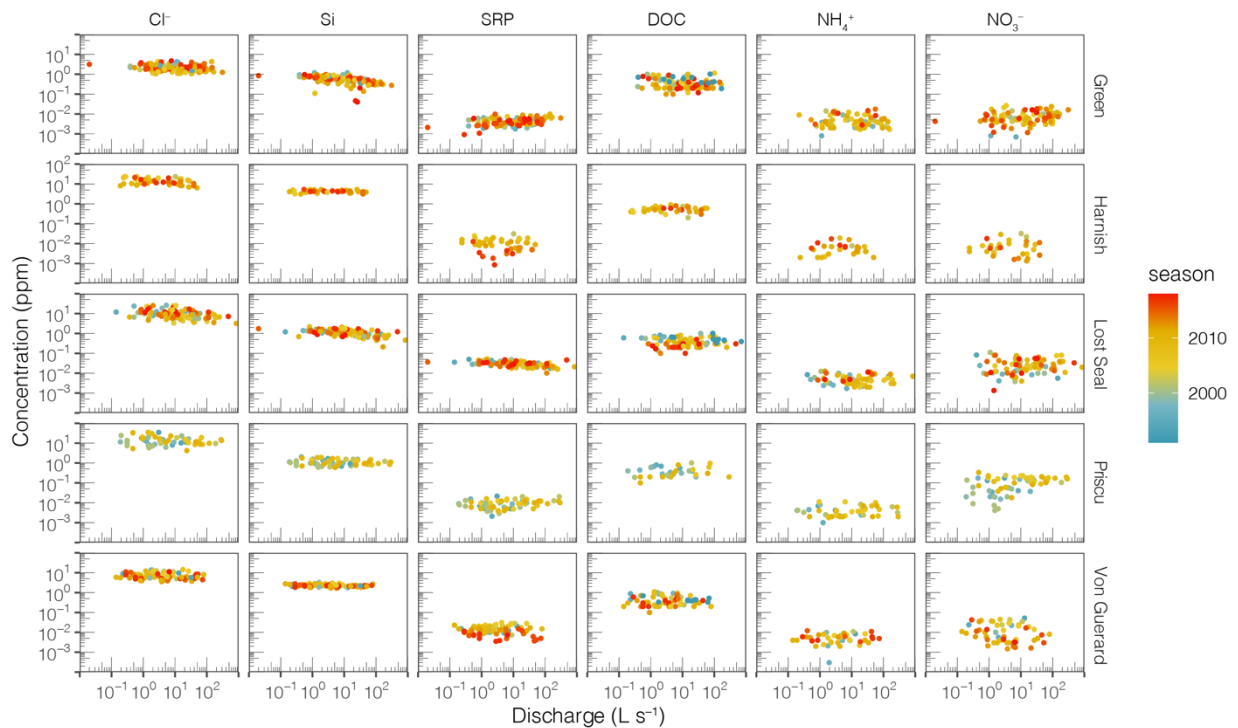
Figure 5.4. Historic C-Q relationships by solute for Green Creek, Lost Seal Stream, Priscu Stream, and Von Guerard Stream. Note that Priscu Stream discharge data ended in 2011 due to lake level rise.
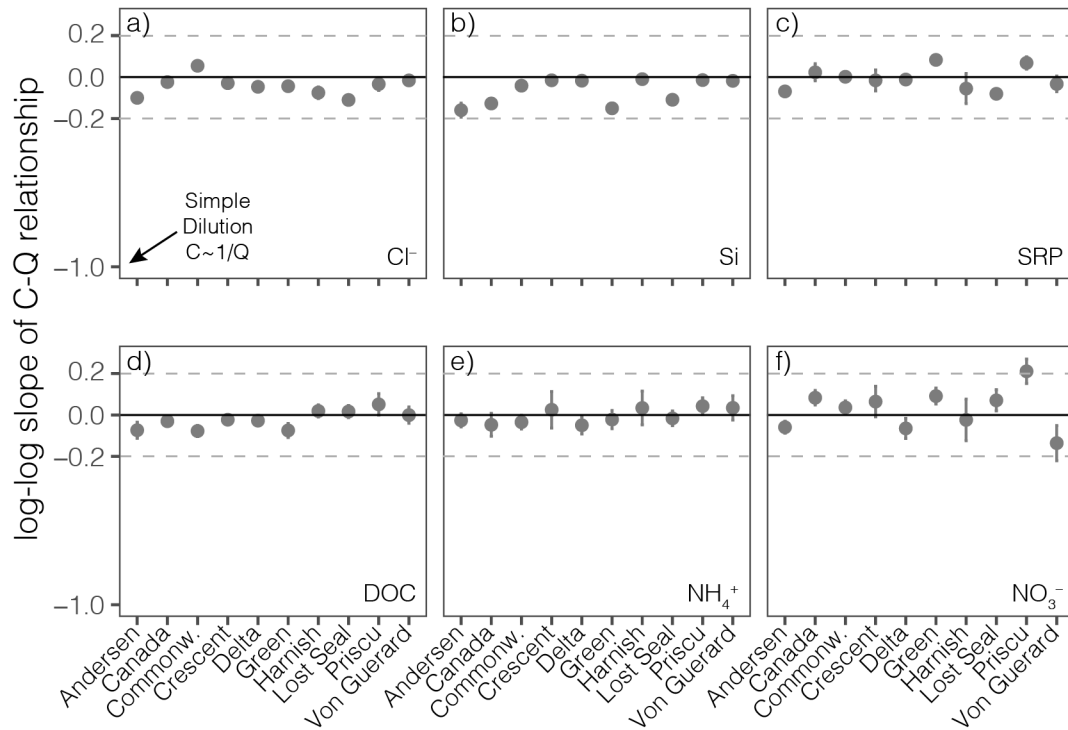
Figure 5.5. Log-log slopes of fitted C-Q relationships (±SE) for each solute by stream over the entire period of record. Dashed lines at ±0.2 indicate the quantitative boundary used to define chemostasis.

The ratio of coefficients of variation exhibited consistent patterns across the long-term record for the 10 streams we studied (Figure 5.6). In particular, CV_C/CV_Q was significantly lower for Si relative to all other solutes ($p < 0.05$, Mann-Whitney U). Variability of Cl^-, SRP, and DOC were not statistically different ($p > 0.35$), while at the other end of the continuum, the relative variability of NO_3^- was greater than for all other solutes ($p < 0.028$), except in comparison to NH_4^+ ($p = 0.68$). Full pairwise statistical test results are provided in Table S5.1.
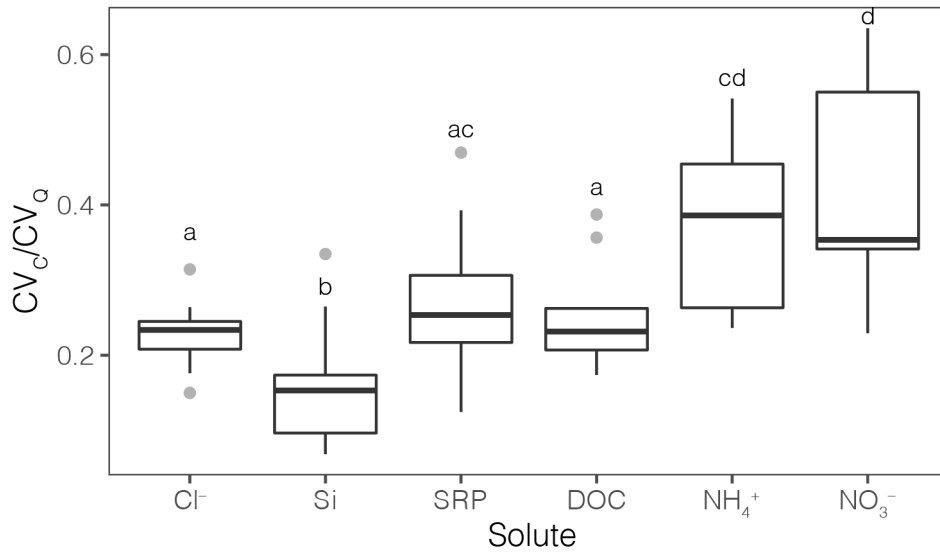
Figure 5.6. Ratio of coefficients of variation by solute across the 10 study streams for all historic data. Lowercase letters denote statistically significant differences among groups ($p < 0.05$, pairwise Mann-Whitney U test).

The observed trend towards higher CV_C/CV_Q among primary nutrients (especially DIN species) than less biologically active geogenic solutes (i.e., Cl and Si) generally held for narrower temporal windows in each stream as well (Figure 5.7). However, five-year moving averages of CV_C/CV_Q were generally more variable than when aggregated over decades. Notably, some longer streams (i.e., Crescent, Delta, Harnish, and Von Guerard) also exhibited larger ranges of CV_C/CV_Q for NH_4^+ and NO_3^- over time. Andersen Creek, which has very little mat coverage and flows closely along the edge of Canada Glacier, exhibited the least structure in CV_C/CV_Q among solutes.
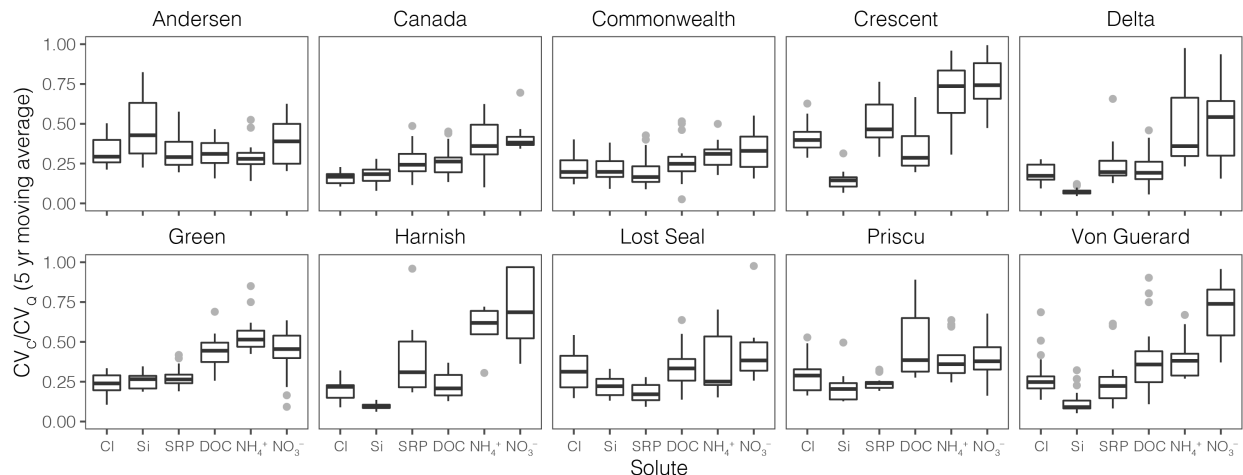
Figure 5.7. Ratio of coefficients of variation from five-year moving window analysis across the historic record for each stream and solute.

Surprisingly, we found that variability within chemostatic relationships was not strongly related to canonical drivers of chemical and biological reactions such as water temperature or PAR, even for nutrients (Figures 5.8 and S5.1-9). Concentration variations did not exhibit relationships with cumulative discharge over the prior 12, 24, and 48 hours or the entire flow season to the time of sample collection. Nor did we find that variations in concentration were controlled by dQ/dt at the time of sample collection. Of the 420 combinations of environmental variables and solutes across the 10 streams, only 117 relationships exhibited a significant linear relationship ($p < 0.05$), but only 44.4% of those had p-values < 0.01. For linear relationships with $p < 0.05$, we found the mean adjusted R^2 was fairly low at 0.10 ± 0.06, while maximum was only 0.32. An example of these generally weak relationships is shown for Canada Stream (Figure 5.9), which had the largest number of grab samples. The same information for all other streams is provided in Figures S5.1-9. The only discernable pattern other than weak linear relationships is an apparent collapse of concentration variability (especially for Si and Cl$^-$) for samples collected at times with larger prior cumulative flows, particularly over shorter preceding window widths (i.e., 12 hours). As the collapse tends towards the mean concentration, it is not possible to determine whether this is merely an artifact of relatively sparse sampling at higher value or actual behavior of the system.
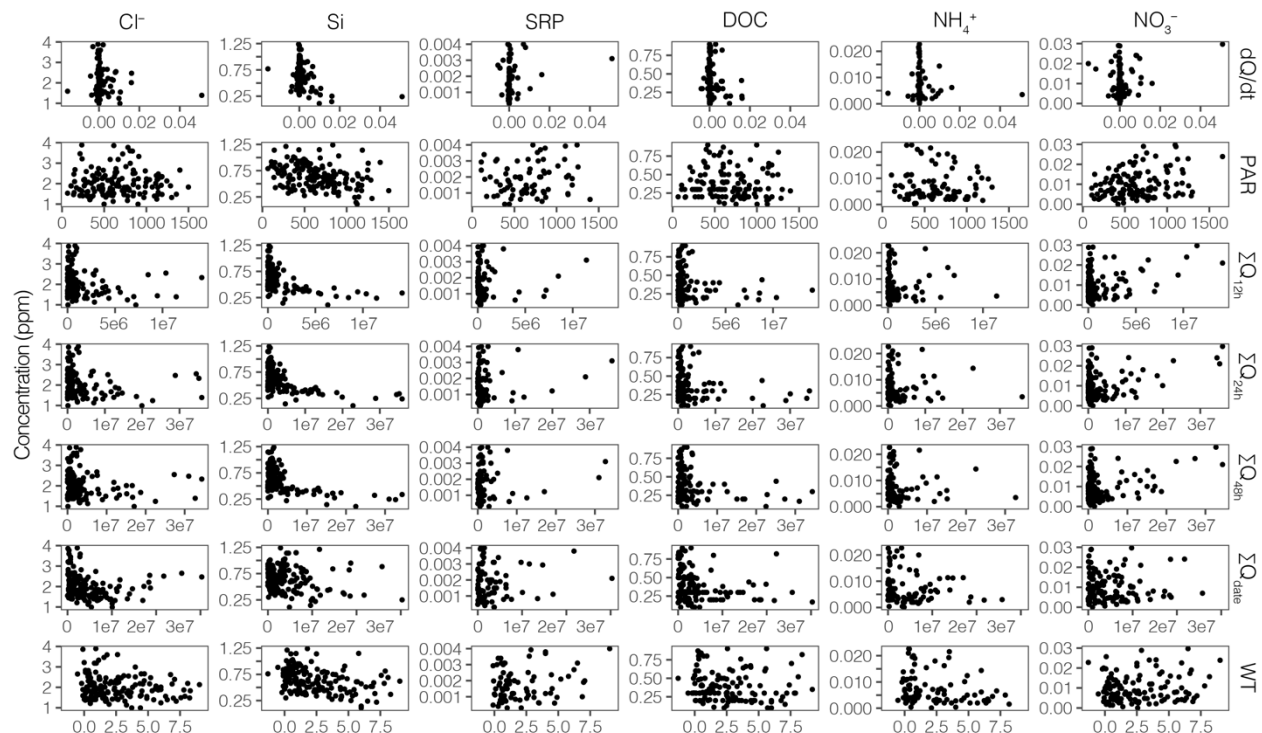
Figure 5.8. Concentration variations of each solute (columns) versus expected environmental drivers (rows) with dQ/dt (L s^{-2}), PAR (μS s^{-1} m^{-2}), cumulative discharge (L) over the prior 12, 24, and 48 hours and season to date, and water temperature (ºC).

We found that few differences in CV_C/CV_Q among streams were explained by stream length, MFMTT, or mean seasonal flashiness (Figure 5.9). As reported by Wlostowski et al. (2018), stream length and MFMTT were negatively correlated to Si CV_C/CV_Q. In contrast, we found that CV_C/CV_Q for SRP, NH$_4^+$ and NO$_3^-$ increased with stream length, although these relationships were not very strong (adjusted $R^2 < 0.33$). Neither DOC nor Cl$^-$ CV_C/CV_Q were related to stream length. MFMTT was only significantly correlated to Si CV_C/CV_Q and flashiness was only weakly positively correlated to NO$_3^-$ CV_C/CV_Q.
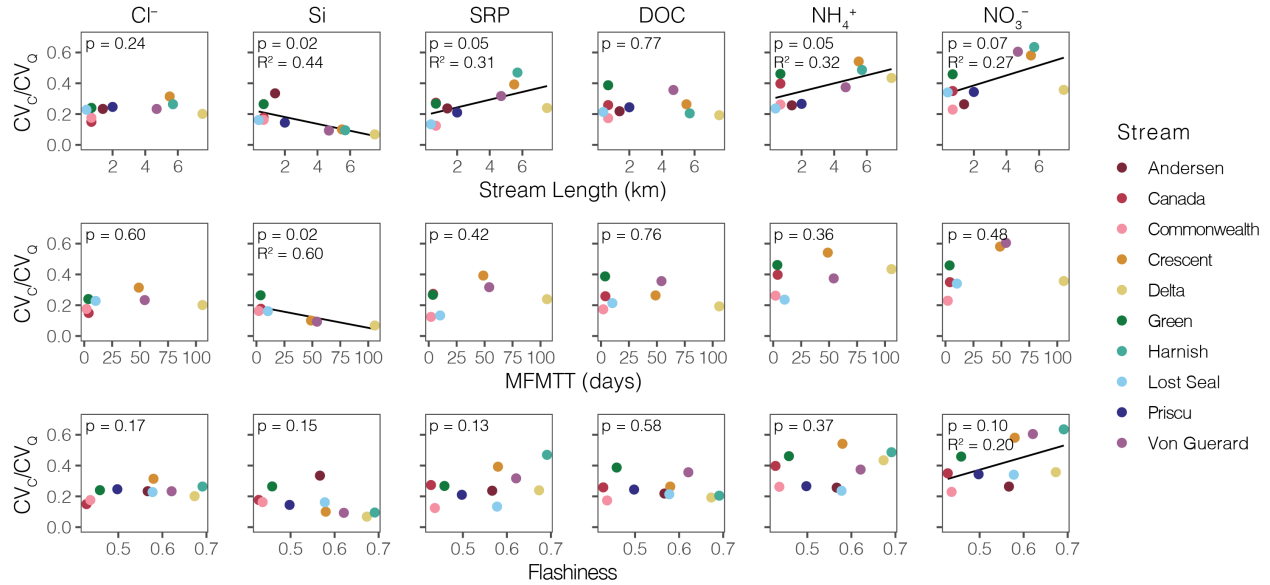
Figure 5.9. Solute CV_C/CV_Q by stream length, median flow mean transit time (MFMTT), and mean seasonal Richards-Baker flashiness index. Adjusted R^2 and linear fit lines are only shown for relationships with $p < 0.10$.

5.5. Discussion

5.5.1 What Causes Nutrient Chemostasis in MDV Streams?

Contrary to H1, we found that chemostasis is remarkably ubiquitous and temporally persistent among all solutes, even primary nutrients (Figures 5.3–5). Prior studies have demonstrated that little to no catchment processes are necessary to bring about and maintain chemostasis of geogenic solutes due to hyporheic weathering in this system (Lyons et al., 2021; Wlostowski et al., 2018). Our findings uniquely demonstrate that chemostasis can also be established and sustained by stream corridor processes for nutrients in a highly oligotrophic system with rapid changes in flow.

In temperate systems, chemostasis is most commonly attributed to large, distributed pools of weathering products, mobilization of "old water" or legacy nutrients from fertilizer applications (Clow & Mast, 2010; Godsey et al., 2009; Marinos et al., 2020; Thompson et al., 2011). Yet, such explanations are unsuitable for MDV streams. Without substantial hydrologic connectivity to hillslopes (Gooseff et al., 2016), stream solute concentrations above those in

relatively dilute glacial meltwater (Bagshaw et al., 2013; Fortner et al., 2005; Fortner & Lyons, 2018) must be primarily sourced from the hyporheic and parafluvial zones (Gooseff et al., 2002). Wlostowski (et al., 2018) explained chemostasis of weathering solutes in MDV streams in terms of chemical equilibrium timescales that are relatively fast compared to transit times in the hyporheic zone. While this explanation may similarly apply to SRP through apatite weathering (Green et al., 1988; Heindel et al., 2018), it does not immediately explain chemostasis of solutes without a geogenic source (i.e., DOC and DIN). Rather, it is likely that the mobilization and remineralization of autochthonous organic matter sustains fluxes from source pools within the hyporheic zone (Heindel et al., 2021; Singley et al., 2021; Chapter IV). It is notable that storage in the stream corridor does not occur predominantly in dissolved, readily mobile forms (Chapter IV). This requires that remineralization processes also be (at least transiently) equal to or faster than exchange timescales and occur over sufficiently large, well-connected hyporheic volumes to prevent shifts towards dilution at higher flows. For DIN species, chemostasis may be further sustained by temporary storage and release of NH_4^+ through reversible sorption to hyporheic sediment (Chapter IV). Thus, chemostasis of nutrients in MDV streams is distinctive in that it (1) does not require anthropogenically enlarged nutrient pools, (2) emerges principally from stream corridor processes, and (3) implies dynamic biogeochemical processing to permit mobilization of solutes in dissolved form.

5.5.2 How and Why does Chemostatic Variability Differ Among Solutes?

Our analysis also demonstrated that variability within chemostatic relationships exhibits system-wide structure by solute over a range of timescales (Figures 5.6 and 5.7). Specifically, Si exhibited the least variability while Cl⁻, SRP, and DOC had intermediate variability and DIN species were the most variable. In temperate and tropical experimental watersheds, larger source pools and export loads stabilize C-Q relationships, resulting in decreased CV_C/CV_Q values for some solutes (Thompson et al., 2011). Although this pattern exists for a few pairwise comparisons in this study (i.e., Si vs NO_3^-), it does not generally hold for MDV streams. In

particular, this explanation is refuted by the statistical similarity of CV_C/CV_Q values for Cl^- and SRP (Figure 5.6), despite their having chemostatic set points and export fluxes that differ by three to four orders of magnitude (Figures 5.3–4). Therefore, the system-wide structure of CV_C/CV_Q in MDV streams is not simply a function of total solute export.

As predicted by H2, we instead found that solutes subject to greater control by biological processes, especially DIN species, exhibit more variability within chemostatic relationships than Si (Figure 5.6) This pattern holds over time, particularly in longer streams (Figure 5.7). We conclude that even when all solutes are sourced from a far more constrained area (i.e., the stream corridor), more variability will emerge in chemostasis due to biological processes. Of course, the temporal changes in biotic processes driving this "noise" may occur contemporaneously with changes in discharge, but persistent directional correlations would result in structured deviations from a C-Q slope near zero, which we do not observe. In other systems, OM mineralization, autotrophic assimilation (of C, N, and P), nitrification, denitrification, gross primary production, and ecosystem respiration have all been shown to exhibit large, multi-scale temporal variation that is controlled by environmental variables such as PAR or temperature, rather than discharge (Griffiths & Tiegs, 2016; Heffernan & Cohen, 2010; Hoellein et al., 2013; Matheson et al., 2012; Rusjan & Mikoš, 2010; Seybold & McGlynn, 2018; Warwick, 1986). The relationship between discharge and temporal variations in biological process kinetics can be further obscured through interactive control by multiple environmental variables (e.g., both light and temperature; Huryn et al., 2014) or lagged coupling between processes (e.g., autotrophic organic matter exudation and denitrification; Heffernan & Cohen, 2010).

It is probable that temporal variations in net reaction rates would contribute to concentration variations in MDV streams, especially given the rapidly changing environmental conditions as well as prior evidence that stream biota respond to rewetting within hours, even after decades of desiccation (McKnight et al., 2007). In contrast to secondary predictions related to H2, observed concentration variations for particular streams and solutes were not well explained by antecedent flow conditions, instantaneous rates of change in discharge, water

temperature, or PAR (Figures 5.9 and S5.1-9). This certainly does not indicate that these variables do not drive changes in biogeochemical cycling, but more likely the magnitude of process rate changes and the response timescale of those changes to environmental drivers differs among individual processes. For instance, autotrophic assimilation capacity for NO_3^- by benthic algal mats may respond strongly and rapidly to large diel fluctuations in streamflow, while nitrification in continuously wetted, thermally buffered hyporheic and parafluvial zones may be more stable throughout daily pulses. Consequently, surface water concentrations at a particular time and location will reflect resulting fluctuations in the net sum of source and sink processes, but may not necessarily exhibit simple relationships to concurrent or antecedent conditions as the number of processes being integrated increases. As these processes are chemically and physically interlinked, increasing the number of coupled processes is not equivalent to summing evermore random independent variables as has been explored for relationships between catchment area and C or Q variability (Egusa et al., 2019; Marinos et al., 2020; Woods et al., 1995). Differences in variability among solutes, as we found in this study, would then arise due to both the number of controlling processes and their individual but interdependent spatiotemporal fluctuations.

Despite the relative simplicity of Si and Cl^- cycling (Figure 5.2) and the abundance of minimally weathered substrate or atmospherically deposited salts (Maurice et al., 2002; Witherow et al., 2006), variability still exists within geogenic solute chemostasis in MDV streams. This suggests that non-biological stream corridor processes also likely contribute to C-Q noise. As in other systems, this may be due to influences of temperature, pH, relative concentrations of ions, and dissolved carbon dioxide concentrations – all of which vary over time – on mineral dissolution rates (Brantley, 2008).

Additionally, solute generation and storage are not homogenously distributed throughout hyporheic and parafluvial zones (Singley et al., 2021). Thompson et al. (2011) demonstrated that more homogenous source pool distribution in catchments would lead to lower CV_C/CV_Q values, which could theoretically apply to the stream corridor itself. In MDV streams, such

heterogeneity in Cl⁻ pools is apparent in visible salt crusts that form in particular locations along stream margins. In contrast, the lower CV_C/CV_Q for Si is likely due to more homogenous sourcing from primary and secondary weathering of minerals (Hirst et al., 2020). The influence of heterogeneity in source pools and microbial process potentials may be even more pronounced for DIN forms due to combinations of habitat suitability, substrate supply, and differences in the timescale and frequency of hydrologic connectivity. Similar to other systems, hyporheic connectivity varies in MDV streams as a function of temperature (Cozzetto et al., 2013) and hyporheic extent changes seasonally due to active layer dynamics (Conovitz et al., 2006). These complexities contribute to hyporheic residence time distributions that range from seconds to months (Gooseff et al., 2003, 2016; Wlostowski et al., 2018) and change over seasonal to interannual timescales (Singley et al., 2017). Modeling has shown that cyclic hydrologic pulsing, as is typical in MDV streams, can also alter hyporheic residence time and efficacy of biogeochemical transformations (Singh et al., 2020). This effect could theoretically result in different observed concentrations at a particular point and flow condition. Unraveling the relative importance of hyporheic solute pool heterogeneity versus time-varying source-sink kinetics in driving the observed patterns is critical but lies outside the scope of the present study.

Our explanations of C-Q variability are also limited by the insufficient information to constrain whether observed variations in chemostasis are driven by time variable solute removal, production, or both in the stream corridor. Regardless of this unresolved distinction, the long-term system-wide behaviors that we present here demonstrate that there is a need to merge investigations into C-Q form and variability with understanding of solute-specific stream corridor processes. By doing so, we have begun to unravel the convolution of stream corridor and catchment biogeochemical signals in long-term C-Q patterns.

5.5.3 Why does Chemostatic Variability Differ Among MDV Streams?

Apart from a few weak relationships, differences in CV_C/CV_Q among streams are not well explained by characteristics related to flow such as length, transit time, or flashiness (Figure

5.9). Large variability in CV_C/CV_Q in short streams for most solutes may reflect the importance of glacial signals rather than the emergence of stream corridor-controlled patterns that dominate solute dynamics in longer streams (Gooseff et al., 2002; Kohler et al., 2018) (Chapter IV). The distances over which this transition occurs is not known and likely differs depending on source glacier as well as physical and biological characteristics (i.e., slope, channel incision, algal mat coverage and composition, etc.). In non-polar settings, increasing dominance of hydrologic exports by precipitation (i.e., similarly dilute inputs with limited sediment or soil contact) reduced the ability of distributed subsurface solute pools to serve as a chemostatic buffer (Thompson et al., 2011). Even for a relatively simple system, our findings reinforce the need to develop biogeochemical reaction rate theories for nutrients and geogenic solutes that integrate hydrologic controls while addressing spatial and temporal heterogeneity at field relevant scales (Li et al., 2021).

5.5.3 Extensions to Other Systems

While hydrologic connectivity and solute sourcing are more narrowly constrained in MDV streams, the over-arching principles guiding our analysis can be extended to more complex systems with greater catchment influence on C-Q patterns. We have shown that stream corridors can imprint variability on chemostatic C-Q relationships that differs systematically across solutes. Although the underlying C-Q pattern in this demonstration case emerges from the stream corridor itself, similar behavior could result in distinct variability about the general form of catchment-driven C-Q relationships. Studies of C-Q relationships and temporal variations in stream biogeochemical processes have not been fully integrated – largely because C-Q studies span much longer timescales than, say, nutrient uptake studies. Developing complementary sampling, modeling, and analysis strategies, that merge these two lines of investigation would greatly advance the development of hydro-biogeochemical theories while connecting catchment and river corridor science (Harvey & Gooseff, 2015; Li et al., 2021).

Further exploration of the structure and relative magnitude of C-Q variability among weathering solutes and nutrients can likely provide more information about heterogeneity of both source pool distributions and reaction rates than has previously been acknowledged – whether these reactions occur in the stream corridor or adjacent hillslopes. It is worth recognizing that regardless of changing catchment connectivity, C-Q data are always observed in the stream corridor. Even if the relative magnitude of signal modulation changes over time or with discharge (Moatar et al., 2017), the filter is may never be completely bypassed. Just as in streams, catchment biogeochemical reaction rates exhibit spatiotemporal variability due to interacting environmental factors (Bond-Lamberty & Thomson, 2010; Chen et al., 2020; Zhi et al., 2020), which could contribute to C-Q variability, as we have discussed here. Although we cannot identify exact causes of C-Q variability, by comparing many solutes and sampling locations, we can identify overarching patterns that lead to narrower hypotheses about processes governing C-Q dynamics. While developing specific techniques to isolate catchment and stream corridor influences on C-Q variability lies beyond the scope of this study, we have demonstrated the need to more directly consider the later in future studies.

5.6 Conclusions

Our analysis of historic data from ephemeral streams in Antarctica shows that while the stream corridor maintenance of chemostasis is ubiquitous across solutes, including nutrients, solutes controlled by biological processes exhibit more variability than weathering solutes. We demonstrate that this pattern is not directly controlled by environmental drivers of biological processes (i.e., light, temperature, and antecedent discharge), but may arise due to spatial and temporal complexity of biogeochemical and hydrologic processes within the stream corridor. Ultimately, our work provides evidence that chemostasis of many solutes can be maintained by stream corridor processes and that what has otherwise been viewed as "noise" in C-Q relationships can provide useful information about the relative variability in coupled biogeochemical processes across solutes. Important questions remain regarding exactly which

biogeochemical processes drive this variability and what controls their fluctuations in space and time. Future studies should draw on comparing variability in C-Q patterns across solutes to identify emergent biogeochemical patterns, consider distinct stream corridor versus catchment effects, and formulate hypotheses that will advance integrated hydro-biogeochemical theories.

References

Alexander, R. B., Bohlke, J. K., Boyer, E. W., David, M. B., Harvey, J. W., Mulholland, P. J., et al. (2009). Dynamic modeling of nitrogen losses in river networks unravels the coupled effects of hydrological and biogeochemical processes. *Biogeochemistry*, *93*(1–2), 91–116. https://doi.org/10.1007/s10533-008-9274-8

Anderson, S. P., Dietrich, W. E., Torres, R., Montgomery, D. R., & Loague, K. (1997). Concentration-discharge relationships in runoff from a steep, unchanneled catchment. *Water Resources Research*, *33*(1), 211–225.

Bagshaw, E. A., Tranter, M., Wadham, J. L., Fountain, A. G., & Mowlem, M. (2011). High-resolution monitoring reveals dissolved oxygen dynamics in an Antarctic cryoconite hole. *Hydrological Processes*, *25*(18), 2868–2877. https://doi.org/https://doi.org/10.1002/hyp.8049

Bagshaw, E. A., Tranter, M., Fountain, A. G., Welch, K. A., Basagic, H. J., & Lyons, W. B. (2013). Do Cryoconite Holes have the Potential to be Significant Sources of C, N, and P to Downstream Depauperate Ecosystems of Taylor Valley, Antarctica? *Arctic, Antarctic, and Alpine Research*, *45*(4), 440–454. https://doi.org/10.1657/1938-4246-45.4.440

Baker, D. B., Richards, R. P., Loftus, T. T., & Kramer, J. W. (2004). A New Flashiness Index: Characteristics and Applications to Midwestern Rivers and Streams. *JAWRA Journal of the American Water Resources Association*, *40*(2), 503–522. https://doi.org/https://doi.org/10.1111/j.1752-1688.2004.tb01046.x

Barrett, J. E., Virginia, R. A., Lyons, W. B., McKnight, D. M., Priscu, J. C., Doran, P. T., Fountain, A. G., Wall, D. H., & Moorhead, D. L. (2007), Biogeochemical stoichiometry of Antarctic Dry Valley ecosystems, *Journal of Geophysical Research*, 112, G01010, https://doi.org/10.1029/2005JG000141

Basu, N. B., Destouni, G., Jawitz, J. W., Thompson, S. E., Loukinova, N. V., Darracq, A., et al. (2010). Nutrient loads exported from managed catchments reveal emergent biogeochemical stationarity. *Geophysical Research Letters*, *37*(23).

Bergstrom, A. J., Gooseff, M. N., Singley, J. G., Cohen, M. J., & Welch, K. A. (2020). Nutrient Uptake in the Supraglacial Stream Network of an Antarctic Glacier. *Journal of Geophysical Research: Biogeosciences*, *125*(9), e2020JG005679. https://doi.org/https://doi.org/10.1029/2020JG005679

Bernhardt, E. S., Likens, G. E., Hall, R. O., Buso, D. C., Fisher, S. G., Burton, T. M., et al. (2005). Can't see the forest for the stream? In-stream processing and terrestrial nitrogen exports. *BioScience*, *55*(3), 219–230.

Bockheim, J. G., Campbell, I. B., & McLeod, M. (2007). Permafrost distribution and active-layer depths in the McMurdo Dry valleys, Antarctica. *Permafrost and Periglacial Processes*, *18*(3), 217–227.

Bond-Lamberty, B., & Thomson, A. (2010). Temperature-associated increases in the global soil respiration record. *Nature*, *464*(7288), 579–582. https://doi.org/10.1038/nature08930

Brantley, S. L. (2008). Kinetics of Mineral Dissolution. In S. L. Brantley, J. D. Kubicki, & A. F. White (Eds.), *Kinetics of Water-Rock Interaction* (pp. 151–210). New York, NY: Springer New York. https://doi.org/10.1007/978-0-387-73563-4_5

Chanat, J. G., Rice, K. C., & Hornberger, G. M. (2002). Consistency of patterns in concentration-discharge plots. *Water Resources Research*, *38*(8).

Chen, Y., Wieder, W. R., Hermes, A. L., & Hinckley, E.-L. S. (2020). The role of physical properties in controlling soil nitrogen cycling across a tundra-forest ecotone of the Colorado Rocky Mountains, U.S.A, *186*, 104369. https://doi.org/10.1016/j.catena.2019.104369

Chinn, T., & Mason, P. (2016, January 1). The first 25 years of the hydrology of the Onyx River, Wright Valley, Dry Valleys, Antarctica. *Polar Record*. Cambridge University Press. https://doi.org/10.1017/S0032247415000212

Chorover, J., Derry, L. A., & McDowell, W. H. (2017, November 1). Concentration-Discharge Relations in the Critical Zone: Implications for Resolving Critical Zone Structure, Function, and Evolution. *Water Resources Research*. Blackwell Publishing Ltd. https://doi.org/10.1002/2017WR021111

Clow, D. W., & Mast, M. A. (2010). Mechanisms for chemostatic behavior in catchments: implications for CO 2 consumption by mineral weathering. *Chemical Geology*, *269*(1), 40–51.

Conovitz, P. A., MacDonald, L. H., & McKnight, D. M. (2006). Spatial and temporal active layer dynamics along three glacial meltwater streams in the McMurdo Dry Valleys, Antarctica. *Arctic, Antarctic, and Alpine Research*, *38*(1), 42–53.

Cozzetto, K. D., Bencala, K. E., Gooseff, M. N., & McKnight, D. M. (2013). The influence of stream thermal regimes and preferential flow paths on hyporheic exchange in a glacial meltwater stream. *Water Resources Research*, *49*(9), 5552–5569.

Creed, I. F., McKnight, D. M., Pellerin, B. A., Green, M. B., Bergamaschi, B. A., Aiken, G. R., et al. (2015). The river as a chemostat: Fresh perspectives on dissolved organic matter flowing down the river continuum. *Canadian Journal of Fisheries and Aquatic Sciences*, *72*(8), 1272–1285. https://doi.org/10.1139/cjfas-2014-0400

Cullis, J. D. S., Stanish, L. F., & McKnight, D. M. (2014). Diel flow pulses drive particulate organic matter transport from microbial mats in a glacial meltwater stream in the McMurdo Dry Valleys. *Water Resources Research*, *50*(1), 86–97. https://doi.org/10.1002/2013WR014061

Doran, P. & A. Fountain (2019). McMurdo Dry Valleys LTER: High frequency measurements from Lake Fryxell Meteorological Station (FRLM) - Taylor Valley, Antarctica - 1993 to present ver 14. *Environmental Data Initiative*. https://doi.org/10.6073/pasta/5eded15437054e7f72f2350e98c44717.

Duncan, J. M., Band, L. E., Groffman, P. M., & Bernhardt, E. S. (2015). Mechanisms driving the seasonality of catchment scale nitrate export: Evidence for riparian ecohydrologic controls. *Water Resources Research*, *51*(6), 3982–3997. https://doi.org/10.1002/2015WR016937

Egusa, T., Kumagai, T., Oda, T., Gomi, T., & Ohte, N. (2019). Contrasting Patterns in the Decrease of Spatial Variability With Increasing Catchment Area Between Stream Discharge and Water Chemistry. *Water Resources Research*, *55*(8), 7419–7435. https://doi.org/10.1029/2018WR024302

Evans, C., & Davies, T. D. (1998). Causes of concentration/discharge hysteresis and its potential as a tool for analysis of episode hydrochemistry. *Water Resources Research*, *34*(1), 129–137.

Fazekas, H. M., Wymore, A. S., & Mcdowell, W. H. (2020). Dissolved Organic Carbon and Nitrate Concentration-Discharge Behavior Across Scales: Land Use, Excursions, and Misclassification. *Water Resources Research*, *56*. https://doi.org/10.1029/2019WR027028

Fortner, S. K., & Lyons, W. B. (2018). Dissolved trace and minor elements in cryoconite holes and supraglacial streams, Canada Glacier, Antarctica. *Frontiers in Earth Science*, *6*, 31. https://doi.org/10.3389/feart.2018.00031

Fortner, S. K., Tranter, M., Fountain, A. G., Lyons, W. B., & Welch, K. A. (2005). The geochemistry of supraglacial streams of Canada Glacier, Taylor Valley (Antarctica), and their evolution into proglacial waters. *Aquatic Geochemistry*, *11*(4), 391–412.

Fountain, A. G., Nylen, T. H., Monaghan, A., Basagic, H. J., & Bromwich, D. (2010). Snow in the McMurdo Dry Valleys, Antarctica. *International Journal of Climatology*, *30*(5), 633–642.

Godsey, S. E., Kirchner, J. W., & Clow, D. W. (2009). Concentration–discharge relationships reflect chemostatic characteristics of US catchments. *Hydrological Processes*, *23*(13), 1844–1864.

Godsey, S. E., Hartmann, J., & Kirchner, J. W. (2019). Catchment chemostasis revisited: Water quality responds differently to variations in weather and climate. *Hydrological Processes*, *33*(24), 3056–3069. https://doi.org/10.1002/hyp.13554

Gooseff, M. N., McKnight, D. M., Lyons, W. B., & Blum, A. E. (2002). Weathering reactions

and hyporheic exchange controls on stream water chemistry in a glacial meltwater stream in the McMurdo Dry Valleys. *Water Resources Research*, *38*(12), 15-1-15–17. https://doi.org/10.1029/2001WR000834

Gooseff, M. N., McKnight, D. M., Runkel, R. L., & Vaughn, B. H. (2003). Determining long time-scale hyporheic zone flow paths in Antarctic streams. *Hydrological Processes*, *17*(9), 1691–1710. https://doi.org/10.1002/hyp.1210

Gooseff, M. N., McKnight, D. M., Runkel, R. L., & Duff, J. H. (2004). Denitrification and hydrologic transient storage in a glacial meltwater stream, McMurdo Dry Valleys, Antarctica. *Limnology and Oceanography*, *49*(5), 1884–1895.

Gooseff, M. N., Wlostowski, A. N., McKnight, D. M., & Jaros, C. (2016). Hydrologic connectivity and implications for ecosystem processes-Lessons from naked watersheds. *Geomorphology*.

Gooseff, M.N. & McKnight, D. M. (2019a). 2019. McMurdo Dry Valleys LTER: High frequency seasonal stream gage measurements from Andersen Creek at H1 in Taylor Valley, Antarctica from 1993 to present ver 10. *Environmental Data Initiative*. https://doi.org/10.6073/pasta/81173c42e5c6a0a4894001eedb3d623a.

Gooseff, M.N. & McKnight, D. M. (2019b). McMurdo Dry Valleys LTER: High frequency seasonal stream gage measurements from Canada Stream at F1 in Taylor Valley, Antarctica from 1990 to present ver 11. *Environmental Data Initiative*. https://doi.org/10.6073/pasta/3b2d96bb09ba5d1b883ab99702e3eb40.

Gooseff, M.N. & McKnight, D. M. (2019c). McMurdo Dry Valleys LTER: High frequency seasonal stream gage measurements from Commonwealth Stream at C1 in Taylor Valley, Antarctica from 1993 to present ver 8. *Environmental Data Initiative*. https://doi.org/10.6073/pasta/b15ef1450799587dc7d60c960fc18142.

Gooseff, M.N. & McKnight, D. M. (2019d). McMurdo Dry Valleys LTER: High frequency seasonal stream gage measurements from Crescent Stream at F8 in Taylor Valley, Antarctica from 1990 to present ver 11. *Environmental Data Initiative*. https://doi.org/10.6073/pasta/86bce67070a2e3b37bf5ca805059feee.

Gooseff, M.N. & McKnight, D. M. (2019e). 2019. McMurdo Dry Valleys LTER: High frequency seasonal stream gage measurements from Delta Stream at F10 in Taylor Valley, Antarctica from 1990 to present ver 11. *Environmental Data Initiative*. https://doi.org/10.6073/pasta/03abc485979246b558d172e01eb81e02.

Gooseff, M.N. & McKnight, D. M. (2019f). McMurdo Dry Valleys LTER: High frequency seasonal stream gage measurements from Green Creek at F9 in Taylor Valley, Antarctica from 1990 to present ver 12. *Environmental Data Initiative*. https://doi.org/10.6073/pasta/bdf09ca40915db102722c4143ed0a0e7.

Gooseff, M.N. & McKnight, D. M. (2019g). McMurdo Dry Valleys LTER: High frequency seasonal stream gage measurements from Harnish Creek at F7 in Taylor Valley, Antarctica

from 2001 to present ver 7. *Environmental Data Initiative*.
https://doi.org/10.6073/pasta/0dbe0da2ff94c833730e855ddc5344b3.

Gooseff, M.N. & McKnight, D. M. (2019i). McMurdo Dry Valleys LTER: High frequency
seasonal stream gage measurements from Lost Seal Stream at F3 in Taylor Valley,
Antarctica from 1990 to present ver 7. *Environmental Data Initiative*.
https://doi.org/10.6073/pasta/fa9c6a1a8ab26074cfd632dbecc339f1.

Gooseff, M.N. & McKnight, D.M.. 2016. McMurdo Dry Valleys Priscu Stream Gage
Measurements ver 7. *Environmental Data Initiative*.
https://doi.org/10.6073/pasta/1567ace50621bb0cee76368c2b59b80a.

Gooseff, M.N. & D. McKnight, D. M. (2019j). McMurdo Dry Valleys LTER: High frequency
seasonal stream gage measurements from Von Guerard Stream at F6 in Taylor Valley,
Antarctica from 1990 to present ver 17. *Environmental Data Initiative*.
https://doi.org/10.6073/pasta/b452c7c780079060e0cd17db08f6089e.

Green, W. J., Angle, M. P., & Chave, K. E. (1988). The geochemistry of Antarctic streams and
their role in the evolution of four lakes of the McMurdo Dry Valleys. *Geochimica et
Cosmochimica Acta*, *52*(5), 1265–1274.

Griffiths, N. A., & Tiegs, S. D. (2016). Organic-matter decomposition along a temperature
gradient in a forested headwater stream. *Freshwater Science*, *35*(2), 518–533.
https://doi.org/10.1086/685657

Harvey, J. W., & Gooseff, M. N. (2015). River corridor science: Hydrologic exchange and
ecological consequences from bedforms to basins. *Water Resources Research*.
https://doi.org/10.1002/2015WR017617

Harvey, J. W., Gomez-Velez, J. D., Schmadel, N. M., Scott, D. T., Boyer, E. W., Alexander, R.
B., et al. (2018, April 9). How Hydrologic Connectivity Regulates Water Quality in River
Corridors. *Journal of the American Water Resources Association*, pp. 369–381.
https://doi.org/10.1111/1752-1688.12691

Hawes, I., & Howard-Williams, C. (1998, January 28). Primary Production Processes in Streams
of the Mcmurdo Dry Valleys, Antarctica. *Ecosystem Dynamics in a Polar Desert: The
Mcmurdo Dry Valleys, Antarctica*. https://doi.org/https://doi.org/10.1029/AR072p0129

Heffernan, J. B., & Cohen, M. J. (2010). Direct and indirect coupling of primary production and
diel nitrate dynamics in a subtropical spring-fed river. *Limnology and Oceanography*, *55*(2),
677–688.

Heindel, R. C., Lyons, W. B., Welch, S. A., Spickard, A. M., & Virginia, R. A. (2018).
Biogeochemical weathering of soil apatite grains in the McMurdo Dry Valleys, Antarctica.
Geoderma, *320*, 136–145. https://doi.org/10.1016/j.geoderma.2018.01.027

Heindel, R. C., Bergstrom, A. J., Singley, J. G., McKnight, D. M., Darling, J., Lukkari, B., et al.
(2021). Diatoms trace the retention and processing of organic matter in hyporheic sediments

in the McMurdo Dry Valleys, Antarctica. *Journal of Geophysical Research-Biogeosciences*. https://doi.org/10.1029/2020JG006097

Hirst, C., Opfergelt, S., Gaspard, F., Hendry, K. R., Hatton, J. E., Welch, S., et al. (2020). Silicon Isotopes Reveal a Non-glacial Source of Silicon to Crescent Stream, McMurdo Dry Valleys, Antarctica. *Frontiers in Earth Science*, *8*. https://doi.org/10.3389/feart.2020.00229

Hoellein, T. J., Bruesewitz, D. A., & Richardson, D. C. (2013). Revisiting Odum (1956): A synthesis of aquatic ecosystem metabolism. *Limnology and Oceanography*, *58*(6), 2089–2100. https://doi.org/10.4319/lo.2013.58.6.2089

Howard-Williams, C., Priscu, J. C., & Vincent, W. F. (1989). Nitrogen dynamics in two antarctic streams. *Hydrobiologia*, *172*(1), 51–61. https://doi.org/10.1007/BF00031612

Huryn, A. D., Benstead, J. P., & Parker, S. M. (2014). Seasonal changes in light availability modify the temperature dependence of ecosystem metabolism in an arctic stream. *Ecology*, *95*(10), 2826–2839. https://doi.org/10.1890/13-1963.1

Keys, J. R., & Williams, K. (1981). Origin of crystalline, cold desert salts in the McMurdo region, Antarctica. *Geochimica et Cosmochimica Acta*, *45*(12), 2299–2309. https://doi.org/10.1016/0016-7037(81)90084-3

Kirchner, J. W. (2003). A double paradox in catchment hydrology and geochemistry. *Hydrological Processes*, *17*(4), 871–874.

Knapp, J. L. A., Von Freyberg, J., Studer, B., Kiewiet, L., & Kirchner, J. W. (2020). Concentration-discharge relationships vary among hydrological events, reflecting differences in event characteristics. *Hydrology and Earth System Sciences*, *24*(5), 2561–2576. https://doi.org/10.5194/hess-24-2561-2020

Koch, J. C., McKnight, D. M., & Baeseman, J. L. (2010). Effect of unsteady flow on nitrate loss in an oligotrophic, glacial meltwater stream. *Journal of Geophysical Research-Biogeosciences*, *115*(G1), G01001. https://doi.org/10.1029/2009jg001030

Kohler, T. J., Stanish, L. F., Crisp, S. W., Koch, J. C., Liptzin, D., Baeseman, J. L., & McKnight, D. M. (2015). Life in the main channel: long-term hydrologic control of microbial mat abundance in McMurdo Dry Valley streams, Antarctica. *Ecosystems*, *18*(2), 310–327.

Kohler, T. J., Stanish, L. F., Liptzin, D., Barrett, J. E., & McKnight, D. M. (2018). Catch and release: Hyporheic retention and mineralization of N-fixing Nostoc sustains downstream microbial mat biomass in two polar desert streams. *Limnology and Oceanography Letters*. https://doi.org/10.1002/lol2.10087

Levy, J. S. (2013). How big are the McMurdo Dry Valleys? Estimating ice-free area using Landsat image data. *Antarctic Science*, *25*(01), 119–120.

Li, L., Sullivan, P. L., Benettin, P., Cirpka, O. A., Bishop, K., Brantley, S. L., et al. (2021). Toward catchment hydro-biogeochemical theories. *Wiley Interdisciplinary Reviews: Water*,

8(1), e1495. https://doi.org/10.1002/wat2.1495

Lyons, B. (2019a). McMurdo Dry Valleys Stream Chemistry - Dissolved Organic Carbon ver 6. *Environmental Data Initiative*. https://doi.org/10.6073/pasta/578d31fa0e142b6b7a6c80095d29b968.

Lyons, B. (2019b). McMurdo Dry Valleys Stream Nutrients (nitrate, nitrite, ammonium, reactive phosphorus) ver 7. *Environmental Data Initiative*. https://doi.org/10.6073/pasta/81cfcad244f7d3f6a6fcdab83ea75849.

Lyons, B. & Welch, K. (2019). McMurdo Dry Valleys Stream Chemistry and Ion Concentrations ver 12. *Environmental Data Initiative*. https://doi.org/10.6073/pasta/be9f781814330116f68844a8957962e4.

Lyons, W. B., Leslie, D. L., & Gooseff, M. N. (2021). Chemical Weathering in the McMurdo Dry Valleys, Antarctica. *Hydrogeology, Chemical Weathering, and Soil Formation*. https://doi.org/https://doi.org/10.1002/9781119563952.ch11

Marinos, R. E., Van Meter, K. J., & Basu, N. B. (2020). Is the River a Chemostat?: Scale Versus Land Use Controls on Nitrate Concentration-Discharge Dynamics in the Upper Mississippi River Basin. *Geophysical Research Letters*, *47*(16). https://doi.org/10.1029/2020GL087051

Martí, E., & Sabater, F. (1996). High variability in temporal and spatial nutrient retention in mediterranean streams. *Ecology*, *77*(3), 854–869. https://doi.org/10.2307/2265506

Matheson, F. E., Quinn, J. M., & Martin, M. L. (2012). Effects of irradiance on diel and seasonal patterns of nutrient uptake by stream periphyton. *Freshwater Biology*, *57*(8), 1617–1630. https://doi.org/10.1111/j.1365-2427.2012.02822.x

Maurice, P. A., McKnight, D. M., Leff, L., Fulghum, J. E., & Gooseff, M. N. (2002). Direct observations of aluminosilicate weathering in the hyporheic zone of an Antarctic Dry Valley stream. *Geochimica et Cosmochimica Acta*, *66*(8), 1335–1347.

McDonnell, J. J., Bonell, M., Stewart, M. K., & Pearce, A. J. (1990). Deuterium variations in storm rainfall: Implications for stream hydrograph separation. *Water Resources Research*, *26*(3), 455–458.

McKnight, D. M., Niyogi, D. K., Alger, A. S., Bomblies, A., Conovitz, P. A., & Tate, C. M. (1999). Dry valley streams in Antarctica: ecosystems waiting for water. *BioScience*, *49*(12), 985–995.

McKnight, D. M., Runkel, R. L., Tate, C. M., Duff, J. H., & Moorhead, D. L. (2004). Inorganic N and P dynamics of Antarctic glacial meltwater streams as controlled by hyporheic exchange and benthic autotrophic communities. *Journal of the North American Benthological Society*, *23*(2), 171–188.

McKnight, D. M., Tate, C. M., Andrews, E. D., Niyogi, D. K., Cozzetto, K. D., Welch, K. A., et al. (2007). Reactivation of a cryptobiotic stream ecosystem in the McMurdo Dry Valleys,

Antarctica: a long-term geomorphological experiment. *Geomorphology*, *89*(1), 186–204.

Moatar, F., Abbott, B. W., Minaudo, C., Curie, F., & Pinay, G. (2017). Elemental properties, hydrology, and biology interact to shape concentration-discharge curves for carbon, nutrients, sediment, and major ions. *Water Resources Research*, *53*(2), 1270–1287. https://doi.org/https://doi.org/10.1002/2016WR019635

Mulholland, P. J. (2004). The importance of in-stream uptake for regulating stream concentrations and outputs of N and P from a forested watershed: Evidence from long-term chemistry records for Walker Branch Watershed. *Biogeochemistry*, *70*(3), 403–426. https://doi.org/10.1007/s10533-004-0364-y

Peterson, B. J., Wollheim, W. M., Mulholland, P. J., Webster, J. R., Meyer, J. L., Tank, J. L., et al. (2001). Control of nitrogen export from watersheds by headwater streams. *Science*, *292*(5514), 86–90.

Pilgrim, D. H., Huff, D. D., & Steele, T. D. (1979). Use of specific conductance and contact time relations for separating flow components in storm runoff. *Water Resources Research*, *15*(2), 329–339.

Rice, K. C., Chanat, J. G., Hornberger, G. M., & Webb, J. R. (2004). Interpretation of concentration-discharge patterns in acid-neutralizing capacity during storm flow in three small, forested catchments in Shenandoah National Park, Virginia. *Water Resources Research*, *40*(5).

Rusjan, S., & Mikoš, M. (2010). Seasonal variability of diurnal in-stream nitrate concentration oscillations under hydrologically stable conditions. *Biogeochemistry*, *97*(2–3), 123–140. https://doi.org/10.1007/s10533-009-9361-5

Savoy, P., Appling, A. P., Heffernan, J. B., Stets, E. G., Read, J. S., Harvey, J. W., & Bernhardt, E. S. (2019). Metabolic rhythms in flowing waters: An approach for classifying river productivity regimes. *Limnology and Oceanography*, *64*(5), 1835–1851. https://doi.org/10.1002/lno.11154

Seybold, E. C., & McGlynn, B. L. (2018). Hydrologic and biogeochemical drivers of dissolved organic carbon and nitrate uptake in a headwater stream network. *Biogeochemistry*, *138*(1), 23–48. https://doi.org/10.1007/s10533-018-0426-1

Simon, K. S., Townsend, C. R., Biggs, B. J. F., & Bowden, W. B. (2005). Temporal variation of N and P uptake in 2 New Zealand streams. *Journal of the North American Benthological Society*, *24*(1), 1–18. https://doi.org/10.1899/0887-3593(2005)024<0001:TVONAP>2.0.CO;2

Singh, T., Gomez-Velez, J. D., Wu, L., Wörman, A., Hannah, D. M., & Krause, S. (2020). Effects of Successive Peak Flow Events on Hyporheic Exchange and Residence Times. *Water Resources Research*, *56*(8). https://doi.org/10.1029/2020WR027113

Singley, J. G., Gooseff, M. N., McKnight, D. M., & Hinckley, E.-L. S. (2021). The Role of

Hyporheic Connectivity in Determining Nitrogen Availability: Insights from an Intermittent Antarctic Stream. *Journal of Geophysical Research: Biogeosciences*, *126*, e2021JG006309. https://doi.org/10.1029/2021JG006309

Thompson, S. E., Basu, N. B., Lascurain, J., Aubeneau, A., & Rao, P. S. C. (2011). Relative dominance of hydrologic versus biogeochemical factors on solute export across impact gradients. *Water Resources Research*, *47*(7). https://doi.org/10.1029/2010WR009605

Warwick, J. J. (1986). Diel variation of in-stream nitrification. *Water Research*, *20*(10), 1325–1332. https://doi.org/10.1016/0043-1354(86)90165-X

Welch, K. A., Lyons, W. B., Whisner, C., Gardner, C. B., Gooseff, M. N., McKnight, D. M., & Priscu, J. C. (2010). Spatial variations in the geochemistry of glacial meltwater streams in the Taylor Valley, Antarctica. *Antarctic Science*, *22*(06), 662–672.

Witherow, R. A., Lyons, W. B., Bertler, N. A. N., Welch, K. A., Mayewski, P. A., Sneed, S. B., et al. (2006). The aeolian flux of calcium, chloride and nitrate to the McMurdo Dry Valleys landscape: Evidence from snow pit analysis. In *Antarctic Science* (Vol. 18, pp. 497–505). https://doi.org/10.1017/S095410200600054X

Wlostowski, A. N., Gooseff, M. N., McKnight, D. M., Jaros, C., & Lyons, W. B. (2016). Patterns of hydrologic connectivity in the McMurdo Dry Valleys, Antarctica: a synthesis of 20 years of hydrologic data. *Hydrological Processes*, *30*, 2958–2975. https://doi.org/10.1002/hyp.10818

Wlostowski, A. N., Gooseff, M. N., McKnight, D. M., & Lyons, W. B. (2018). Transit Times and Rapid Chemical Equilibrium Explain Chemostasis in Glacial Meltwater Streams in the McMurdo Dry Valleys, Antarctica. *Geophysical Research Letters*, *45*(24), 13,322-13,331. https://doi.org/10.1029/2018GL080369

Woods, R., Sivapalan, M., & Duncan, M. (1995). Investigating the representative elementary area concept: An approach based on field data. *Hydrological Processes*, *9*(3–4), 291–312. https://doi.org/10.1002/hyp.3360090306

Zhi, W., Williams, K. H., Carroll, R. W. H., Brown, W., Dong, W., Kerins, D., & Li, L. (2020). Significant stream chemistry response to temperature variations in a high-elevation mountain watershed. *Communications Earth & Environment*, *1*(1), 1–10. https://doi.org/10.1038/s43247-020-00039-w

Chapter VI

Conclusions

The spatial and temporal patterning of stream corridor connectivity influences water quality and the export of nutrients to downstream systems (Harvey & Gooseff, 2015). Hyporheic connectivity, in particular, exerts a strong control on hydrologic transport, biogeochemical reactions, and the provisioning of ecological refugia (Harvey et al., 2018; Harvey & Bencala, 1993; Lewandowski et al., 2019; Ward, 2016). Hydrologic connectivity and N cycling are particularly complex in intermittent stream corridors, which are both globally pervasive and challenging to characterize (Allen et al., 2020; Datry et al., 2014; Larned et al., 2014) With this dissertation, I advance quantitative analysis of (1) how hyporheic connectivity is spatially structured and (2) how this connectivity controls the availability and retention of N in intermittent streams with few external N inputs. Altogether, this research advances understanding of processes that are difficult to measure or are often overlooked in typical studies of temperate stream corridors. Specifically, I demonstrated that machine learning can be utilized to characterize multi-scale heterogeneity of hyporheic connectivity into functional zones. I also leveraged field sampling, laboratory assays, numerical modeling, and remote sensing to characterize the surprising fate of N in highly oligotrophic and intermittent Antarctic streams.

Chapter II introduced a method to analyze inverted ER models using unsupervised hierarchical clustering to delimit the extent of hyporheic exchange and to characterize functional zones with distinct transport behaviors within the subsurface. I used this method to show that total hyporheic extent and the spatial heterogeneity of exchange respond differently to seasonal baseflow recession between adjacent (< 10 m) transects in a mountain stream. To our knowledge, this represents the first application of machine learning to classify statistically unique spatial patterning of hyporheic exchange during tracer studies and represents a major advance in data-driven characterization of multi-scale transport heterogeneity.

In Chapters III – V, I turned to the relatively simple ephemeral streams of the McMurdo Dry Valleys to isolate stream corridor processes governing autochthonous N cycling, transport and storage. The results of Chapter III challenge the typical conceptualization of the hyporheic zone as an N sink, which is based mostly on studies of temperate perennial streams with relatively large allochthonous N inputs. My findings highlight the need to develop more nuanced representations of autochthonously sourced N cycling in oligotrophic intermittent stream systems, and especially their hyporheic zones. Ultimately, this work demonstrates the potential for hyporheic connectivity both to enhance the contributions of internal N sources to nutrient budgets in oligotrophic streams and control how tightly and in what form it cycles this material.

Chapter IV highlighted the surprising magnitude of N storage that is possible in an MDV stream corridor relative to annual import and export fluxes. Even in a system devoid of higher plants, hillslope connectivity, and allochthonous N inputs, large amounts of N are stored, especially in the hyporheic zone. This chapter also demonstrated the potential to quantify the spatial heterogeneity of periphyton biomass and nutrient content over much larger scales than has previously been attempted. In doing so, we illustrate the potential to contextualize N flux modulation by stream corridors in terms of broad-scale storage processes.

In Chapter V, I demonstrated that stream corridor processes can sustain chemostasis even of nutrients and that biological processes appear to generate more concentration variability than physical processes alone. Traditionally, chemostasis has been explained almost exclusively in terms of distributed catchment storage and release of solutes. This work provides evidence that stream corridors can more strongly influence the form of C-Q relationships than is often recognized and that what has otherwise been viewed as "noise" in C-Q relationships may provide useful information about the relative variability in coupled biogeochemical processes across solutes. Moreover, in showing that the additional variability in C for biologically active solutes is not directly correlated with canonical drivers of biological activity, my work demonstrates that even in a relatively simple system the consequences of temporally varying coupled hydro-biogeochemical processes are not easy to predict or infer from discrete sampling. A forthcoming

modeling component that addresses the dynamic balance of stream corridor N uptake and release processes necessary to sustain chemostasis in these intermittent streams will be added to this chapter prior to publication.

Taken together, Chapter III – V represent a major shift in how MDV stream N cycling has been characterized over the past three decades from simple N removal by assimilatory uptake to hydrologically linked interdependence of autotrophic periphyton (both capable and incapable of N fixation) and heterotrophic microbial communities. My research demonstrates the central importance of autochthonous N sourcing and the physical and biogeochemical processes that allow in-stream N fixation to influence downstream N availability in the absence of allochthonous inputs. This research also establishes that beyond hyporheic exchange, other physical processes such as entrainment of N containing organic matter and reversible sorption in the hyporheic zone influence the availability of N in a hyper-oligotrophic system. Of course, this shift in conceptual understanding of N cycling and a greater appreciation for the importance of instream N fixation potentially applies to other intermittent stream systems in low N environments.

More broadly, this work demonstrates the potential to advance linked understanding of hydrological and biogeochemical processes through data-driven investigations of systems and processes that are often overlooked, assumed to be of negligible importance, or overly simplified despite recognized complexity. Relatedly, in order to address pressing questions about how the biogeochemical function of stream corridors will respond to global change (i.e., increasing prevalence of intermittency due to climate change), future studies should focus on analytical approaches that promote cross-site and cross-scale comparisons. My cluster-based analysis of hyporheic exchange represents one such pathway, as does my analysis of long-term C-Q variability of many solutes from many streams. Similar applications of pattern extraction to repeated remote sensing analysis has the potential to further link point-scale sampling with process-based understanding of ecosystem resilience and sensitivity to hydrologic variability. With high spatial and temporal resolution data from networks becoming increasingly common,

conducting data-driven analyses that promote cross-site synthesis is both feasible and necessary to address applied and basic questions about the influence of stream corridor connectivity on ecosystem function and water quality.

Bibliography

Aber, J. D., K. J. Nadelhoffer, P. Steudler, & J. M. Melillo (1989). *Nitrogen Saturation in Northern Forest Ecosystems,* Published by: University of California Press on behalf of the American Institute of Biological Sciences, http://www.jstor.org/stable/1311067 . BioScience 39:378–386.

Acuña, V., Muñoz, I., Giorgi, A., Omella, M., Sabater, F., & Sabater, S. (2005). Drought and postdrought recovery cycles in an intermittent Mediterranean stream: structural and functional aspects. *Journal of the North American Benthological Society*, *24*(4), 919–933.

Acuña, V., Casellas, M., Corcoll, N., Timoner, X., & Sabater, S. (2015). Increasing extent of periods of no flow in intermittent waterways promotes heterotrophy. *Freshwater Biology*, *60*(9), 1810–1823. https://doi.org/10.1111/fwb.12612

Adams, B. J., R. D. Bardgett, E. Ayres, D. H. Wall, J. Aislabie, S. Bamforth, R. Bargagli, C. Cary, P. Cavacini, L. Connell, P. Convey, J. W. Fell, F. Frati, I. D. Hogg, K. K. Newsham, A. O'Donnell, N. Russell, R. D. Seppelt, & M. I. Stevens (2006). Diversity and distribution of Victoria Land biota. *Soil Biology and Biochemistry* 38:3003–3018.

Aghabozorgi, S., Seyed Shirkhorshidi, A., Ying Wah, T., Shirkhorshidi, A. S., & Wah, Y. (2015). Time-series clustering – A decade review. *Information Systems*, *53*, 16–38. https://doi.org/10.1016/j.is.2015.04.007

Alexander, R. B., Boyer, E. W., Smith, R. A., Schwarz, G. E., and Moore, R. B. (2007). The role of headwater streams in downstream water quality1. *JAWRA Journal of the American Water Resources Association*, *43*(1), 41–59.

Alexander, R. B., Bohlke, J. K., Boyer, E. W., David, M. B., Harvey, J. W., Mulholland, P. J., et al. (2009). Dynamic modeling of nitrogen losses in river networks unravels the coupled effects of hydrological and biogeochemical processes. *Biogeochemistry*, *93*(1–2), 91–116. https://doi.org/10.1007/s10533-008-9274-8

Alger, A. S. (1997). Ecological processes in a cold desert ecosystem: the abundance and species distribution of algal mats in glacial meltwater streams in Taylor Valley, Antarctica. *Occasional Paper/University of Colorado*.

Allen, D. C., Datry, T., Boersma, K. S., Bogan, M. T., Boulton, A. J., Bruno, D., et al. (2020). River ecosystem conceptual models and non-perennial rivers: A critical review. *Wiley Interdisciplinary Reviews: Water*. John Wiley and Sons Inc. https://doi.org/10.1002/wat2.1473

Anderson, S. P., Dietrich, W. E., Torres, R., Montgomery, D. R., & Loague, K. (1997). Concentration-discharge relationships in runoff from a steep, unchanneled catchment. *Water Resources Research*, *33*(1), 211–225.

Arce, I. M., Sanchez-Montoya, M. D., Vidal-Abarca, M. R., Suarez, M. L., & Gomez-Velez, J. D. (2014). Implications of flow intermittency on sediment nitrogen availability and

processing rates in a Mediterranean headwater stream. *Aquatic Sciences*, *76*(2), 173–186. https://doi.org/10.1007/s00027-013-0327-2

Bagshaw, E. A., Tranter, M., Wadham, J. L., Fountain, A. G., & Mowlem, M. (2011). High-resolution monitoring reveals dissolved oxygen dynamics in an Antarctic cryoconite hole. *Hydrological Processes*, *25*(18), 2868–2877. https://doi.org/https://doi.org/10.1002/hyp.8049

Bagshaw, E. A., Tranter, M., Fountain, A. G., Welch, K. A., Basagic, H. J., & Lyons, W. B. (2013). Do Cryoconite Holes have the Potential to be Significant Sources of C, N, and P to Downstream Depauperate Ecosystems of Taylor Valley, Antarctica? *Arctic, Antarctic, and Alpine Research*, *45*(4), 440–454. https://doi.org/10.1657/1938-4246-45.4.440

Baker, D. B., Richards, R. P., Loftus, T. T., & Kramer, J. W. (2004). A New Flashiness Index: Characteristics and Applications to Midwestern Rivers and Streams. *JAWRA Journal of the American Water Resources Association*, *40*(2), 503–522. https://doi.org/https://doi.org/10.1111/j.1752-1688.2004.tb01046.x

Barr, D. M. (1999). Biotic and abiotic regulation of nitrogen dynamics in biological soil crusts. Northern Arizona University.

Barrett, J. E., Virginia, R. A., Lyons, W. B., McKnight, D. M., Priscu, J. C., Doran, P. T., Fountain, A. G., Wall, D. H., & Moorhead, D. L. (2007), Biogeochemical stoichiometry of Antarctic Dry Valley ecosystems, *Journal of Geophysical Research*, 112, G01010, https://doi.org/10.1029/2005JG000141

Barrett, J. E., M. N. Gooseff, and C. D. Takacs-Vesbach (2009). Spatial variation in soil active-layer geochemistry across hydrologic margins in polar desert ecosystems. *Hydrology and Earth System Sciences*, 13:2349–2358.

Basu, N. B., Destouni, G., Jawitz, J. W., Thompson, S. E., Loukinova, N. V., Darracq, A., et al. (2010). Nutrient loads exported from managed catchments reveal emergent biogeochemical stationarity. *Geophysical Research Letters*, *37*(23).

Benjamini, Y., & Hochberg, Y. (1995). Controlling the False Discovery Rate: A Practical and Powerful Approach to Multiple Testing. *Journal of the Royal Statistical Society: Series B (Methodological)*, *57*(1), 289–300. https://doi.org/10.1111/j.2517-6161.1995.tb02031.x

Bentley, L. R., & Gharibi, M. (2004). Two-and three-dimensional electrical resistivity imaging at a heterogeneous remediation site. *Geophysics*, 69(3), 674-680.

Bergstrom, A. J., Gooseff, M. N., Singley, J. G., Cohen, M. J., & Welch, K. A. (2020a). Nutrient Uptake in the Supraglacial Stream Network of an Antarctic Glacier. *Journal of Geophysical Research: Biogeosciences*, *125*(9), e2020JG005679. https://doi.org/https://doi.org/10.1029/2020JG005679

Bergstrom, A.J., Gooseff, M.N. (2021a). Chemical and sediment characteristics of ice cores collected from the ablation zones of Canada, Commonwealth, Howard, Hughes, and Seuss

Glaciers in the McMurdo Dry Valleys, Antarctica from 2015 to 2019. *Environmental Data Initiative*. DOI: 10.6073/pasta/9943dc9f5b04e9d24424911c19349b58. Dataset accessed 3 June 2021.

Bergstrom, A.J., Gooseff, M.N. (2021b). Chemical characteristics of supraglacial stream water on Canada Glacier, McMurdo Dry Valleys, Antarctica during the 2015-2016 austral summer. *Environmental Data Initiative*. DOI: 10.6073/pasta/ea75e039fb7b6314e1c555c9ff8a5009. Dataset accessed 3 June 2021.

Bernal, S., Butturini, A., & Sabater, F. (2005). Seasonal variations of dissolved nitrogen and DOC:DON ratios in an intermittent Mediterranean stream. *Biogeochemistry*, *75*(2), 351–372. https://doi.org/10.1007/s10533-005-1246-7

Bernal, S., & Sabater, F. (2012). Changes in discharge and solute dynamics between hillslope and valley-bottom intermittent streams. *Hydrology and Earth System Sciences*, *16*(6), 1595–1605. https://doi.org/10.5194/hess-16-1595-2012

Bernal, S., von Schiller, D., Sabater, F., & Martí, E. (2013). Hydrological extremes modulate nutrient dynamics in mediterranean climate streams across different spatial scales. *Hydrobiologia*, *719*(1), 31–42. https://doi.org/10.1007/s10750-012-1246-2

Bernal, S., Lupon, A., Wollheim, W. M., Sabater, F., Poblador, S., & Martí, E. (2019). Supply, Demand, and In-Stream Retention of Dissolved Organic Carbon and Nitrate During Storms in Mediterranean Forested Headwater Streams. *Frontiers in Environmental Science*, *7*(May), 60. https://doi.org/10.3389/fenvs.2019.00060

Bernhardt, E. S., Likens, G. E., Hall, R. O., Buso, D. C., Fisher, S. G., Burton, T. M., et al. (2005). Can't see the forest for the stream? In-stream processing and terrestrial nitrogen exports. *BioScience*, *55*(3), 219–230.

Bernhardt, E. S., Blaszczak, J. R., Ficken, C. D., Fork, M. L., Kaiser, K. E., & Seybold, E. C. (2017). Control Points in Ecosystems: Moving Beyond the Hot Spot Hot Moment Concept. *Ecosystems*, *20*(4), 665–682. https://doi.org/10.1007/s10021-016-0103-y

Bernot, M. J., & Dodds, W. K. (2005). Nitrogen retention, removal, and saturation in lotic ecosystems. *Ecosystems*. Springer. https://doi.org/10.1007/s10021-003-0143-y

Bertilsson, S., & Jones, J. B. (2003). Supply of Dissolved Organic Matter to Aquatic Ecosystems: Autochthonous Sources. In S. E. G. Findlay & R. L. Sinsabaugh (Eds.), *Aquatic Ecosystems - Interactivity of Dissolved Organic Matter* (pp. 3–24). Academic Press.

Binley, A. M., & Kemna, A. (2005). Electrical Methods. In Y. Rubin & S. S. Hubbard (Eds.), *Hydrogeophysics* (pp. 129–156). Springer.

Binley, A. M. (2015). Tools and Techniques: Electrical Methods. In *Treatise on Geophysics: Second Edition* (Vol. 11, pp. 233–259). Elsevier Inc. https://doi.org/10.1016/B978-0-444-53802-4.00192-5

Binley, A. M. (2019). R2: Summary. Retrieved from
    http://www.es.lancs.ac.uk/people/amb/Freeware/R2/R2_readme.pdf

Blöschl, G., M. F. P. Bierkens, A. Chambel, C. Cudennec, et al. (2019) Twenty-three unsolved
    problems in hydrology (UPH) – a community perspective, *Hydrological Sciences Journal*,
    64:10, 1141-1158, https://doi.org/10.1080/02626667.2019.1620507

Boano, F., J. W. Harvey, Boano, F., Harvey, J. W., et al. (2014), Hyporheic flow and transport
    processes: Mechanisms, models, and biogeochemical implications, *Rev. Geophys.*, 52, 603–
    679, https://doi.org/10.1002/2012RG000417.

Bockheim, J. G., Campbell, I. B., & McLeod, M. (2007). Permafrost distribution and active-layer
    depths in the McMurdo Dry valleys, Antarctica. *Permafrost and Periglacial Processes*,
    18(3), 217–227.

Bond-Lamberty, B., & Thomson, A. (2010). Temperature-associated increases in the global soil
    respiration record. *Nature*, *464*(7288), 579–582. https://doi.org/10.1038/nature08930

Borchers, H. W. (2021). pracma: Practical Numerical Math Functions.

Bottacin-Busolin, A. (2019). Modeling the effect of hyporheic mixing on stream solute transport.
    Water Resources Research, 55, 9995– 10011. https://doi.org/10.1029/2019WR025697

Boyer, E. W., C. L. Goodale, N. A. Jaworski, and R. W. Howarth (2002). Anthropogenic
    nitrogen sources and relationships to riverine nitrogen export in the northeastern USA.
    Biogeochemistry 57:137–169.

Brantley, S. L. (2008). Kinetics of Mineral Dissolution. In S. L. Brantley, J. D. Kubicki, & A. F.
    White (Eds.), *Kinetics of Water-Rock Interaction* (pp. 151–210). New York, NY: Springer
    New York. https://doi.org/10.1007/978-0-387-73563-4_5

Briggs, M. A., Lautz, L. K., & Hare, D. K. (2014). Residence time control on hot moments of net
    nitrate production and uptake in the hyporheic zone. *Hydrological Processes*, *28*(11), 3741–
    3751.

Briggs, M. A., Day-Lewis, F. D., Zarnetske, J. P., & Harvey, J. W. (2015). A physical
    explanation for the development of redox microzones in hyporheic flow. *Geophysical
    Research Letters*, *42*(11), 4402–4410. https://doi.org/10.1002/2015GL064200

Burrows, R. M., H. Rutlidge, N. R. Bond, S. M. Eberhard, A. Auhl, M. S. Andersen, D. G.
    Valdez, & M. J. Kennard (2017). High rates of organic carbon processing in the hyporheic
    zone of intermittent streams. *Scientific Reports*, 7:1–11.

Buttle, J. M., Boon, S., Peters, D. L., Spence, C., (Ilja) van Meerveld, H. J., & Whitfield, P. H.
    (2012). An Overview of Temporary Stream Hydrology in Canada. *Canadian Water
    Resources Journal / Revue Canadienne Des Ressources Hydriques*, *37*(4), 279–310.
    https://doi.org/10.4296/cwrj2011-903

Cardenas, M. B., & Markowski, M. S. (2011). Geoelectrical imaging of hyporheic exchange and mixing of river water and groundwater in a large regulated river. *Environmental Science and Technology*, *45*(4), 1407–1411. https://doi.org/10.1021/es103438a

Chanat, J. G., Rice, K. C., & Hornberger, G. M. (2002). Consistency of patterns in concentration-discharge plots. *Water Resources Research*, *38*(8).

Chen, Y., Wieder, W. R., Hermes, A. L., & Hinckley, E.-L. S. (2020). The role of physical properties in controlling soil nitrogen cycling across a tundra-forest ecotone of the Colorado Rocky Mountains, U.S.A, *186*, 104369. https://doi.org/10.1016/j.catena.2019.104369

Chinn, T., & Mason, P. (2016). The first 25 years of the hydrology of the Onyx River, Wright Valley, Dry Valleys, Antarctica. *Polar Record*. Cambridge University Press. https://doi.org/10.1017/S0032247415000212

Chorover, J., Derry, L. A., & McDowell, W. H. (2017). Concentration-Discharge Relations in the Critical Zone: Implications for Resolving Critical Zone Structure, Function, and Evolution. *Water Resources Research*. Blackwell Publishing Ltd. https://doi.org/10.1002/2017WR021111

Clow, D. W., & Mast, M. A. (2010). Mechanisms for chemostatic behavior in catchments: implications for CO 2 consumption by mineral weathering. *Chemical Geology*, *269*(1), 40–51.

Conovitz, P. A., MacDonald, L. H., & McKnight, D. M. (2006). Spatial and temporal active layer dynamics along three glacial meltwater streams in the McMurdo Dry Valleys, Antarctica. *Arctic, Antarctic, and Alpine Research*, *38*(1), 42–53.

Cozzetto, K. D., Bencala, K. E., Gooseff, M. N., & McKnight, D. M. (2013). The influence of stream thermal regimes and preferential flow paths on hyporheic exchange in a glacial meltwater stream. *Water Resources Research*, *49*(9), 5552–5569.

Creed, I. F., McKnight, D. M., Pellerin, B. A., Green, M. B., Bergamaschi, B. A., Aiken, G. R., et al. (2015). The river as a chemostat: Fresh perspectives on dissolved organic matter flowing down the river continuum. *Canadian Journal of Fisheries and Aquatic Sciences*, *72*(8), 1272–1285. https://doi.org/10.1139/cjfas-2014-0400

Cullis, J. D. S., Stanish, L. F., & McKnight, D. M. (2014). Diel flow pulses drive particulate organic matter transport from microbial mats in a glacial meltwater stream in the McMurdo Dry Valleys. *Water Resources Research*, *50*(1), 86–97. https://doi.org/10.1002/2013WR014061

Dahm, C. N., Baker, M. A., Moore, D. I., & Thibault, J. R. (2003). Coupled biogeochemical and hydrological responses of streams and rivers to drought. *Freshwater Biology*, *48*(7), 1219–1231.

Datry, T., Larned, S. T., & Tockner, K. (2014). Intermittent Rivers: A Challenge for Freshwater Ecology. *BioScience*, *64*(3), 229–235. https://doi.org/10.1093/biosci/bit027

Datry, T., Bonada, N., Boulton, A. J., Datry, T., Bonada, N., & Boulton, A. J. (2017). *Intermittent Rivers and Ephemeral Streams - Ecology and Management*. Cambridge, MA, United States: Academic Press.

Davidson, E. A., David, M. B., Galloway, J. N., Goodale, C. L., Haeuber, R., Harrison, J. A., et al. (2011). Excess nitrogen in the US environment: trends, risks, and solutions. *Issues in Ecology*, (15).

Day-Lewis, F. D., Singha, K., & Binley, A. (2005). The application of petrophysical models to radar and electrical resistivity tomograms: resolution-dependent limitations. *Journal of Geophysical Research*, 110, B08206, https:doi.org/10.1029/2004JB003569

Delignette-Muller, M. L., & C. Dutang (2015). fitdistrplus: An R Package for Fitting Distributions. *Journal of Statistical Software*, 64:1–34.

Dodds, W. K., & Jones, R. D. (1987). Potential Rates of Nitrification and Denitrification in an Oligotrophic Freshwater Sediment System. *Microbial Ecology*, *14*, 91–100.

Dodds, W. K., Gudder, D. A., & Mollenhauer, D. (1995). The Ecology of Nostoc. *Journal of Phycology*, *31*(1), 2–18. https://doi.org/10.1111/j.0022-3646.1995.00002.x

Dodds, W. K., V. H. Smith, & K. Lohman (2002). Nitrogen and phosphorus relationships to benthic algal biomass in temperate streams. *Canadian Journal of Fisheries and Aquatic Sciences*, 59:865–874.

Dodds, W. K. (2006). Eutrophication and trophic state in rivers and streams. *Limnology and Oceanography,* 51, 671–680). https://doi.org/10.4319/lo.2006.51.1_part_2.0671

Doran, P. & A. Fountain (2019). McMurdo Dry Valleys LTER: High frequency measurements from Lake Fryxell Meteorological Station (FRLM) - Taylor Valley, Antarctica - 1993 to present ver 14. *Environmental Data Initiative*. https://doi.org/10.6073/pasta/5eded15437054e7f72f2350e98c44717.

Doughty, M., Sawyer, A. H., Wohl, E., & Singha, K. (2020). Mapping increases in hyporheic exchange from channel-spanning logjams. *Journal of Hydrology*, *587*, 124931. https://doi.org/https://doi.org/10.1016/j.jhydrol.2020.124931

Drummond, J. D., S. Bernal, D. Von Schiller, & E. Martí (2016). Linking in-stream nutrient uptake to hydrologic retention in two headwater streams. *Freshwater Science*, 35:1176–1188.

Dubnick, A., Wadham, J. L., Tranter, M., Sharp, M., Orwin, J., Barker, J., et al. (2017). Trickle or treat: The dynamics of nutrient export from polar glaciers. *Hydrological Processes*, *31*(9), 1776–1789. https://doi.org/10.1002/hyp.11149

Duncan, J. M., Band, L. E., Groffman, P. M., & Bernhardt, E. S. (2015). Mechanisms driving the seasonality of catchment scale nitrate export: Evidence for riparian ecohydrologic controls. *Water Resources Research*, *51*(6), 3982–3997. https://doi.org/10.1002/2015WR016937

Egusa, T., Kumagai, T., Oda, T., Gomi, T., & Ohte, N. (2019). Contrasting Patterns in the Decrease of Spatial Variability With Increasing Catchment Area Between Stream Discharge and Water Chemistry. *Water Resources Research*, *55*(8), 7419–7435. https://doi.org/10.1029/2018WR024302

Evans, C., & Davies, T. D. (1998). Causes of concentration/discharge hysteresis and its potential as a tool for analysis of episode hydrochemistry. *Water Resources Res. 34*(1), 129–137.

Fazekas, H. M., Wymore, A. S., & Mcdowell, W. H. (2020). Dissolved Organic Carbon and Nitrate Concentration-Discharge Behavior Across Scales: Land Use, Excursions, and Misclassification. *Water Resources Research*, *56*. https://doi.org/10.1029/2019WR027028

Fellman, J. B., Dogramaci, S., Skrzypek, G., Dodson, W., & Grierson, P. F. (2011). Hydrologic control of dissolved organic matter biogeochemistry in pools of a subtropical dryland river. *Water Resources Research*, *47*(6). https://doi.org/10.1029/2010WR010275

Fenoglio, S., Bo, T., Cammarata, M., López-Rodríguez, M. J., & Tierno De Figueroa, J. M. (2015). Seasonal variation of allochthonous and autochthonous energy inputs in an Alpine stream. *Journal of Limnology*, *74*(2), 272–277. https://doi.org/10.4081/jlimnol.2014.1082

Fortner, S. K., Tranter, M., Fountain, A. G., Lyons, W. B., & Welch, K. A. (2005). The geochemistry of supraglacial streams of Canada Glacier, Taylor Valley (Antarctica), and their evolution into proglacial waters. *Aquatic Geochemistry*, *11*(4), 391–412.

Fortner, S. K., & Lyons, W. B. (2018). Dissolved trace and minor elements in cryoconite holes and supraglacial streams, Canada Glacier, Antarctica. *Frontiers in Earth Science*, *6*, 31. https://doi.org/10.3389/feart.2018.00031

Fountain, A. G., Nylen, T. H., Monaghan, A., Basagic, H. J., & Bromwich, D. (2010). Snow in the McMurdo Dry Valleys, Antarctica. *International Journal of Climatology*, *30*(5), 633–642.

Fowler, D., Coyle, M., Skiba, U., Sutton, M. A., Cape, J. N., Reis, S., et al. (2013). The global nitrogen cycle in the Twentyfirst century. *Philosophical Transactions of the Royal Society B: Biological Sciences*, *368*(1621). https://doi.org/10.1098/rstb.2013.0164

Fu, T. C. (2011). A review on time series data mining. *Engineering Applications of Artificial Intelligence*. Elsevier Ltd. https://doi.org/10.1016/j.engappai.2010.09.007

Glibert, P. M., & Bronk, D. A. (1994). Release of dissolved organic nitrogen by marine diazotrophic cyanobacteria, Trichodesmium spp. *Applied and Environmental Microbiology*, *60*(11), 3996–4000. https://doi.org/10.1128/aem.60.11.3996-4000.1994

Godsey, S. E., Kirchner, J. W., & Clow, D. W. (2009). Concentration–discharge relationships reflect chemostatic characteristics of US catchments. *Hydrological Processes*, *23*(13), 1844–1864.

Godsey, S. E., Hartmann, J., & Kirchner, J. W. (2019). Catchment chemostasis revisited: Water

quality responds differently to variations in weather and climate. *Hydrological Processes*, *33*(24), 3056–3069. https://doi.org/10.1002/hyp.13554

Gomez-Velez, J. D., J. W. Harvey, M. Bayani Cardenas, and B. Kiel (2015). Denitrification in the Mississippi River network controlled by flow through river bedforms. *Nature Geoscience*, 8:941.

Gómez, R., García, V., Vidal-Abarca, M. R., & Suárez, L. (2009). Effect of intermittency on N spatial variability in an arid Mediterranean stream. *Journal of the North American Benthological Society*, *28*(3), 572–583.

Gómez, R., Arce, I. M., Sánchez, J. J., & del Mar Sánchez-Montoya, M. (2012). The effects of drying on sediment nitrogen content in a Mediterranean intermittent stream: A microcosms study. *Hydrobiologia*, *679*(1), 43–59. https://doi.org/10.1007/s10750-011-0854-6

Gooseff, M. N., McKnight, D. M., Lyons, W. B., & Blum, A. E. (2002). Weathering reactions and hyporheic exchange controls on stream water chemistry in a glacial meltwater stream in the McMurdo Dry Valleys. *Water Resources Research*, *38*(12), 15-1-15–17. https://doi.org/10.1029/2001WR000834

Gooseff, M. N., McKnight, D. M., Runkel, R. L., & Vaughn, B. H. (2003). Determining long time-scale hyporheic zone flow paths in Antarctic streams. *Hydrological Processes*, *17*(9), 1691–1710. https://doi.org/10.1002/hyp.1210

Gooseff, M. N., D. M. McKnight, and R. L. Runkel (2004a). Reach-Scale Cation Exchange Controls on Major Ion Chemistry of an Antarctic Glacial Meltwater Stream. Aquatic Geochemistry 10:221–238.

Gooseff, M. N., D. M. McKnight, R. L. Runkel, and J. H. Duff (2004b). Denitrification and hydrologic transient storage in a glacial meltwater stream, McMurdo Dry Valleys, Antarctica. Limnology and Oceanography 49:1884–1895.

Gooseff, M. N. (2010). Defining hyporheic zones - advancing our conceptual and operational definitions of where stream water and groundwater meet. *Geography Compass*. https://doi.org/10.1111/j.1749-8198.2010.00364.x

Gooseff, M. N., D. M. McKnight, P. T. Doran, A. G. Fountain, & W. B. Lyons (2011). Hydrological connectivity of the landscape of the McMurdo Dry Valleys, Antarctica. *Geography Compass*, 5:666–681.

Gooseff, M. N., Wlostowski, A. N., McKnight, D. M., & Jaros, C. (2016). Hydrologic connectivity and implications for ecosystem processes-Lessons from naked watersheds. *Geomorphology*.

Gooseff, M.N. & McKnight, D.M. (2016). McMurdo Dry Valleys Priscu Stream Gage Measurements ver 7. *Environmental Data Initiative*. https://doi.org/10.6073/pasta/1567ace50621bb0cee76368c2b59b80a.

Gooseff, M.N. & McKnight, D. M. (2019a). McMurdo Dry Valleys LTER: High frequency seasonal stream gage measurements from Andersen Creek at H1 in Taylor Valley, Antarctica from 1993 to present ver 10. *Environmental Data Initiative*. https://doi.org/10.6073/pasta/81173c42e5c6a0a4894001eedb3d623a.

Gooseff, M.N. & McKnight, D. M. (2019b). McMurdo Dry Valleys LTER: High frequency seasonal stream gage measurements from Canada Stream at F1 in Taylor Valley, Antarctica from 1990 to present ver 11. *Environmental Data Initiative*. https://doi.org/10.6073/pasta/3b2d96bb09ba5d1b883ab99702e3eb40.

Gooseff, M.N. & McKnight, D. M. (2019c). McMurdo Dry Valleys LTER: High frequency seasonal stream gage measurements from Commonwealth Stream at C1 in Taylor Valley, Antarctica from 1993 to present ver 8. *Environmental Data Initiative*. https://doi.org/10.6073/pasta/b15ef1450799587dc7d60c960fc18142.

Gooseff, M.N. & McKnight, D. M. (2019d). McMurdo Dry Valleys LTER: High frequency seasonal stream gage measurements from Crescent Stream at F8 in Taylor Valley, Antarctica from 1990 to present ver 11. *Environmental Data Initiative*. https://doi.org/10.6073/pasta/86bce67070a2e3b37bf5ca805059feee.

Gooseff, M.N. & McKnight, D. M. (2019e). 2019. McMurdo Dry Valleys LTER: High frequency seasonal stream gage measurements from Delta Stream at F10 in Taylor Valley, Antarctica from 1990 to present ver 11. *Environmental Data Initiative*. https://doi.org/10.6073/pasta/03abc485979246b558d172e01eb81e02.

Gooseff, M.N. & McKnight, D. M. (2019f). McMurdo Dry Valleys LTER: High frequency seasonal stream gage measurements from Green Creek at F9 in Taylor Valley, Antarctica from 1990 to present ver 12. *Environmental Data Initiative*. https://doi.org/10.6073/pasta/bdf09ca40915db102722c4143ed0a0e7.

Gooseff, M.N. & McKnight, D. M. (2019g). McMurdo Dry Valleys LTER: High frequency seasonal stream gage measurements from Harnish Creek at F7 in Taylor Valley, Antarctica from 2001 to present ver 7. *Environmental Data Initiative*. https://doi.org/10.6073/pasta/0dbe0da2ff94c833730e855ddc5344b3.

Gooseff, M.N. & D. McKnight, D. M. (2019j). McMurdo Dry Valleys LTER: High frequency seasonal stream gage measurements from Von Guerard Stream at F6 in Taylor Valley, Antarctica from 1990 to present ver 17. *Environmental Data Initiative*. https://doi.org/10.6073/pasta/b452c7c780079060e0cd17db08f6089e.

Gooseff, M.N. & McKnight, D. M. (2019i). McMurdo Dry Valleys LTER: High frequency seasonal stream gage measurements from Lost Seal Stream at F3 in Taylor Valley, Antarctica from 1990 to present ver 7. *Environmental Data Initiative*. https://doi.org/10.6073/pasta/fa9c6a1a8ab26074cfd632dbecc339f1.

Green, W. J., Angle, M. P., & Chave, K. E. (1988). The geochemistry of Antarctic streams and their role in the evolution of four lakes of the McMurdo Dry Valleys. *Geochimica et Cosmochimica Acta*, *52*(5), 1265–1274.

Griffiths, N. A., & Tiegs, S. D. (2016). Organic-matter decomposition along a temperature gradient in a forested headwater stream. *Freshwater Science*, *35*(2), 518–533. https://doi.org/10.1086/685657

Grimm, N. B. (1987). Nitrogen Dynamics During Succession in a Desert Stream. *Ecology* 68:1157–1170.

Grimm, N. B., & Petrone, K. C. (1997). Nitrogen fixation in a desert stream ecosystem. *Biogeochemistry*, *37*(1), 33–61. https://doi.org/10.1023/A:1005798410819

Hall, R. O., & Tank, J. L. (2003). Ecosystem metabolism controls nitrogen uptake in streams in Grand Teton National Park, Wyoming. *Limnology and Oceanography*, *48*(3), 1120–1128. https://doi.org/10.4319/lo.2003.48.3.1120

Hamada, Y., B. L. O'Connor, A. B. Orr, & K. K. Wuthrich (2016). Mapping ephemeral stream networks in desert environments using very-high-spatial-resolution multispectral remote sensing. *Journal of Arid Environments*, 130:40–48.

Hamilton, S. K., Tank, J. L., Raikow, D. F., Siler, E. R., Dorn, N. J., & Leonard, N. E. (2004). The role of instream vs allochthonous N in stream food webs: modeling the results of an isotope addition experiment. *Journal of the North American Benthological Society*, *23*(3), 429–448. https://doi.org/10.1899/0887-3593(2004)023<0429:TROIVA>2.0.CO;2

Harvey, J. W., & Bencala, K. E. (1993). The Effect of streambed topography on surface-subsurface water exchange in mountain catchments. *Water Resources Research*, *29*(1), 89–98. https://doi.org/10.1029/92WR01960

Harvey, J. W., Wagner, B. J., & Bencala, K. E. (1996). Evaluating the reliability of the stream tracer approach to characterize stream-subsurface water exchange. *Water Resources Research*, *32*(8), 2441–2451. https://doi.org/10.1029/96WR01268

Harvey, J. W., Bohlke, J. K., Voytek, M. A., Scott, D. T., & Tobias, C. R. (2013). Hyporheic zone denitrification: Controls on effective reaction depth and contribution to whole-stream mass balance. *Water Resources Research*, *49*(10), 6298–6316. https://doi.org/10.1002/wrcr.20492

Harvey, J. W., & Gooseff, M. N. (2015). River corridor science: Hydrologic exchange and ecological consequences from bedforms to basins. *Water Resources Research*. https://doi.org/10.1002/2015WR017617

Harvey, J. W., Gomez-Velez, J. D., Schmadel, N. M., Scott, D. T., Boyer, E. W., Alexander, R. B., et al. (2018). How Hydrologic Connectivity Regulates Water Quality in River Corridors. *Journal of the American Water Resources Association*, pp. 369–381. https://doi.org/10.1111/1752-1688.12691

Hawes, I., & Howard-Williams, C. (1998). Primary Production Processes in Streams of the Mcmurdo Dry Valleys, Antarctica. *Ecosystem Dynamics in a Polar Desert: The Mcmurdo Dry Valleys, Antarctica*. https://doi.org/https://doi.org/10.1029/AR072p0129

Heffernan, J. B., & Cohen, M. J. (2010). Direct and indirect coupling of primary production and diel nitrate dynamics in a subtropical spring-fed river. *Limnology and Oceanography*, *55*(2), 677–688.

Heindel, R. C., Bergstrom, A. J., Singley, J. G., McKnight, D. M., Darling, J., Lukkari, B., et al. (2021). Diatoms trace the retention and processing of organic matter in hyporheic sediments in the McMurdo Dry Valleys, Antarctica. *Journal of Geophysical Research-Biogeosciences*. https://doi.org/10.1029/2020JG006097

Heindel, R. C., J. G. Singley, A. J. Bergstrom, J. Darling, K. A. Welch, D. M. McKnight, and M. N. Gooseff (2021). Hyporheic sediment characteristics from Von Guerard Stream, Taylor Valley, McMurdo Dry Valleys, Antarctica in January 2019 ver 2. *Environmental Data Initiative*.

Heindel, R. C., Lyons, W. B., Welch, S. A., Spickard, A. M., & Virginia, R. A. (2018). Biogeochemical weathering of soil apatite grains in the McMurdo Dry Valleys, Antarctica. *Geoderma*, *320*, 136–145. https://doi.org/10.1016/j.geoderma.2018.01.027

Hermes, A. L., Wainwright, H. M., Wigmore, O., Falco, N., Molotch, N. P., & Hinckley, E.-L. S. (2020). From Patch to Catchment: A Statistical Framework to Identify and Map Soil Moisture Patterns Across Complex Alpine Terrain. *Frontiers in Water*, *2*. https://doi.org/10.3389/frwa.2020.578602

Hillebrand, H. (2008). Grazing Regulates the Spatial Variability of Periphyton. *Ecology* 89:165–173.

Hirst, C., Opfergelt, S., Gaspard, F., Hendry, K. R., Hatton, J. E., Welch, S., et al. (2020). Silicon Isotopes Reveal a Non-glacial Source of Silicon to Crescent Stream, McMurdo Dry Valleys, Antarctica. *Frontiers in Earth Science*, *8*. https://doi.org/10.3389/feart.2020.00229

Hoellein, T. J., Bruesewitz, D. A., & Richardson, D. C. (2013). Revisiting Odum (1956): A synthesis of aquatic ecosystem metabolism. *Limnology and Oceanography*, *58*(6), 2089–2100. https://doi.org/10.4319/lo.2013.58.6.2089

Hopkins, D. W., Sparrow, A. D., Elberling, B., Gregorich, E. G., Novis, P. M., Greenfield, L. G., & Tilston, E. L. (2006). Carbon, nitrogen and temperature controls on microbial activity in soils from an Antarctic dry valley. *Soil Biology and Biochemistry*, *38*(10), 3130–3140. https://doi.org/10.1016/j.soilbio.2006.01.012

Horne, A. J., & Carmiggelt, C. J. W. (1975). Algal nitrogen fixation in Californian streams: seasonal cycles. *Freshwater Biology*, *5*(5), 461–470. https://doi.org/10.1111/j.1365-2427.1975.tb00148.x

Horner, R. R. & E. B. Welch (1981). Stream Periphyton Development in Relation to Current Velocity and Nutrients. *Canadian Journal of Fisheries and Aquatic Sciences*, 38:449–457.

Hou, Z., Scheibe, T. D., Murray, C. J., Perkins, W. A., Arntzen, E. V., Ren, H., et al. (2019). Identification and mapping of riverbed sediment facies in the Columbia River through

integration of field observations and numerical simulations. *Hydrological Processes*, *33*(8), 1245–1259. https://doi.org/10.1002/hyp.13396

Howard-Williams, C., Priscu, J. C., & Vincent, W. F. (1989). Nitrogen dynamics in two antarctic streams. *Hydrobiologia*, *172*(1), 51–61. https://doi.org/10.1007/BF00031612

Huryn, A. D., Benstead, J. P., & Parker, S. M. (2014). Seasonal changes in light availability modify the temperature dependence of ecosystem metabolism in an arctic stream. *Ecology*, *95*(10), 2826–2839. https://doi.org/10.1890/13-1963.1

Jacobson, P. J., & Jacobson, K. M. (2013). Hydrologic controls of physical and ecological processes in Namib Desert ephemeral rivers: Implications for conservation and management. *Journal of Arid Environments*, *93*, 80–93. https://doi.org/10.1016/j.jaridenv.2012.01.010

Jensen, C. K., McGuire, K. J., & Prince, P. S. (2017). Headwater stream length dynamics across four physiographic provinces of the Appalachian Highlands. *Hydrological Processes*.

Jones, J. B., Fisher, S. G., & Grimm, N. B. (1995a). Nitrification in the Hyporheic Zone of a Desert Stream Ecosystem. *Journal of the North American Benthological Society*, *14*(2), 249–258. https://doi.org/10.2307/1467777

Jones, J. B., Fisher, S. G., & Grimm, N. B. (1995b). Vertical hydrologic exchange and ecosystem metabolism in a Sonoran Desert stream. *Ecology*, *76*(3), 942–952.

Kasahara, T., & Wondzell, S. M. (2003). Geomorphic controls on hyporheic exchange flow in mountain streams. *Water Resources Research*, *39*(1), SBH 3-1-SBH 3-14. https://doi.org/10.1029/2002wr001386

Kelleher, C., Ward, A., Knapp, J. L. A., Blaen, P. J., Kurz, M. J., Drummond, J. D., et al. (2019). Exploring tracer information and model framework trade-offs to improve estimation of stream transient storage processes. *Water Resources Research*, 55, 3481– 3501. https://doi.org/10.1029/2018WR023585

Kemp, M. J., & Dodds, W. K. (2001). Centimeter-scale patterns in dissolved oxygen and nitrification rates in a prairie stream. *Journal of the North American Benthological Society*, *20*(3), 347–357. https://doi.org/10.2307/1468033

Kemp, M. J., & Dodds, W. K. (2002). Comparisons of nitrification and denitrification in prairie and agriculturally influenced streams. *Ecological Applications*, *12*(4), 998–1009. https://doi.org/10.1890/1051-0761(2002)012[0998:CONADI]2.0.CO;2

Keys, J. R., & Williams, K. (1981). Origin of crystalline, cold desert salts in the McMurdo region, Antarctica. *Geochimica et Cosmochimica Acta*, *45*(12), 2299–2309. https://doi.org/10.1016/0016-7037(81)90084-3

Kirchner, J. W. (2003). A double paradox in catchment hydrology and geochemistry. *Hydrological Processes*, *17*(4), 871–874.

Knapp, J. L. A., González-Pinzón, R., & Haggerty, R. (2018). The Resazurin-Resorufin System: Insights From a Decade of "Smart" Tracer Development for Hydrologic Applications. *Water Resources Research*, *54*(9), 6877–6889. https://doi.org/10.1029/2018WR023103

Knapp, J. L. A., Von Freyberg, J., Studer, B., Kiewiet, L., & Kirchner, J. W. (2020). Concentration-discharge relationships vary among hydrological events, reflecting differences in event characteristics. *Hydrology and Earth System Sciences*, *24*(5), 2561–2576. https://doi.org/10.5194/hess-24-2561-2020

Knights, D., Sawyer, A. H., Barnes, R. T., Musial, C. T., & Bray, S. (2017). Tidal controls on riverbed denitrification along a tidal freshwater zone. *Water Resources Research*, *53*(1), 799–816. https://doi.org/10.1002/2016WR019405

Koch, J. C., McKnight, D. M., & Baeseman, J. L. (2010). Effect of unsteady flow on nitrate loss in an oligotrophic, glacial meltwater stream. *Journal of Geophysical Research-Biogeosciences*, *115*(G1), G01001. https://doi.org/10.1029/2009jg001030

Koch, J. C., D. M. McKnight, & R. M. Neupauer (2011). Simulating unsteady flow, anabranching, and hyporheic dynamics in a glacial meltwater stream using a coupled surface water routing and groundwater flow model. *Water Resources Research*, 47.

Koch, R., D. Kerling, & J. M. O'Brien (2018). Effects of chronic elevated nitrate concentrations on the structure and function of river biofilms. *Freshwater Biology*, 63:1199–1210.

Kohler, T. J., Stanish, L. F., Crisp, S. W., Koch, J. C., Liptzin, D., Baeseman, J. L., & McKnight, D. M. (2015). Life in the main channel: long-term hydrologic control of microbial mat abundance in McMurdo Dry Valley streams, Antarctica. *Ecosystems*, *18*(2), 310–327.

Kohler, T. J., Stanish, L. F., Liptzin, D., Barrett, J. E., & McKnight, D. M. (2018). Catch and release: Hyporheic retention and mineralization of N-fixing Nostoc sustains downstream microbial mat biomass in two polar desert streams. *Limnology and Oceanography Letters*. https://doi.org/10.1002/lol2.10087

Kohler, T. J. (2018). McMurdo Dry Valleys Microbial mat biomass, isotopes, and nutrient ratios sampled over a longitudinal gradient of two McMurdo Dry Valley streams ver 2. *Environmental Data Initiative*.

Koohafkan, M. C., & B. A. Younis (2015). Open-channel computation with R. *The R Journal*, 7:249–262.

Krause, S., et al. (2017), Ecohydrological interfaces as hot spots of ecosystem processes, *Water Resources Research*, 53, 6359– 6376, https://doi.org/10.1002/2016WR019516.

Krysanova, V., Vetter, T., & Hattermann, F. (2008). Detection of change in drought frequency in the Elbe basin: comparison of three methods. *Hydrological Sciences Journal*, *53*(3), 519–537.

Kunza, L. A., & Hall, R. O. (2014). Nitrogen fixation can exceed inorganic nitrogen uptake

fluxes in oligotrophic streams. *Biogeochemistry*, *121*(3), 537–549.

Lansdown, K., Heppell, C. M., Trimmer, M., Binley, A. M., Heathwaite, A. L., Byrne, P., & Zhang, H. (2015). The interplay between transport and reaction rates as controls on nitrate attenuation in permeable, streambed sediments. *Journal of Geophysical Research G: Biogeosciences*, *120*(6), 1093–1109. https://doi.org/10.1002/2014JG002874

Larned, S. T., Datry, T., Arscott, D. B., & Tockner, K. (2010). Emerging concepts in temporary-river ecology. *Freshwater Biology*, *55*(4), 717–738.

Lee, A., Aubeneau, A. F., & Cardenas, M. B. (2020). The Sensitivity of Hyporheic Exchange to Fractal Properties of Riverbeds. *Water Resources Research*, *56*(5). https://doi.org/10.1029/2019WR026560

Leigh, C., Boulton, A. J., Courtwright, J. L., Fritz, K., May, C. L., Walker, R. H., & Datry, T. (2016). Ecological research and management of intermittent rivers: an historical review and future directions. *Freshwater Biology*, *61*(8), 1181–1199. https://doi.org/10.1111/fwb.12646

Levy, J. S. (2013). How big are the McMurdo Dry Valleys? Estimating ice-free area using Landsat image data. *Antarctic Science*, *25*(01), 119–120.

Lewandowski, J., Arnon, S., Banks, E., et al. (2019). Is the hyporheic zone relevant beyond the scientific community? *Water*, *11*(11), 2230. https://doi.org/10.3390/w11112230

Li, L., Sullivan, P. L., Benettin, P., Cirpka, O. A., Bishop, K., Brantley, S. L., et al. (2021). Toward catchment hydro-biogeochemical theories. *Wiley Interdisciplinary Reviews: Water*, *8*(1), e1495. https://doi.org/10.1002/wat2.1495

Lovett, G. M., & C. L. Goodale (2011). A New Conceptual Model of Nitrogen Saturation Based on Experimental Nitrogen Addition to an Oak Forest. *Ecosystems* 14:615–631.

Luce, J. J., A. Cattaneo, and M. F. Lapointe (2010). Spatial patterns in periphyton biomass after low-magnitude flow spates: geomorphic factors affecting patchiness across gravel–cobble riffles. *Journal of the North American Benthological Society*, 29:614–626.

Lyons, W. B. (2015). McMurdo Dry Valleys Stream Nutrients (nitrate, nitrite, ammonium, reactive phosphorus). *Environmental Data Initiative*. https://doi.org/10.6073/pasta/81cfcad244f7d3f6a6fcdab83ea75849

Lyons, B. (2019a). McMurdo Dry Valleys Stream Chemistry - Dissolved Organic Carbon ver 6. *Environmental Data Initiative*. https://doi.org/10.6073/pasta/578d31fa0e142b6b7a6c80095d29b968.

Lyons, B. (2019b). McMurdo Dry Valleys Stream Nutrients (nitrate, nitrite, ammonium, reactive phosphorus) ver 7. *Environmental Data Initiative*. https://doi.org/10.6073/pasta/81cfcad244f7d3f6a6fcdab83ea75849.

Lyons, B. & Welch, K. (2019). McMurdo Dry Valleys Stream Chemistry and Ion Concentrations

ver 12. *Environmental Data Initiative*.
https://doi.org/10.6073/pasta/be9f781814330116f68844a8957962e4.

Lyons, W. B., Leslie, D. L., & Gooseff, M. N. (2021). Chemical Weathering in the McMurdo Dry Valleys, Antarctica. *Hydrogeology, Chemical Weathering, and Soil Formation*. https://doi.org/https://doi.org/10.1002/9781119563952.ch11

Magliozzi, C., Grabowski, R. C., Packman, A. I., & Krause, S. (2018). Toward a conceptual framework of hyporheic exchange across spatial scales. *Hydrology and Earth System Sciences*, *22*(12), 6163–6185. https://doi.org/10.5194/hess-22-6163-2018

Marcarelli, A. M., & Wurtsbaugh, W. A. (2006). Temperature and nutrient supply interact to control nitrogen fixation in oligotrophic streams: An experimental examination. *Limnology and Oceanography*, *51*(5), 2278–2289. https://doi.org/10.4319/lo.2006.51.5.2278

Marcarelli, A. M., Baker, M. A., & Wurtsbaugh, W. A. (2008). Is in-stream N2 fixation an important N source for benthic communities and stream ecosystems? *Journal of the North American Benthological Society*. https://doi.org/10.1899/07-027.1

Marinos, R. E., Van Meter, K. J., & Basu, N. B. (2020). Is the River a Chemostat?: Scale Versus Land Use Controls on Nitrate Concentration-Discharge Dynamics in the Upper Mississippi River Basin. *Geophysical Research Letters*, *47*(16). https://doi.org/10.1029/2020GL087051

Marion, A., Zaramella, M., & Packman, A. I. (2003). Parameter Estimation of the Transient Storage Model for Stream–Subsurface Exchange. *Journal of Environmental Engineering*, *129*(5), 456–463. https://doi.org/10.1061/(asce)0733-9372(2003)129:5(456)

Martí, E., & Sabater, F. (1996). High variability in temporal and spatial nutrient retention in mediterranean streams. *Ecology*, *77*(3), 854–869. https://doi.org/10.2307/2265506

Martí, E., Grimm, N. B., & Fisher, S. G. (1997). Pre-and post-flood retention efficiency of nitrogen in a Sonoran Desert stream. *Journal of the North American Benthological Society*, *16*(4), 805–819.

Marzadri, A., Tonina, D., & Bellin, A. (2011). A semianalytical three-dimensional process-based model for hyporheic nitrogen dynamics in gravel bed rivers. *Water Resour. Res.*, 47, W11518, https://doi.org/10.1029/2011WR010583

Matheson, F. E., Quinn, J. M., & Martin, M. L. (2012). Effects of irradiance on diel and seasonal patterns of nutrient uptake by stream periphyton. *Freshwater Biology*, *57*(8), 1617–1630. https://doi.org/10.1111/j.1365-2427.2012.02822.x

Maurice, P. A., McKnight, D. M., Leff, L., Fulghum, J. E., & Gooseff, M. N. (2002). Direct observations of aluminosilicate weathering in the hyporheic zone of an Antarctic Dry Valley stream. *Geochimica et Cosmochimica Acta*, *66*(8), 1335–1347.

Mayland, H. F., McIntosh, T. H., & Fuller, W. H. (1966). Fixation of Isotopic Nitrogen on a Semiarid Soil by Algal Crust Organisms. *Soil Science Society of America Journal*, *30*(1),

56–60. https://doi.org/10.2136/sssaj1966.03615995003000010022x

McDonnell, J. J., Bonell, M., Stewart, M. K., & Pearce, A. J. (1990). Deuterium variations in storm rainfall: Implications for stream hydrograph separation. *Water Resources Research*, *26*(3), 455–458.

McKnight, D. M., A. Alger, C. Tate, G. Shupe, and S. Spaulding (1998). Longitudinal Patterns in Algal Abundance and Species Distribution In Meltwater Streams In Taylor Valley, Southern Victoria Land, Antarctica. Pages 109–127 *in* J. C. Priscu (editor*). Ecosystem Dynamics in a Polar Desert: The McMurdo Dry Valleys, Antarctica*. American Geophysical Union (AGU).

McKnight, D. M., Niyogi, D. K., Alger, A. S., Bomblies, A., Conovitz, P. A., & Tate, C. M. (1999). Dry valley streams in Antarctica: ecosystems waiting for water. *BioScience*, *49*(12), 985–995.

McKnight, D. M., K. D. Cozzetto, J. D. S. Cullis, M. N. Gooseff, C. Jaros, J. C. Koch, W. B. Lyons, R. Neupauer, and A. N. Wlostowski (2015). Potential for real-time understanding of coupled hydrologic and biogeochemical processes in stream ecosystems: Future integration of telemetered data with process models for glacial meltwater streams. *Water Resources Research*, 51:6725–6738.

McKnight, D. M., Runkel, R. L., Tate, C. M., Duff, J. H., & Moorhead, D. L. (2004). Inorganic N and P dynamics of Antarctic glacial meltwater streams as controlled by hyporheic exchange and benthic autotrophic communities. *Journal of the North American Benthological Society*, *23*(2), 171–188.

McKnight, D. M., Tate, C. M., Andrews, E. D., Niyogi, D. K., Cozzetto, K. D., Welch, K. A., et al. (2007). Reactivation of a cryptobiotic stream ecosystem in the McMurdo Dry Valleys, Antarctica: a long-term geomorphological experiment. *Geomorphology*, *89*(1), 186–204.

McKnight, D. M., Tate, C. M., Andrews, E. D., Niyogi, D. K., Cozzetto, K. D., Welch, K. A., et al. (2007). Reactivation of a cryptobiotic stream ecosystem in the McMurdo Dry Valleys, Antarctica: a long-term geomorphological experiment. *Geomorphology*, *89*(1), 186–204.

McKnight, D. M. (2019). McMurdo Dry Valleys LTER: Algal microbial mat biomass measurements from the McMurdo Dry Valleys and Cape Royds, Antarctica from 1994 to present. *Environmental Data Initiative*.

McLachlan, P. J., Chambers, J. E., Uhlemann, S. S., & Binley, A. M. (2017). Geophysical characterisation of the groundwater–surface water interface. *Advances in Water Resources*, *109*, 302–319. https://doi.org/10.1016/J.ADVWATRES.2017.09.016

Mendoza-Lera, C., Ribot, M., Foulquier, A., Martí, E., Bonnineau, C., Breil, P., & Datry, T. (2019). Exploring the role of hydraulic conductivity on the contribution of the hyporheic zone to in-stream nitrogen uptake. *Ecohydrology*, *12*(7). https://doi.org/10.1002/eco.2139

Merbt, S. N., Proia, L., Prosser, J. I., Martí, E., Casamayor, E. O., & von Schiller, D. (2016).

Stream drying drives microbial ammonia oxidation and first-flush nitrate export. *Ecology*, *97*(9), 2192–2198. https://doi.org/10.1002/ecy.1486

Mikucki, J., Auken, E., Tulaczyk, S. et al. (2015) Deep groundwater and potential subsurface habitats beneath an Antarctic dry valley. *Nature Communications*, 6, 6831, https://doi.org/10.1038/ncomms7831

Moatar, F., Abbott, B. W., Minaudo, C., Curie, F., & Pinay, G. (2017). Elemental properties, hydrology, and biology interact to shape concentration-discharge curves for carbon, nutrients, sediment, and major ions. *Water Resources Research*, *53*(2), 1270–1287. https://doi.org/https://doi.org/10.1002/2016WR019635

Montero, P., & Vilar, J. A. (2014). TSclust: An R package for Time Series Clustering. *Journal of Statistical Software2*, *62*(1), 1–43.

Mueen, A., & Keogh, E. (2016). Extracting optimal performance from dynamic time warping. In *Proceedings of the ACM SIGKDD International Conference on Knowledge Discovery and Data Mining* (Vol. 13-17-August-2016, pp. 2129–2130). New York, NY, USA: Association for Computing Machinery. https://doi.org/10.1145/2939672.2945383

Mulholland, P. J., C. S. Fellows, J. L. Tank, N. B. Grimm, et al. (2001), Inter-biome comparison of factors controlling stream metabolism. *Freshwater Biology*, 46: 1503-1517. https://doi.org/10.1046/j.1365-2427.2001.00773.x

Mulholland, P. J. (2004). The importance of in-stream uptake for regulating stream concentrations and outputs of N and P from a forested watershed: Evidence from long-term chemistry records for Walker Branch Watershed. *Biogeochemistry*, *70*(3), 403–426. https://doi.org/10.1007/s10533-004-0364-y

Mulholland, P. J., Helton, A. M., Poole, G. C., Hall, R. O., Hamilton, S. K., Peterson, B. J., et al. (2008). Stream denitrification across biomes and its response to anthropogenic nitrate loading. *Nature*, *452*(7184), 202–205. https://doi.org/10.1038/nature06686

Nadoushani, S. S. M., Dehghanian, N., & Saghafian, B. (2018). A fuzzy hybrid clustering method for identifying hydrologic homogeneous regions. *Journal of Hydroinformatics*, *20*(6), 1367–1386. https://doi.org/10.2166/hydro.2018.004

Naiman, R. J. & J. M. Melillo (1984). Nitrogen budget of a subarctic stream altered by beaver (Castor canadensis). *Oecologia*, 62:150–155.

O'Brien, J. M., S. K. Hamilton, L. Podzikowski, & N. Ostrom (2012). The fate of assimilated nitrogen in streams: An in situ benthic chamber study. *Freshwater Biology*, 57:1113–1125.

Oviedo-Vargas, D., Royer, T. V., & Johnson, L. T. (2013). Dissolved organic carbon manipulation reveals coupled cycling of carbon, nitrogen, and phosphorus in a nitrogen-rich stream. *Limnology and Oceanography*, *58*(4), 1196–1206. https://doi.org/10.4319/lo.2013.58.4.1196

Park, P. J., Manjourides, J., Bonetti, M., & Pagano, M. (2009). A permutation test for determining significance of clusters with applications to spatial and gene expression data. *Computational Statistics and Data Analysis*, *53*(12), 4290–4300. https://doi.org/10.1016/j.csda.2009.05.031

Peterson, B. J., Wollheim, W. M., Mulholland, P. J., Webster, J. R., Meyer, J. L., Tank, J. L., et al. (2001). Control of nitrogen export from watersheds by headwater streams. *Science*, *292*(5514), 86–90.

Pidlisecky, A., Singha, K., & Day-Lewis, F. D. (2011). A distribution-based parameterization for improved tomographic imaging of solute plumes. *Geophysical Journal International*, 187(1), doi: 10.1111/j.1365-246X.2011.05131.x

Pilgrim, D. H., Huff, D. D., & Steele, T. D. (1979). Use of specific conductance and contact time relations for separating flow components in storm runoff. *Water Resources Research*, *15*(2), 329–339.

R Core Team. (2019). R: A Language and Environment for Statistical Computing. Vienna, Austria: R Foundation for Statistical Computing.

Rice, K. C., Chanat, J. G., Hornberger, G. M., & Webb, J. R. (2004). Interpretation of concentration-discharge patterns in acid-neutralizing capacity during storm flow in three small, forested catchments in Shenandoah National Park, Virginia. *Water Resources Research*, *40*(5).

Robinson, C. T., Tonolla, D., Imhof, B., Vukelic, R., & Uehlinger, U. (2016). Flow intermittency, physico-chemistry and function of headwater streams in an Alpine glacial catchment. *Aquatic Sciences*, *78*(2), 327–341.

Rucker, D. F., Tsai, C. H., Carroll, K. C., Brooks, S., Pierce, E. M., Ulery, A., & Derolph, C. (2021). Bedrock architecture, soil texture, and hyporheic zone characterization combining electrical resistivity and induced polarization imaging. *Journal of Applied Geophysics*, *188*, 104306. https://doi.org/10.1016/j.jappgeo.2021.104306

Runkel, R. L., McKnight, D. M., & Andrews, E. D. (1998). Analysis of transient storage subject to unsteady flow: diel flow variation in an Antarctic stream. *Journal of the North American Benthological Society*, 143–154.

Runkel, R. L. (2002). A new metric for determining the importance of transient storage. *Journal of the North American Benthological Society*, *21*(4), 529–543. https://doi.org/10.2307/1468428

Rusjan, S., & Mikoš, M. (2010). Seasonal variability of diurnal in-stream nitrate concentration oscillations under hydrologically stable conditions. *Biogeochemistry*, *97*(2–3), 123–140. https://doi.org/10.1007/s10533-009-9361-5

Sabater, S. (2008). Alterations of the global water cycle and their effects on river structure, function and services. *Freshwater Reviews*, *1*(1), 75–88.

Salvatore, M. R., S. R. Borges, J. E. Barrett, E. R. Sokol, L. F. Stanish, S. N. Power, and P. Morin (2020). Remote characterization of photosynthetic communities in the Fryxell basin of Taylor Valley, Antarctica. *Antarctic Science*, 32:255–270.

Sassen, D. S., Hubbard, S. S., Bea, S. A., Chen, J., Spycher, N., & Denham, M. E. (2012). Reactive facies: An approach for parameterizing field-scale reactive transport models using geophysical methods. *Water Resources Research*, *48*(10), 10526. https://doi.org/10.1029/2011WR011047

Savoy, P., Appling, A. P., Heffernan, J. B., Stets, E. G., Read, J. S., Harvey, J. W., & Bernhardt, E. S. (2019). Metabolic rhythms in flowing waters: An approach for classifying river productivity regimes. *Limnology and Oceanography*, *64*(5), 1835–1851. https://doi.org/10.1002/lno.11154

Schade, J. D., Welter, J. R., Martí, E., & Grimm, N. B. (2005). Hydrologic exchange and N uptake by riparian vegetation in an arid-land stream. *Journal of the North American Benthological Society*, *24*(1), 19–28. https://doi.org/10.1899/0887-3593(2005)024<0019:HEANUB>2.0.CO;2

Schmadel, N. M., Ward, A. S., & Wondzell, S. M. (2017). Hydrologic controls on hyporheic exchange in a headwater mountain stream. *Water Resources Research*, *53*(7), 6260–6278. https://doi.org/10.1002/2017WR020576

Schmidt, E. L., & Belser, L. W. (1994). Autotrophic Nitrifying Bacteria. In P. S. Bottomley, J. S. Angle, & R. W. Weaver (Eds.), *Methods of Soil Analysis: Part 2 – Microbiological and Biochemical Properties* (pp. 159–177). Madison, WI: Soil Science Society of America. https://doi.org/10.2136/sssabookser5.2.c10

Seitzinger, S. P., W. S. Gardner, & A. K. Spratt (1991). The effect of salinity on ammonium sorption in aquatic sediments: Implications for benthic nutrient recycling. *Estuaries*, 14:167–174.

Seybold, E. C., & McGlynn, B. L. (2018). Hydrologic and biogeochemical drivers of dissolved organic carbon and nitrate uptake in a headwater stream network. *Biogeochemistry*, *138*(1), 23–48. https://doi.org/10.1007/s10533-018-0426-1

Shumilova, O., D. Zak, T. Datry, D. Schiller, R. Corti, A. Foulquier, B. Obrador, K. Tockner, D. et al. (2019). Simulating rewetting events in intermittent rivers and ephemeral streams: A global analysis of leached nutrients and organic matter. *Global Change Biology*, 25:1591–1611.

Simon, K. S., Townsend, C. R., Biggs, B. J. F., & Bowden, W. B. (2005). Temporal variation of N and P uptake in 2 New Zealand streams. *Journal of the North American Benthological Society*, *24*(1), 1–18. https://doi.org/10.1899/0887-3593(2005)024<0001:TVONAP>2.0.CO;2

Singh, T., Gomez-Velez, J. D., Wu, L., Wörman, A., Hannah, D. M., & Krause, S. (2020). Effects of Successive Peak Flow Events on Hyporheic Exchange and Residence Times.

Water Resources Research, *56*(8). https://doi.org/10.1029/2020WR027113

Singha, K., Pidlisecky, A., Day-Lewis, F. D., & Gooseff, M. N. (2008). Electrical characterization of non-Fickian transport in groundwater and hyporheic systems. *Water Resources Research*, *46*(4), 0–07. https://doi.org/10.1029/2008WR007048

Singley, J. G., Wlostowski, A. N., Bergstrom, A. J., Sokol, E. R., Torrens, C. L., Jaros, C., et al. (2017). Characterizing hyporheic exchange processes using high-frequency electrical conductivity-discharge relationships on subhourly to interannual timescales. *Water Resources Research*, *53*(5), 4124–4141. https://doi.org/10.1002/2016WR019739

Singley, J. G., Gooseff, M. N., McKnight, D. M., & Hinckley, E.-L. S. (2021a). The Role of Hyporheic Connectivity in Determining Nitrogen Availability: Insights from an Intermittent Antarctic Stream. *Journal of Geophysical Research: Biogeosciences*, *126*, e2021JG006309. https://doi.org/10.1029/2021JG006309

Singley, J. G., Gooseff, M. N., McKnight, D. M., & Hinckley, E.-L. S. (2021b). Surface and hyporheic porewater chemistry and sediment nitrification potentials in Von Guerard Stream, McMurdo Dry Valleys, Antarctica (2018-2020) ver 2. Environmental Data Initiative. https://doi.org/10.6073/pasta/d6e4301bf93fba0fef6fd5c33a092aaf

Spence, C., & S. Mengistu (2016). Deployment of an unmanned aerial system to assist in mapping an intermittent stream. *Hydrological Processes*, 30:493–500.

Stelzer, R. S., & G. A. Lamberti (2001). Effects of N: P ratio and total nutrient concentration on stream periphyton community structure, biomass, and elemental composition. *Limnology and Oceanography*, 46:356–367.

Stream Solute Workshop. (1990). Concepts and methods for assessing solute dynamics in stream ecosystems. *Journal of the North American Benthological Society*, *9*(2), 95–119. https://doi.org/10.2307/1467445

Tank, J. L., Rosi-Marshall, E. J., Griffiths, N. A., Entrekin, S. A., & Stephen, M. L. (2010). A review of allochthonous organic matter dynamics and metabolism in streams. *Journal of the North American Benthological Society*, *29*(1), 118–146. https://doi.org/10.1899/08-170.1

Taylor, J. R. (1997). *An Introduction to Error Analysis: The Study of Uncertainties in Physical Measurements* (2nd ed.). Sausalito, CA: University Science Books.

Thompson, S. E., Basu, N. B., Lascurain, J., Aubeneau, A., & Rao, P. S. C. (2011). Relative dominance of hydrologic versus biogeochemical factors on solute export across impact gradients. *Water Resources Research*, *47*(7). https://doi.org/10.1029/2010WR009605

Tonina, D., & Buffington, J. M. (2007). Hyporheic exchange in gravel bed rivers with pool-riffle morphology: Laboratory experiments and three-dimensional modeling. *Water Resources Research*, *43*(1). https://doi.org/10.1029/2005WR004328

Triska, F. J., J. R. Sedell, K. Cromack, S. V. Gregory, & F. M. McCorison (1984). Nitrogen

Budget for a Small Coniferous Forest Stream. *Ecological Monographs*, 54:119–140.

Triska, F. J., A. P. Jackman, J. H. Duff, & R. J. Avanzino (1994). Ammonium sorption to channel and riparian sediments: A transient storage pool for dissolved inorganic nitrogen. *Biogeochemistry*, 26:67–83.

Vidal-Abarca, M. R., Gómez, R., & Suarez, M. L. (2004). Los ríos de las regiones semiáridas. *Revista Ecosistemas*, *13*(1), 15–28.

Vitousek, P. M., & W. A. Reiners (1975). Ecosystem Succession and Nutrient Retention: A Hypothesis. *BioScience*, 25:376–381.

von Schiller, D., E. Martí, J. L. Riera, & F. Sabater (2007). Effects of nutrients and light on periphyton biomass and nitrogen uptake in Mediterranean streams with contrasting land uses. *Freshwater Biology*, 52:891–906.

von Schiller, D., Acuña, V., Graeber, D., Martí, E., Ribot, M., Sabater, S., et al. (2011). Contraction, fragmentation and expansion dynamics determine nutrient availability in a Mediterranean forest stream. *Aquatic Sciences*, *73*(4), 485. https://doi.org/10.1007/s00027-011-0195-6

von Schiller, D., Bernal, S., Dahm, C. N., & Martí, E. (2017). Nutrient and Organic Matter Dynamics in Intermittent Rivers and Ephemeral Streams. *Intermittent Rivers and Ephemeral Streams*, 135–160. https://doi.org/10.1016/B978-0-12-803835-2.00006-1

Wainwright, H. M., Chen, J., Sassen, D. S., & Hubbard, S. S. (2014). Bayesian hierarchical approach and geophysical data sets for estimation of reactive facies over plume scales. *Water Resources Research*, *50*(6), 4564–4584. https://doi.org/10.1002/2013WR013842

Ward, A. S., Gooseff, M. N., & Singha, K. (2010a). Characterizing hyporheic transport processes - Interpretation of electrical geophysical data in coupled stream-hyporheic zone systems during solute tracer studies. *Advances in Water Resources*, *33*(11), 1320–1330. https://doi.org/10.1016/j.advwatres.2010.05.008

Ward, A. S., Gooseff, M. N., & Singha, K. (2010b). Imaging hyporheic zone solute transport using electrical resistivity. *Hydrological Processes*, *24*(7), 948–953. https://doi.org/10.1002/hyp.7672

Ward, A. S., Fitzgerald, M., Gooseff, M. N., Voltz, T. J., Binley, A. M., & Singha, K. (2012). Hydrologic and geomorphic controls on hyporheic exchange during base flow recession in a headwater mountain stream. *Water Resources Research*, *48*(4), 4513. https://doi.org/10.1029/2011WR011461

Ward, A. S., Gooseff, M. N., Fitzgerald, M., Voltz, T. J., & Singha, K. (2014). Spatially distributed characterization of hyporheic solute transport during baseflow recession in a headwater mountain stream using electrical geophysical imaging. *Journal of Hydrology*, *517*, 362–377. https://doi.org/10.1016/j.jhydrol.2014.05.036

Ward, A. S. (2016). The evolution and state of interdisciplinary hyporheic research. *Wiley Interdisciplinary Reviews: Water*, *3*(1), 83–103. https://doi.org/10.1002/wat2.1120

Ward, A. S., Schmadel, N. M., Wondzell, S. M., Gooseff, M. N., & Singha, K. (2017). Dynamic hyporheic and riparian flow path geometry through base flow recession in two headwater mountain stream corridors. *Water Resources Research*, *53*(5), 3988–4003. https://doi.org/10.1002/2016WR019875

Ward, A. S., Wondzell, S. M., Schmadel, N. M., Herzog, S., Zarnetske, J. P., Baranov, V., et al. (2019). Spatial and temporal variation in river corridor exchange across a 5th-order mountain stream network. *Hydrology and Earth System Sciences*, *23*(12), 5199–5225. https://doi.org/10.5194/hess-23-5199-2019

Ward, A. S., K. Singha, and M. N. Gooseff (2020). Hyporheic exchange studies in H.J. Andrews Watersheds 01 and 03, summer 2010, HydroShare, https://doi.org/10.4211/hs.8207c26f492e49f0be33e7a2427ccfea

Warren Liao, T. (2005). Clustering of time series data - A survey. *Pattern Recognition*, *38*(11), 1857–1874. https://doi.org/10.1016/j.patcog.2005.01.025

Warwick, J. J. (1986). Diel variation of in-stream nitrification. *Water Research*, *20*(10), 1325–1332. https://doi.org/10.1016/0043-1354(86)90165-X

Webster, J. R., Mulholland, P. J., Tank, J. L., Valett, H. M., Dodds, W. K., Peterson, B. J., Bowden, W. B., Dahm, C. N., Findlay, S., Gregory, S. V., et al. (2003). Factors affecting ammonium uptake in streams - an inter-biome perspective. *Freshwater Biology*, *48*(8), 1329–1352. https://doi.org/10.1046/j.1365-2427.2003.01094.x

Welch, K. A., Lyons, W. B., Whisner, C., Gardner, C. B., Gooseff, M. N., McKnight, D. M., & Priscu, J. C. (2010). Spatial variations in the geochemistry of glacial meltwater streams in the Taylor Valley, Antarctica. *Antarctic Science*, *22*(06), 662–672.

Witherow, R. A., Lyons, W. B., Bertler, N. A. N., Welch, K. A., Mayewski, P. A., Sneed, S. B., et al. (2006). The aeolian flux of calcium, chloride and nitrate to the McMurdo Dry Valleys landscape: Evidence from snow pit analysis. In *Antarctic Science* (Vol. 18, pp. 497–505). https://doi.org/10.1017/S095410200600054X

Wlostowski, A. N., Gooseff, M. N., McKnight, D. M., Jaros, C., & Lyons, W. B. (2016). Patterns of hydrologic connectivity in the McMurdo Dry Valleys, Antarctica: a synthesis of 20 years of hydrologic data. *Hydrological Processes*, *30*, 2958– 2975. https://doi.org/10.1002/hyp.10818

Wlostowski, A. N., Gooseff, M. N., & Adams, B. J. (2018). Soil Moisture Controls the Thermal Habitat of Active Layer Soils in the McMurdo Dry Valleys, Antarctica. *Journal of Geophysical Research: Biogeosciences*, *123*(1), 46–59. https://doi.org/10.1002/2017JG004018

Wlostowski, A. N., Gooseff, M. N., McKnight, D. M., & Lyons, W. B. (2018). Transit Times

and Rapid Chemical Equilibrium Explain Chemostasis in Glacial Meltwater Streams in the McMurdo Dry Valleys, Antarctica. *Geophysical Research Letters*, *45*(24), 13,322-13,331. https://doi.org/10.1029/2018GL080369

Wondzell, S. M. (2006). Effect of morphology and discharge on hyporheic exchange flows in two small streams in the Cascade Mountains of Oregon, USA. *Hydrological Processes*, *20*(2), 267–287. https://doi.org/10.1002/hyp.5902

Wondzell, S. M., & Gooseff, M. N. (2013). 9.13 Geomorphic controls on hyporheic exchange across scales: Watersheds to particles. *Treatise on Geomorphology*, 203–218.

Woods, R., Sivapalan, M., & Duncan, M. (1995). Investigating the representative elementary area concept: An approach based on field data. *Hydrological Processes*, *9*(3–4), 291–312. https://doi.org/10.1002/hyp.3360090306

Yang, K., and L. C. Smith (2013). Supraglacial streams on the greenland ice sheet delineated from combined spectral-shape information in high-resolution satellite imagery. *IEEE Geoscience and Remote Sensing Letters*, 10:801–805.

Zarnetske, J. P., Haggerty, R., Wondzell, S. M., & Baker, M. A. (2011). Dynamics of nitrate production and removal as a function of residence time in the hyporheic zone. *Journal of Geophysical Research-Biogeosciences*, *116*. https://doi.org/10.1029/2010jg001356

Zarnetske, J. P., Haggerty, R., Wondzell, S. M., Bokil, V. A., & González-Pinzón, R. (2012). Coupled transport and reaction kinetics control the nitrate source-sink function of hyporheic zones. *Water Resources Research*, *48*(11). https://doi.org/10.1029/2012WR011894

Zhi, W., Williams, K. H., Carroll, R. W. H., Brown, W., Dong, W., Kerins, D., & Li, L. (2020). Significant stream chemistry response to temperature variations in a high-elevation mountain watershed. *Communications Earth & Environment*, *1*(1), 1–10. https://doi.org/10.1038/s43247-020-00039-w

Zimmer, M. A., & Lautz, L. K. (2014). Temporal and spatial response of hyporheic zone geochemistry to a storm event. *Hydrological Processes*, *28*(4), 2324–2337. https://doi.org/10.1002/hyp.9778

Chapter III Supplemental Information
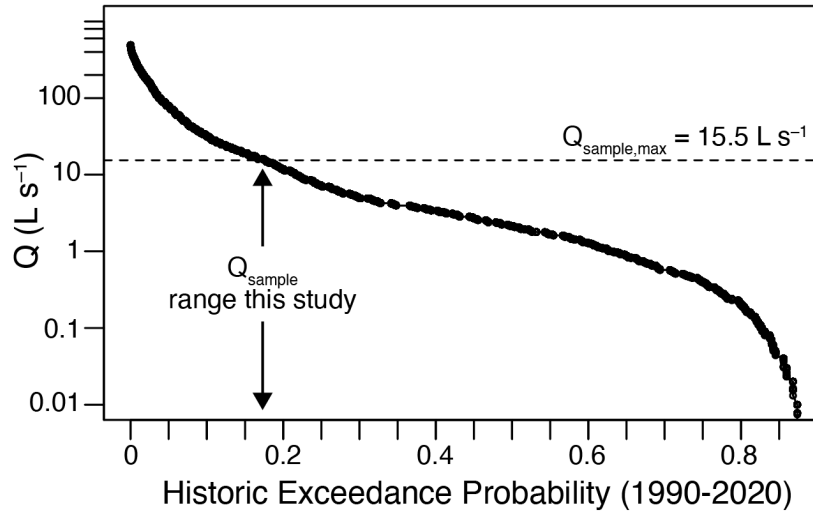
Figure S3.1. Flow exceedance curve for 15-minute Q data from Von Guerard Stream and sampling range of present study.
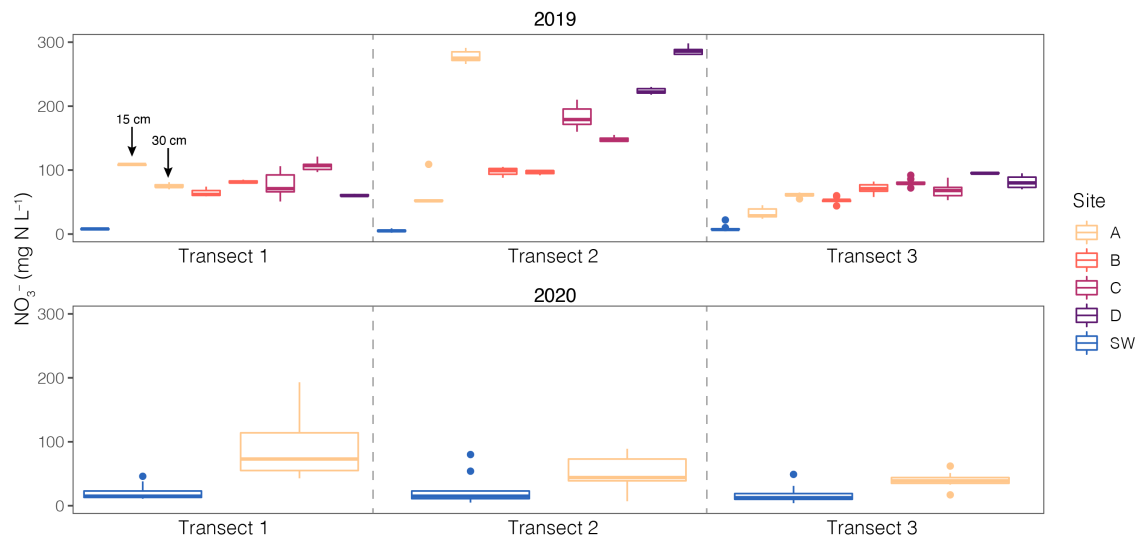
Figure S3.2. Nitrate concentrations by transect, lateral sampling site, and depth.
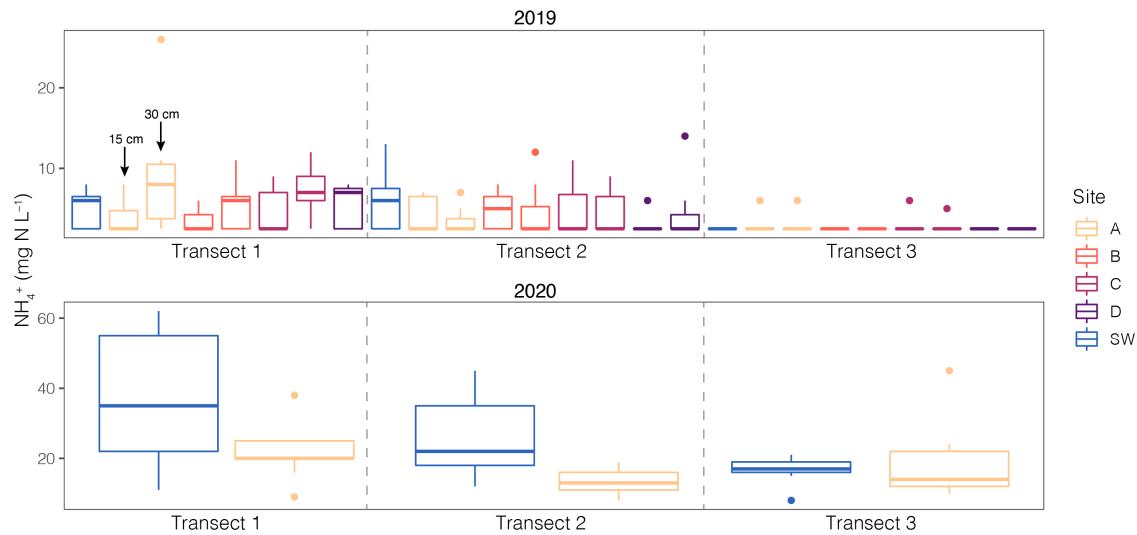
Figure S3.3. Ammonium concentrations by transect, lateral sampling site, and depth.
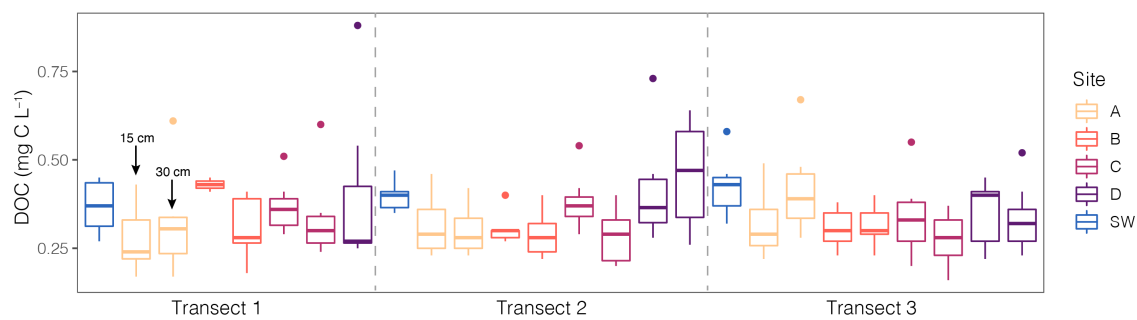
Figure S3.4. Dissolved organic carbon concentrations by transect, lateral sampling site, and depth.
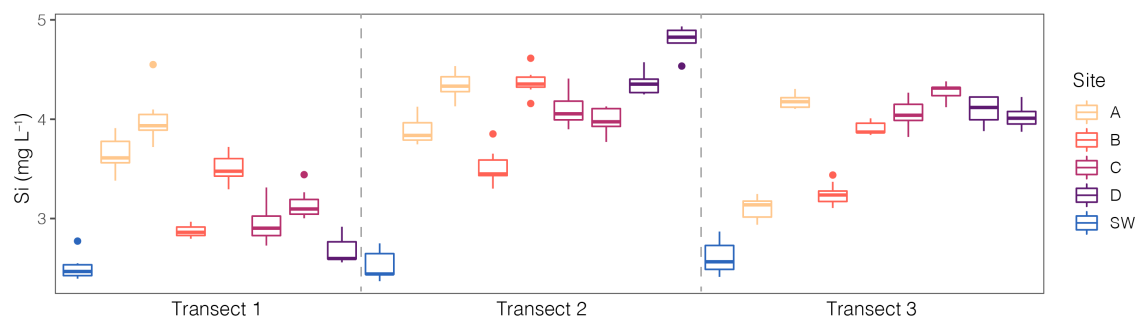
Figure S3.5. Dissolved silica concentrations by transect, lateral sampling site, and depth.
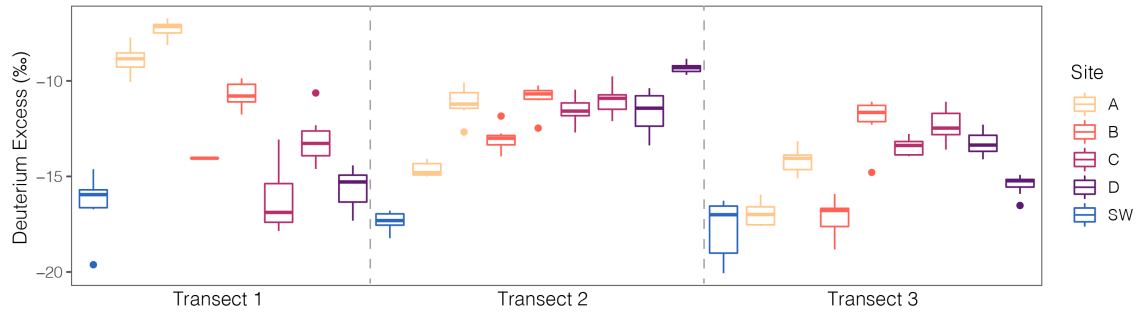
Figure S3.6. Deuterium excess by transect, lateral sampling site, and depth.
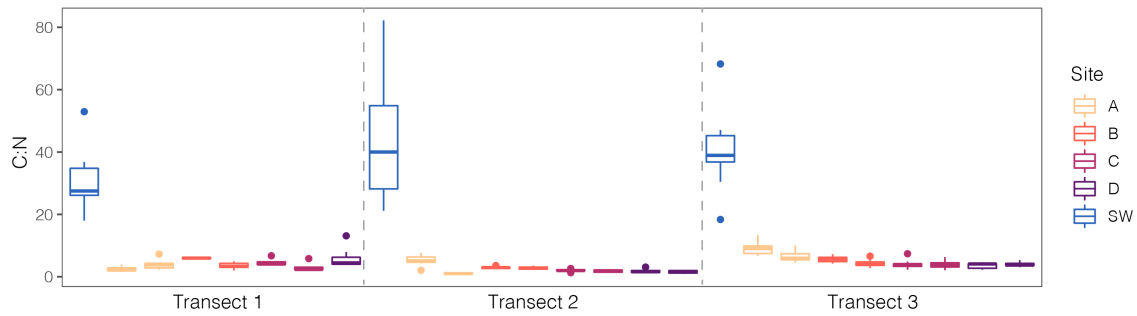
Figure S3.7. Carbon to nitrogen ratio (as mg C DOC to mg N DIN) by transect, lateral sampling site, and depth.

Table S3.1. Results for pairwise comparison of mean dissolved nitrate by sampling site. Surface water samples are denoted as "Surface". All values are p-values resulting from a Mann-Whitney U test rounded to the nearest hundredth. No samples were collected from the 30 cm depth at T1 site D during the 2019 season.

| Season				A		B		C		D	
				15 cm	30 cm	15 cm	30 cm	15 cm	30 cm	15 cm	30 cm
2019	T1	A	Surface	<0.01	<0.01	<0.01	<0.01	<0.01	<0.01	<0.01	-
			15 cm	-	<0.01	<0.01	<0.01	<0.01	0.30	<0.01	-
			30 cm	-	-	0.11	<0.01	0.90	<0.01	<0.01	-
		B	15 cm	-	-	-	0.02	0.49	0.02	0.49	-
			30 cm	-	-	-	-	0.70	<0.01	<0.01	-
		C	15 cm	-	-	-	-	-	0.015	0.06	-
			30 cm	-	-	-	-	-	-	<0.01	-
		D	15 cm	-	-	-	-	-	-	-	-
	T2	A	Surface	<0.01	<0.01	<0.01	<0.01	<0.01	<0.01	<0.01	<0.01
			15 cm	-	<0.01	0.03	0.03	<0.01	<0.01	<0.01	<0.01
			30 cm	-	-	<0.01	<0.01	<0.01	<0.01	<0.01	0.08
		B	15 cm	-	-	-	0.65	<0.01	<0.01	<0.01	<0.01
			30 cm	-	-	-	-	<0.01	<0.01	<0.01	<0.01
		C	15 cm	-	-	-	-	-	<0.01	<0.01	<0.01
			30 cm	-	-	-	-	-	-	<0.01	<0.01
		D	15 cm	-	-	-	-	-	-	-	<0.01
	T3	A	Surface	<0.01	<0.01	<0.01	<0.01	<0.01	<0.01	<0.01	<0.01
			15 cm	-	<0.01	<0.01	<0.01	<0.01	<0.01	<0.01	<0.01
			30 cm	-	-	<0.01	0.01	<0.01	0.14	<0.01	<0.01
		B	15 cm	-	-	-	<0.01	<0.01	<0.01	<0.01	<0.01
			30 cm	-	-	-	-	0.03	0.43	<0.01	0.06
		C	15 cm	-	-	-	-	-	<0.01	<0.01	0.96
			30 cm	-	-	-	-	-	-	<0.01	0.02
		D	15 cm	-	-	-	-	-	-	-	<0.01
2020	T1		Surface	<0.01	-	-	-	-	-	-	-
	T2		Surface	0.06	-	-	-	-	-	-	-
	T3		Surface	<0.01	-	-	-	-	-	-	-

Table S3.2. Results for pairwise comparison of mean dissolved ammonium by sampling site. Surface water samples are denoted as "Surface". All values are p-values resulting from a Mann-Whitney U test rounded to the nearest hundredth. No samples were collected from the 30 cm depth at T1 site D during the 2019 season.

Season				A		B		C		D	
				15 cm	30 cm	15 cm	30 cm	15 cm	30 cm	15 cm	30 cm
2019	T1	A	Surface	0.52	0.27	0.46	0.79	0.99	0.15	0.64	-
			15 cm	-	0.09	0.99	0.48	0.65	0.06	0.35	-
			30 cm	-	-	0.24	0.39	0.18	0.95	0.29	-
		B	15 cm	-	-	-	0.46	0.61	0.11	0.33	-
			30 cm	-	-	-	-	0.89	0.22	0.74	-
		C	15 cm	-	-	-	-	-	0.15	0.68	-
			30 cm	-	-	-	-	-	-	0.32	-
		D	15 cm	-	-	-	-	-	-	-	-
	T2	A	SW	0.45	0.20	0.69	0.48	0.52	0.58	0.12	0.40
			15 cm	-	0.55	0.73	0.99	0.99	0.94	0.29	0.71
			30 cm	-	-	0.29	0.81	0.81	0.50	0.70	0.94
		B	15 cm	-	-	-	0.67	0.72	0.89	0.17	0.48
			30 cm	-	-	-	-	0.99	0.88	0.56	0.99
		C	15 cm	-	-	-	-	-	0.99	0.56	0.99
			30 cm	-	-	-	-	-	-	0.29	0.71
		D	15 cm	-	-	-	-	-	-	-	0.63
	T3	A	SW	0.35	0.37	-	-	0.37	0.37	-	-
			15 cm	-	0.99	-	-	0.99	0.93	-	-
			30 cm	-	-	-	-	0.99	0.99	-	-
		B	15 cm	-	-	-	-	0.37	0.37	-	-
			30 cm	-	-	-	-	0.37	0.37	-	-
		C	15 cm	-	-	-	-	-	0.99	-	-
			30 cm	-	-	-	-	-	-	-	-
		D	15 cm	-	-	-	-	-	-	-	-
2020	T1		Surface	0.09	-	-	-	-	-	-	-
	T2		Surface	<0.01	-	-	-	-	-	-	-
	T3		Surface	0.79	-	-	-	-	-	-	-

Table S3.3. Results for pairwise comparison of mean dissolved organic carbon by sampling site. Surface water samples are denoted as "Surface". All values are p-values resulting from a Mann-Whitney U test rounded to the nearest hundredth. No samples were collected from the 30 cm depth at T1 site D during the 2019 season.

Season				A		B		C		D	
				15 cm	30 cm	15 cm	30 cm	15 cm	30 cm	15 cm	30 cm
2019	T1	A	Surface	0.07	0.30	0.39	0.28	0.99	0.25	0.43	-
			15 cm	-	0.67	0.11	0.44	0.95	0.27	0.25	-
			30 cm	-	-	0.24	0.83	0.25	0.89	0.94	-
		B	15 cm	-	-	-	0.08	0.24	0.19	0.46	-
			30 cm	-	-	-	-	0.28	0.99	0.95	-
		C	15 cm	-	-	-	-	-	0.20	0.31	-
			30 cm	-	-	-	-	-	-	0.99	-
		D	15 cm	-	-	-	-	-	-	-	-
	T2	A	SW	0.06	0.02	<0.01	0.01	0.56	0.02	0.57	0.89
			15 cm	-	0.85	0.85	0.56	0.16	0.44	0.15	0.09
			30 cm	-	-	0.75	0.80	0.05	0.70	0.10	0.07
		B	15 cm	-	-	-	0.40	0.04	0.48	0.06	0.10
			30 cm	-	-	-	-	0.03	0.90	0.07	0.05
		C	15 cm	-	-	-	-	-	0.07	0.99	0.57
			30 cm	-	-	-	-	-	-	0.09	0.07
		D	15 cm	-	-	-	-	-	-	-	0.75
	T3	A	SW	0.03	0.75	<0.01	<0.01	0.03	<0.01	0.17	0.03
			15 cm	-	0.10	0.77	0.96	0.66	0.60	0.64	0.70
			30 cm	-	-	0.06	0.07	0.12	0.02	0.37	0.15
		B	15 cm	-	-	-	0.96	0.82	0.27	0.39	0.82
			30 cm	-	-	-	-	0.82	0.25	0.43	0.69
		C	15 cm	-	-	-	-	-	0.27	0.59	0.99
			30 cm	-	-	-	-	-	-	0.18	0.27
		D	15 cm	-	-	-	-	-	-	-	0.75

Table S3.4. Results for pairwise comparison of mean dissolved silica by sampling site. Surface water samples are denoted as "Surface". All values are p-values resulting from a Mann-Whitney U test rounded to the nearest hundredth. No samples were collected from the 30 cm depth at T1 site D during the 2019 season.

Season				A		B		C		D	
				15 cm	30 cm	15 cm	30 cm	15 cm	30 cm	15 cm	30 cm
			Surface	<0.01	<0.01	<0.01	<0.01	<0.01	<0.01	0.02	-
	T1	A	15 cm	-	0.01	0.02	0.25	<0.01	<0.01	<0.01	-
			30 cm	-	-	0.02	<0.01	<0.01	<0.01	<0.01	-
		B	15 cm	-	-	-	0.02	0.82	0.02	0.11	-
			30 cm	-	-	-	-	<0.01	<0.01	<0.01	-
		C	15 cm	-	-	-	-	-	0.10	0.02	-
			30 cm	-	-	-	-	-	-	<0.01	-
		D	15 cm	-	-	-	-	-	-	-	-
			SW	<0.01	<0.01	<0.01	<0.01	<0.01	<0.01	<0.01	<0.01
	T2	A	15 cm	-	<0.01	0.02	<0.01	0.05	0.20	<0.01	<0.01
			30 cm	-	-	<0.01	0.61	0.02	<0.01	0.94	<0.01
		B	15 cm	-	-	-	<0.01	<0.01	<0.01	<0.01	<0.01
2019			30 cm	-	-	-	-	0.02	<0.01	0.89	<0.01
		C	15 cm	-	-	-	-	-	0.34	0.03	<0.01
			30 cm	-	-	-	-	-	-	<0.01	<0.01
		D	15 cm	-	-	-	-	-	-	-	<0.01
			SW	<0.01	<0.01	<0.01	<0.01	<0.01	<0.01	<0.01	<0.01
	T3	A	15 cm	-	<0.01	0.03	<0.01	<0.01	<0.01	<0.01	<0.01
			30 cm	-	-	<0.01	<0.01	0.06	0.02	0.37	<0.01
		B	15 cm	-	-	-	<0.01	<0.01	<0.01	<0.01	<0.01
			30 cm	-	-	-	-	0.05	<0.01	<0.01	0.01
		C	15 cm	-	-	-	-	-	<0.01	0.67	0.48
			30 cm	-	-	-	-	-	-	<0.01	<0.01
		D	15 cm	-	-	-	-	-	-	-	0.19

Table S3.5. Results for pairwise comparison of mean deuterium excess by sampling site. Surface water samples are denoted as "Surface". All values are p-values resulting from a Mann-Whitney U test rounded to the nearest hundredth. No samples were collected from the 30 cm depth at T1 site D during the 2019 season.

Season				A 15 cm	A 30 cm	B 15 cm	B 30 cm	C 15 cm	C 30 cm	D 15 cm	D 30 cm
2019	T1	A	Surface	<0.01	<0.01	0.06	<0.01	0.70	<0.01	0.44	-
			15 cm	-	<0.01	<0.01	<0.01	<0.01	<0.01	<0.01	-
			30 cm	-	-	<0.01	<0.01	<0.01	<0.01	<0.01	-
		B	15 cm	-	-	-	0.06	0.19	0.46	0.06	-
			30 cm	-	-	-	-	<0.01	0.01	<0.01	-
		C	15 cm	-	-	-	-	-	0.02	0.37	-
			30 cm	-	-	-	-	-	-	<0.01	-
		D	15 cm	-	-	-	-	-	-	-	-
	T2	A	Surface	<0.01	<0.01	<0.01	<0.01	<0.01	<0.01	<0.01	<0.01
			15 cm	-	<0.01	<0.01	<0.01	<0.01	<0.01	<0.01	<0.01
			30 cm	-	-	<0.01	0.44	0.22	0.90	0.62	<0.01
		B	15 cm	-	-	-	<0.01	<0.01	<0.01	0.04	<0.01
			30 cm	-	-	-	-	0.13	0.44	0.22	<0.01
		C	15 cm	-	-	-	-	-	0.22	0.99	<0.01
			30 cm	-	-	-	-	-	-	0.52	<0.01
		D	15 cm	-	-	-	-	-	-	-	<0.01
	T3	A	Surface	0.47	<0.01	0.48	<0.01	<0.01	<0.01	<0.01	<0.01
			15 cm	-	<0.01	0.77	<0.01	<0.01	<0.01	<0.01	<0.01
			30 cm	-	-	<0.01	<0.01	0.02	<0.01	0.04	<0.01
		B	15 cm	-	-	-	<0.01	<0.01	<0.01	<0.01	<0.01
			30 cm	-	-	-	-	<0.01	0.12	0.01	<0.01
		C	15 cm	-	-	-	-	-	<0.01	0.92	<0.01
			30 cm	-	-	-	-	-	-	0.06	<0.01
		D	15 cm	-	-	-	-	-	-	-	<0.01

Table S3.6. Results for pairwise comparison of mean dissolved C:N by sampling site. Surface water samples are denoted as "Surface". All values are p-values resulting from a Mann-Whitney U test rounded to the nearest hundredth. No samples were collected from the 30 cm depth at T1 site D during the 2019 season.

Season				A		B		C		D	
				15 cm	30 cm	15 cm	30 cm	15 cm	30 cm	15 cm	30 cm
	T1	A	Surface	<0.01	<0.01	0.07	<0.01	<0.01	<0.01	<0.01	-
			15 cm	-	0.05	0.06	0.04	<0.01	0.28	<0.01	-
			30 cm	-	-	0.24	0.83	0.43	0.22	0.17	-
		B	15 cm	-	-	-	0.06	0.19	0.11	0.46	-
			30 cm	-	-	-	-	0.20	0.25	0.10	-
		C	15 cm	-	-	-	-	-	0.02	0.61	-
			30 cm	-	-	-	-	-	-	0.02	-
		D	15 cm	-	-	-	-	-	-	-	-
2019	T2	A	Surface	<0.01	<0.01	<0.01	<0.01	<0.01	<0.01	<0.01	<0.01
			15 cm	-	<0.01	0.03	0.03	<0.01	<0.01	<0.01	<0.01
			30 cm	-	-	<0.01	<0.01	<0.01	<0.01	0.01	0.10
		B	15 cm	-	-	-	0.44	<0.01	<0.01	0.04	<0.01
			30 cm	-	-	-	-	0.02	0.01	0.03	<0.01
		C	15 cm	-	-	-	-	-	0.31	0.43	0.22
			30 cm	-	-	-	-	-	-	0.83	0.43
		D	15 cm	-	-	-	-	-	-	-	0.58
	T3	A	Surface	<0.01	<0.01	<0.01	<0.01	<0.01	<0.01	<0.01	<0.01
			15 cm	-	0.04	<0.01	<0.01	<0.01	<0.01	<0.01	<0.01
			30 cm	-	-	0.40	0.01	<0.01	0.02	<0.01	<0.01
		B	15 cm	-	-	-	0.03	0.01	0.04	<0.01	<0.01
			30 cm	-	-	-	-	0.72	0.72	0.29	0.54
		C	15 cm	-	-	-	-	-	0.86	0.92	0.99
			30 cm	-	-	-	-	-	-	0.53	0.93
		D	15 cm	-	-	-	-	-	-	-	0.60

Chapter IV Supplemental Information

Table S4.1. N pool mass estimates from Monte Carlo uncertainty propagation (n = 10,000).

| Mass N (kg)	Hyporheic OM	Algal Biomass	Algal Biomass (Remotely Sensed)	Sediment Sorbed NH_4^+	Hyporheic Dissolved NO_3^-
1st Quartile	3624.0	87.5	162.4	17.2	0.3
Median	4769.0	201.5	276.3	31.6	0.4
Mean	5051.8	297.2	349.7	35.7	0.4
3rd Quartile	6161.1	405.4	456.6	49.1	0.5

Chapter V Supplemental Information

Figure S5.1. Concentration variations of each solute (columns) versus expected environmental drivers (rows) with dQ/dt (L s^{-2}), PAR (μS s^{-1} m^{-2}), cumulative discharge (L) over the prior 12, 24, and 48 hours and season to date, and water temperature (ºC) for Andersen Creek.
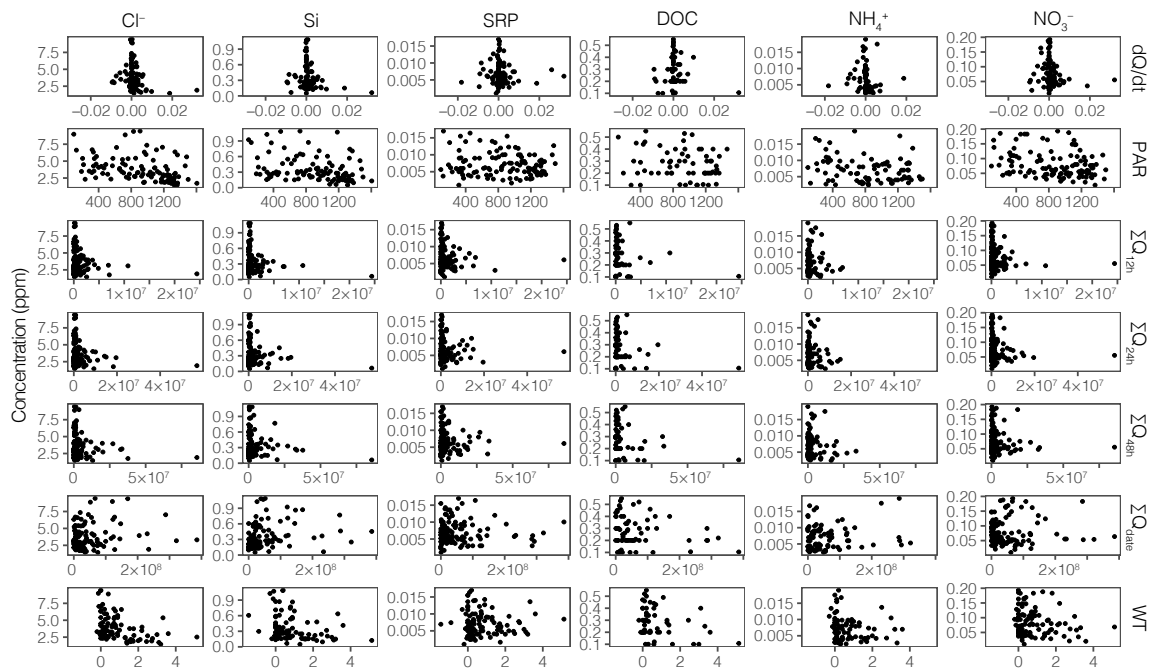
Figure S5.2. Concentration variations of each solute (columns) versus expected environmental drivers (rows) with dQ/dt (L s⁻²), PAR (µS s⁻¹ m⁻²), cumulative discharge (L) over the prior 12, 24, and 48 hours and season to date, and water temperature (ºC) for Commonwealth Stream.
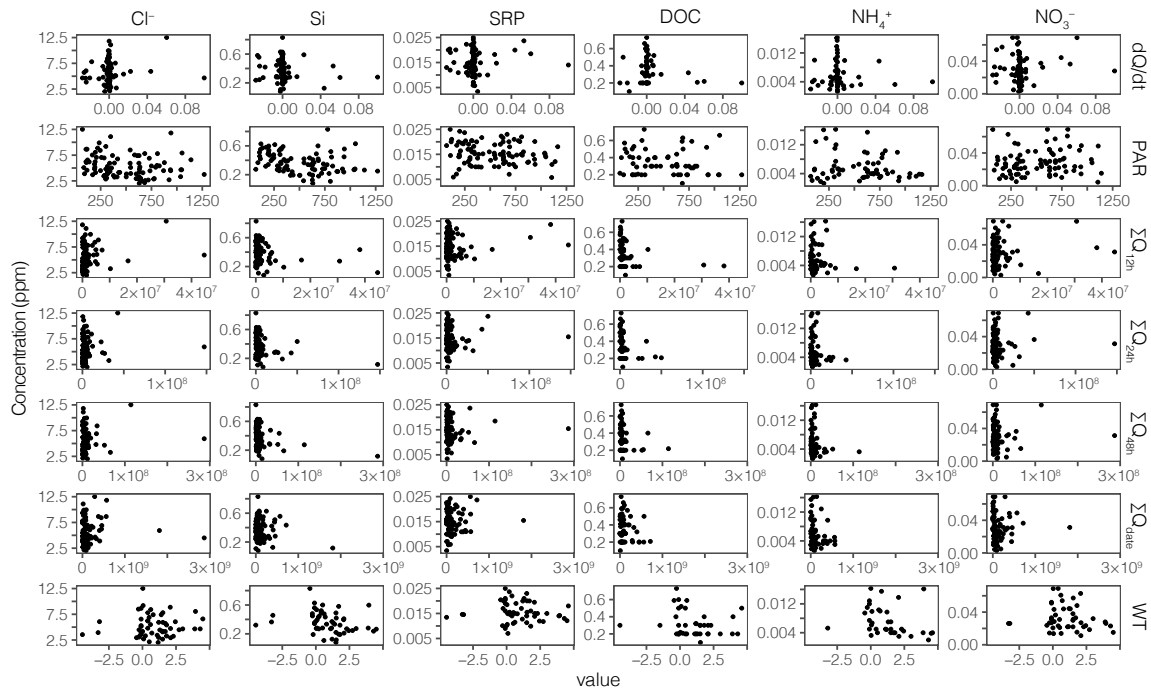
Figure S5.3. Concentration variations of each solute (columns) versus expected environmental drivers (rows) with dQ/dt (L s⁻²), PAR (µS s⁻¹ m⁻²), cumulative discharge (L) over the prior 12, 24, and 48 hours and season to date, and water temperature (ºC) for Crescent Stream.
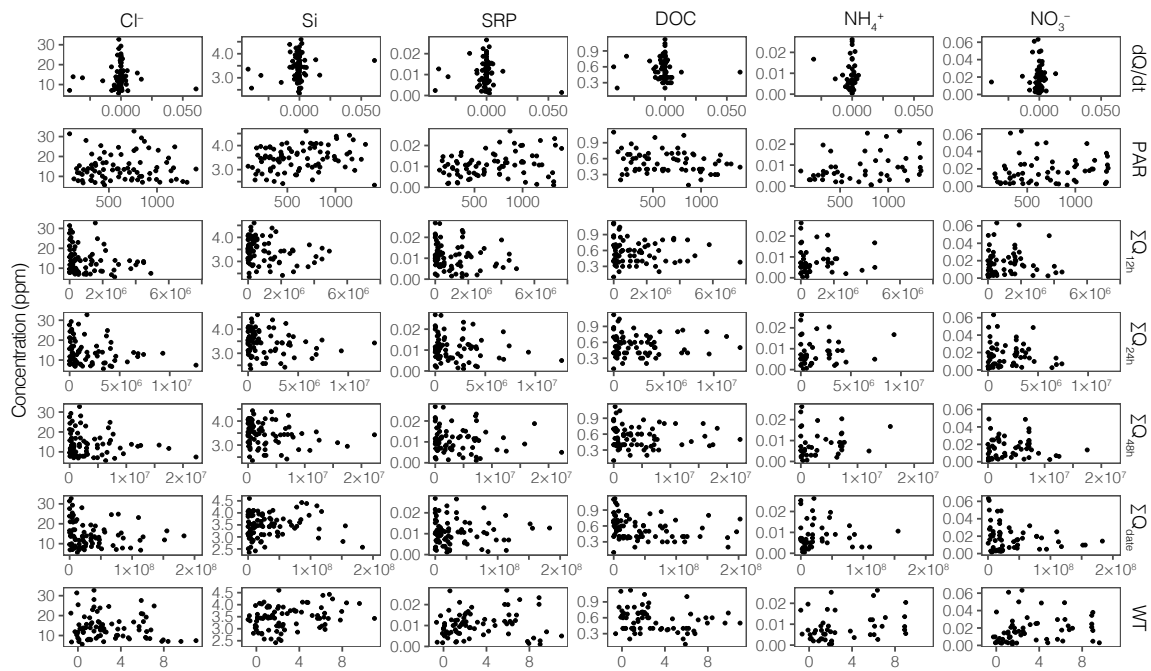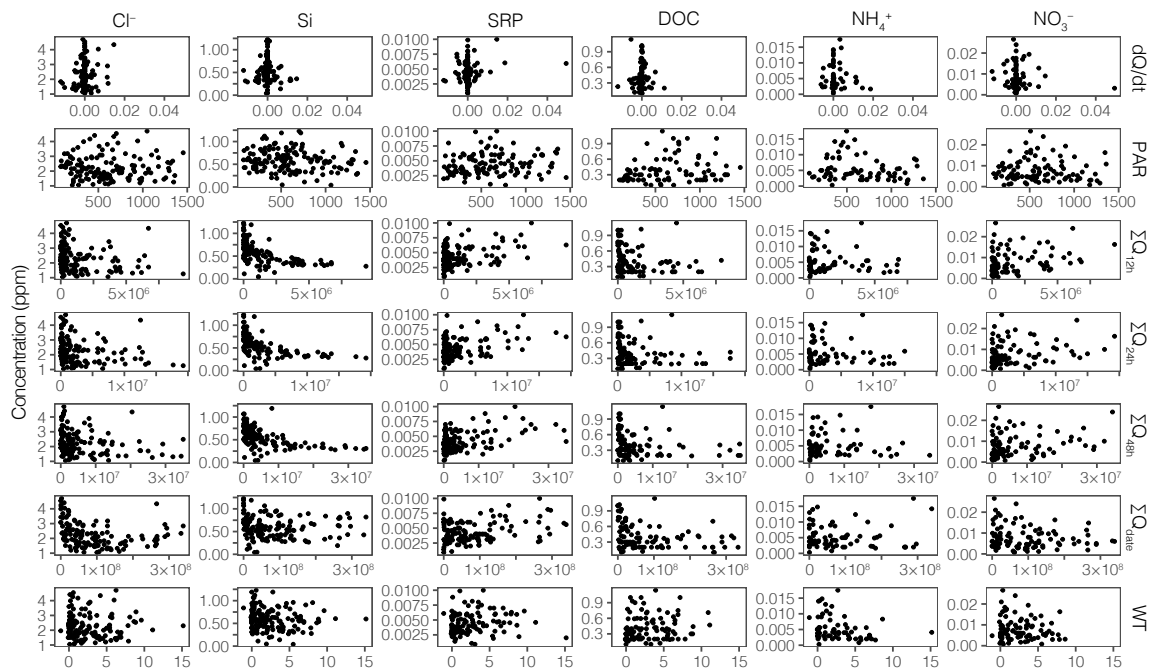
Figure S5.4. Concentration variations of each solute (columns) versus expected environmental drivers (rows) with dQ/dt (L s^{-2}), PAR (µS s^{-1} m^{-2}), cumulative discharge (L) over the prior 12, 24, and 48 hours and season to date, and water temperature (ºC) for Delta Stream.
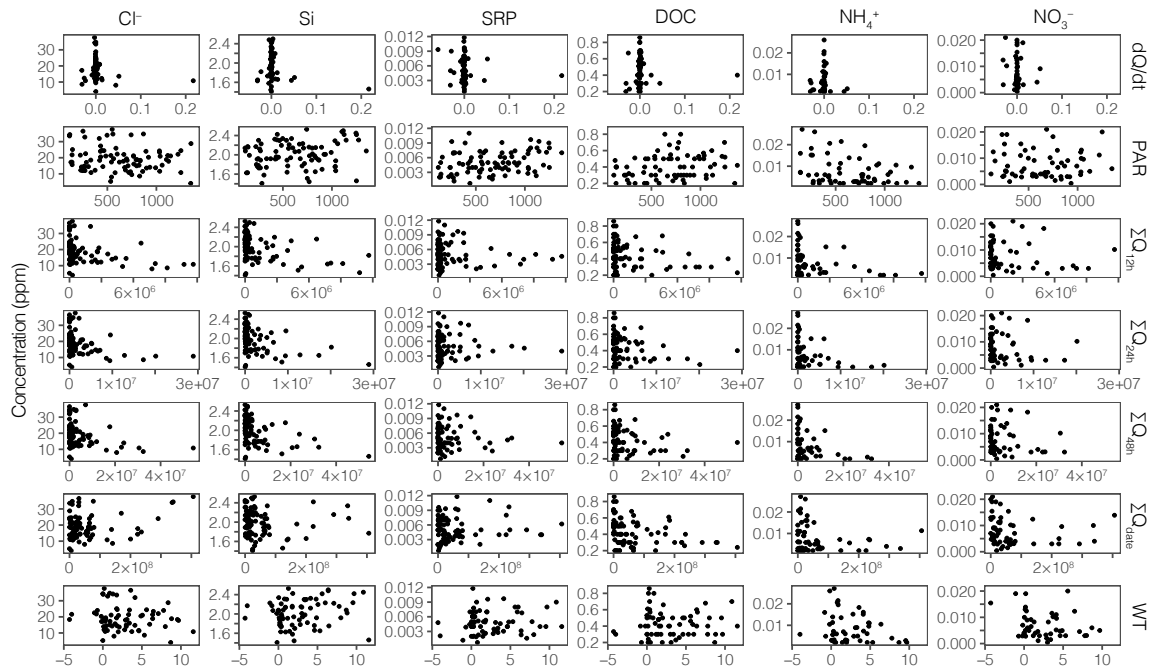
Figure S5.5. Concentration variations of each solute (columns) versus expected environmental drivers (rows) with dQ/dt (L s^{-2}), PAR (µS s^{-1} m^{-2}), cumulative discharge (L) over the prior 12, 24, and 48 hours and season to date, and water temperature (ºC) for Green Creek.
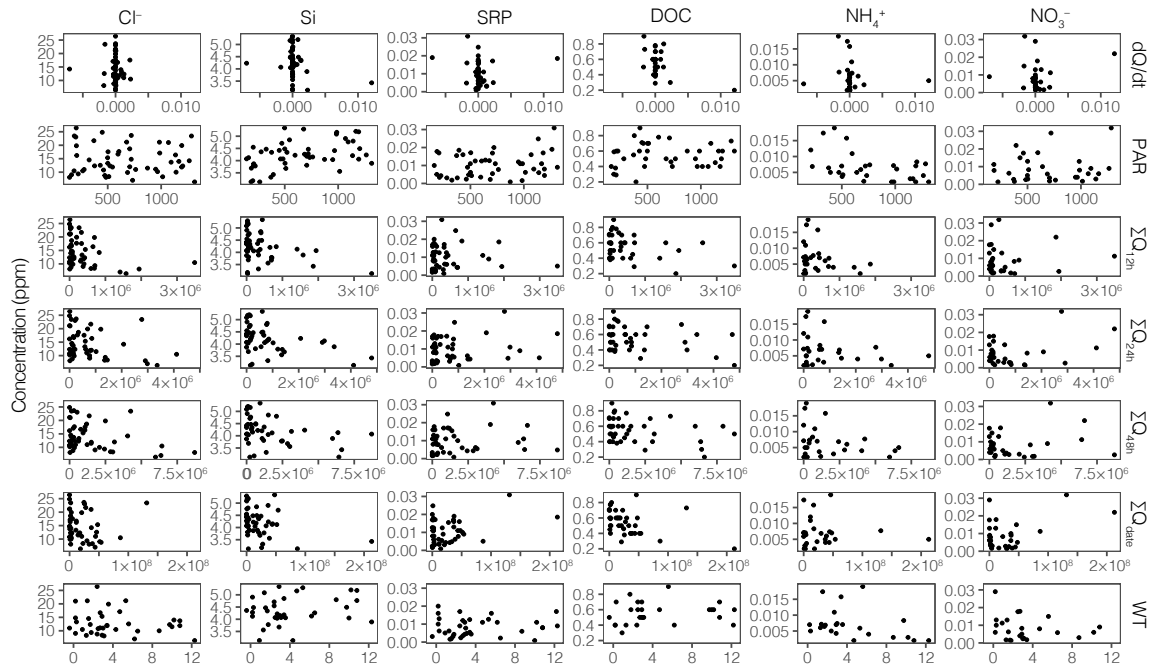
Figure S5.6. Concentration variations of each solute (columns) versus expected environmental drivers (rows) with dQ/dt (L s^{-2}), PAR (μS s^{-1} m^{-2}), cumulative discharge (L) over the prior 12, 24, and 48 hours and season to date, and water temperature (ºC) for Harnish Creek.
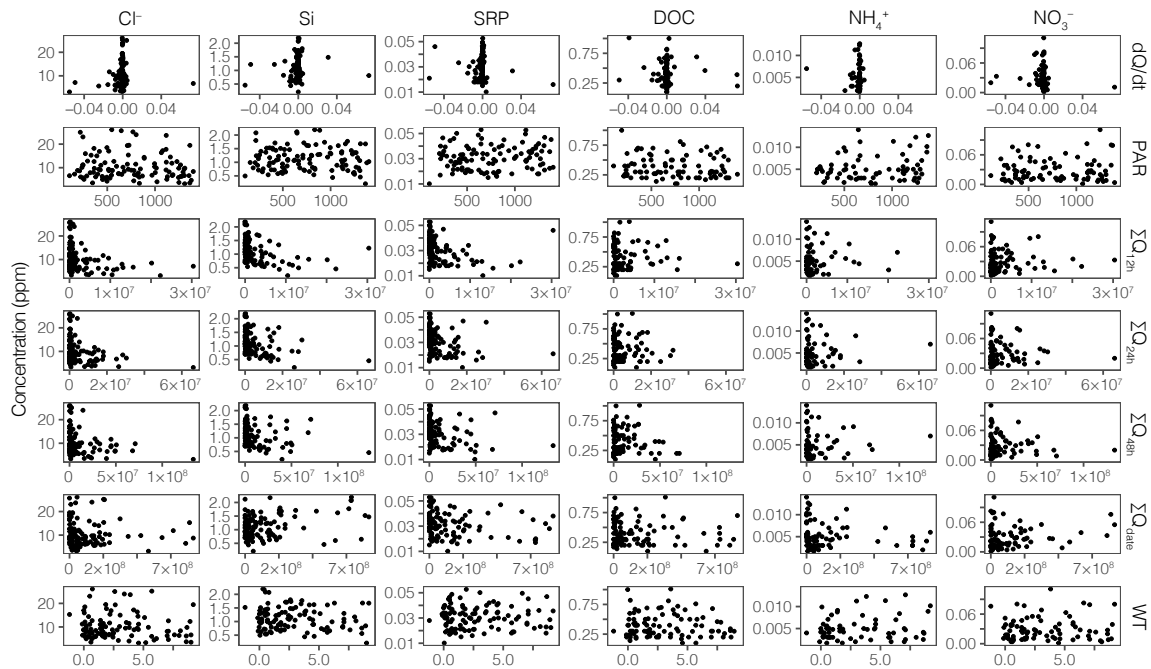

Figure S5.7. Concentration variations of each solute (columns) versus expected environmental drivers (rows) with dQ/dt (L s^{-2}), PAR (μS s^{-1} m^{-2}), cumulative discharge (L) over the prior 12, 24, and 48 hours and season to date, and water temperature (ºC) for Lost Seal Stream.

Figure S5.8. Concentration variations of each solute (columns) versus expected environmental drivers (rows) with dQ/dt (L s^{-2}), PAR (μS s^{-1} m^{-2}), cumulative discharge (L) over the prior 12, 24, and 48 hours and season to date, and water temperature (ºC) for Lawson Stream.
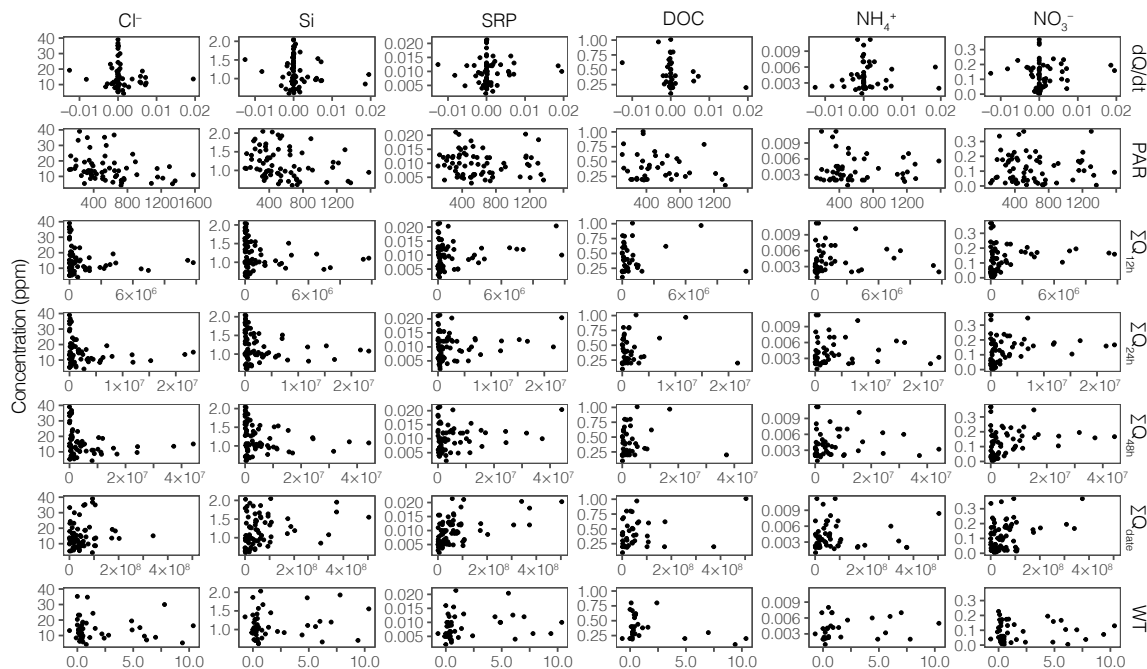

Figure S5.9. Concentration variations of each solute (columns) versus expected environmental drivers (rows) with dQ/dt (L s^{-2}), PAR (μS s^{-1} m^{-2}), cumulative discharge (L) over the prior 12, 24, and 48 hours and season to date, and water temperature (ºC) for Von Guerard Stream.